SECTION 13

Distillation

PERRY'S CHEMICAL ENGINEERS' HANDBOOK

8TH EDITION

M. F. DOHERTY, Z. T. FIDKOWSKI
M. F. MALONE, R. TAYLOR

0-07-154220-5

The material in this eBook also appears in the print version of this title: 0-07-151136-9.

DOI: 10.1036/0071511369

This page intentionally left blank

Section 13

Distillation*

M. F. Doherty, Ph.D. *Professor of Chemical Engineering, University of California—Santa Barbara (Section Editor)*

Z. T. Fidkowski, Ph.D. *Process Engineer, Air Products and Chemicals Inc. (Distillation Systems)*

M. F. Malone, Ph.D. *Professor of Chemical Engineering and Dean of Engineering, University of Massachusetts—Amherst (Batch Distillation)*

R. Taylor, Ph.D. *Professor of Chemical Engineering, Clarkson University (Simulation of Distillation Processes)*

*Certain portions of this section draw heavily on the work of J. D. Seader, Jeffrey J. Siirola, and Scott D. Barnicki, authors of this section in the 7th edition.

DEGREES OF FREEDOM AND DESIGN VARIABLES

DISTILLATION SYSTEMS

ENHANCED DISTILLATION

PETROLEUM AND COMPLEX-MIXTURE DISTILLATION

BATCH DISTILLATION

Nomenclature and Units

Symbol	Definition	SI units	U.S. Customary System units
A	Absorption factor		
A	Area	m^2	ft^2
C	Number of chemical species		
D	Distillate flow rate	kg·mol/s	lb·mol/h
D	Diffusion coefficient	m^2/s	ft^2/h
E	Efficiency		
E	Energy flux	kW/m^2	$Btu/(ft^2·h)$
$\mathcal{E}$	Energy transfer rate	kW	Btu/h
F	Feed flow rate	kg·mol/s	lb·mol/h
H	Column height	m	ft
H	Enthalpy	J/(kg·mol)	Btu/(lb·mol)
H	Liquid holdup	kg·mol	lb·mol
$\mathbb{H}$	Height of a transfer unit	m	ft
K	Vapor-liquid equilibrium ratio (K value)		
K_D	Chemical equilibrium constant for dimerization		
K_d	Liquid-liquid distribution ratio		
L	Liquid flow rate	kg·mol/s	lb·mol/h
N	Number of equilibrium stages		
N_c	Number of relationships		
N_i	Number of design variables		
N_{min}	Minimum number of equilibrium stages		
N_p	Number of phases		
N_r	Number of repetition variables		
N_o	Number of variables		
$\mathcal{N}$	Rate of mass transfer	kg·mol/s	lb·mol/h
N	Molar flux	$kg·mol/(m^2·s)$	$lb·mol/(ft^2·h)$
$\mathbb{N}$	Number of transfer units		
P	Pressure	Pa	psia
P^{sat}	Vapor pressure	Pa	psia
Q	Heat-transfer rate	kW	Btu/h
Q_c	Condenser duty	kW	Btu/h
Q_r	Reboiler duty	kW	Btu/h
R	External-reflux ratio		
R_{min}	Minimum-reflux ratio		
S	Sidestream flow rate	kg·mol/s	lb·mol/h
S	Stripping factor		
S	Vapor-sidestream ratio		
Sc	Schmidt number		
T	Temperature	K	°R
U	Liquid-sidestream rate	kg·mol/s	lb·mol/h
V	Vapor flow rate	kg·mol/s	lb·mol/h
W	Vapor-sidestream rate	kg·mol/s	lb·mol/h
X	Relative mole fraction in liquid phase		
Y	Relative mole fraction in vapor phase		
a	Activity		
a	Area	m^2	ft^2
b	Component flow rate in bottoms	kg·mol/s	lb·mol/h
c	Number of chemical species		
c	Molar density	$kg·mol/m^3$	$lb·mol/ft^3$
d	Component flow rate in distillate	kg·mol/s	lb·mol/h
d	Mass-transfer driving force		
e	Rate of heat transfer	kW	Btu/h
f	Component flow rate in feed	kg·mol/s	lb·mol/h
f	Fugacity	Pa	psia

Symbol	Definition	SI units	U.S. Customary System units
h	Height	m	ft
h	Heat-transfer coefficient	kW/m^2	$Btu/(ft^2·h)$
k	Mass-transfer coefficient	m/s	ft/h
ℓ	Component flow rate in liquid	kg·mol/s	lb·mol/h
p	Pressure	kPa	psia
q	Measure of thermal condition of feed		
q	Heat flux	kW/m^2	$Btu/(ft^2·h)$
q_c	Condenser duty	kW	Btu/h
q_r	Reboiler duty	kW	Btu/h
r	Sidestream ratio		
s	Liquid-sidestream ratio		
t	Time	s	H
u	Velocity	m/s	ft/h
v	Component flow rate in vapor	kg·mol/s	lb·mol/h
w	Weight fraction		
x	Mole fraction in liquid		
y	Mole fraction in vapor		
z	Mole fraction in feed		

Greek Symbols

α	Relative volatility		
γ	Activity coefficient		
ε	TBK efficiency		
ξ	Dimensionless time		
ρ	Density	kg/m^3	lb/ft^3
μ	Viscosity	N/m^2	
σ	Surface tension	N/m	
θ	Time for batch distillation	s	h
Θ	Parameter in Underwood equations		
Φ	Fugacity coefficient of pure component		
$\hat{\Phi}$	Fugacity coefficient in mixture		
Φ_A	Fraction of a component in feed vapor that is not absorbed		
Φ_S	Fraction of a component in entering liquid that is not stripped		
Ψ	Factor in Gilliland correlation		

Subscripts and Superscripts

EQ	Equilibrium
f	Froth
hk	Heavy key
i	Component index
j	Stage index
L	Liquid
lk	Light key
MV	Murphree vapor
o	Overall
s	Superficial
t	Mixture or total
V	Vapor
$*$	Equilibrium composition

Acronyms

HETP	Height equivalent to a theoretical plate
n.b.p.	Normal boiling point (1-atm pressure)
NTU	Number of transfer units

General References: Billet, *Distillation Engineering,* Chemical Publishing, New York, 1979. Doherty and Malone, *Conceptual Design of Distillation Systems*, McGraw-Hill, New York, 2001. Fair and Bolles, "Modern Design of Distillation Columns," *Chem. Eng.,* **75**(9), 156 (Apr. 22, 1968). Fredenslund, Gmehling, and Rasmussen, *Vapor-Liquid Equilibria Using UNIFAC, A Group Contribution Method,* Elsevier, Amsterdam, 1977. Friday and Smith, "An Analysis of the Equilibrium Stage Separation Problem—Formulation and Convergence," *AIChE J.,* **10,** 698 (1964). Hengstebeck, *Distillation—Principles and Design Procedures,* Reinhold, New York, 1961. Henley and Seader, *Equilibrium-Stage Separation Operations in Chemical Engineering,* Wiley, New York, 1981. Hoffman, *Azeotropic and Extractive Distillation,* Wiley, New York, 1964. Holland, *Fundamentals and Modeling of Separation Processes,* Prentice-Hall, Englewood Cliffs, N.J., 1975. Holland, *Fundamentals of Multicomponent Distillation,* McGraw-Hill, New York, 1981. King, *Separation Processes,* 2d ed., McGraw-Hill, New York, 1980. Kister, *Distillation Design,* McGraw-Hill, New York, 1992. Kister, *Distillation Operation,* McGraw-Hill, New York, 1990. Robinson and Gilliland, *Elements of Fractional Distillation,* 4th ed., McGraw-Hill, New York, 1950. Rousseau, ed., *Handbook of Separation Process Technology,* Wiley-Interscience, New York, 1987. Seader, "The B. C. (Before Computers) and A.D. of Equilibrium-Stage Operations," *Chem. Eng. Educ.,* **14**(2) (Spring 1985). Seader, *Chem. Eng. Progress,* **85**(10), 41 (1989). Smith, *Design of Equilibrium Stage Processes,* McGraw-Hill, New York, 1963. Seader and Henley, *Separation Process Principles*, Wiley, New York, 1998. Taylor and Krishna, *Multicomponent Mass Transfer,* Wiley, New York, 1993. Treybal, *Mass Transfer Operations,* 3d ed., McGraw-Hill, New York, 1980. *Ullmann's Encyclopedia of Industrial Chemistry,* vol. **B3,** VCH, Weinheim, 1988. Van Winkle, *Distillation,* McGraw-Hill, New York, 1967.

INTRODUCTION TO DISTILLATION OPERATIONS

GENERAL PRINCIPLES

Separation operations achieve their objective by the creation of two or more coexisting zones which differ in temperature, pressure, composition, and/or phase state. Each molecular species in the mixture to be separated responds in a unique way to differing environments offered by these zones. Consequently, as the system moves toward equilibrium, each species establishes a different concentration in each zone, and this results in a separation between the species.

The separation operation called *distillation* utilizes vapor and liquid phases at essentially the same temperature and pressure for the coexisting zones. Various kinds of devices such as *random* or *structured packings* and *plates* or *trays* are used to bring the two phases into intimate contact. Trays are stacked one above the other and enclosed in a cylindrical shell to form a *column.* Packings are also generally contained in a cylindrical shell between hold-down and support plates. The column may be operated continuously or in batch mode depending on a number of factors such as scale and flexibility of operations and solids content of feed. A typical tray-type continuous distillation column plus major external accessories is shown schematically in Fig. 13-1.

The *feed* material, which is to be separated into fractions, is introduced at one or more points along the column shell. Because of the difference in density between vapor and liquid phases, liquid runs down the column, cascading from tray to tray, while vapor flows up the column, contacting liquid at each tray.

Liquid reaching the bottom of the column is partially vaporized in a heated *reboiler* to provide *boil-up,* which is sent back up the column. The remainder of the bottom liquid is withdrawn as *bottoms,* or bottom product. Vapor reaching the top of the column is cooled and condensed to liquid in the *overhead condenser.* Part of this liquid is returned to the column as *reflux* to provide liquid overflow. The remainder of the overhead stream is withdrawn as *distillate,* or overhead product. In some cases only part of the vapor is condensed so that a vapor distillate can be withdrawn.

This overall flow pattern in a distillation column provides countercurrent contacting of vapor and liquid streams on all the trays through the column. Vapor and liquid phases on a given tray approach thermal, pressure, and composition equilibria to an extent dependent upon the efficiency of the contacting tray.

The *lighter* (lower-boiling temperature) components tend to concentrate in the vapor phase, while the *heavier* (higher-boiling temperature) components concentrate in the liquid phase. The result is a vapor phase that becomes richer in light components as it passes up the column and a liquid phase that becomes richer in heavy components as it cascades downward. The overall separation achieved between the distillate and the bottoms depends primarily on the *relative volatilities* of the components, the number of contacting trays in each column section, and the ratio of the liquid-phase flow rate to the vapor-phase flow rate in each section.

If the feed is introduced at one point along the column shell, the column is divided into an upper section, which is often called the *rectifying* section, and a lower section, which is often referred to as the *stripping* section. In *multiple-feed* columns and in columns from which a liquid or vapor *sidestream* is withdrawn, there are more than two column sections between the two end-product streams. The notion of a column section is a useful concept for finding alternative *systems* (or *sequences*) of columns for separating multicomponent mixtures, as described below in the subsection Distillation Systems.

All separation operations require energy input in the form of heat or work. In the conventional distillation operation, as typified in Fig. 13-1, energy required to separate the species is added in the form of heat to the reboiler at the bottom of the column, where the temperature is highest. Also heat is removed from a condenser at the top of the column, where the temperature is lowest. This frequently results in a

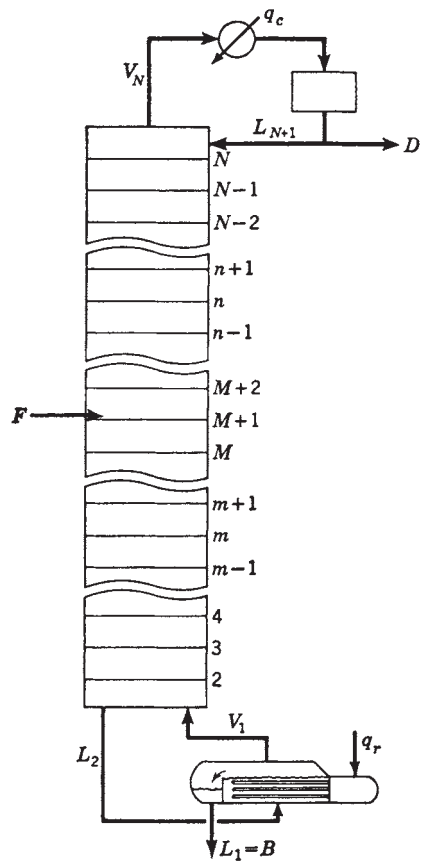

FIG. 13-1 Schematic diagram and nomenclature for a simple continuous distillation column with one feed, a total overhead condenser, and a partial reboiler.

large energy-input requirement and low overall thermodynamic efficiency, especially if the heat removed in the condenser is wasted. Complex distillation operations that offer higher thermodynamic efficiency and lower energy-input requirements have been developed and are also discussed below in the subsection Distillation Systems.

Batch distillation is preferred for small feed flows or seasonal production which is carried out intermittently in "batch campaigns." In this mode the feed is charged to a still which provides vapor to a column where the separation occurs. Vapor leaving the top of the column is condensed to provide liquid reflux back to the column as well as a distillate stream containing the product. Under normal operation, this is the only stream leaving the device. In addition to the batch rectifier just described, other batch configurations are possible as discussed in the subsection Batch Distillation. Many of the concepts and methods discussed for continuous distillation are useful for developing models and design methods for batch distillation.

EQUILIBRIUM AND NONEQUILIBRIUM-STAGE CONCEPTS

The transfer processes taking place in an actual distillation column are a complicated interplay between the thermodynamic phase equilibrium properties of the mixture, rates of intra- and interphase mass and energy transport, and multiphase flows. Simplifications are necessary to develop tractable models. The landmark concept of the *equilibrium-stage model* was developed by Sorel in 1893, in which the liquid in each stage is considered to be well mixed and such that the vapor and liquid streams leaving the stage are in thermodynamic equilibrium with each other. This is needed so that thermodynamic phase equilibrium relations can be used to determine the temperature and composition of the equilibrium streams at a given pressure. A hypothetical column composed of equilibrium stages (instead of actual contact trays) is designed to accomplish the separation specified for the actual column. The number of hypothetical equilibrium stages required is then converted to a number of actual trays by means of *tray efficiencies*, which describe the extent to which the performance of an actual contact tray duplicates the performance of an equilibrium stage. Alternatively and preferably, tray inefficiencies can be accounted for by using rate-based models that are described below.

Use of the equilibrium-stage concept separates the design of a distillation column into three major steps: (1) Thermodynamic data and methods needed to predict equilibrium-phase compositions are assembled. (2) The number of equilibrium stages and the energy input required to accomplish a specified separation, or the separation that will be accomplished in a given number of equilibrium stages for a given energy input, are calculated. (3) The number of equilibrium stages is converted to an equivalent number of actual contact trays or height of packing, and the column diameter is determined. Much of the third step is eliminated if a rate-based model is used. This section deals primarily with equilibrium and rate-based models of distillation. Section 4 covers the first step, but a summary of methods and some useful data are included in this section. Section 14 covers equipment design.

RELATED SEPARATION OPERATIONS

The simple and complex distillation operations just described all have two things in common: (1) Both rectifying and stripping sections are provided so that a separation can be achieved between two components that are adjacent in volatility; and (2) the separation is effected only by the addition and removal of energy and not by the addition of any mass separating agent (MSA) such as in liquid-liquid extraction.

Sometimes, alternative single- or multiple-stage vapor-liquid separation operations, of the types shown in Fig. 13-2, may be more suitable than distillation for the specified task.

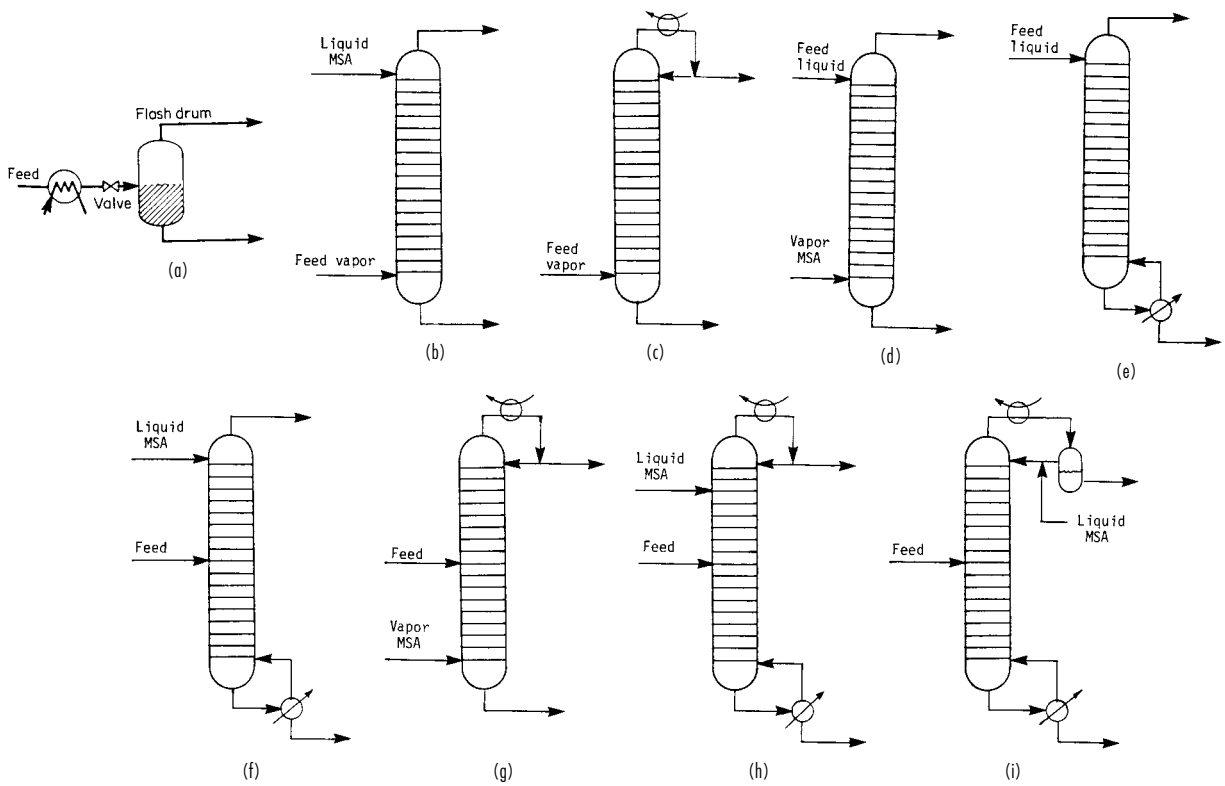

FIG. 13-2 Separation operations related to distillation. (*a*) Flash vaporization or partial condensation. (*b*) Absorption. (*c*) Rectifier. (*d*) Stripping. (*e*) Reboiled stripping. (*f*) Reboiled absorption. (*g*) Refluxed stripping. (*h*) Extractive distillation. (*i*) Azeotropic distillation.

A single-stage flash, as shown in Fig. 13-2*a,* may be appropriate if (1) the relative volatility between the two components to be separated is very large; (2) the recovery of only one component in one of the two product streams is to be achieved, without regard to the separation of the other components; or (3) only a partial separation is to be made. A common example is the separation of light gases such as hydrogen and methane from aromatics. The desired temperature and pressure of a flash may be established by the use of heat exchangers, a valve, a compressor, and/or a pump upstream of the vessel, used to separate the product vapor and liquid phases. Depending on the original condition of the feed, it may be partially condensed or partially vaporized in a so-called flash operation.

If the recovery of only one component is required rather than a sharp separation between two components of adjacent volatility, their absorption or stripping in a single section of stages may be sufficient. If the feed is vapor at separation conditions, absorption is used either with a liquid MSA absorbent of relatively low volatility, as in Fig. 13-2*b,* or with reflux produced by an overhead partial condenser, as in Fig. 13-2*c.* The choice usually depends on the ease of partially condensing the overhead vapor or of recovering and recycling the absorbent. If the feed is liquid at separation conditions, stripping is used, either with an externally supplied vapor stripping agent of relatively high volatility, as shown in Fig. 13-2*d,* or with boil-up produced by a partial reboiler, as in Fig. 13-2*e.* The choice depends on the ease of partially reboiling the bottoms or of recovering and recycling the stripping agent.

If a relatively sharp separation is required between two components of adjacent volatility, but either an undesirably low temperature is required to produce reflux at the column operating pressure or an undesirably high temperature is required to produce boil-up, then refluxed stripping, as shown in Fig. 13-2*g,* or reboiled absorption, as shown in Fig. 13-2*f,* may be used. In either case, the choice of MSA follows the same consideration given for simple absorption and stripping.

When the volatility difference between the two components to be separated is so small that a very large number of stages would be required, then extractive distillation, as shown in Fig. 13-2*h,* should be considered. Here, an MSA is selected that increases the volatility difference sufficiently to reduce the stage requirement to a reasonable number. Usually, the MSA is a polar compound of low volatility that leaves in the bottoms, from which it is recovered and recycled. It is introduced in an appreciable amount near the top stage of the column so as to affect the volatility difference over most of the stages. Some reflux to the top stage is used to minimize the MSA content in the distillate. An alternative to extractive distillation is azeotropic distillation, which is shown in Fig. 13-2*i* in just one of its many modes. In a common mode, an MSA that forms a heterogeneous minimum-boiling azeotrope with one or more components of the feed is used. The azeotrope is taken overhead, and the MSA-rich phase is decanted and returned to the top of the column as reflux.

Numerous other multistaged configurations are possible. One important variation of a stripper, shown in Fig. 13-2*d,* is a refluxed stripper, in which an overhead condenser is added. Such a configuration is sometimes used to steam-strip sour water containing NH_3, H_2O, phenol, and HCN.

All the separation operations shown in Fig. 13-2, as well as the simple and complex distillation operations described earlier, are referred to here as distillation-type separations because they have much in common with respect to calculations of (1) thermodynamic properties, (2) vapor-liquid equilibrium stages, and (3) column sizing. In fact, as will be evident from the remaining treatment of this section, the trend is toward single generalized digital computer program packages that compute many or all distillation-type separation operations.

This section also includes a treatment of distillation-type separations from a rate-based point of view that uses principles of mass- and heat-transfer rates. Section 14 also presents details of that subject as applied to absorption and stripping.

THERMODYNAMIC DATA AND MODELS

Reliable thermodynamic data are essential for the accurate design or analysis of distillation columns. Failure of equipment to perform at specified levels is often attributable, at least in part, to the lack of such data.

This subsection summarizes and presents examples of phase equilibrium data currently available to the designer. The thermodynamic concepts used are presented in the subsection Thermodynamics of Sec. 4.

PHASE EQUILIBRIUM DATA

For a binary mixture, pressure and temperature fix the equilibrium vapor and liquid compositions. Thus, experimental data are frequently presented in the form of tables of vapor mole fraction y and liquid mole fraction x for one constituent over a range of temperature T for a fixed pressure P or over a range of pressure for a fixed temperature. A small selection of such data, at a pressure of 101.3 kPa (1 atm, 1.013 bar), for four nonideal binary systems is given in Table 13-1. More extensive presentations and bibliographies of such data may be found in Hala, Wichterle, Polak, and Boublik (*Vapour-Liquid Equilibrium Data at Normal Pressures,* Pergamon, Oxford, 1968); Hirata, Ohe, and Nagahama (*Computer Aided Data Book of Vapor-Liquid Equilibria,* Elsevier, Amsterdam, 1975); Wichterle, Linek, and Hala (*Vapor-Liquid Equilibrium Data Bibliography,* Elsevier, Amsterdam, 1973, Supplement I, 1976, Supplement II, 1979); Ohe (*Vapor-Liquid Equilibrium Data,* Elsevier, Amsterdam, 1989); Ohe (*Vapor-Liquid Equilibrium Data at High Pressure,* Elsevier, Amsterdam, 1990); Walas (*Phase Equilibria in Chemical Engineering,* Butterworth, Boston, 1985); and, particularly, Gmehling and Onken [*Vapor-Liquid Equilibrium Data Collection,* DECHEMA Chemistry Data ser., vol. 1 (parts 1–10), Frankfurt, 1977]. Extensive databases of phase equilibrium measurements are readily available in most process simulators together with models for correlating, interpolating, and extrapolating (care is needed here) the data. Many of these simulators also provide graphical display of the data for easy visualization and interpretation.

For application to distillation (a nearly isobaric process) binary-mixture data are frequently plotted, for a fixed pressure, as y versus x, with a line of 45° slope included for reference, and as T versus y and x, as shown in Figs. 13-3 to 13-8. In some binary systems, one of the components is more volatile than the other over the entire composition range. This is the case in Figs. 13-3 and 13-4 for the benzene-toluene system at pressures of both 101.3 and 202.6 kPa (1 and 2 atm), where benzene is more volatile than toluene.

For other binary systems, one of the components is more volatile over only a part of the composition range. Two systems of this type, ethyl acetate–ethanol and chloroform-acetone, are shown in Figs. 13-5 to 13-7. Figure 13-5 shows that chloroform is less volatile than acetone below a concentration of 66 mol % chloroform and that ethyl acetate is more volatile than ethanol below a concentration of 53 mol % ethyl acetate. Above these concentrations, volatility is reversed. Such mixtures are known as azeotropic mixtures, and the composition in which the reversal occurs, which is the composition in which vapor and liquid compositions are equal, is the azeotropic composition, or azeotrope. The azeotropic liquid may be homogeneous or heterogeneous (two immiscible liquid phases). Two of the binary mixtures of Table 13-1 form homogeneous azeotropes. Non-azeotrope-forming mixtures such as benzene and toluene in Figs. 13-3 and 13-4 can be separated by simple distillation into two essentially pure products. By contrast, simple distillation of azeotropic mixtures will at best yield the azeotrope and one essentially pure species. The distillate and bottoms products obtained depend upon the feed composition and whether a minimum-boiling azeotrope is formed as with the ethyl acetate–ethanol mixture in Fig. 13-6 or a maximum-boiling azeotrope is formed as with the chloroform-acetone mixture in Fig. 13-7. For example, if a mixture of 30 mol % chloroform and 70 mol % acetone is fed to a simple distillation column, such as that

TABLE 13-1 Constant-Pressure Liquid-Vapor Equilibrium Data for Selected Binary Systems

Component		Temperature, °C	Mole fraction *A* in		Total pressure, kPa	Reference
A	*B*		Liquid	Vapor		
Acetone	Chloroform	62.50	0.0817	0.0500	101.3	1
		62.82	0.1390	0.1000		
		63.83	0.2338	0.2000		
		64.30	0.3162	0.3000		
		64.37	0.3535	0.3500		
		64.35	0.3888	0.4000		
		64.02	0.4582	0.5000		
		63.33	0.5299	0.6000		
		62.23	0.6106	0.7000		
		60.72	0.7078	0.8000		
		58.71	0.8302	0.9000		
		57.48	0.9075	0.9500		
Acetone	Water	74.80	0.0500	0.6381	101.3	2
		68.53	0.1000	0.7301		
		65.26	0.1500	0.7716		
		63.59	0.2000	0.7916		
		61.87	0.3000	0.8124		
		60.75	0.4000	0.8269		
		59.95	0.5000	0.8387		
		59.12	0.6000	0.8532		
		58.29	0.7000	0.8712		
		57.49	0.8000	0.8950		
		56.68	0.9000	0.9335		
		56.30	0.9500	0.9627		
Ethyl acetate	Ethanol	78.3	0.0	0.0	101.3	3
		76.6	0.050	0.102		
		75.5	0.100	0.187		
		73.9	0.200	0.305		
		72.8	0.300	0.389		
		72.1	0.400	0.457		
		71.8	0.500	0.516		
		71.8	0.540	0.540		
		71.9	0.600	0.576		
		72.2	0.700	0.644		
		73.0	0.800	0.726		
		74.7	0.900	0.837		
		76.0	0.950	0.914		
		77.1	1.000	1.000		
Ethylene glycol	Water	69.5	0.0	0.0	30.4	4
		76.1	0.23	0.002		
		78.9	0.31	0.003		
		83.1	0.40	0.010		
		89.6	0.54	0.020		
		103.1	0.73	0.06		
		118.4	0.85	0.13		
		128.0	0.90	0.22		
		134.7	0.93	0.30		
		145.0	0.97	0.47		
		160.7	1.00	1.00		

NOTE: To convert degrees Celsius to degrees Fahrenheit, °C = (°F − 32)/1.8. To convert kilopascals to pounds-force per square inch, multiply by 0.145.

[1]Kojima, Kato, Sunaga, and Hashimoto, *Kagaku Kogaku,* **32,** 337 (1968).

[2]Kojima, Tochigi, Seki, and Watase, *Kagaku Kogaku,* **32,** 149 (1968).

[3]Chu, Getty, Brennecke, and Paul, *Distillation Equilibrium Data,* New York, 1950.

[4]Trimble and Potts, *Ind. Eng. Chem.,* **27,** 66 (1935).

shown in Fig. 13-1, operating at 101.3 kPa (1 atm), the distillate could approach pure acetone and the bottoms could approach the maximum-boiling azeotrope.

An example of heterogeneous-azeotrope formation is shown in Fig. 13-8 for the water–normal butanol system at 101.3 kPa. At liquid compositions between 0 and 3 mol % butanol and between 40 and 100 mol % butanol, the liquid phase is homogeneous. Phase splitting into two separate liquid phases (one with 3 mol % butanol and the other with 40 mol % butanol) occurs for any overall liquid composition between 3 and 40 mol % butanol. A minimum-boiling heterogeneous azeotrope occurs at 92°C (198°F) when the vapor composition and the overall composition of the two liquid phases are 25 mol % butanol.

For mixtures containing more than two species, an additional degree of freedom is available for each additional component. Thus, for a four-component system, the equilibrium vapor and liquid compositions are fixed only if the pressure, temperature, and mole fractions of two components are set. Representation of multicomponent vapor-liquid equilibrium data in tabular or graphical form of the type shown earlier for binary systems is either difficult or impossible. Instead, such data, as well as binary-system data, are commonly represented in terms of *K* values (vapor-liquid equilibrium ratios), which are defined by

$$K_i = \frac{y_i}{x_i} \tag{13-1}$$

and are correlated empirically or theoretically in terms of temperature, pressure, and phase compositions in the form of tables, graphs, and equations. The *K* values are widely used in multicomponent distillation calculations, and the ratio of the *K* values of two species, called the relative volatility,

$$\alpha_{ij} = \frac{K_i}{K_j} \tag{13-2}$$

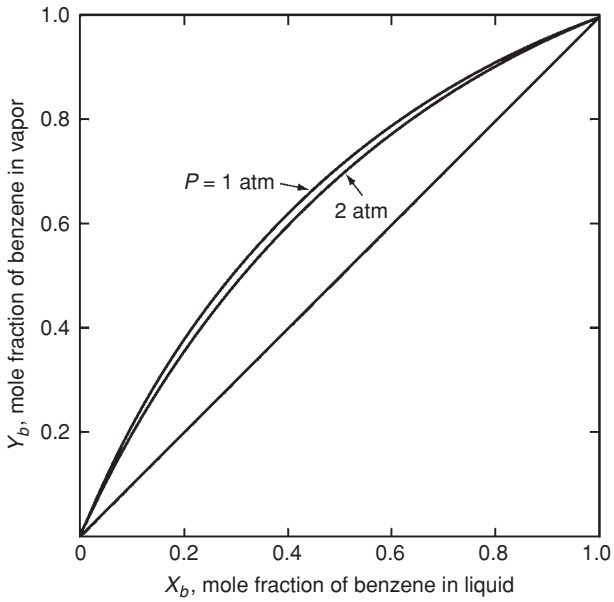

FIG. 13-3 Isobaric *y-x* curves for benzene-toluene. (*Brian,* Staged Cascades in Chemical Processing, *Prentice-Hall, Englewood Cliffs, N.J., 1972.*)

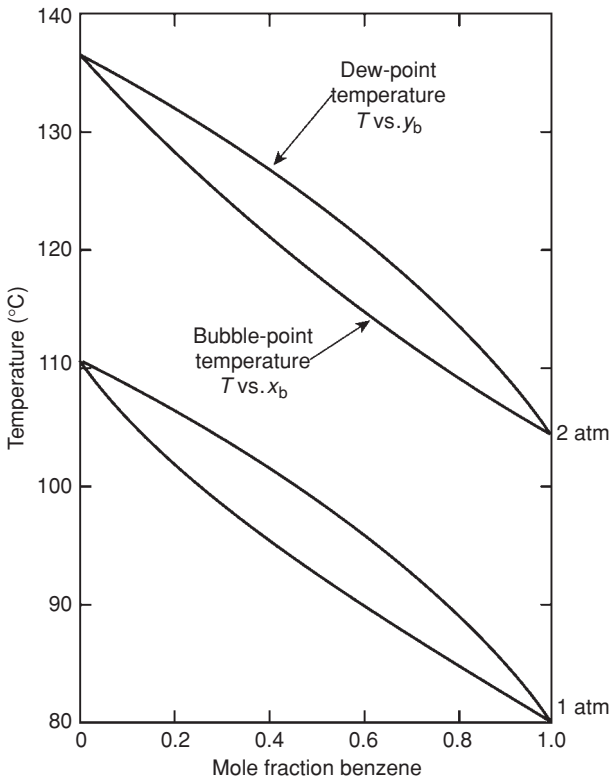

FIG. 13-4 Isobaric vapor-liquid equilibrium curves for benzene-toluene. (*Brian,* Staged Cascades in Chemical Processing, *Prentice-Hall, Englewood Cliffs, N.J., 1972.*)

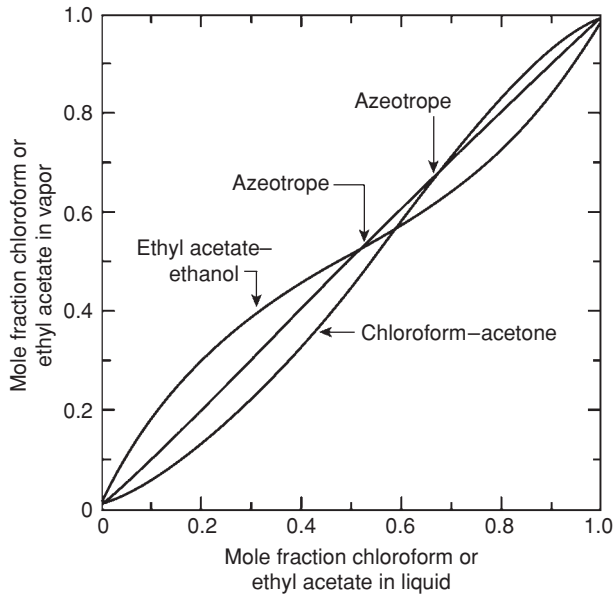

FIG. 13-5 Vapor-liquid equilibria for the ethyl acetate–ethanol and chloroform-acetone systems at 101.3 kPa (1 atm).

is a convenient index of the relative ease or difficulty of separating components *i* and *j* by distillation. Rarely is distillation used on a large scale if the relative volatility is less than 1.05, with *i* more volatile than *j*.

GRAPHICAL *K* VALUE CORRELATIONS

As discussed in Sec. 4, the *K* value of a species is a complex function of temperature, pressure, and equilibrium vapor- and liquid-phase compositions. However, for mixtures of compounds of similar molecular structure and size, the *K* value depends mainly on temperature and pressure. For example, several major graphical *K* value correlations are available for light-hydrocarbon systems. The easiest to use are the DePriester charts [*Chem. Eng. Prog. Symp. Ser.* 7, **49,** 1 (1953)],

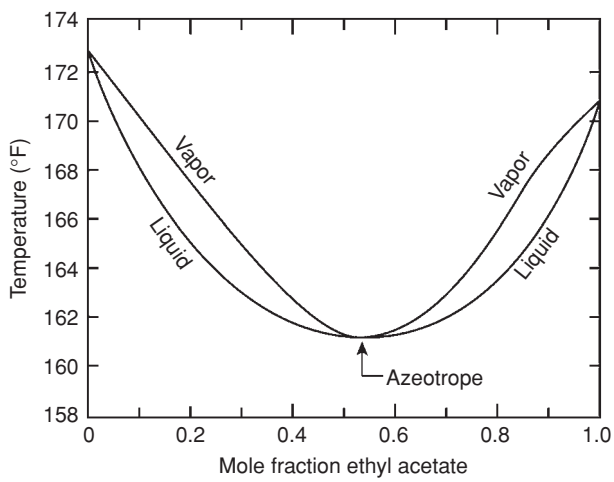

FIG. 13-6 Liquid boiling points and vapor condensation temperatures for minimum-boiling azeotrope mixtures of ethyl acetate and ethanol at 101.3-kPa (1-atm) total pressure.

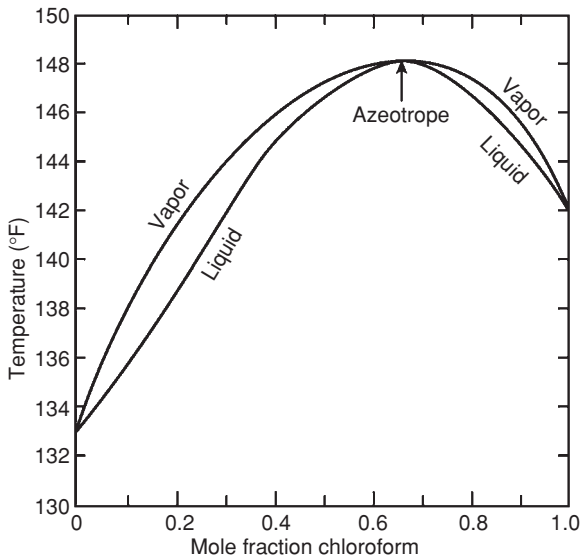

FIG. 13-7 Liquid boiling points and vapor condensation temperatures for maximum-boiling azeotrope mixtures of chloroform and acetone at 101.3-kPa (1-atm) total pressure.

which cover 12 hydrocarbons (methane, ethylene, ethane, propylene, propane, isobutane, isobutylene, *n*-butane, isopentane, *n*-pentane, *n*-hexane, and *n*-heptane). These charts are a simplification of the Kellogg charts (*Liquid-Vapor Equilibria in Mixtures of Light Hydrocarbons, MWK Equilibrium Constants, Polyco Data,* 1950) and include additional experimental data. The Kellogg charts, and hence the DePriester charts, are based primarily on the Benedict-Webb-Rubin equation of state [*Chem. Eng. Prog.,* **47,** 419 (1951); **47,** 449 (1951)], which can represent both the liquid and the vapor phases and can predict *K* values quite accurately when the equation constants are available for the components in question.

A trial-and-error procedure is required with any *K* value correlation that takes into account the effect of composition. One cannot calculate *K* values until phase compositions are known, and those cannot be known until the *K* values are available to calculate them. For *K* as a function of *T* and *P* only, the DePriester charts provide good starting values for the iteration. These nomographs are shown in Fig. 13-9*a* and *b.* SI versions of these charts have been developed by Dadyburjor [*Chem. Eng. Prog.,* **74**(4), 85 (1978)].

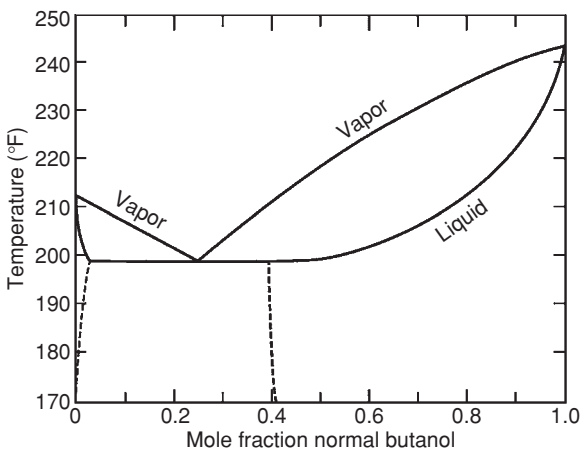

FIG. 13-8 Vapor-liquid equilibrium data for an *n*-butanol–water system at 101.3 kPa (1 atm); phase splitting and heterogeneous-azeotrope formation.

The Kellogg and DePriester charts and their subsequent extensions and generalizations use the molar average boiling points of the liquid and vapor phases to represent the composition effect. An alternative measure of composition is the convergence pressure of the system, which is defined as that pressure at which the *K* values for all the components in an isothermal mixture converge to unity. It is analogous to the critical point for a pure component in the sense that the two phases become indistinguishable. The behavior of a complex mixture of hydrocarbons for a convergence pressure of 34.5 MPa (5000 psia) is illustrated in Fig. 13-10.

Two major graphical correlations based on convergence pressure as the third parameter (besides temperature and pressure) are the charts published by the Gas Processors Association (GPA, *Engineering Data Book,* 9th ed., Tulsa, 1981) and the charts of the American Petroleum Institute (API, *Technical Data Book—Petroleum Refining,* New York, 1966) based on the procedures from Hadden and Grayson [*Hydrocarbon Process., Pet. Refiner,* **40**(9), 207 (1961)]. The former uses the method proposed by Hadden [*Chem. Eng. Prog. Symp. Ser. 7,* **49,** 53 (1953)] for the prediction of convergence pressure as a function of composition. The basis for Hadden's method is illustrated in Fig. 13-11, where it is shown that the critical loci for various mixtures of methane-propane-pentane fall within the area circumscribed by the three binary loci. (This behavior is not always typical of more nonideal systems.) The critical loci for the ternary mixtures vary linearly, at constant temperature, with weight percent propane on a methane-free basis. The essential point is that critical loci for mixtures are independent of the concentration of the lightest component in a mixture. This permits representation of a multicomponent mixture as a pseudobinary. The light component in this pseudobinary is the lightest species present (to a reasonable extent) in the multicomponent mixture. The heavy component is a pseudosubstance whose critical temperature is an average of all other components in the multicomponent mixture. This pseudocritical point can then be located on a *P-T* diagram containing the critical points for all compounds covered by the charts, and a critical locus can be drawn for the pseudobinary by interpolation between various real binary curves. Convergence pressure for the mixture at the desired temperature is read from the assumed loci at the desired system temperature. This method is illustrated in the left half of Fig. 13-12 for the methane-propane-pentane ternary. Associated *K* values for pentane at 104°C (220°F) are shown to the right as a function of mixture composition (or convergence pressure).

The GPA convergence pressure charts are primarily for alkane and alkene systems but do include charts for nitrogen, carbon dioxide, and hydrogen sulfide. The charts may not be valid when appreciable amounts of naphthenes or aromatics are present; the API charts use special procedures for such cases. Useful extensions of the convergence pressure concept to more varied mixtures include the nomographs of Winn [*Chem. Eng. Prog. Symp. Ser. 2,* **48,** 121 (1952)], Hadden and Grayson (op. cit.), and Cajander, Hipkin, and Lenoir [*J. Chem. Eng. Data,* **5,** 251 (1960)].

ANALYTICAL *K* VALUE CORRELATIONS

The widespread availability and use of digital computers for distillation calculations have given impetus to the development of analytical expressions for *K* values. McWilliams [*Chem. Eng.,* **80**(25), 138 (1973)] presents a regression equation and accompanying regression coefficients that represent the DePriester charts of Fig. 13-9. Regression equations and coefficients for various versions of the GPA convergence pressure charts are available from the GPA.

Preferred analytical correlations are less empirical and most often are theoretically based on one of two exact thermodynamic formulations, as derived in Sec. 4. When a single pressure-volume-temperature *(P-V-T)* equation of state is applicable to both vapor and liquid phases, the formulation used is

$$K_i = \frac{\hat{\Phi}_i^L}{\hat{\Phi}_i^V} \tag{13-3}$$

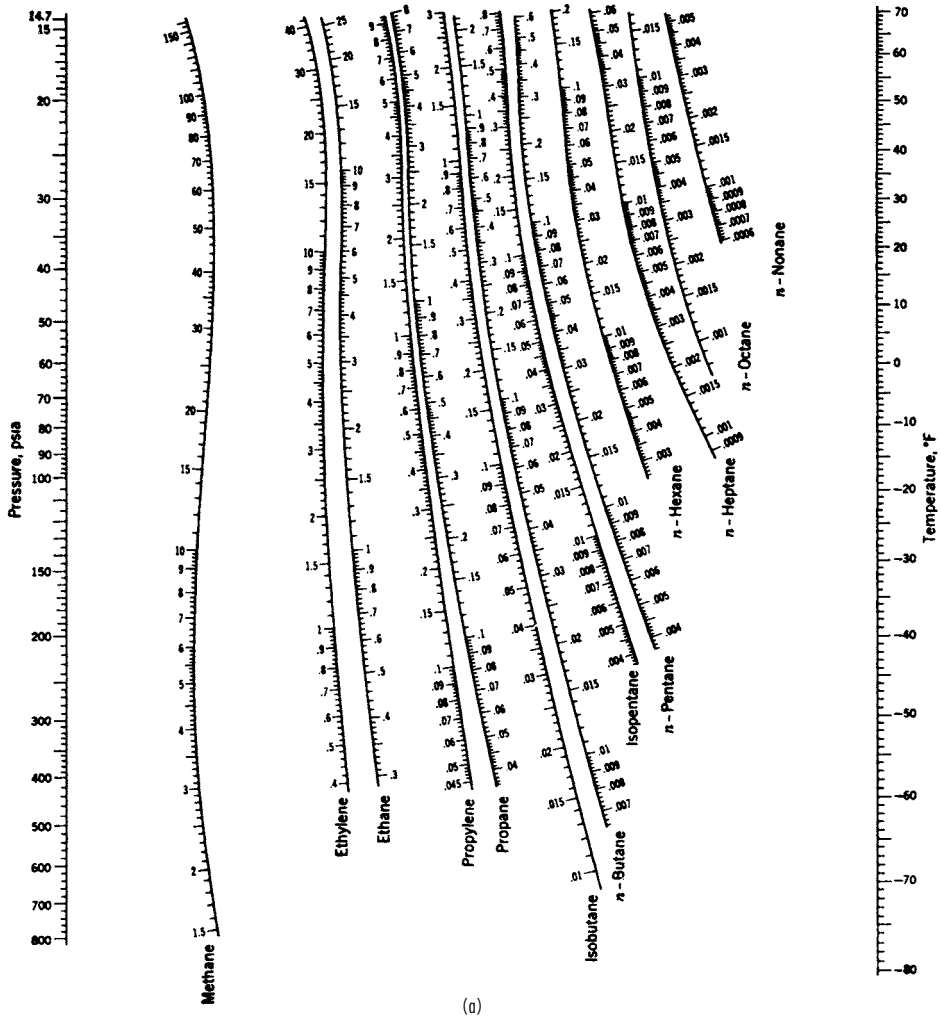

FIG. 13-9 The K values ($K = y/x$) in light-hydrocarbon systems. (*a*) Low-temperature range. (*b*) High-temperature range. [*DePriester*, Chem. Eng. Prog. Symp., *Ser. 7,* ***49****, 1 (1953).*]

where the mixture fugacity coefficients $\hat{\Phi}_i^L$ for the liquid and $\hat{\Phi}_i^V$ for the vapor are derived by classical thermodynamics from the *P-V-T* expression. Consistent equations for enthalpy can be similarly derived.

Until recently, equations of state that have been successfully applied to Eq. (13-3) have been restricted to mixtures of nonpolar compounds, namely, hydrocarbons and light gases. These equations include those of Benedict-Webb-Rubin (BWR), Soave (SRK) [*Chem. Eng. Sci.,* **27,** 1197 (1972)], who extended the remarkable Redlich-Kwong equation, and Peng-Robinson (PR) [*Ind. Eng. Chem. Fundam.,* **15,** 59 (1976)]. The SRK and PR equations belong to a family of so-called cubic equations of state. The Starling extension of the BWR equation (*Fluid Thermodynamic Properties for Light Petroleum Systems,* Gulf, Houston, 1973) predicts K values and enthalpies of the normal paraffins up through *n*-octane, as well as isobutane, isopentane, ethylene, propylene, nitrogen, carbon dioxide, and hydrogen sulfide, including the cryogenic region. Computer programs for K values derived from the SRK, PR, and other equations of state are widely available in all computer-aided process design and simulation programs. The ability of the SRK correlation to predict K values even when the pressure approaches the convergence pressure is shown for a multicomponent system in Fig. 13-13. Similar results are achieved with the PR correlation. The Wong-Sandler mixing rules for cubic equations of state now permit such equations to be extended to mixtures of organic chemicals, as shown in a reformulated version by Orbey and Sandler [*AIChE J.,* **41,** 683 (1995)].

An alternative K value formulation that has received wide application to mixtures containing polar and/or nonpolar compounds is

$$K_i = \frac{\gamma_i^L \Phi_i^L}{\hat{\Phi}_i^V} \tag{13-4}$$

where different equations of state may be used to predict the pure-component liquid fugacity coefficient Φ_i^L and the vapor-mixture fugacity coefficient, and any one of a number of mixture free-energy models may be used to obtain the liquid activity coefficient γ_i^L. At low to moderate pressures, accurate prediction of the latter is crucial to the application of Eq. (13-4).

When either Eq. (13-3) or Eq. (13-4) can be applied, the former is generally preferred because it involves only a single equation of state applicable to both phases and thus would seem to offer greater consistency. In addition, the quantity Φ_i^L in Eq. (13-4) is hypothetical for any components that are supercritical. In that case, a modification of Eq. (13-4) that uses Henry's law is sometimes applied.

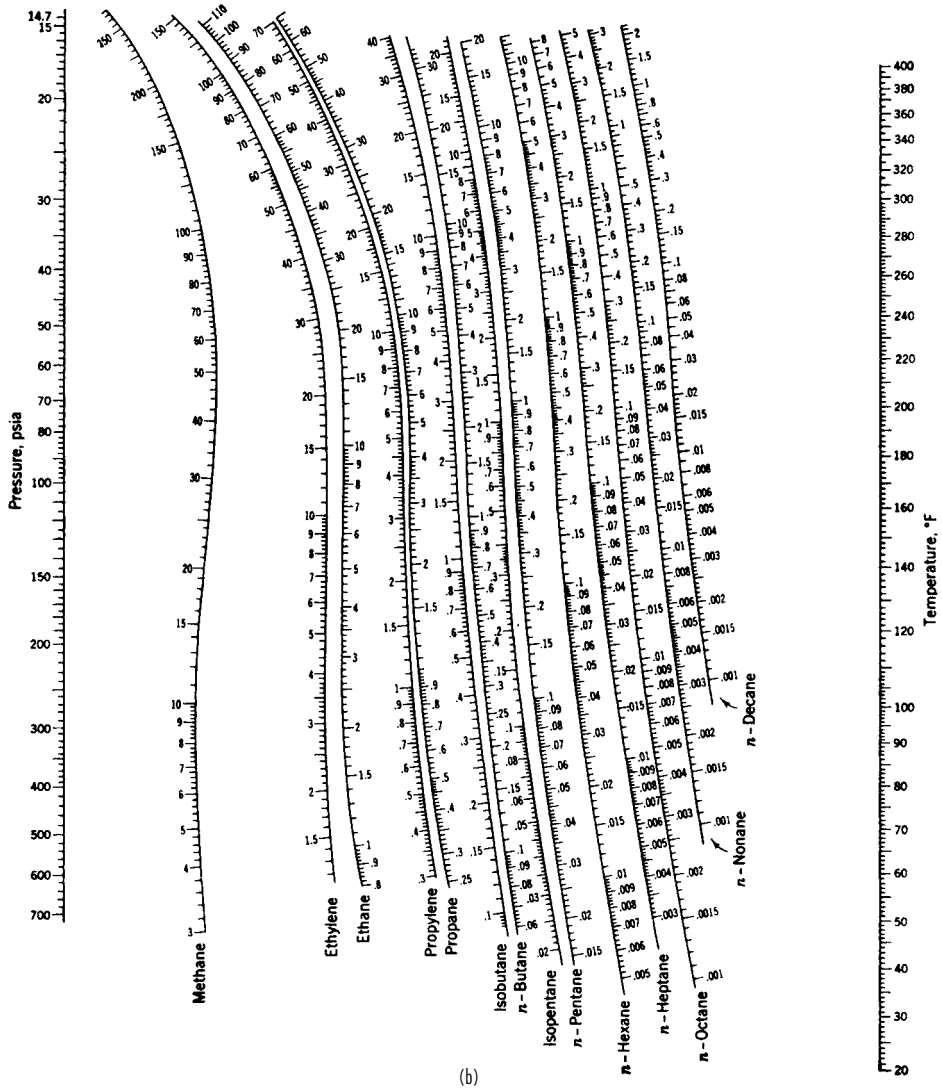

FIG. 13-9 (*Continued*)

For mixtures of hydrocarbons and light gases, Chao and Seader (CS) [*AIChE J.*, **7,** 598 (1961)] applied Eq. (13-4) by using an empirical expression for Φ_i^L based on the generalized corresponding-states *P-V-T* correlation of Pitzer et al., the Redlich-Kwong equation of state for $\hat{\Phi}_i^V$, and the regular solution theory of Scatchard and Hildebrand for γ_i^L. The predictive ability of the last-named theory is exhibited in Fig. 13-14 for the heptane-toluene system at 101.3 kPa (1 atm). Five pure-component constants for each species (T_v, P_v, ω, δ, and v^L) are required to use the CS method which, when applied within the restrictions discussed by Lenoir and Koppany [*Hydrocarbon Process.*, **46**(11), 249 (1967)], gives good results. Revised coefficients of Grayson and Streed (GS) (Paper 20-P07, Sixth World Pet. Conf. Frankfurt, June, 1963) for the Φ_i^L expression permit application of the CS correlation to higher temperatures and pressures and give improved predictions for hydrogen. Jin, Greenkorn, and Chao [*AIChE J*, **41,** 1602 (1995)] present a revised correlation for the standard-state liquid fugacity of hydrogen, applicable from 200 to 730 K.

For mixtures containing polar substances, more complex predictive equations for γ_i^L that involve binary-interaction parameters for each pair of components in the mixture are required for use in Eq. (13-4), as discussed in Sec. 4. Six popular expressions are the Margules, van Laar, Wilson, NRTL, UNIFAC, and UNIQUAC equations. The preferred expressions for representing activity coefficients are the NRTL and UNIQUAC equations. Extensive listings of binary-interaction parameters for use in all but the UNIFAC equation are given by Gmehling and Onken (op. cit.). They obtained the parameters for binary systems at 101.3 kPa (1 atm) from best fits of the experimental *T-y-x* equilibrium data by setting Φ_i^V and Φ_i^L to their ideal-gas, ideal-solution limits of 1.0 and P^{sat}/P, respectively, with the vapor pressure P^{sat} given by a three-constant Antonie equation, whose values they tabulate. Table 13-2 lists their parameters for selected binary systems based on the binary system activity coefficient equation forms given in Table 13-3.

Consistent Antoine vapor pressure constants and liquid molar volumes are listed in Table 13-4. The Wilson equation is particularly useful for systems that are highly nonideal but do not undergo phase splitting, as exemplified by the ethanol-hexane system, whose activity coefficients are shown in Fig. 13-15. For systems such as this, in which activity coefficients in dilute regions may exceed values of

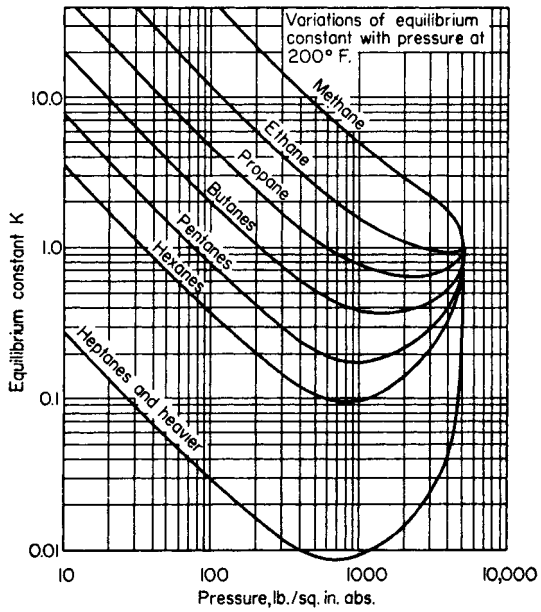

FIG. 13-10 Typical variation of K values with total pressure at constant temperature for a complex mixture. Light hydrocarbons in admixture with crude oil. [*Katz and Hachmuth*, Ind. Eng. Chem., **29,** *1072 (1937).*]

approximately 7.5, the van Laar equation erroneously predicts phase splitting.

Tables 13-2 and 13-4 include data on formic acid and acetic acid, two substances that tend to dimerize in the vapor phase according to the chemical equilibrium expression

$$K_D = \frac{P_D}{P_M^2} = 10^{A+B/T} \tag{13-5}$$

where K_D is the chemical equilibrium constant for dimerization, P_D and P_M are partial pressures of dimer and monomer, respectively, in torr,

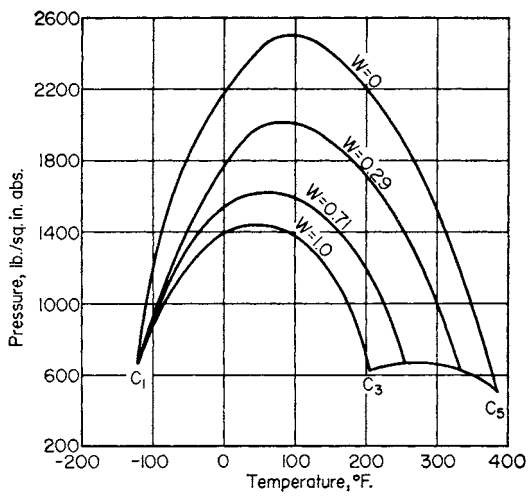

FIG. 13-11 Critical loci for a methane-propane-pentane system according to Hadden [Chem. Eng. Prog. Symp. Sec. 7, **49,** *53 (1953)*]. Parameter W is weight fraction propane on a methane-free basis.

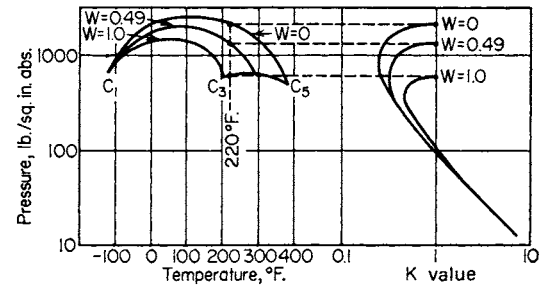

FIG. 13-12 Effect of mixture composition on K value for n-pentane at 104°C (220°F). The K values are shown for various values of W, weight fraction propane on a methane-free basis for the methane-propane-pentane system. [*Hadden*, Chem. Eng. Prog. Symp. Sec. 7, **49,** *58 (1953).*]

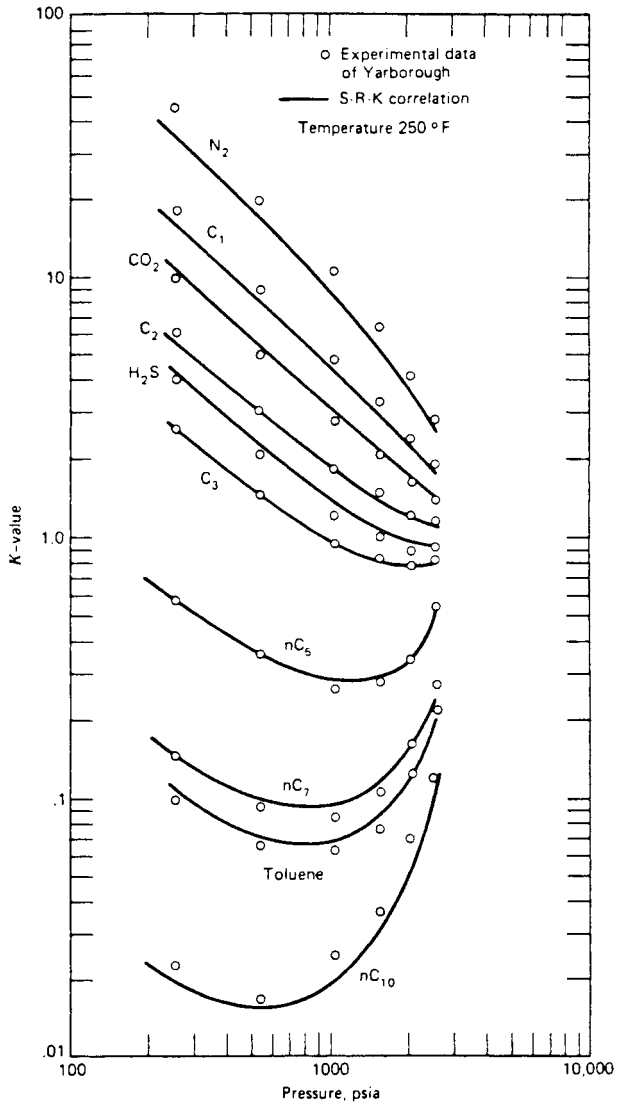

FIG. 13-13 Comparison of experimental K value data and SRK correlation. [*Henley and Seader*, Equilibrium-Stage Separation Operations in Chemical Engineering, *Wiley, New York, 1981; data of Yarborough,* J. Chem. Eng. Data, **17,** *129 (1972).*]

TABLE 13-2 Binary-Interaction Parameters*

System	Margules		van Laar		Wilson (cal/mol)	
	$\overline{A}_{12}$	$\overline{A}_{21}$	A_{12}	A_{21}	$(\lambda_{12}-\lambda_{11})$	$(\lambda_{21}-\lambda_{22})$
Acetone (1), chloroform (2)	–0.8404	–0.5610	–0.8643	–0.5899	116.1171	–506.8519
Acetone (1), methanol (2)	0.6184	0.5788	0.6184	0.5797	–114.4047	545.2942
Acetone (1), water (2)	2.0400	1.5461	2.1041	1.5555	344.3346	1482.2133
Carbon tetrachloride (1), benzene (2)	0.0948	0.0922	0.0951	0.0911	7.0459	59.6233
Chloroform (1), methanol (2)	0.8320	1.7365	0.9356	1.8860	–361.7944	1694.0241
Ethanol (1), benzene (2)	1.8362	1.4717	1.8570	1.4785	1264.4318	266.6118
Ethanol (1), water (2)	1.6022	0.7947	1.6798	0.9227	325.0757	953.2792
Ethyl acetate (1) ethanol (2)	0.8557	0.7476	0.8552	0.7526	58.8869	570.0439
n-Hexane (1), ethanol (2)	1.9398	2.7054	1.9195	2.8463	320.3611	2189.2896
Methanol (1), benzene (2)	2.1411	1.7905	2.1623	1.7925	1666.4410	227.2126
Methanol (1), ethyl acetate (2)	1.0016	1.0517	1.0017	1.0524	982.2689	–172.9317
Methanol (1), water (2)	0.7923	0.5434	0.8041	0.5619	82.9876	520.6458
Methyl acetate (1), methanol (2)	0.9605	1.0120	0.9614	1.0126	–93.8900	847.4348
1-Propanol (1), water (2)	2.7070	0.7172	2.9095	1.1572	906.5256	1396.6398
2-Propanol (1), water (2)	2.3319	0.8976	2.4702	1.0938	659.5473	1230.2080
Tetrahydrofuran (1), water (2)	2.8258	1.9450	3.0216	1.9436	1475.2583	1844.7926
Water (1), acetic acid (2)	0.4178	0.9533	0.4973	1.0623	705.5876	111.6579
Water (1), 1-butanol (2)	0.8608	3.2051	1.0996	4.1760	1549.6600	2050.2569
Water (1), formic acid (2)	–0.2966	–0.2715	–0.2935	–0.2757	–310.1060	1180.8040

*Abstracted from Gmehling and Onken, *Vapor-Liquid Equilibrium Data Collection,* DECHEMA Chemistry Data ser., vol. 1 (parts1–10). Frankfurt, 1977.

and T is in kelvins. Values of A and B for the first four normal aliphatic acids are

	A	B
Formic acid	–10.743	3083
Acetic acid	–10.421	3166
n-Propionic acid	–10.843	3316
n-Butyric acid	–10.100	3040

As shown by Marek and Standart [*Collect. Czech. Chem. Commun.,* **19,** 1074 (1954)], it is preferable to correlate and use liquid-phase activity coefficients for the dimerizing component by considering separately the partial pressures of the monomer and dimer. For example, for a binary system of components 1 and 2, when only compound 1 dimerizes in the vapor phase, the following equations apply if an ideal gas is assumed:

$$P_1 = P_D + P_M \tag{13-6}$$

$$y_1 = \frac{P_M + 2P_D}{P} \tag{13-7}$$

These equations when combined with Eq. (13-5) lead to the following equations for liquid-phase activity coefficients in terms of measurable quantities:

$$\gamma_1 = \frac{Py_1}{P_1^{\text{sat}}x_1}\left\{\frac{1+(1+4K_DP_1^{\text{sat}})^{0.5}}{1+[1+4K_DPy_1(2-y_1)]^{0.5}}\right\} \tag{13-8}$$

$$\gamma_2 = \frac{Py_1}{P_2^{\text{sat}}x_2}\left(\frac{2(1-y_1+[1+4K_DPy_1(2-y_1)]^{0.5}}{(2-y_1)\{1+[1+4K_DPy_1(2-y_1)]^{0.5}\}}\right) \tag{13-9}$$

Detailed procedures, including computer programs for evaluating binary-interaction parameters from experimental data and then using these parameters to predict K values and phase equilibria, are given in terms of the UNIQUAC equation by Prausnitz et al. (*Computer Calculations for Multicomponent Vapor-Liquid and Liquid-Liquid Equilibria,* Prentice-Hall, Englewood Cliffs, N.J., 1980) and in terms of the UNIFAC group contribution method by Fredenslund, Gmehling, and Rasmussen (*Vapor-Liquid Equilibria Using UNIFAC,* Elsevier, Amsterdam, 1980). Both use the method of Hayden and O'Connell [*Ind. Eng. Chem. Process Des. Dev.,* **14,** 209 (1975)] to compute $\hat{\Phi}_i^V$ in Eq. (13-4). When the system temperature is greater than the critical

TABLE 13-3 Activity-Coefficient Equations in Binary Form for Use with Parameters and Constants in Tables 13-2 and 13-4

Type of equation	Adjustable parameters	Equations in binary form
Margules	$\overline{A}_{12}$	$\ln\gamma_1 = [\overline{A}_{12} + 2(\overline{A}_{21}-\overline{A}_{12})x_1]x_2^2$
	$\overline{A}_{21}$	$\ln\gamma_2 = [\overline{A}_{21} + 2(\overline{A}_{12}-\overline{A}_{21})x_2]x_1^2$
van Laar	A_{12}	$\ln\gamma_1 = A_{12}\left(\frac{A_{21}x_2}{A_{12}x_1+A_{21}x_2}\right)^2$
	A_{21}	$\ln\gamma_2 = A_{21}\left(\frac{A_{12}x_1}{A_{12}x_1+A_{21}x_2}\right)^2$
Wilson	$\lambda_{12}-\lambda_{11}$	$\ln\gamma_1 = -\ln(x_1+\Lambda_{12}x_2) + x_2\left(\frac{\Lambda_{12}}{x_1+\Lambda_{12}x_2} - \frac{\Lambda_{21}}{\Lambda_{21}x_1+x_2}\right)$
	$\lambda_{21}-\lambda_{22}$	$\ln\gamma_2 = -\ln(x_2+\Lambda_{21}x_1) - x_1\left(\frac{\Lambda_{12}}{x_1+\Lambda_{12}x_2} - \frac{\Lambda_{21}}{\Lambda_{21}x_1+x_2}\right)$

where $\Lambda_{12} = \frac{v_2^L}{v_1^L}\exp\left(-\frac{\lambda_{12}-\lambda_{11}}{RT}\right)$ $\Lambda_{21} = \frac{v_1^L}{v_2^L}\exp\left(-\frac{\lambda_{21}-\lambda_{22}}{RT}\right)$

v_i^L = molar volume of pure-liquid component i
λ_{ij} = interaction energy between components i and j, $\lambda_{ij} = \lambda_{ji}$

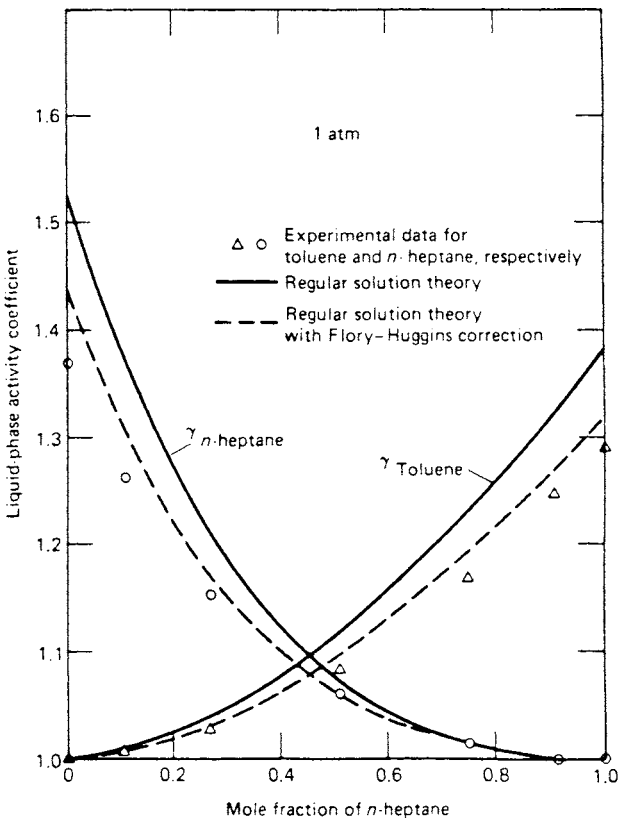

FIG. 13-14 Liquid-phase activity coefficients for an *n*-heptane–toluene system at 101.3 kPa (1 atm). [*Henley and Seader,* Equilibrium-Stage Separation Operations in Chemical Engineering, *Wiley, New York, 1981; data of Yerazunis et al.,* AIChE J., ***10,*** *660 (1964).*]

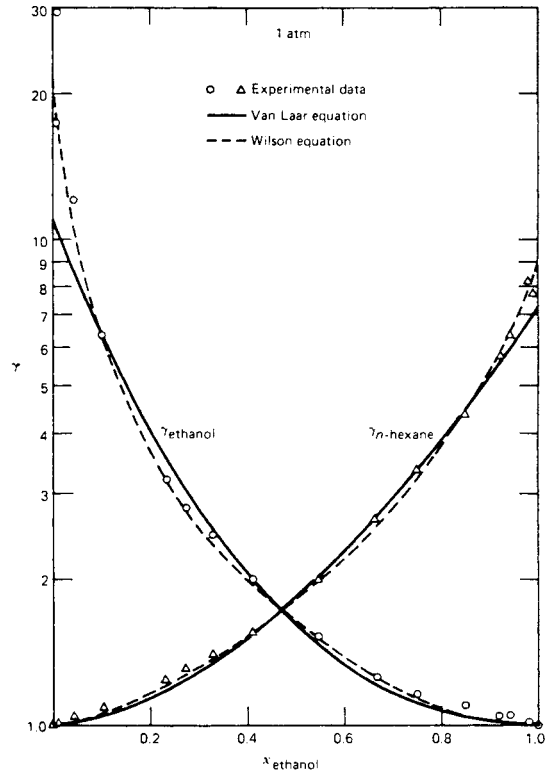

FIG. 13-15 Liquid-phase activity coefficients for an ethanol–*n*-hexane system. [*Henley and Seader,* Equilibrium-Stage Separation Operations in Chemical Engineering, *Wiley, New York, 1981; data of Sinor and Weber,* J. Chem. Eng. Data, **5,** *243–247 (1960).*]

TABLE 13-4 Antoine Vapor-Pressure Constants and Liquid Molar Volume*

Species	Antoine constants† A	B	C	Applicable temperature region, °C	v^L, liquid molar volume, cm³/g-mol
Acetic acid	8.02100	1936.010	258.451	18–118	57.54
Acetone	7.11714	1210.595	229.664	(–13)–55	74.05
Benzene	6.87987	1196.760	219.161	8–80	89.41
1-Butanol	7.36366	1305.198	173.427	89–126	91.97
Carbon tetrachloride	6.84083	1177.910	220.576	(–20)–77	97.09
Chloroform	6.95465	1170.966	226.232	(–10)–60	80.67
Ethanol	7.58670	1281.590	193.768	78–203	58.68
Ethanol	8.11220	1592.864	226.184	20–93	58.68
Ethyl acetate	7.10179	1244.951	217.881	16–76	98.49
Formic acid	6.94459	1295.260	218.000	36–108	37.91
n-Hexane	6.91058	1189.640	226.280	(–30)–170	131.61
Methanol	8.08097	1582.271	239.726	15–84	40.73
Methyl acetate	7.06524	1157.630	219.726	2–56	79.84
1-Propanol	8.37895	1788.020	227.438	(–15)–98	75.14
2-Propanol	8.87829	2010.320	252.636	(–26)–83	76.92
Tetrahydrofuran	6.99515	1202.290	226.254	23–100	81.55
Water	8.07131	1730.630	233.426	1–100	18.07

*Abstracted from Gmehling and Onken, *Vapor-Liquid Equilibrium Data Collection,* DECHEMA Chemistry Data ser., vol. 1 (parts 1–10), Frankfurt, 1977.
†Antoine equation is $\log P^{sat} = A - B/(T + C)$ with P^{sat} in torr and T in °C.
NOTE: To convert degrees Celsius to degrees Fahrenheit, °F = 1.8°C + 32. To convert cubic centimeters per gram-mole to cubic feet per pound-mole, multiply by 0.016.

temperature of one or more components in the mixture, Prausnitz et al. use a Henry's law constant $H_{i,M}$ in place of the product $\gamma_i^L \Phi_i^L$ in Eq. (13-4). Otherwise Φ_i^L is evaluated from vapor pressure data with a Poynting saturated-vapor fugacity correction. When the total pressure is less than about 202.6 kPa (2 atm) and all components in the mixture have a critical temperature that is greater than the system temperature, then $\Phi_i^L = P_i^{sat}/P$ and $\Phi_i^V = 1.0$. Equation (13-4) then reduces to

$$K_i = \frac{\gamma_i^L P_i^{sat}}{P} \tag{13-10}$$

which is referred to as a modified Raoult's law K value. If, furthermore, the liquid phase is ideal, then $\gamma_i^L = 1.0$ and

$$K_i = \frac{P_i^{sat}}{P} \tag{13-11}$$

which is referred to as a Raoult's law K value that is dependent solely on the vapor pressure P_i^{sat} of the component in the mixture. The UNIFAC method is being periodically updated with new group contributions; e.g., see Hansen et al. [*Ind. Eng. Chem. Res.*, **30,** 2352 (1991)].

SINGLE-STAGE EQUILIBRIUM FLASH CALCULATIONS

The simplest continuous distillation process is the adiabatic single-stage equilibrium flash process pictured in Fig. 13-16. Feed temperature and the pressure drop across the valve are adjusted to vaporize the feed to the desired extent, while the drum provides disengaging space to allow the vapor to separate from the liquid. The expansion across the valve is at constant enthalpy, and this fact can be used to calculate T_2 (or T_1 to give a desired T_2).

A degrees-of-freedom analysis indicates that the variables subject to the designer's control are $C + 3$ in number. The most common way to use these is to specify the feed rate, composition, and pressure ($C + 1$ variables) plus the drum temperature T_2 and pressure P_2. This operation will give one point on the *equilibrium flash curve* shown in Fig. 13-17. This curve shows the relation at constant pressure between the fraction V/F of the feed flashed and the drum temperature. The temperature at $V/F = 0.0$ when the first bubble of vapor is about to form (saturated liquid) is the *bubble point* temperature of the feed mixture, and the value at $V/F = 1.0$ when the first droplet of liquid is about to form (saturated vapor) is the *dew point* temperature.

BUBBLE POINT AND DEW POINT

For a given drum pressure and feed composition, the bubble and dew point temperatures bracket the temperature range of the equilibrium flash. At the bubble point temperature, the total vapor pressure exerted by the mixture becomes equal to the confining drum pressure, and it follows that $\sum y_i = 1.0$ in the bubble formed. Since $y_i = K_i x_i$ and since the x_i's still equal the feed compositions (denoted by z_i), calculation of the bubble point temperature involves a trial-and-error search for the temperature which, at the specified pressure, makes $\sum K_i z_i = 1.0$. If instead the temperature is specified, one can find the bubble point pressure that satisfies this relationship.

At the dew point temperature y_i still equals z_i and the relationship $\sum x_i = \sum z_i/K_i = 1.0$ must be satisfied. As in the case of the bubble point, a trial-and-error search for the dew point temperature at a specified pressure is involved. Or, if the temperature is specified, the dew point pressure can be calculated.

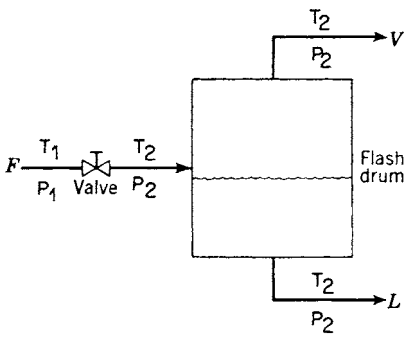

FIG. 13-16 Equilibrium flash separator.

ISOTHERMAL FLASH

The calculation for a point on the flash curve that is intermediate between the bubble point and the dew point is referred to as an isothermal flash calculation because T_2 is specified. Except for an ideal binary mixture, procedures for calculating an isothermal flash are iterative. A popular and recommended method is the following, due to Rachford and Rice [*J. Pet. Technol.*, **4**(10), sec. 1, p. 19, and sec. 2, p. 3 (October 1952)]. The component mole balance ($Fz_i = Vy_i + Lx_i$), phase distribution relation ($K_i = y_i/x_i$), and total mole balance ($F = V + L$) can be combined to give

$$x_i = \frac{z_i}{1 + (V/F)(K_i - 1)} \tag{13-12}$$

$$y_i = \frac{K_i z_i}{1 + (V/F)(K_i - 1)} \tag{13-13}$$

Since $\sum x_i - \sum y_i = 0$,

$$f\left(\frac{V}{F}\right) = \sum_i \frac{z_i(1 - K_i)}{1 + (V/F)(K_i - 1)} = 0 \tag{13-14}$$

Equation (13-14) is solved iteratively for V/F, followed by the calculation of values of x_i and y_i from Eqs. (13-12) and (13-13) and L from the total mole balance. Any one of a number of numerical root-finding procedures such as the Newton-Raphson, secant, false-position, or bisection method can be used to solve Eq. (13-14). Values of K_i are constants if they are independent of liquid and vapor compositions. Then the resulting calculations are straightforward. Otherwise, the K_i values must be periodically updated for composition effects, perhaps

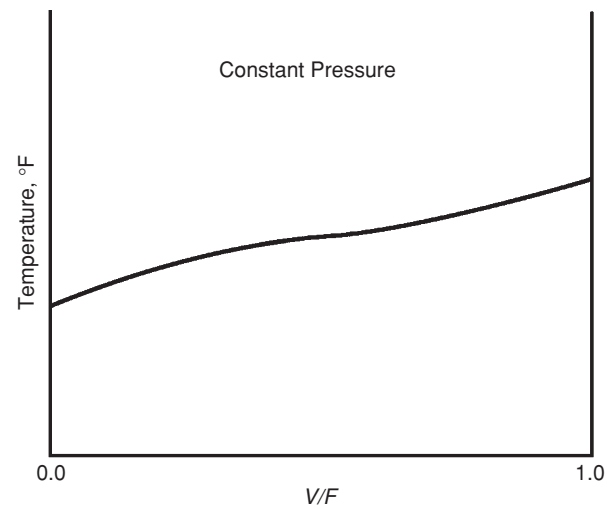

FIG. 13-17 Equilibrium flash curve.

after each iteration, using prorated values of x_i and y_i from Eqs. (13-12) and (13-13). Generally the iterations are continued until the change in the absolute value of V/F is sufficiently small and until the absolute value of the residual $f(V/F)$ is close to zero. When converged, $\sum x_i$ and $\sum y_i$ will each be very close to a value of 1, and, if desired, T_1 can be computed from an energy balance around the valve if no heat exchanger is used. Alternatively, if T_1 is fixed, as mentioned earlier, a heat exchanger must be added before, after, or in place of the valve with the required heat duty being calculated from an energy balance. The limits of applicability of Eqs. (13-12) to (13-14) are the bubble point, at which $V = 0$ and $x_i = z_i$, and the dew point, at which $L = 0$ and $y_i = z_i$. At these limits Eq. (13-14) reduces to the bubble point equation

$$\sum_i K_i x_i = 1 \tag{13-15}$$

and the dew point equation, respectively,

$$\sum_i \frac{y_i}{K_i} = 1 \tag{13-16}$$

For a *binary feed,* specification of the flash drum temperature and pressure fixes the equilibrium-phase compositions, which are related to the K values by

$$x_1 = \frac{1 - K_2}{K_1 - K_2} \quad \text{and} \quad y_1 = \frac{K_1 K_2 - K_1}{K_2 - K_1}$$

The mole balance can be rearranged to

$$\frac{V}{F} = \frac{z_1(K_1 - K_2)/(1 - K_2) - 1}{K_1 - 1}$$

If K_1 and K_2 are functions of temperature and pressure only (ideal solutions), the flash curve can be calculated directly without iteration.

ADIABATIC FLASH

In Fig. 13-16, if P_2 and the feed-stream conditions (that is, F, z_i, T_1, P_1) are known, then the calculation of T_2, V, L, y_i, and x_i is referred to as an adiabatic flash. In addition to Eqs. (13-12) to (13-14) and the total mole balance, the following energy balance around both the valve and the flash drum combined must be included:

$$H^F F = H^V V + H^L L \tag{13-17}$$

By taking a basis of $F = 1.0$ mol and eliminating L with the total mole balance, Eq. (13-17) becomes

$$f_2\{V, T_2\} = H^F - V(H^V - H^L) - H^L = 0 \tag{13-18}$$

With T_2 now unknown, Eq. (13-14) becomes

$$f_1\{V, T_2\} = \sum_i \frac{z_i(1 - K_i)}{1 + V(K_i - 1)} = 0 \tag{13-19}$$

A number of iterative procedures have been developed for solving Eqs. (13-18) and (13-19) simultaneously for V and T_2. Frequently, and especially if the feed contains components of a narrow range of volatility, convergence is rapid for a tearing method in which a value of T_2 is assumed, Eq. (13-19) is solved iteratively by the isothermal flash procedure, and, using that value of V, Eq. (13-18) is solved iteratively for a new approximation of T_2, which is then used to initiate the next cycle until T_2 and V converge. However, if the feed contains components of a wide range of volatility, it may be best to invert the sequence and assume a value for V, solve Eq. (13-19) for T_2, solve Eq. (13-18) for V, and then repeat the cycle. If the K values and/or enthalpies are sensitive to the unknown phase compositions, it may be necessary to solve Eqs. (13-18) and (13-19) simultaneously by a Newton or other suitable iterative technique. Alternatively, the two-tier method of Boston and Britt [*Comput. Chem. Eng.,* **2,** 109 (1978)], which is also suitable for difficult isothermal flash calculations, may be applied.

OTHER FLASH SPECIFICATIONS

Flash drum specifications in addition to (P_2, T_2) and (P_2, adiabatic) are possible but must be applied with care, as discussed by Michelsen [*Comp. Chem. Engng.,* **17,** 431 (1993)]. Most computer-aided process design and simulation programs permit a wide variety of flash specifications.

THREE-PHASE FLASH

Single-stage equilibrium flash calculations become considerably more complex when an additional liquid phase can form, as in mixtures of water with hydrocarbons, water with ethers, and water with higher alcohols (containing four or more carbon atoms). Procedures for computing such situations are referred to as three-phase flash methods, which are given for the general case by Henley and Rosen (*Material and Energy Balance Computations,* Wiley, New York, 1968, chap. 8). When the two liquid phases are almost mutually insoluble, they can be considered separately and relatively simple procedures apply, as discussed by Smith (*Design of Equilibrium Stage Processes,* McGraw-Hill, New York, 1963). Condensation of such mixtures may result in one liquid phase being formed before the other. Computer-aided process design and simulation programs all contain a Gibbs free-energy routine that can compute a three-phase flash by minimization of the Gibbs free energy. Many important and subtle aspects of three-phase flash calculations are discussed by Michelsen [*Fluid Phase Equil.,* **9,** 1, 21 (1982)], McDonald and Floudas [*AIChE J.*, **41,** 1798 (1995)], and Wasylkiewicz et al. [*Ind. Eng. Chem. Research*, **35,** 1395 (1996)].

COMPLEX MIXTURES

Feed analyses in terms of component compositions are usually not available for complex hydrocarbon mixtures with a final normal boiling point above about 38°C (100°F) (*n*-pentane). One method of handling such a feed is to break it down into pseudocomponents (narrow-boiling fractions) and then estimate the mole fraction and K value for each such component. Edmister [*Ind. Eng. Chem.,* **47,** 1685 (1955)] and Maxwell (*Data Book on Hydrocarbons,* Van Nostrand, Princeton, N.J., 1958) give charts that are useful for this estimation. Once K values are available, the calculation proceeds as described above for multicomponent mixtures. Another approach to complex mixtures is to obtain an American Society for Testing and Materials (ASTM) or true-boiling point (TBP) curve for the mixture and then use empirical correlations to construct the atmospheric-pressure equilibrium flash vaporization (EFV) curve, which can then be corrected to the desired operating pressure. A discussion of this method and the necessary charts is presented in a later subsection Petroleum and Complex-Mixture Distillation.

GRAPHICAL METHODS FOR BINARY DISTILLATION

Multistage distillation under continuous, steady-state operating conditions is widely used in practice to separate a variety of mixtures. Table 13-5, taken from the study of Mix, Dweck, Weinberg, and Armstrong [*AIChE Symp. Ser.* **76,** 192, 10 (1980)] lists key components along with typical stage requirements to perform the separation for 27 industrial distillation processes. The design of multistage columns can be accomplished by graphical techniques when the feed mixture contains only two components. The *x-y* diagram method developed by McCabe and Thiele [*Ind. Eng. Chem.,* **17,** 605 (1925)] uses only phase equilibrium and mole balance relationships. The method assumes an adiabatic column (no heat losses through the column walls) and constant latent heat for the binary mixture at all compositions (which requires, among other things, equal latent heat for both components). The method is exact only for those systems in which energy effects on vapor and liquid rates leaving the stages are negligible. However, the approach is simple and gives a useful first estimate of the column design which can be refined by using the enthalpy composition diagram method of Ponchon [*Tech. Mod.,* **13,**

TABLE 13-5 Key Components and Typical Number of (Real) Stages Required to Perform the Separation for Distillation Processes of Industrial Importance

Key components	Typical number of trays
Hydrocarbon systems	
Ethylene-ethane	73
Propylene-propane	138
Propyne–1–3-butadiene	40
1–3 Butadiene-vinyl acetylene	130
Benzene-toluene	34, 53
Benzene-ethyl benzene	20
Benzene–diethyl benzene	50
Toluene–ethyl benzene	28
Toluene-xylenes	45
Ethyl benzene–styrene	34
o-Xylene-*m*-xylene	130
Organic systems	
Methonol-formaldehyde	23
Dichloroethane-trichloroethane	30
Acetic acid–acetic anhydride	50
Acetic anhydride–ethylene diacetate	32
Vinyl acetate–ethyl acetate	90
Ethylene glycol–diethylene glycol	16
Cumene-phenol	38
Phenol-acetophenone	39, 54
Aqueous systems	
HCN-water	15
Acetic acid–water	40
Methanol-water	60
Ethanol-water	60
Isopropanol-water	12
Vinyl acetate–water	35
Ethylene oxide–water	50
Ethylene glycol–water	16

20, 55 (1921)] and Savarit [*Arts Metiers,* **65,** 142, 178, 241, 266, 307 (1922)]. This approach uses the energy balance in addition to mole balance and phase equilibrium relationships and is rigorous when enough calorimetric data are available to construct the diagram without assumptions.

With the widespread availability of computers, the preferred approach to design is equation-based since it provides answers rapidly and repeatedly without the tedium of redrawing graphs. Such an approach is especially useful for sensitivity analysis, which gives insight into how a design changes under variations or uncertainty in design parameters such as thermodynamic properties; feed flow rate, composition, temperature, and pressure; and desired product compositions. Nevertheless, diagrams are useful for quick approximations, for interpreting the results of equation-based methods, and for demonstrating the effect of various design variables. The *x-y* diagram is the most convenient for these purposes, and its use is developed in detail here. The use of the enthalpy composition diagram is given by Smith (*Design of Equilibrium Stage Processes,* McGraw-Hill, New York, 1963) and Henley and Seader (*Equilibrium-Stage Separation Operations in Chemical Engineering,* Wiley, New York, 1981). An approximate equation-based approach based on the enthalpy composition diagram was proposed by Peters [*Ind. Eng. Chem.,* **14,** 476 (1922)] with additional aspects developed later by others. Doherty and Malone (*Conceptual Design of Distillation Systems*, McGraw-Hill, 2001, app. A) describe this method for binary mixtures and extend it to multicomponent systems. The approach is exact when the enthalpy composition surfaces are linear.

PHASE EQUILIBRIUM DIAGRAMS

Three types of binary phase equilibrium curves are shown in Fig. 13-18. The *y-x* diagram is almost always plotted for the component that is the more volatile (denoted by the subscript 1) in the region where distillation is to take place. Curve *A* shows the common case in which component 1 remains more volatile over the entire composition range. Curve *B* is typical of many systems (e.g., ethanol-water) in which the

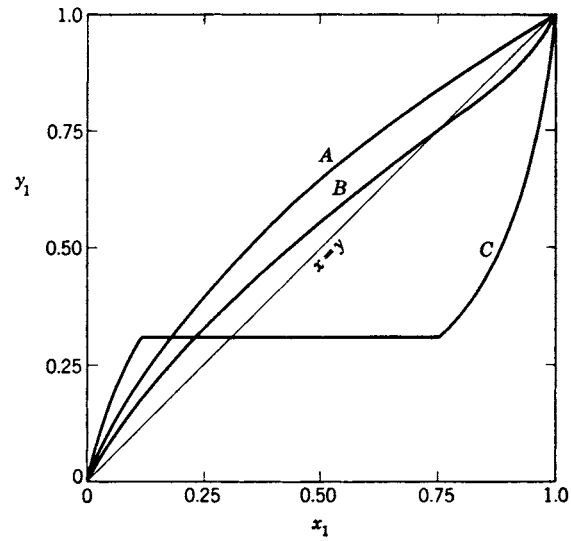

FIG. 13-18 Typical binary equilibrium curves. Curve *A,* system with normal volatility. Curve *B,* system with homogeneous azeotrope (one liquid phase). Curve *C,* system with heterogeneous azeotrope (two liquid phases in equilibrium with one vapor phase).

component that is more volatile at low values of x_1 becomes less volatile than the other component at high values of x_1. The vapor and liquid compositions are identical for the homogeneous azeotrope where curve *B* crosses the 45° diagonal (that is, $x_1 = y_1$). A heterogeneous azeotrope is formed by curve *C,* in which there are two equilibrium liquid phases and one equilibrium vapor phase.

An azeotrope limits the separation that can be obtained between components by simple distillation. For the system described by curve *B,* the maximum overhead-product concentration that could be obtained from a feed with $z_1 = 0.25$ is the azeotropic composition. Similarly, a feed with $x_1 = 0.9$ could produce a bottom-product composition no lower than the azeotrope.

The phase rule permits only two variables to be specified arbitrarily in a binary two-phase mixture at equilibrium. Consequently, the curves in Fig. 13-18 can be plotted at either constant temperature or constant pressure but not both. The latter is more common, and data in Table 13-1 correspond to that case. The *y-x* diagram can be plotted in mole, weight, or volume fractions. The units used later for the phase flow rates must, of course, agree with those used for the equilibrium data. Mole fractions, which are almost always used, are applied here.

It is sometimes permissible to assume constant *relative volatility* to approximate the equilibrium curve quickly. Then by applying Eq. (13-2) to components 1 and 2,

$$\alpha = \frac{K_1}{K_2} = \frac{y_1 x_2}{x_1 y_2}$$

which can be rewritten as (using $x_2 = 1 - x_1$ and $y_2 = 1 - y_1$)

$$y_1 = \frac{x_1 \alpha}{1 + (\alpha - 1) x_1} \tag{13-20}$$

With a constant value for α this equation provides a simple, approximate expression for representing the equilibrium $y = x$ diagram. Doherty and Malone (*Conceptual Design of Distillation Systems,* McGraw-Hill, 2001, sec. 2.3) discuss this approximation in greater detail and give a selection of binary mixtures for which the approximation is reasonable. At a constant pressure of 1 atm these include benzene + toluene, $\alpha = 2.34$; benzene + *p*-xylene, $\alpha = 4.82$; and hexane + *p*-xylene, $\alpha = 7.00$.

McCABE-THIELE METHOD

Operating Lines The McCabe-Thiele method is based upon representation of the material balance equations as operating lines on the *y-x* diagram. The lines are made straight by the assumption of *constant molar overflow*, which eliminates the need for an energy balance. The liquid-phase flow rate is assumed to be constant from tray to tray in each section of the column between addition (feed) and withdrawal (product) points. If the liquid rate is constant, the vapor rate must also be constant.

The constant-molar-overflow assumption rests on several underlying thermodynamic assumptions. The most important one is equal molar heats of vaporization for the two components. The other assumptions are adiabatic operation (no heat leaks) and no heat of mixing or sensible heat effects. These assumptions are most closely approximated for close-boiling isomers. The result of these assumptions on the calculation method can be illustrated with Fig. 13-19, which shows two material balance envelopes cutting through the top section (above the top feed stream or sidestream) of the column. If the liquid flow rate L_{n+1} is assumed to be identical to L_{n-1}, then $V_n = V_{n-2}$ and the component material balance for both envelopes 1 and 2 can be represented by

$$y_n = \left(\frac{L}{V}\right)x_{n+1} + \frac{Dx_D}{V} \tag{13-21}$$

where y and x have a stage subscript n or $n+1$, but L and V need be identified only with the section of the column to which they apply. Equation (13-21) has the analytical form of a straight line where L/V is the slope and Dx_D/V is the y intercept at $x = 0$.

The effect of a sidestream withdrawal point is illustrated by Fig. 13-20. The material balance equation for the column section below the sidestream is

$$y_n = \frac{L'}{V'}x_{n+1} + \frac{Dx_D + Sx_S}{V'} \tag{13-22}$$

where the primes designate the L and V below the sidestream. Since the sidestream must be a saturated phase, $V = V'$ if a liquid sidestream is withdrawn and $L = L'$ if it is a vapor.

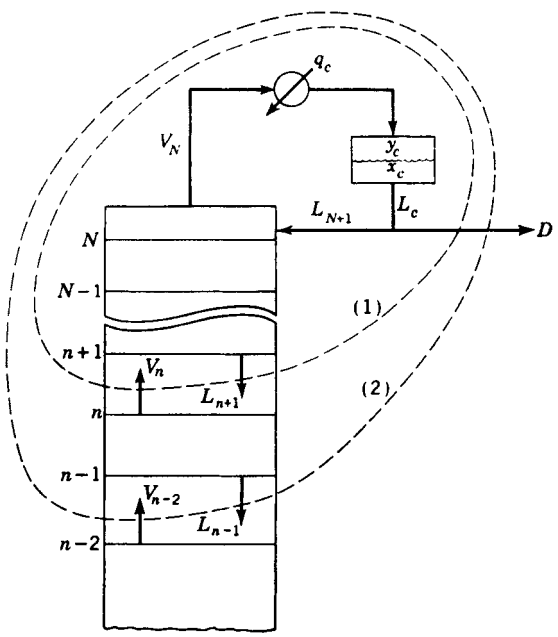

FIG. 13-19 Two material balance envelopes in the top section of a distillation column.

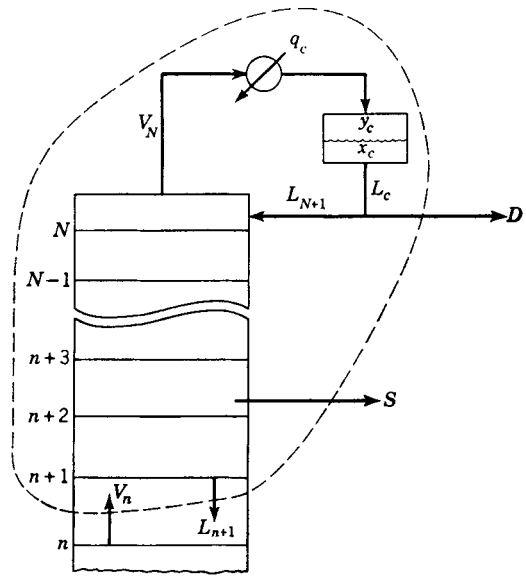

FIG. 13-20 Material balance envelope which contains two external streams D and S, where S represents a sidestream product withdrawn above the feed plate.

If the sidestream in Fig. 13-20 is a feed (not necessarily a saturated liquid or vapor), the balance for the section below the feed becomes

$$y_n = \frac{L'}{V'}x_{n+1} + \frac{Dx_D - Fz_F}{V'} \tag{13-23}$$

Similar equations can be written for the bottom section of the column. For the envelope shown in Fig. 13-21,

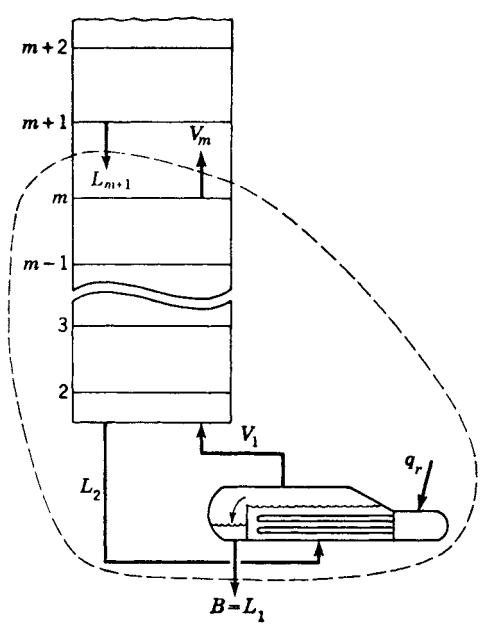

FIG. 13-21 Material balance envelope around the bottom end of the column. The partial reboiler is equilibrium stage 1.

$$y_m = \frac{L'}{V'} x_{m+1} - \frac{Bx_B}{V'} \tag{13-24}$$

where the subscript m is used to identify the stage number in the bottom section.

Equations such as (13-21) through (13-24), when plotted on the y-x diagram, furnish a set of *operating lines.* A point on an operating line represents two *passing streams,* and the operating line itself is the locus of all possible pairs of passing streams within the column section to which the line applies.

An operating line can be located on the y-x diagram if (1) two points on the line are known or (2) one point and the slope are known. The known points on an operating line are usually its intersection with the y-x diagonal and/or its intersection with another operating line.

The slope L/V of the operating line is termed the *internal reflux ratio.* This ratio in the operating line equation for the top section of the column [see Eq. (13-21)] is related to the *external reflux ratio* $R = L_{N+1}/D$ by

$$\frac{L}{V} = \frac{L_{N+1}}{V_N} = \frac{RD}{(1+R)D} = \frac{R}{1+R} \tag{13-25}$$

when the reflux stream L_{N+1} is a saturated liquid.

Thermal Condition of the Feed The slope of the operating line changes whenever a feed stream or a sidestream is passed. To calculate this change, it is convenient to introduce a quantity q which is defined by the following equations for a feed stream F:

$$L' = L + qF \tag{13-26}$$

$$V = V' + (1-q)F \tag{13-27}$$

The primes denote the streams below the stage to which the feed is introduced. The value of q is a measure of the thermal condition of the feed and represents the moles of saturated liquid formed in the feed stage per mole of feed. The value of q for a particular feed can be estimated from

$$q = \frac{\text{energy to convert 1 mol of feed to saturated vapor}}{\text{molar heat of vaporization}}$$

It takes on the following values for various thermal conditions of the feed:

Subcooled liquid feed:	$q > 1$
Saturated liquid feed:	$q = 1$
Partially flashed feed:	$0 < q < 1$
Saturated vapor feed:	$q = 0$
Superheated vapor feed:	$q < 0$

Equations analogous to (13-26) and (13-27) can be written for a sidestream, but the value of q will be either 1 or 0 depending upon whether the sidestream is taken from the liquid or the vapor stream.

The quantity q can be used to derive the "q line equation" for a feed stream or a sidestream. The q line is the locus of all points of intersection of the two operating lines, which meet at the feed stream or sidestream stage. This intersection must occur along that section of the q line between the equilibrium curve and the $y = x$ diagonal. At the point of intersection, the same y, x point must satisfy both the operating line equation above the feed stream (or sidestream) stage and the one below the feed stream (or sidestream) stage. Subtracting one equation from the other gives for a feed stage

$$(V - V')y = (L - L')x + Fz_F$$

which, when combined with Eqs. (13-26) and (13-27), gives the q line equation

$$y = \frac{q}{q-1} x - \frac{z_F}{q-1} \tag{13-28}$$

A q line construction for a partially flashed feed is given in Fig. 13-22. It is easily shown that the q line must intersect the diagonal at z_F.

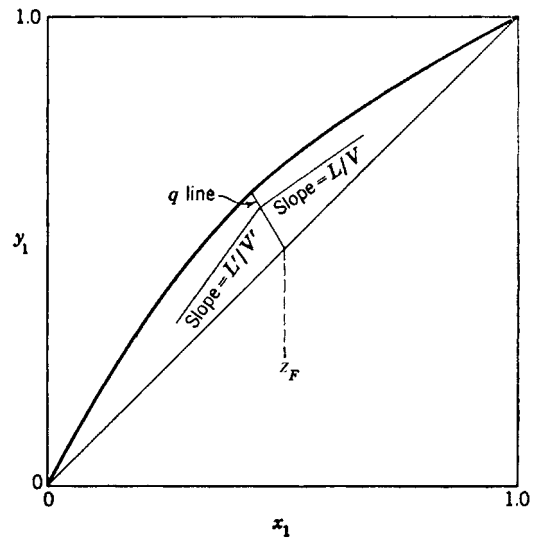

FIG. 13-22 Typical intersection of the two operating lines at the q line for a feed stage. The q line shown is for a partially flashed feed.

The slope of the q line is $q/(q-1)$. All five q line cases are shown in Fig. 13-23. Note that when $q = 1$, the q line has infinite slope and is vertical.

The derivation of Eq. (13-28) assumes a single-feed column and no sidestream. However, the same result is obtained for other column configurations. Typical q line constructions for sidestream stages are shown in Fig. 13-24. Note that the q line for a sidestream must always intersect the diagonal at the composition (y_S or x_S) of the sidestream. Figure 13-24 also shows the intersections of the operating lines with the diagonal construction line. The top operating line must always intersect the diagonal at the overhead-product composition x_D. This can be shown by substituting $y = x$ in Eq. (13-21) and using $V - L = D$ to reduce the resulting equation to $x = x_D$. Similarly (except for columns in which open steam is introduced at the bottom), the bottom operating line must always intersect the diagonal at the bottom-product composition x_B.

Equilibrium-Stage Construction Use of the equilibrium curve and the operating lines to "step off" equilibrium stages is illustrated in Fig. 13-25. The plotted portions of the equilibrium curve (curved) and the operating line (straight) cover the composition range existing in the column section shown in the lower right-hand corner of the figure. If y_n and x_n represent the compositions (in terms of the more volatile

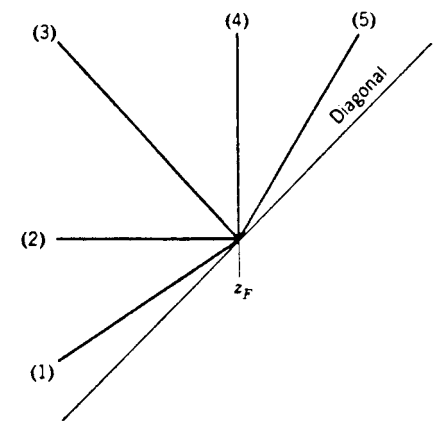

FIG. 13-23 All five cases of q lines: (1) superheated vapor feed, (2) saturated vapor feed, (3) partially vaporized feed, (4) saturated liquid feed, and (5) subcooled liquid feed. Slope of q line is $q/(q-1)$.

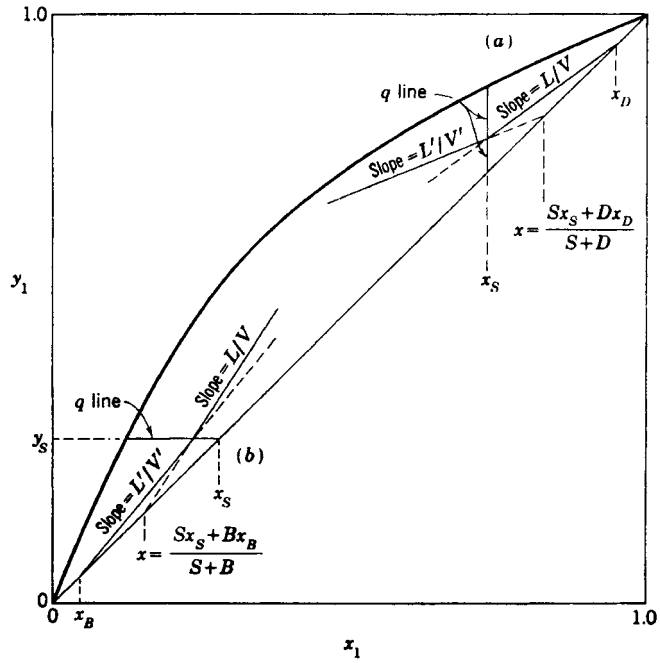

FIG. 13-24 Typical construction for a sidestream showing the intersection of the two operating lines with the q line and with the x-y diagonal. (*a*) Liquid sidestream near the top of the column. (*b*) Vapor sidestream near the bottom of the column.

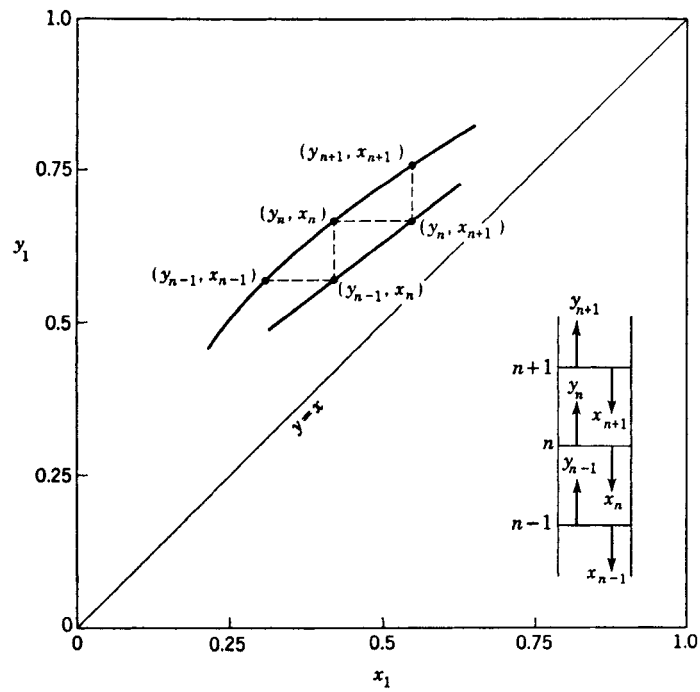

FIG. 13-25 Illustration of how equilibrium stages can be located on the x-y diagram through the alternating use of the equilibrium curve and the operating line.

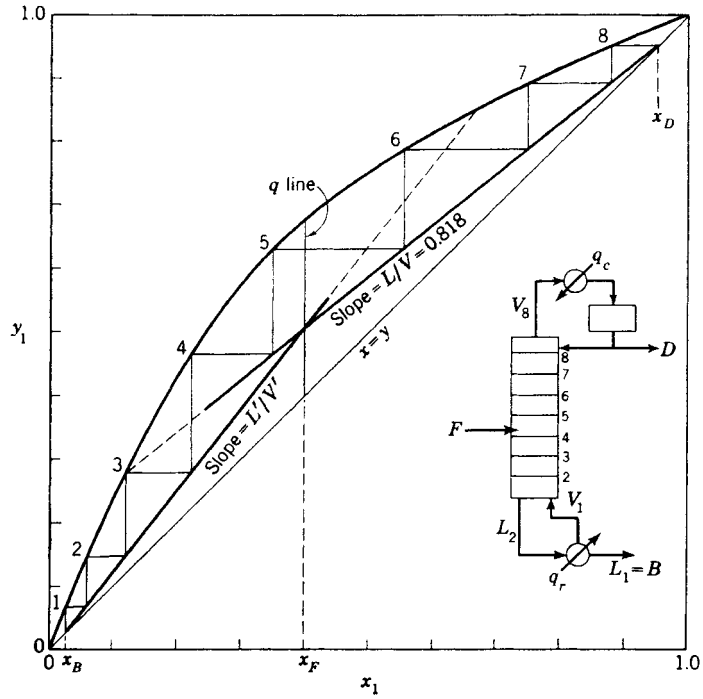

FIG. 13-26 Construction for a column with a bubble point feed, a total condenser, and a partial reboiler.

component) of the equilibrium vapor and liquid leaving stage n, then point (y_n, x_n) on the equilibrium curve must represent the equilibrium stage n. The operating line is the locus for compositions of all possible pairs of passing streams within the section, and therefore a horizontal line (dashed) at y_n must pass through the point (y_n, x_{n+1}) on the operating line since y_n and x_{n+1} represent passing streams. Likewise, a vertical line (dashed) at x_n must intersect the operating line at point (y_{n-1}, x_n). The equilibrium stages above and below stage n can be located by a vertical line through (y_n, x_{n+1}) to find (y_{n+1}, x_{n+1}) and a horizontal line through (y_{n-1}, x_n) to find (y_{n-1}, x_{n-1}). This procedure can be repeated by alternating the use of equilibrium and operating lines upward or downward through the column to find the total number of equilibrium stages.

Total Column Construction The graphical construction for an entire column is shown in Fig. 13-26. The process, pictured in the lower right-hand corner of the diagram, is an existing column with a number of actual trays equivalent to eight equilibrium stages. A partial reboiler (equivalent to an equilibrium stage) and a total condenser are used. This column configuration has $C + 2N + 9$ design variables (degrees of freedom) which must be specified to define one unique operation [see subsection Degrees of Freedom and Design Variables, especially Fig. 13-62 and Eq. (13-111)]. These may be used as follows as the basis for a graphical solution:

Specifications	Degrees of freedom
Stage pressures (including reboiler)	N
Condenser pressure	1
Stage heat leaks (except reboiler)	$N - 1$
Pressure and heat leak in reflux divider	2
Feed stream	$C + 2$
Feed-stage location	1
Total number of stages N	1
One overhead purity	1
Reflux temperature	1
Eternal reflux ratio	1
	$C + 2N + 9$

Pressures can be specified at any level below the safe working pressure of the column. The condenser pressure will be set at 275.8 kPa (40 psia), and all pressure drops within the column will be neglected. The equilibrium curve in Fig. 13-26 represents data at that pressure. All heat leaks will be assumed to be zero. The feed composition is 40 mol % of the more volatile component 1, and the feed rate is 0.126 kg·mol/s (1000 lb·mol/h) of saturated liquid ($q = 1$). The feed-stage location is fixed at stage 4 and the total number of stages at eight.

The overhead purity is specified as $x_D = 0.95$. The reflux temperature is the bubble point temperature (saturated reflux), and the external reflux ratio is set at $R = 4.5$.

Answers are desired to the following two questions. First, what bottom-product composition x_B will the column produce under these specifications? Second, what is the value of the top vapor rate V_N in this operation, and will it exceed the maximum vapor rate capacity for this column, which is assumed to be 0.252 kg·mol/s (2000 lb·mol/h) at the top-tray conditions?

The solution is started by using Eq. (13-25) to convert the external reflux ratio of 4.5 to an internal reflux ratio of $L/V = 0.818$. The distillate composition $x_D = 0.95$ is then located on the diagonal, and the upper operating line is drawn as shown in Fig. 13-26.

If the x_B value were known, the bottom operating line could be immediately drawn from the x_B value on the diagonal up to its required intersection point with the upper operating line on the feed q line. In this problem, since the number of stages is fixed, the value of x_B which gives a lower operating line that will require exactly eight stages must be found by trial and error. An x_B value is assumed, and the resulting lower operating line is drawn. The stages can be stepped off by starting from either x_B or x_D; x_B was used in this case.

Note that the lower operating line is used until the fourth stage is passed, at which time the construction switches to the upper operating line. This is necessary because the vapor and liquid streams passing each other between the fourth and fifth stages must fall on the upper line.

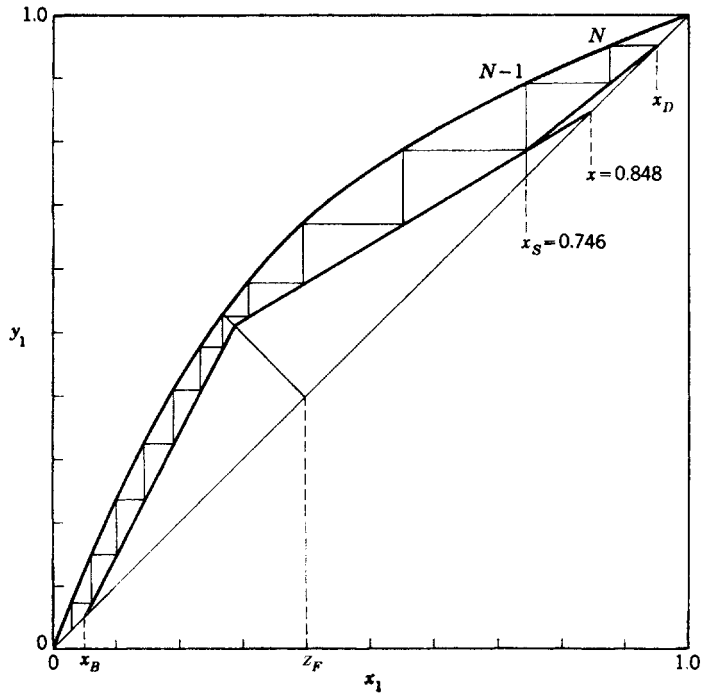

FIG. 13-27 Graphical solution for a column with a partially flashed feed, a liquid sidestream, and a total condenser.

The x_B that requires exactly eight equilibrium stages is $x_B = 0.026$. An overall component balance gives $D = 0.051$ kg·mol/s (405 lb·mol/h). Then

$$V_N = V_B = L_{N+1} + D = D(R + 1) = 0.051(4.5 + 1.0)$$

$$= 0.280 \text{ kg·mol/s (2230 lb·mol/h)}$$

which exceeds the column capacity of 0.252 kg·mol/s (2007 lb·mol/h). This means that the column cannot provide an overhead-product yield of 40.5 percent at 95 percent purity. Either the purity specification must be reduced, or we must be satisfied with a lower yield. If the distillate specification ($x_D = 0.95$) is retained, the reflux rate must be reduced. This will cause the upper operating line to pivot upward around its fixed point of $x_D = 0.95$ on the diagonal. The new intersection of the upper line with the q line will lie closer to the equilibrium curve. The x_B value must then move upward along the diagonal because the eight stages will not "reach" as far as before. The higher x_B composition will reduce the recovery of component 1 in the 95 percent overhead product.

Another entire column with a partially vaporized feed, a liquid sidestream rate equal to D withdrawn from the second stage from the top, and a total condenser is shown in Fig. 13-27. The specified compositions are $z_F = 0.40$, $x_B = 0.05$, and $x_D = 0.95$. The specified L/V ratio in the top section is 0.818. These specifications permit the top operating line to be located and the two top stages stepped off to determine the liquid sidestream composition $x_s = 0.746$. The operating line below the sidestream must intersect the diagonal at the "blend" of the sidestream and the overhead stream. Since S was specified to be equal to D in rate, the intersection point is

$$x = \frac{(1.0)(0.746) + (1.0)(0.95)}{1.0 + 1.0} = 0.848$$

This point plus the point of intersection of the two operating lines on the sidestream q line (vertical at $x_s = 0.746$) permits the location of the middle operating line. (The slope of the middle operating line could also have been used.) The lower operating line must run from the specified x_B value on the diagonal to the required point of intersection on the feed q line. The stages are stepped off from the top down in this case. The sixth stage from the top is the feed stage, and a total of about 11.4 stages are required to reach the specified $x_B = 0.05$.

Fractional equilibrium stages have meaning. The 11.4 will be divided by a tray efficiency, and the rounding up to an integral number of actual trays should be done after that division. For example, if the average tray efficiency for the process modeled in Fig. 13-27 is 80 percent, then the number of actual trays required is 11.4/0.8 = 14.3, which is rounded up to 15.

Feed-Stage Location The *optimum* feed-stage location is that location which, with a given set of other operating specifications, will result in the widest separation between x_D and x_B for a given number of stages. Or, if the number of stages is not specified, the optimum feed location is the one that requires the lowest number of stages to accomplish a specified separation between x_D and x_B. Either of these criteria will always be satisfied if the operating line farthest from the equilibrium curve is used in each step, as in Fig. 13-26.

It can be seen from Fig. 13-26 that the optimum feed location would have been the fifth tray for that operation. If a new column were being designed, that should be the designer's choice. However, when an existing column is being modeled, the feed stage on the diagram should correspond as closely as possible to the actual feed tray in the column. It can be seen that a badly mislocated feed (a feed that requires one to remain with an operating line until it closely approaches the equilibrium curve) can be very wasteful insofar as the effectiveness of the stages is concerned.

Minimum Stages A column operating at total reflux is represented in Fig. 13-28*a*. Enough material has been charged to the column to fill the reboiler, the trays, and the overhead condensate drum to their working levels. The column is then operated with no feed and with all the condensed overhead stream returned as reflux ($L_{N+1} = V_N$ and $D = 0$). Also all the liquid reaching the reboiler is

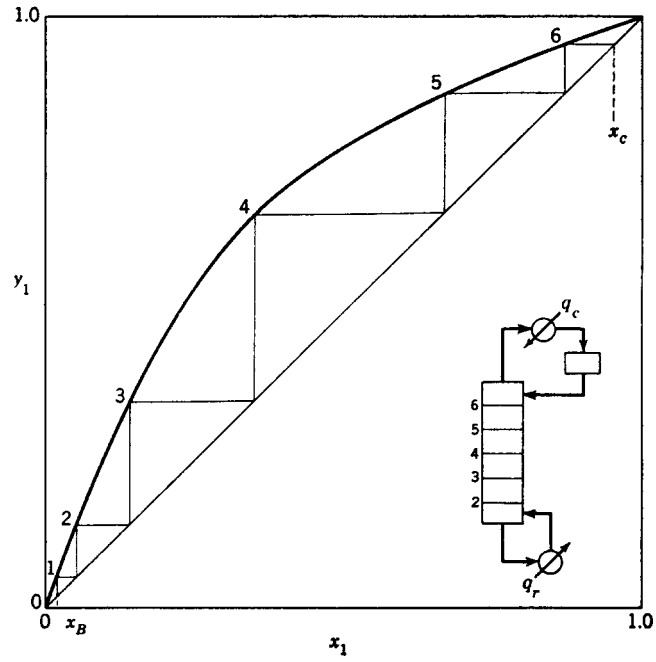

(a)

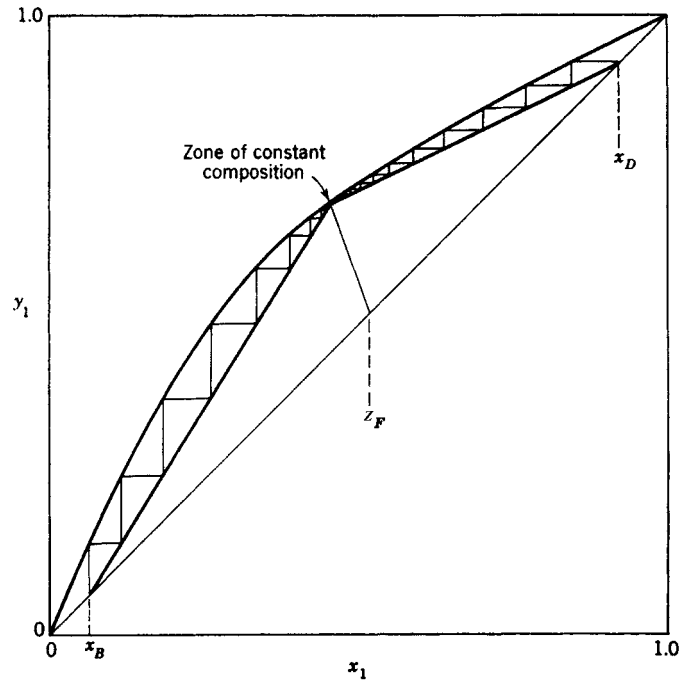

(b)

FIG. 13-28 McCabe-Thiele diagrams for limiting cases. (*a*) Minimum stages for a column operating at total reflux with no feeds or products. (*b*) Minimum reflux for a binary system of normal volatility.

vaporized and returned to the column as vapor. Since F, D, and B are all zero, $L_{n+1} = V_n$ at all points in the column. With a slope of unity ($L/V = 1.0$), the operating line must coincide with the diagonal throughout the column. Total reflux operation gives the minimum number of stages required to effect a specified separation between x_B and x_D.

Minimum Reflux The minimum reflux ratio is defined as that ratio which if decreased by an infinitesimal amount would require an infinite number of stages to accomplish a specified separation between two components. The concept has meaning only if a separation between two components is specified and the number of stages is not specified. Figure 13-28*b* illustrates the minimum reflux condition. As the reflux ratio is reduced, the two operating lines swing upward, pivoting around the specified x_B and x_D values, until one or both touch the equilibrium curve. For equilibrium curves shaped like the one shown, the contact occurs at the feed q line, resulting in a *feed pinch point*. Often an equilibrium curve will dip down closer to the diagonal at higher compositions. In such cases, the upper operating line may make contact before its intersection point on the q line reaches the equilibrium curve, resulting in a *tangent pinch point*. Wherever the contact appears, the intersection of the operating line with the equilibrium curve produces a pinch point which contains a very large number of stages, and a zone of constant composition is formed (see Doherty and Malone, 2001, chap. 3 and sec. 4.6 for additional information).

Intermediate Reboilers and Condensers When a large temperature difference exists between the ends of the column due to a wide boiling point difference between the components, intermediate reboilers and/or condensers may be used to add heat at a lower temperature, or remove heat at a higher temperature, respectively. [A distillation column of this type is shown in *Perry's Chemical Engineers' Handbook*, 7th ed. (1986), Fig. 13-2*a*.] A column operating with an intermediate reboiler and an intermediate condenser in addition to a regular reboiler and a condenser is illustrated with the solid lines in Fig. 13-29. The dashed lines correspond to simple distillation with only a bottoms reboiler and an overhead condenser. Total boiling and condensing heat loads are the same for both columns. As shown by Kayihan [*AIChE Symp. Ser.* **76,** 192, 1 (1980)], the addition of intermediate reboilers and intermediate condensers increases thermodynamic efficiency but requires additional stages, as is clear from the positions of the operating lines in Fig. 13-29.

Optimum Reflux Ratio The general effect of the operating reflux ratio on fixed costs, operating costs, and the sum of these is shown in Fig. 13-30. In ordinary situations, the minimum on the total cost curve will generally occur at an operating reflux ratio in the interval 1.1 to 2 times the minimum value. Generally, the total cost curve rises slowly from its minimum value as the operating reflux ratio increases, and very steeply as the operating reflux ratio decreases. In the absence of a detailed cost analysis for the specific separation of interest, it is recommended to select operating reflux ratios closer to 1.5 to 2.0 times the minimum value (see Doherty and Malone, 2001, chap. 6 for additional discussion).

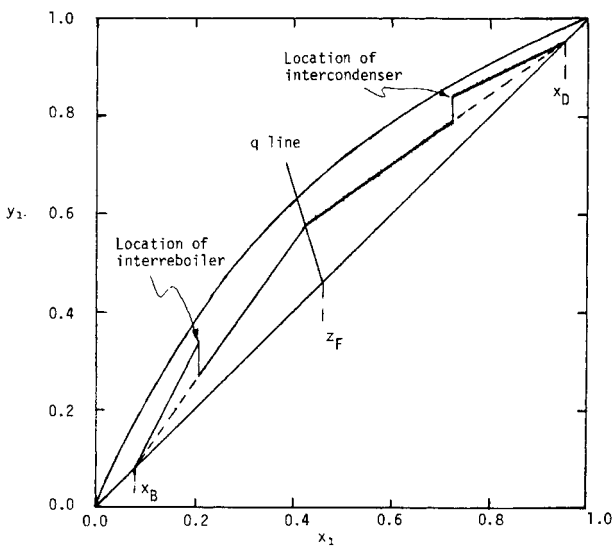

FIG. 13-29 McCabe-Thiele diagram for columns with and without an intermediate reboiler and an intermediate condenser.

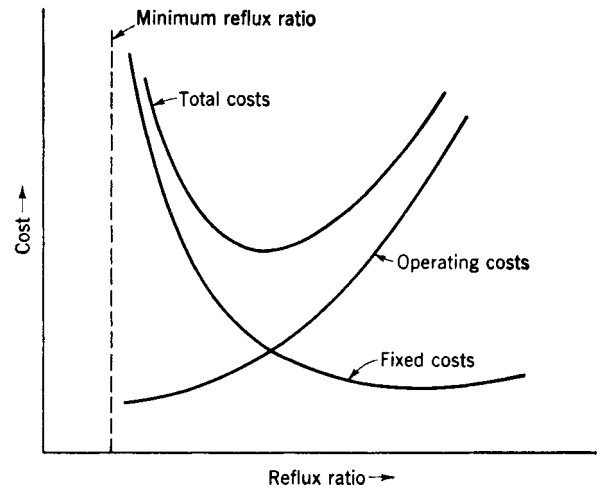

FIG. 13-30 Location of the optimum reflux for a given feed and specified separation.

Difficult Separations Some binary separations may pose special problems because of extreme purity requirements for one or both

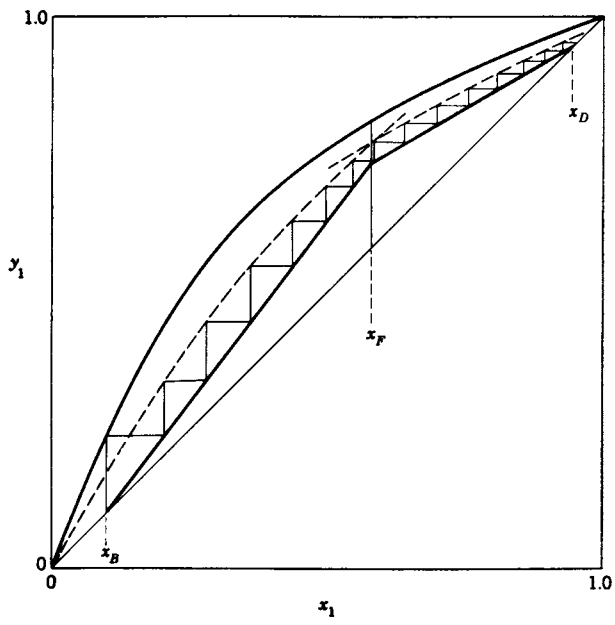

FIG. 13-31 Application of a 50 percent Murphree vapor-phase efficiency to each stage (excluding the reboiler) in the column. Each step in the diagram corresponds to an actual stage.

products or because of a relative volatility close to 1. The *y-x* diagram is convenient for stepping off stages at extreme purities if it is plotted on log-log paper. However, such cases are best treated by equation-based design methods.

Equation-Based Design Methods Exact design equations have been developed for mixtures with constant relative volatility. Minimum stages can be computed with the Fenske equation, minimum reflux from the Underwood equation, and the total number of stages in each section of the column from either the Smoker equation (*Trans. Am. Inst. Chem. Eng.,* **34,** 165 (1938); the derivation of the equation is shown, and its use is illustrated by Smith, op. cit.), or Underwood's method. A detailed treatment of these approaches is given in Doherty and Malone (op. cit., chap. 3). Equation-based methods have also been developed for nonconstant relative volatility mixtures (including nonideal and azeotropic mixtures) by Julka and Doherty [*Chem. Eng. Sci*., **45,** 1801 (1990); *Chem. Eng. Sci*., **48,** 1367 (1993)], and Fidkowski et al. [*AIChE J.*, **37,** 1761 (1991)]. Also see Doherty and Malone (op. cit., chap. 4).

Stage Efficiency The use of the *Murphree plate efficiency* is particularly convenient on *y-x* diagrams. The Murphree efficiency is defined for the vapor phase as

$$E^{MV} = \frac{y_n - y_{n-1}}{y_n^* - y_{n-1}} \tag{13-29}$$

where y_n^* is the composition of the vapor that would be in equilibrium with the liquid leaving stage n and is the value read from the equilibrium curve. The y_{n-1} and y_n are the actual (nonequilibrium) values for vapor streams leaving the $n-1$ and n stages, respectively. Note that for the y_{n-1} and y_n values we assume that the vapor streams are completely mixed and uniform in composition. An analogous efficiency can be defined for the liquid phase.

The application of a 50 percent Murphree vapor-phase efficiency on a *y-x* diagram is illustrated in Fig. 13-31. A pseudoequilibrium curve is drawn halfway (on a vertical line) between the operating lines and the true equilibrium curve. The true equilibrium curve is used for the first stage (the partial reboiler is assumed to be an equilibrium stage), but for all other stages the vapor leaving each stage is assumed to approach the equilibrium value y_n^* only 50 percent of the way. Consequently, the steps in Fig. 13-31 represent actual trays.

In general, application of a constant efficiency to each stage as in Fig. 13-31 will not give the same answer as obtained when the number of equilibrium stages (obtained by using the true equilibrium curve) is divided by the same efficiency factor.

The prediction and use of stage efficiencies are described in detail in Sec. 14. Alternative approaches based on mass-transfer rates are preferred, as described in the subsection below, Nonequilibrium Modeling.

Miscellaneous Operations The *y-x* diagrams for several other column configurations have not been presented here. The omitted items are *partial condensers, rectifying columns* (feed introduced to the bottom stage), *stripping columns* (feed introduced to the top stage), total reflux in the top section but not in the bottom section, multiple feeds, and introduction of *open steam* to the bottom stage to eliminate the reboiler. These configurations are discussed in Smith (op. cit.) and Henley and Seader (op. cit.), who also describe the more rigorous Ponchon-Savarit method, which is not covered here.

APPROXIMATE MULTICOMPONENT DISTILLATION METHODS

Some approximate calculation methods for the solution of multicomponent, multistage separation problems continue to serve useful purposes even though computers are available to provide more rigorous solutions. The available phase equilibrium and enthalpy data may not be accurate enough to justify the longer rigorous methods. Or in extensive design and optimization studies, a large number of cases can be worked quickly and cheaply by an approximate method to define roughly the optimum specifications, which can then be investigated more exactly with a rigorous method.

Two approximate multicomponent shortcut methods for simple distillation are the Smith-Brinkley (SB) method, which is based on an analytical solution of the finite-difference equations that can be written for staged separation processes when stages and interstage flow rates are known or assumed, and the Fenske-Underwood-Gilliland (FUG) method, which combines Fenske's total reflux equation and Underwood's minimum reflux equation with a graphical correlation by Gilliland that relates actual column performance to total and minimum reflux conditions for a specified separation between two key components. Thus, the SB and FUG methods are rating and design methods, respectively. Both methods work best when mixtures are nearly ideal.

The SB method is not presented here, but is presented in detail in the 6th edition of *Perry's Chemical Engineers' Handbook.* Extensions of the SB method to nonideal mixtures and complex configurations are developed by Eckert and Hlavacek [*Chem. Eng. Sci.,* **33,** 77 (1978)] and Eckert [*Chem. Eng. Sci.,* **37,** 425 (1982)], respectively, but are not discussed here. However, the approximate and very useful method of Kremser [*Nat. Pet. News,* **22**(21), 43 (May 21, 1930)] for application to absorbers and strippers is discussed at the end of this subsection.

FENSKE-UNDERWOOD-GILLILAND (FUG) SHORTCUT METHOD

In this approach, Fenske's equation [*Ind. Eng. Chem.,* **24,** 482 (1932)] is used to calculate N_{min}, which is the number of plates required to make a specified separation at total reflux, i.e., the minimum value of N. Underwood's equations [*J. Inst. Pet.,* **31,** 111 (1945); **32,** 598 (1946); **32,** 614 (1946); and *Chem. Eng. Prog.,* **44,** 603 (1948)] are used to estimate the minimum reflux ratio R_{min}. The empirical correlation of Gilliland [*Ind. Eng. Chem.,* **32,** 1220 (1940)] shown in Fig. 13-32 then uses these values to give N for any specified R, or R for any specified N. Limitations of the Gilliland correlation are discussed by Henley and Seader (*Equilibrium-Stage Separation Operations in Chemical Engineering,* Wiley, New York, 1981). The following equation, developed by Molokanov et al. [*Int. Chem. Eng.,* **12**(2), 209 (1972)], satisfies the endpoints and fits the Gilliland curve reasonably well:

$$\frac{N - N_{min}}{N+1} = 1 - \exp\left(\frac{1 + 54.4\Psi}{11 + 117.2\Psi} \times \frac{\Psi - 1}{\Psi^{0.5}}\right) \tag{13-30}$$

where $\Psi = (R - R_{min})/(R+1)$.

The Fenske total reflux equation can be written as

$$\left(\frac{x_i}{x_r}\right)_D = (\alpha_i)^{N_{min}}\left(\frac{x_i}{x_r}\right)_B \tag{13-31}$$

or as

$$N_{min} = \frac{\log[(Dx_D/Bx_B)_i(Bx_B/Dx_D)_r]}{\log \alpha_i} \tag{13-32}$$

where i is any component and r is an arbitrarily selected reference component in the definition of relative volatilities

$$\alpha_i = \frac{K_i}{K_r} = \frac{y_i x_r}{y_r x_i} \tag{13-33}$$

The particular value of α_i used in Eqs. (13-31) and (13-32) is the effective value calculated from Eq. (13-34) defined in terms of values for each stage in the column by

$$\alpha^N = \alpha_N \alpha_{N-1} \cdots \alpha_2 \alpha_1 \tag{13-34}$$

Equations (13-31) and (13-32) are exact relationships between the splits obtained for components i and r in a column at total reflux.

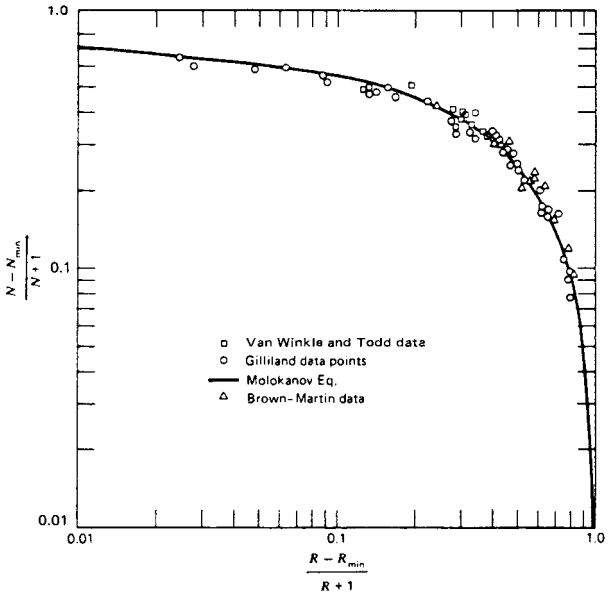

FIG. 13-32 Comparison of rigorous calculations with Gilliland correlation. [*Henley and Seader,* Equilibrium-Stage Separation Operations in Chemical Engineering, *Wiley, New York, 1981; data of Van Winkle and Todd,* Chem. Eng., **78**(*21), 136 (Sept. 20, 1971); data of Gilliland,* Elements of Fractional Distillation, *4th ed., McGraw-Hill, New York, 1950; data of Brown and Martin,* Trans. Am. Inst. Chem. Eng., **35,** *679 (1939).*]

However, the value of α_i must always be estimated, and this is where the approximation enters. It is usually estimated from

$$\alpha = (\alpha_{top}\alpha_{bottom})^{1/2} \tag{13-35}$$

or

$$\alpha = (\alpha_{top}\alpha_{middle}\alpha_{bottom})^{1/3} \tag{13-36}$$

As a side note, the separation that will be accomplished in a column with a known number of equilibrium stages can often be reasonably well estimated by specifying the split of one component (designated as the reference component *r*), setting N_{min} equal to 40 to 60 percent of the number of equilibrium stages (not actual trays), and then using Eq. (13-32) to estimate the splits of all the other components. This is an iterative calculation because the component splits must first be arbitrarily assumed to give end compositions that can be used to give initial end-temperature estimates. The α_{top} and α_{bottom} values corresponding to these end temperatures are used in Eq. (13-5) to give α_i values for each component. The iteration is continued until the α_i values do not change from trial to trial.

The Underwood minimum reflux equations of main interest are those that apply when some of the components do not appear in either the distillate or the bottom products at minimum reflux. These equations are

$$\sum_i \frac{\alpha_i (x_{iD})_{min}}{\alpha_i - \Theta} = R_{min} + 1 \tag{13-37}$$

and

$$\sum_i \frac{\alpha_i z_{iF}}{\alpha_i - \Theta} = 1 - q \tag{13-38}$$

The relative volatilities α_i are defined by Eq. (13-33), R_{min} is the minimum reflux ratio, and *q* describes the thermal condition of the feed (1 for a saturated liquid feed and 0 for a saturated vapor feed). The $z_{i,F}$ values are available from the given feed composition. The Θ is the common root for the top section equations and the bottom section equations developed by Underwood for a column at minimum reflux with separate zones of constant composition in each section. The common root value must fall between α_{hk} and α_{lk}, where *hk* and *lk* stand for *heavy key* and *light key,* respectively. The *key components* are the ones the designer wants to separate. In the butane-pentane splitter problem in Example 1, the light key is *n*-C_4 and the heavy key is *i*-C_5.

The α_i values in Eqs. (13-37) and (13-38) are effective values obtained from Eq. (13-35) or Eq. (13-36). Once these values are available, Θ can be calculated in a straightforward iteration from Eq. (13-38). Since the α-Θ difference can be small, Θ should be determined to four decimal places to avoid numerical difficulties.

The $(x_{iD})_{min}$ values in Eq. (13-37) are minimum reflux values, i.e., the overhead composition that would be produced by the column operating at the minimum reflux with an infinite number of stages. When the light key and the heavy key are adjacent in relative volatility and the specified split between them is sharp or the relative volatilities of the other components are not close to those of the two keys, only the two keys will distribute at minimum reflux and the $(x_{iD})_{min}$ values are easily determined. This is often the case and is the only one considered here. Other cases in which some of or all the nonkey components distribute between distillate and bottom products are discussed in detail by Henley and Seader (op. cit.).

The FUG method is convenient for new column design with the following specifications:

1. A value for R/R_{min}
2. Desired split on the reference component (usually chosen as the heavy key)
3. Desired split on one other component (usually the light key)

However, the total number of equilibrium stages *N*, N/N_{min}, or the external reflux ratio can be substituted for one of these three specifications. Note that the feed location is automatically specified as the optimum one; this is assumed in the Underwood equations. The assumption of saturated liquid reflux is also inherent in the Fenske and Underwood equations (i.e., the reflux is *not* subcooled). An important limitation on the Underwood equations is the assumption of constant molar overflow. As discussed by Henley and Seader (op. cit.), this assumption can lead to a prediction of the minimum reflux that is considerably lower than the actual value. No such assumption is inherent in the Fenske equation. An exact calculation technique for minimum reflux is given by Tavana and Hansen [*Ind. Eng. Chem. Process Des. Dev.*, **18,** 154 (1979)]. Approximate explicit expressions for minimum reflux for various types of splits in three- and four-component mixtures were developed by Glinos and Malone [*Ind. Eng. Chem. Process Des. Dev.*, **23,** 764 (1984)] as well as lumping rules for applying their expressions to mixtures containing more than four components. These expressions are fairly accurate (usually within 5 percent of the exact value for R_{min}) and are extremely convenient for using in the FUG method since they remove the tedious calculation of R_{min} via the Underwood equations. A computer program for the FUG method is given by Chang [*Hydrocarbon Process.*, **60**(8), 79 (1980)]. The method is best applied to mixtures that form ideal or nearly ideal solutions, and should not be used for strongly nonideal or azeotropic mixtures.

Example 1: Application of FUG Method A large butane-pentane splitter is to be shut down for repairs. Some of its feed will be diverted temporarily to an available smaller column, which has only 11 trays plus a partial reboiler. The feed enters on the middle tray. Past experience with similar feeds indicates that the 11 trays plus the reboiler are roughly equivalent to 10 equilibrium stages and that the column has a maximum top vapor capacity of 1.75 times the feed rate on a mole basis. The column will operate at a condenser pressure of 827.4 kPa (120 psia). The feed will be at its bubble point ($q = 1.0$) at the feed tray conditions and has the following composition on the basis of 0.0126 kg·mol/s (100 lb·mol/h):

Component	Fx_{iF}
C_3	5
i-C_4	15
n-C_4	25
i-C_5	20
n-C_5	35
	100

The original column normally has less than 7 mol % i-C_5 in the overhead and less than 3 mol % n-C_4 in the bottom product when operating at a distillate rate of $D/F = 0.489$. Can these product purities be produced on the smaller column at $D/F = 0.489$?

Pressure drops in the column will be neglected, and the K values will be read at 827 kPa (120 psia) in both column sections from the DePriester nomograph in Fig. 13-9*b*. When constant molar overflow is assumed in each section, the rates in pound moles per hour in the upper and lower sections are as follows:

Top section	Bottom section
$D = (0.489)(100) = 48.9$	$B = 100 - 48.9 = 51.1$
$V = (1.75)(100) = 175$	$V' = V = 175$
$L = 175 - 48.9 = 126.1$	$L' = L + F = 226.1$
$\frac{V}{L} = 1.388$	$\frac{V'}{L'} = 0.7739$

$$\frac{L}{L'} = \frac{126.1}{226.1} = 0.5577$$

$$R = \frac{126.1}{48.9} = 2.579$$

NOTE: To convert pound-moles per hour to kilogram-moles per second, multiply by 1.26×10^{-4}.

Application of the FUG method is demonstrated on the splitter. Specifications necessary to model the existing column include these:

1. $N = 10$, total number of equilibrium stages
2. Optimum feed location (which may or may not reflect the actual location)
3. Maximum V/F at the top tray of 1.75
4. Split on one component given in the following paragraphs

The solution starts with an assumed arbitrary split of all the components to give estimates of top and bottom compositions that can be used to get initial end temperatures. The α_i's evaluated at these temperatures are averaged with the α at the feed-stage temperature (assumed to be the bubble point of the feed) by using Eq. (13-36). The initial assumption for the split on i-C_5 is $Dx_D/Bx_B = 3.15/16.85$. As mentioned earlier, N_{min} usually ranges from $0.4N$ to $0.6N$, and the initial N_{min} value assumed here will be $(0.6)(10) = 6.0$. Equation (13-32) can be rewritten as

$$\left(\frac{Dx_D}{Fx_F - Dx_D}\right)_i = \alpha_i^{6.0}\left(\frac{3.15}{16.85}\right) = \alpha_i^{6.0}(0.1869)$$

or

$$Dx_{iD} = \frac{0.1869\alpha_i^{6.0}}{1 + 0.1869\alpha_i^{6.0}} Fx_{iF}$$

The evaluation of this equation for each component is as follows:

Component	α_i	$\alpha_i^{6.0}$	$0.1869\alpha_i^{6.0}$	Fx_{iF}	Dx_{iD}	Bx_{iB}
C_3	5.00			5	5.0	0.0
i-C_4	2.63	330	61.7	15	14.8	0.2
n-C_4	2.01	66	12.3	25	25.1	1.9
i-C_5	1.00	1.00	0.187	20	3.15	16.85
n-C_5	0.843	0.36	0.0672	35	2.20	32.80
				100	48.25	51.75

The end temperatures corresponding to these product compositions are 344 K (159°F) and 386 K (236°F). These temperatures plus the feed bubble point temperature of 358 K (185°F) provide a new set of α_i's which vary only slightly from those used earlier. Consequently, the $D = 48.25$ value is not expected to vary greatly and will be used to estimate a new i-C_5 split. The desired distillate composition for i-C_5 is 7 percent; so it will be assumed that $Dx_D = (0.07)(48.25) = 3.4$ for i-C_5 and that the split on that component will be 3.4/16.6. The results obtained with the new α_i's and the new i-C_5 split are as follows:

Component	$\alpha_i^{6.0}$	$0.2048\alpha_i^{6.0}$	Fx_{iF}	Dx_{iD}	Bx_{iB}	x_{iD}	x_{iB}
C_3			5	5.0	0.0	0.102	0.000
i-C_4	322	65.9	15	14.8	0.2	0.301	0.004
n-C_4	68	13.9	25	23.3	1.7	0.473	0.033
i-C_5	1.00	0.205	20	3.4	16.6	0.069	0.327
n-C_5	0.415	0.085	35	2.7	32.3	0.055	0.636
			100	49.2	50.8	1.000	1.000

The calculated i-C_5 composition in the overhead stream is 6.9 percent, which is close enough to the target value of 7.0 for now.

Table 13-6 shows subsequent calculations using the Underwood minimum reflux equations. The α and x_D values in Table 13-6 are those from the Fenske total reflux calculation. As noted earlier, the x_D values should be those at minimum reflux. This inconsistency may reduce the accuracy of the Underwood method; but to be useful, a shortcut method must be fast, and it has not been shown that a more rigorous estimation of x_D values results in an overall improvement in accuracy. The calculated R_{min} is 0.9426. The actual reflux assumed is obtained from the specified maximum top vapor rate of 0.022 kg·mol/s [175 lb·(mol/h)] and the calculated D of 49.2 (from the Fenske equation).

$$L_{N+1} = V_N - D$$

$$R = \frac{V_N}{D} - 1 = \frac{175}{49.2} - 1 = 2.557$$

The values of $R_{min} = 0.9426$, $R = 2.557$, and $N = 10$ are now used with the Gilliland correlation in Fig. 13-32 or Eq. (13-30) to check the initially assumed value of 6.0 for N_{min}. Equation (13-30) gives $N_{min} = 6.95$, which differs from the assumed value.

Repetition of the calculations with $N_{min} = 7$ gives $R = 2.519$, $R_{min} = 0.9782$, and a calculated check value of $N_{min} = 6.85$, which is close enough. The final product compositions and the α values used are as follows:

Component	α_i	Dx_{iD}	Bx_{iB}	x_{iD}	x_{iB}
C_3	4.98	5.00	0	0.1004	0.0
i-C_4	2.61	14.91	0.09	0.2996	0.0017
n-C_4	2.02	24.16	0.84	0.4852	0.0168
i-C_5	1.00	3.48	16.52	0.0700	0.3283
n-C_5	0.851	2.23	32.87	0.0448	0.6532
		49.78	50.32	1.0000	1.0000

These results indicate that the 7 percent composition of i-C_5 in D and the 3 percent composition of i-C_4 in B obtained in the original column can also be obtained with the smaller column. These results disagree somewhat with the answers obtained from a rigorous computer solution, as shown in the following comparison. However, given the approximations that went into the FUG method, the agreement is good.

	x_{iD}		x_{iB}	
Component	Rigorous	FUG	Rigorous	FUG
C_3	0.102	0.100	0.0	0.0
i-C_4	0.299	0.300	0.006	0.002
n-C_4	0.473	0.485	0.037	0.017
i-C_5	0.073	0.070	0.322	0.328
n-C_5	0.053	0.045	0.635	0.653
	1.000	1.000	1.000	1.000

TABLE 13-6 Application of Underwood Equations

Component	x_F	α	αx_F	$\theta = 1.36$		$\theta = 1.365$		x_D	αx_D	$\alpha - \theta$	$\frac{\alpha x_D}{\alpha - \theta}$
				$\alpha - \theta$	$\frac{\alpha x_F}{\alpha - \theta}$	$\alpha - \theta$	$\frac{\alpha x_F}{\alpha - \theta}$				
C_3	0.05	4.99	0.2495	3.63	0.0687	3.625	0.0688	0.102	0.5090	3.6253	0.1404
i-C_4	0.15	2.62	0.3930	1.26	0.3119	1.255	0.3131	0.301	0.7886	1.2553	0.6282
n-C_4	0.25	2.02	0.5050	0.66	0.7651	0.655	0.7710	0.473	0.9555	0.6553	1.4581
i-C_5	0.20	1.00	0.2000	−0.36	−0.5556	−0.365	−0.5479	0.069	0.0690	−0.3647	−0.1892
n-C_5	0.35	0.864	0.3024	−0.496	−0.6097	−0.501	−0.6036	0.055	0.0475	−0.5007	−0.0949
	1.00				−0.0196		+0.0014	1.000			$1.9426 = R_m + 1$

Interpolation gives $\theta = 1.3647$.

KREMSER EQUATION

Starting with the classical method of Kremser (op. cit.), approximate methods of increasing complexity have been developed to calculate the behavior of groups of equilibrium stages for a countercurrent cascade, such as is used in simple absorbers and strippers of the type shown in Fig. 13-2*b* and *d*. However, none of these methods can adequately account for stage temperatures that are considerably higher or lower than the two entering stream temperatures for absorption and stripping, respectively, when appreciable composition changes occur. Therefore, only the simplest form of the Kremser method is presented here. Fortunately, rigorous computer methods described later can be applied when accurate results are required. The Kremser method is most useful for making preliminary estimates of absorbent and stripping agent flow rates or equilibrium-stage requirements. The method can also be used to extrapolate quickly results of a rigorous solution to a different number of equilibrium stages.

Consider the general adiabatic countercurrent cascade of Fig. 13-33 where v and ℓ are molar component flow rates. Regardless of whether the cascade is an absorber or a stripper, components in the entering vapor will tend to be absorbed and components in the entering liquid will tend to be stripped. If more moles are stripped than absorbed, the cascade is a stripper; otherwise, the cascade is an absorber. The Kremser method is general and applies to either case. Application of component material balance and phase equilibrium equations successively to stages 1 through $N-1$, 1 through $N-2$, etc., as shown by Henley and Seader (op. cit.), leads to the following equations originally derived by Kremser. For each component i,

$$(v_i)_N = (v_i)_0(\Phi_i)_A = (l_i)_{N+1}[1 - (\Phi_i)_s] \tag{13-39}$$

where

$$(\Phi_i)_A = \frac{(A_i)_c - 1}{(A_i)_c^{N+1} - 1} \tag{13-40}$$

is the fraction of component i in the entering vapor that is not absorbed,

$$(\Phi_i)_s = \frac{(S_i)_c - 1}{(S_i)_c^{N+1} - 1} \tag{13-41}$$

is the fraction of component i in the entering liquid that is not stripped,

$$(A_i)_e = \left(\frac{L}{K_i V}\right)_e \tag{13-42}$$

is the effective or average absorption factor for component i, and

$$(S_i)_e = \frac{1}{(A_i)_e} \tag{13-43}$$

is the effective or average stripping factor for component i. When the entering streams are at the same temperature and pressure and negligible absorption and stripping occur, effective component absorption and stripping factors are determined simply by entering stream conditions. Thus, if K values are composition-independent, then

$$(A_i)_e = \frac{1}{(S_i)_e} = \frac{L_{N+1}}{K_i(T_{N+1}, P_{N+1})V_0} \tag{13-44}$$

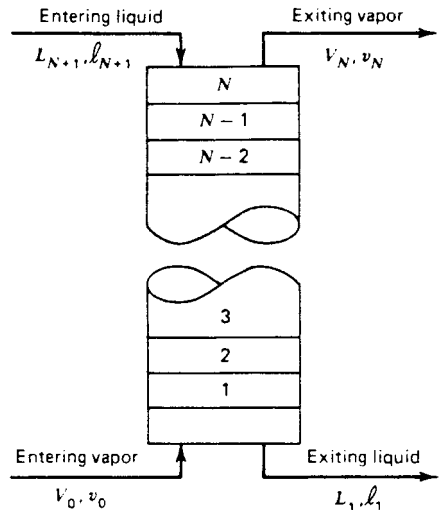

FIG. 13-33 General adiabatic countercurrent cascade for simple absorption or stripping.

When entering stream temperatures differ and/or moderate to appreciable absorption and/or stripping occurs, values of A_i and S_i should be based on effective average values of L, V, and K_i in the cascade. However, even then Eq. (13-44) with T_{N+1} replaced by $(T_{N+1} + T_0)/2$ may be able to give a first-order approximation of $(A_i)_e$. In the case of an absorber, $L_{N+1} < L_e$ and $V_0 > V_e$ will be compensated to some extent by $K_i\{(T_{N+1} + T_0)/2,\ P)\} < K_i\{T_e,\ P\}$. A similar compensation, but in opposite directions, will occur in the case of a stripper. Equations (13-40) and (13-41) are plotted in Fig. 13-34. Components having large values of A_e or S_e absorb or strip, respectively, to a large extent. Corresponding values of Φ_A and Φ_S approach a value of 1 and are almost independent of the number of equilibrium stages.

An estimate of the minimum absorbent flow rate for a specified amount of absorption from the entering gas of some key component K for a cascade with an infinite number of equilibrium stages is obtained from Eq. (13-40) as

$$(L_{N+1})_{\min} = K_K V_0[1 - (\Phi_K)_A] \tag{13-45}$$

The corresponding estimate of minimum stripping agent flow rate for a stripper is obtained as

$$(V_0)_{\min} = \frac{L_{N+1}[1 - (\Phi_K)_s]}{K_K} \tag{13-46}$$

Example 2: Calculation of Kremser Method For the simple absorber specified in Fig. 13-35, a rigorous calculation procedure as described below gives the results in Table 13-7. Values of Φ were computed from component

TABLE 13-7 Results of Calculations for Simple Absorber of Fig. 13-35

	$N = 6$ (rigorous method)				$N = 12$ (Kremser method)					
	(lb·mol)/h						(lb·mol)/h			
Component	$(v_i)_6$	$(\ell_i)_1$	$(\Phi_i)_A$	$(\Phi_i)_S$	$(A_i)_e$	$(S_i)_e$	$(v_i)_{12}$	$(\ell_i)_1$	$(\Phi_i)_A$	$(\Phi_i)_S$
C_1	147.64	12.36	0.9228		0.0772		147.64	12.36	0.9228	
C_2	276.03	94.97	0.7460		0.2541		275.98	94.02	0.7459	
C_3	105.42	134.58	0.4393		0.5692		103.46	136.54	0.4311	
nC_4	1.15	23.85	0.0460		1.3693		0.16	24.84	0.0063	
nC_5	0.0015	4.9985	0.0003		3.6		0	5.0	0.0	
Absorber oil	0.05	164.95		0.9997		0.0003	0.05	164.95		0.9997
Totals	530.29	435.71					527.29	437.71		

NOTE: To convert pound-moles per hour to kilogram-moles per hour, multiply by 0.454.

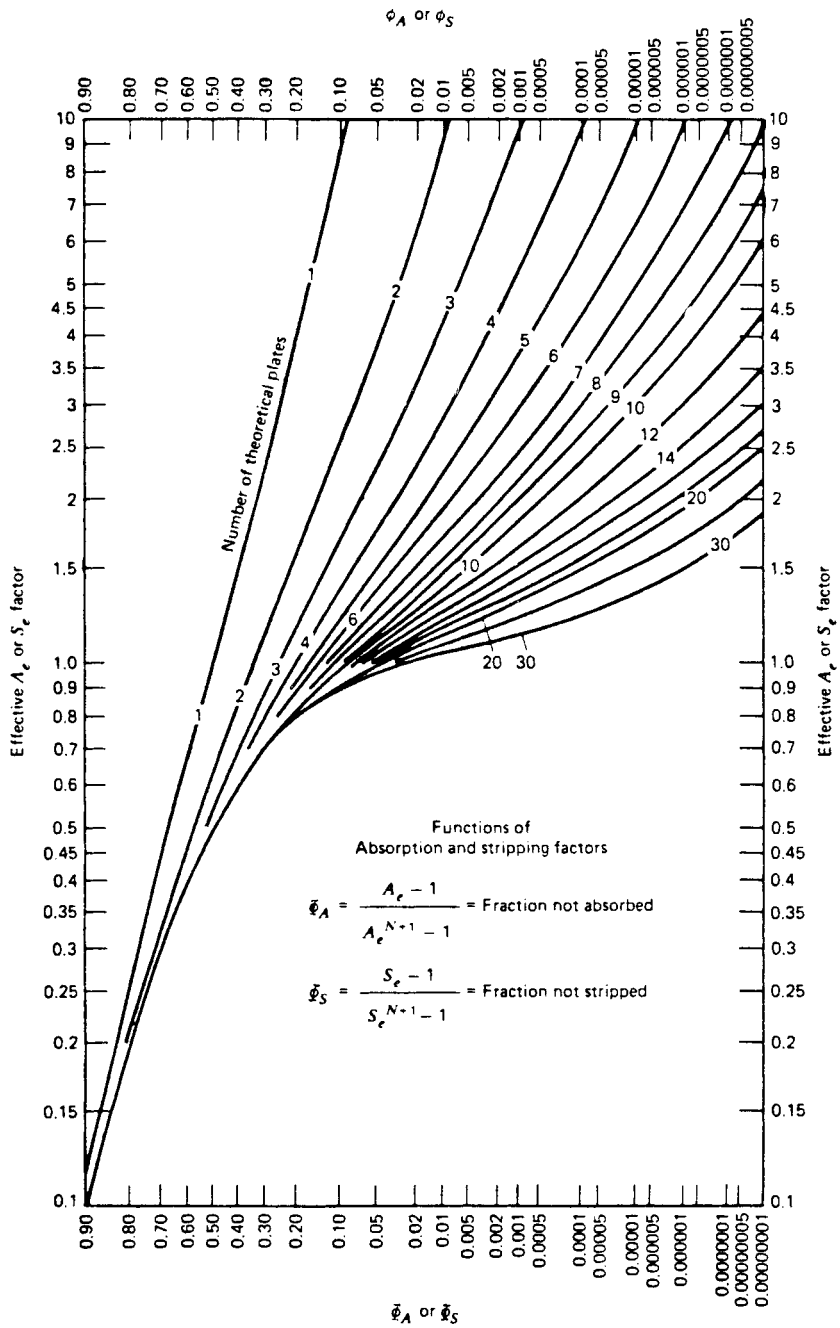

FIG. 13-34 Absorption and stripping factors. [*W. C. Edmister,* AIChE J., **3,** *165–171 (1957).*]

product flow rates, and corresponding effective absorption and stripping factors were obtained by iterative calculations in using Eqs. (13-40) and (13-41) with $N = 6$. Use the Kremser method to estimate component product rates if N is doubled to a value of 12.

Assume that values of A_e and S_e will not change with a change in N. Application of Eqs. (13-40), (13-41), and (13-39) gives the results in the last four columns of Table 13-7. Because of its small value of A_e, the extent of absorption of C_1 is unchanged. For the other components, somewhat increased amounts of absorption occur. The degree of stripping of the absorber oil is essentially unchanged. Overall, only an additional 0.5 percent of absorption occurs. The greatest increase in absorption occurs for n-C_4, to the extent of about 4 percent.

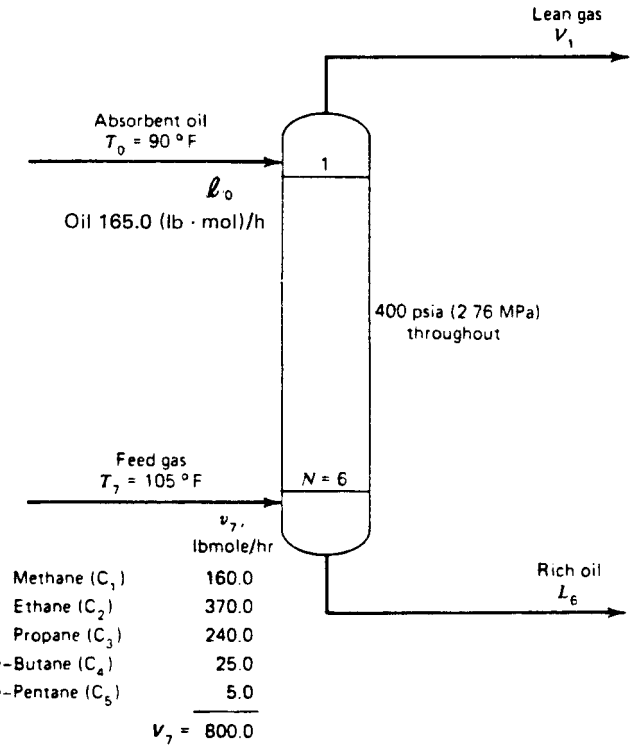

FIG. 13-35 Specifications for the absorber example.

SIMULATION OF DISTILLATION PROCESSES

Chemical engineers have been solving distillation problems by using the *equilibrium-stage model* since 1893 when Sorel outlined the concept to describe the distillation of alcohol. Since that time, it has been used to model a wide variety of distillation-like processes, including simple distillation (single-feed, two-product columns), complex distillation (multiple-feed, multiple-product columns), extractive and azeotropic distillation, petroleum distillation, absorption, liquid-liquid extraction, stripping, and supercritical extraction.

Real distillation processes, however, nearly always operate away from equilibrium. In recent years it has become possible to simulate distillation and absorption as the mass-transfer rate-based operations that they really are, using what have become known as *nonequilibrium* (NEQ) or *rate-based* models [Taylor et al., *CEP* (July 28, 2003)].

The computer simulation of distillation processes, whether done using equilibrium or nonequilibrium models, requires us to address the following topics:

- Formulation of the model equations
- Physical property data and calculations (see Sec. 4 of this handbook)
- Degrees-of-freedom analysis
- Solution of large linear and strongly nonlinear systems of equations

These are the topics we consider in what follows. We also discuss the use of simulation tools in the modeling of real distillation columns.

EQUILIBRIUM-STAGE MODELING

A schematic diagram of an equilibrium stage is shown in Fig. 13-36*a*. Vapor from the stage below and liquid from a stage above are brought into contact on the stage together with any fresh or recycle feeds. The vapor and liquid streams leaving the stage are assumed to be in equilibrium with each other. A complete separation process is modeled as a sequence of these *equilibrium stages,* as shown in Fig. 13-36*b*.

The MESH Equations (the 2*c* + 3 Formulation) The equations that model equilibrium stages often are referred to as the MESH equations. The M equations are the material balance equations, E stands for equilibrium equations, S stands for mole fraction summation equations, and H refers to the heat or enthalpy balance equations.

There are two types of material balance: the total material balance

$$V_{j+1} + L_{j-1} + F_j - (1 + r_j^V)V_j - (1 + r_j^L)L_j = 0 \qquad (13\text{-}47)$$

and the component material balance

$$V_{j+1}y_{i,j+1} + L_{j-1}x_{i,j-1} + F_j z_{i,j} - (1 + r_j^V)V_j y_{i,j} - (1 + r_j^L)L_j x_{i,j} = 0 \qquad (13\text{-}48)$$

In the material balance equations given above, r_j is the ratio of sidestream flow to interstage flow:

$$r_j^V = \frac{U_j}{V_j} \quad r_j^L = \frac{W_j}{L_j} \qquad (13\text{-}49)$$

Mole fractions must be forced to sum to unity, thus

$$\sum_{i=1}^{c} x_{i,j} = 1 \quad \sum_{i=1}^{c} y_{i,j} = 1 \quad \sum_{i=1}^{c} z_{i,j} = 1 \qquad (13\text{-}50)$$

The enthalpy balance is given by

$$V_{j+1}H_{j+1}^V + L_{j-1}H_{j-1}^L + F_j H_j^F - (1 + r_j^V)V_j H_j^V - (1 + r_j^L)L_j H_j^L - Q_j = 0 \qquad (13\text{-}51)$$

The superscripted H's are the enthalpies of the appropriate phase.

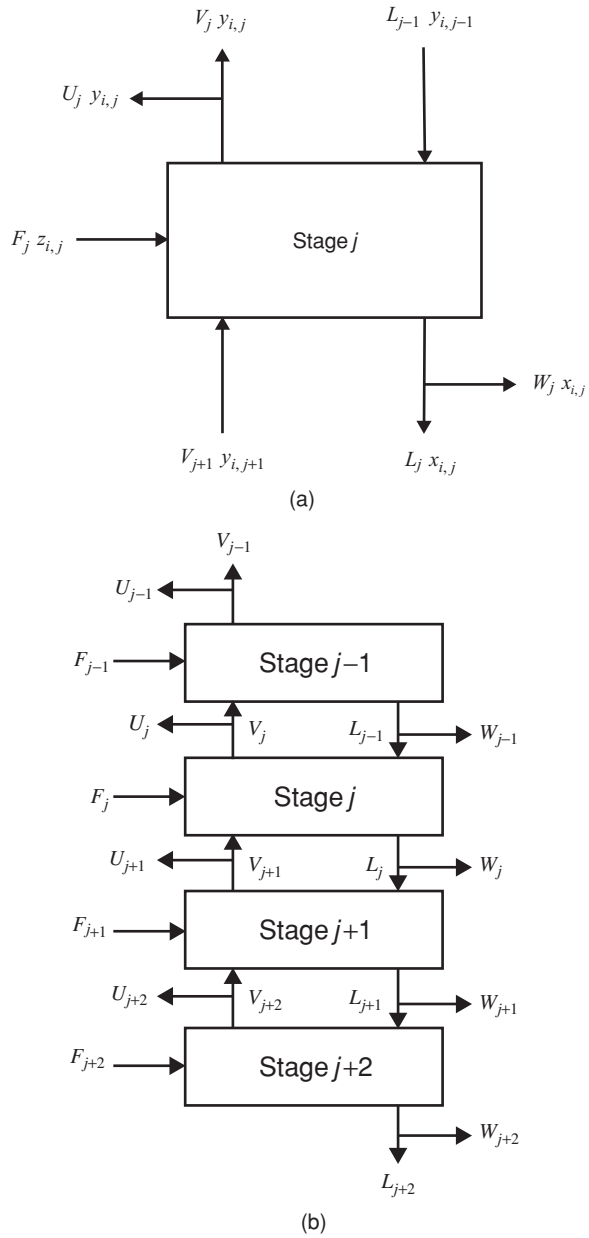

FIG. 13-36 (*a*) The equilibrium stage. (*b*) Multistage column.

To complete the model, it is usual to add equations that relate the compositions of the two streams leaving the stage. In the standard model of a distillation column, we assume that these two streams are in equilibrium with each other. Thus, the mole fractions in the exiting streams are related by the familiar equations of phase equilibrium:

$$y_{i,j} = K_{i,j} x_{i,j} \tag{13-52}$$

The $K_{i,j}$ are the equilibrium ratios or K values for species i on stage j.

Degrees-of-Freedom Analysis and Problem Formulation Table 13-8 summarizes the equations for a single equilibrium stage (in a sequence of stages). There are $2c + 4$ equations per stage, of which only $2c + 3$ are independent. Thus, one of these equations must be ignored in a (computer-based) method to solve the equations. In some methods we disregard the total material balance; an alternative is to combine the vapor and liquid mole fraction summation equations (as was done for flash calculations by Rachford and Rice, op. cit.). Note that the mole fraction summation equations for the feed are omitted here, as are the mole fraction summation equations for interstage vapor and liquid traffic; the latter "belong" to the equation set for adjacent stages (see, however, the subsection Degrees of Freedom below in which this topic is revisited in greater detail).

TABLE 13-8 Equations for an Equilibrium Stage

Equation	Equation no.	Number
Total mass balance	(13-47)	1
Component mass balances	(13-48)	c
Total energy balance	(13-51)	1
Mole fraction summation equations	(13-50)	2
Equilibrium equations	(13-52)	c
		$2c + 4$

The quantities for stage j that appear in these equations are summarized in Table 13-9. The total number of variables appearing in these equations is $3c + 10$. Note that the K values and enthalpies that also appear in the MESH equations are not included in the table of variables, nor are equations for their estimation included in the list of equations. Thermodynamic properties are functions of temperature, pressure, and composition, quantities that do appear in the table of variables.

The $2c + 3$ unknown variables normally determined by solving the MESH equations are the c vapor mole fractions $y_{i,j}$; the c liquid mole fractions $x_{i,j}$; the stage temperature T_j; and the vapor and liquid flow V_j and L_j. The remaining variables, $c + 7$ in number (the difference between the number of variables and the number of independent equations), that need to be specified are the stage pressure P_j, the feed flow rate, $c - 1$ mole fractions in the feed (the last is then computed directly from the feed mole fraction summation equation, which was not included in the equations for stage j in Table 13-8), temperature and pressure of the feed, the stage heat duty Q_j, and the sidestream flows U_j and W_j. It is important to recognize that the other flows and composition variables appearing in the MESH equations are associated with the equivalent equations for adjacent stages.

For a column of N stages, we must solve $N(2c + 3)$ equations. The table below shows how we may need to solve hundreds or even thousands of equations.

c	N	$N(2c + 3)$
2	10	70
3	20	180
5	50	650
10	30	690
40	100	8300

TABLE 13-9 Variables for an Equilibrium Stage

Variable	Symbol	Number
Vapor flow rate	V_j	1
Liquid flow rate	L_j	1
Feed flow rate	F_j	1
Vapor sidestream flow	W_j	1
Liquid sidestream flow	U_j	1
Vapor-phase mole fractions	$y_{i,j}$	c
Liquid-phase mole fractions	$x_{i,j}$	c
Feed composition	$z_{i,j}$	c
Stage temperature	T_j	1
Stage pressure	P_j	1
Feed temperature		1
Feed pressure		1
Stage heat duty	Q_j	1
		$3c + 10$

The $2c + 1$ Formulation An alternative form of the MESH equations is used in many algorithms. In this variation, we make use of the component flow defined by

$$v_{ij} = V_j y_{ij} \quad l_{ij} = L_j x_{ij} \quad f_{ij} = F_j z_{ij} \tag{13-53}$$

In terms of the component flow, the component material balance becomes

$$v_{i,j+1} + l_{i,j-1} + f_{i,j} - (1 + r_j^V) v_{i,j} - (1 + r_j^L) l_{i,j} = 0 \tag{13-54}$$

Since the total vapor and liquid flow rates are, by definition, the sum of the component flow rates of the respective phases, the summation equations and total mass balance equation are satisfied automatically. Thus, the number of equations and variables per stage has been reduced by 2 to $2c + 1$.

The $c + 3$ Formulation The number of unknown variables per stage can be reduced to only $c + 3$ if we use the equilibrium relations to eliminate the vapor-phase mole fractions from the component mass balances

$$V_{j+1} K_{i,j+1} x_{i,j+1} + L_{j-1} x_{i,j-1} + F_j z_{i,j} - (1 + r_j^V) V_j K_{i,j} x_{i,j} - (1 + r_j^L) L_j x_{i,j} = 0 \tag{13-55}$$

and from the summation equation

$$\sum_{i=1}^{c} K_{i,j} x_{i,j} = 1 \tag{13-56}$$

This equation is familiar to us from bubble point calculations. In this formulation of the MESH equations, the vapor-phase mole fractions no longer are independent variables but are defined by Eq. (13-52). This formulation of the MESH equations has been used in quite a number of algorithms. It is less useful if vapor-phase nonideality is important (and, therefore, the K values depend on the vapor-phase composition).

Condenser and Reboiler The MESH equations given above apply to all the interior stages of a column. In addition, any reboiler and condenser must be considered. On an actual plant, a total condenser may be followed by a reflux accumulator and a stream divider. The accumulator does not add any equations to a steady-state model (but it is important to consider in an un-steady-state model), but the stream splitter is a separate unit with its own temperature, pressure, and heat loss, and modeled by the appropriate balance equations (see the section below on Degrees of Freedom where we address this topic in greater detail). In practice the condenser and reflux splitter often are modeled as a single combined unit, and the MESH equations described above may be used to model these stages with only some minor modifications. For example, for a total condenser *and* the reflux stream splitter at the top of a distillation column, the liquid distillate is U_1 and the reflux ratio $R = 1/r_1^L$. For a partial condenser (with no stream splitter needed) the vapor product is V_1 and the reflux ratio $R = L_1/V_1$. A condenser/splitter device unit that provides both vapor and liquid products is given by a combination of these two units. Finally, for a partial reboiler at the base of a column, the bottoms flow rate is L_N. Note that an equilibrium stage with a sidestream is considered here to be a single unit in essentially the same way.

In computer-based methods for solving the MESH equations, it is common to replace the energy balance of the condenser (with or without the associated stream splitter) and reboiler with a specification equation. Possible specifications include

- The flow rate of the distillate/bottoms product stream
- The mole fraction of a component in either the distillate or bottoms product stream
- Component flow rate in either the distillate or bottoms product stream
- A reflux/reboil ratio or rate
- The temperature of the condenser or reboiler
- The heat duty to the condenser or reboiler

If the condenser and/or reboiler heat duties are not specified, it is possible to calculate them from the energy balances after all the other model equations have been solved.

For a total condenser, the vapor composition used in the equilibrium relations is that determined during a bubble point calculation based on the actual pressure and liquid compositions found in the condenser. These vapor mole fractions are not used in the component mass balances since there is no vapor stream from a total condenser. It often happens that the temperature of the reflux stream is below the bubble point temperature of the condensed liquid (subcooled condenser). In such cases it is necessary to specify either the actual temperature of the reflux stream or the difference in temperature between the reflux stream and the bubble point of the condensate.

Solution of the MESH Equations We may identify several classes of methods of solving the *equilibrium*-stage model equations:

- *Graphical methods.* These methods were developed before modern computer methods became widely adopted. Some graphical methods retain their value for a variety of reasons and were discussed at length in a prior subsection.
- *Approximate methods.* In these a great many simplifying assumptions are made to obtain solutions of the model equations. These methods were the subject of the immediately preceding subsection.
- *Computer-based methods.* Indeed, from the late 1950s to the early 1990s hardly a year passed without the publication of at least one (and usually many more than one) new algorithm for solving these equations (Seader, op. cit.). It is possible to make the case that it was the equilibrium model that brought computing into chemical engineering in the first place! One of the incentives for this activity has always been a desire to solve problems with which existing methods have trouble. The evolution of algorithms for solving the stage model equations has been influenced by, among other things, the availability (or lack) of sufficient computer storage and speed, the development of mathematical techniques that can be exploited, the complexity of physical property (K value and enthalpy) correlations, and the form of the model equations being solved. We continue with a brief discussion of computer-based methods. Readers interested in complete details of the methods discussed should consult the references cited below. In addition, many computer-based methods are discussed at length in a number of textbooks [see, e.g., Holland, op. cit.; King, op. cit.; Seader and Henley, op. cit.; Haas (in Kister op. cit. 1992)]. Seader (op. cit.) has written an interesting history of equilibrium-stage simulation.

The MESH equations form a set of nonlinear, algebraic equations (in the sense that no derivatives or integrals are involved) and must, therefore, be solved by some iterative process. There are two key steps in the development of an algorithm for solving systems of nonlinear equations:

- The selection of particular numerical methods
- The selection of the order in which the equations are to be solved

We may identify several classes of methods for numerically solving the MESH equations:

1. Tearing methods in which the equations are divided into groups and each group is solved separately
2. Inside-out (IO) methods
3. Simultaneous convergence (SC) methods in which all the equations are solved at the same time simultaneously by using Newton's method (or a variant thereof)
4. Relaxation methods in which the MESH equations are cast in unsteady-state form and integrated numerically until the steady-state solution has been found
5. Continuation methods
6. Collocation methods
7. Optimization methods

The methods for solving the MESH equations that are used most widely fall into categories 1 through 3 and 5—tearing methods, inside-out methods, simultaneous convergence methods, and continuation method. Following the sections on each of these three classes of method, we discuss homotopy continuation methods. For many years the older tearing methods formed the backbone of sequential modular flow sheet simulation programs; such methods have largely been replaced by the inside-out methods that now are standard in all major (and many less widely used) flow sheet simulation programs. Simultaneous convergence methods also now are available in many of these systems. Even homotopy methods (sometimes considered to belong

to the domain of specialists) are finding increasing use in commercial software.

Tearing Methods Equation tearing involves breaking a system of nonlinear equations into small groups and solving each group of equations in turn. In solving any subset of the complete set of equations, only a corresponding number of variables, the "tear" variables, can be determined. To start the calculations, therefore, it is necessary to assume values for the remaining variables. The "torn" set of equations is then solved for the "tear" variables, assuming that the values assigned to all other variables are correct. Successive groups of equations and variables are *torn* or *decoupled* from the full set of equations and variables until all the variables have been updated. At this point, the process starts over and is repeated until all the equations are satisfied simultaneously.

A great many tearing methods for solving the MESH equations have been proposed. According to Friday and Smith (1964), tearing methods may be analyzed in the following terms:

- The order in which the equations are grouped
- The order in which each group of equations is solved
- The selection of which variables are to be computed from which equation

Subsequent issues are

- The method(s) used to solve the M and E equations
- The method of calculating the new stage temperatures
- The method of calculating the new flow rates V_j and L_j

Most tearing methods are based on keeping all the equations of a given type together, e.g., the M equations or the H equations, for all the stages at once.

The classic papers by Lewis and Matheson [*Ind. Eng. Chem.,* **24,** 496 (1932)] and Thiele and Geddes [*Ind. Eng. Chem.,* **25,** 290 (1933)] represent the first attempts at solving the MESH equations for multicomponent systems numerically (the graphical methods for binary systems discussed earlier had already been developed by Ponchon, by Savarit, and by McCabe and Thiele). At that time the computer had yet to be invented, and since modeling a column could require hundreds, possibly thousands, of equations, it was necessary to divide the MESH equations into smaller subsets if hand calculations were to be feasible. Despite their essential simplicity and appeal, stage-to-stage calculation procedures are not used now as often as they used to be.

Matrix techniques were first used in separation process calculations by Amundson and Pontinen [*Ind. Eng. Chem.,* **50,** 730 (1958)] who demonstrated that the combined M + E equations (the $c + 3$ formulation) could be conveniently written in tridiagonal matrix form.

Three quite different approaches to the problem of computing the flow rates and temperatures have evolved:

1. In the bubble point (BP) method, the S + E equations are used to determine the stage temperatures from a bubble point calculation. The vapor and liquid flow rates are computed from the energy balances and total material balances. The BP method was introduced by Amundson and Pontinen (op. cit.) who used matrix inversion to solve equations. A significant improvement in the BP method was introduced by Wang and Henke [*Hydrocarbon Process.,* **45**(8), 155 (1966)] who used a form of Gaussian elimination known as the Thomas algorithm that can be used to solve a tridiagonal system very efficiently. Holland and coworkers (Holland, op. cit.) have combined some of these ideas with the "theta method" of convergence acceleration.

2. In the sum rates (SR) method, the vapor and liquid flow rates are computed directly from the summation equations and the stage temperatures determined from the energy balances. The SR algorithm was due originally to Sujuta [*Hydrocarbon Process.,* **40**(12), 137 (1961)] and Friday and Smith (op. cit.). Sujuta used the $2c + 1$ version of the MESH equations in his work and the tridiagonal system of combined M + E equations was written in terms of the component flow rates in the liquid phase. Burningham and Otto [*Hydrocarbon Process.,* **46**(10), 163 (1967)] incorporated the Thomas algorithm in their implementation of the SR method. Sridhar and Lucia [*Comput. Chem. Eng.* **14,** 901 (1990)] developed a modified SR method that is capable of solving problems involving narrow, intermediate, and wide-boiling mixtures alike.

3. In the Newton-Raphson methods, the bubble point equations and energy balances are solved simultaneously for the stage temperatures and vapor flow rates; the liquid flow rates follow from the total material balances [Tierney and coworkers, *AIChE J.,* **13,** 556 (1967); **15,** 897 (1969); Billingsley and Boynton, *AIChE J.,* **17,** 65 (1971)]. Similar methods are described by Holland (op. cit.) and by Tomich [*AIChE J.,* **16,** 229 (1970)].

Inside-Out Methods First proposed by Boston and Sullivan [*Can. J. Chem. Engr.,* **52,** 52 (1974)] and further developed by Boston and coworkers [*Comput. Chem. Engng.,* **2,** 109 (1978); *ACS Symp. Ser.* No. 124, 135 (1980); *Comput. Chem. Engng.,* **8,** 105 (1984); and *Chem. Eng. Prog.,* **86** (8), 45–54 (1990)], Jelinek [*Comput. Chem. Engng.,* **12,** 195 (1988)], and Simandl and Svrcek [*Comput. Chem. Engng.,* **15,** 337 (1991)], inside-out methods really belong in the group of tearing methods; however, their very widespread use in many commercial simulation programs demands that they be granted a category all to themselves. In these methods, complicated equilibrium and enthalpy expressions are replaced by simple models, and the iteration variables T, V, x, y are replaced by variables within the simple models that are relatively free of interactions with each other. Seader and Henley (op. cit.) provide complete details of the somewhat lengthy algorithm. Inside-out methods have replaced many of the older algorithms in commercial simulation programs, the modified version of Russell [*Chem. Eng.,* **90,** (20), 53 (1983)] being the basis for some of them.

Simultaneous Convergence Methods One drawback of some tearing methods is their relatively limited range of application. For example, the BP methods are more successful for distillation, and the SR-type methods are considered better for mixtures that exhibit a wide range of (pure-component) boiling points (see, however, our remarks above on modified BP and SR methods). Other possible drawbacks (at least in some cases) include the number of times physical properties must be evaluated (several times per outer loop iteration) if temperature- and composition-dependent physical properties are used. It is the physical properties calculations that generally dominate the computational cost of chemical process simulation problems. Other problems can arise if any of the iteration loops are hard to converge.

The development of methods for solving all the equations at the same time was tackled independently by a number of investigators. Simultaneous solution of all the MESH equations was suggested as a method of last resort by Friday and Smith (op. cit.) in a classic paper analyzing the reasons why other algorithms fail. They did not, however, implement such a technique. The two best-known papers are those of Goldstein and Stanfield [*Ind. Eng. Chem. Process Des. Dev.,* **9,** 78 (1970)] and Naphtali and Sandholm [*AIChE J.,* **17,** 148 (1971)], the latter providing more details of an application of Newton's method described by Naphtali at an AIChE meeting in May 1965. A method to solve all the MESH equations for all stages at once by using Newton's method was implemented by Whitehouse [Ph.D. Thesis, University of Manchester Institute of Science and Technology (1964)] (see Stainthorp and Whitehouse [*I. Chem. E. Symp. Series*, **23,** 181 (1967)]). Among other things, Whitehouse's code allowed for specifications of purity, T, V, L, or Q on any stage. Interlinked systems of columns and nonideal solutions could be dealt with even though no examples of the latter type were solved by Whitehouse.

Many others have since employed Newton's method or a related method to solve the MESH equations. Such methods have become standard in commercial process simulation programs, most often for simulating systems for which tearing and inside-out methods are less successful (typically those that involve strongly nonideal mixtures). Simultaneous convergence procedures have shown themselves to be generally fast and reliable, having a locally quadratic convergence rate in the case of Newton's method, and these methods are much less sensitive to difficulties associated with nonideal solutions than are tearing methods. Seader (Sec. 13, *Perry's Chemical Engineers' Handbook,* 7th ed., 1986) discusses the design of simultaneous convergence methods.

Continuation Methods (for Really Difficult Problems) For those problems that other methods fail to solve, we may use continuation

methods. These methods begin with a known solution of a companion set of equations and follow a path to the desired solution of the set of equations to be solved. In most cases, the path exists and can be followed. We can identify the following categories of continuation method that have been used for solving the equilibrium-stage MESH equations:

1. Mathematical methods which place the MESH equations into a homotopy equation of purely mathematical origin
2. Physical continuation methods in which the nature of the equations being solved is exploited in some way

The first to use the Newton homotopy for separation process problems were Hlavacek and coworkers [*Chem. Eng. Sci.*, **36,** 1599 (1981); *Chem. Eng. Commun.*, **28,** 165 (1984)]. In papers of considerable significance Wayburn and Seader [*Comput. Chem. Engng.,* **11,** 7–25 (1987); *Proc. Second Intern. Conf. Foundations of Computer-Aided Process Design,* CACHE, Austin, Tex., 765–862 (1984); *AIChE Monograph Series,* AIChE, New York, **81,** No. 15 (1985)] used the Newton homotopy in their solution of the MESH equations for interlinked distillation columns. Kovach and Seider [*Comput. Chem. Engng.,* **11,** 593 (1987)] used the Newton homotopy for solving distillation problems involving highly nonideal mixtures.

In the category of physical continuation methods are the thermodynamic homotopies of Vickery and Taylor [*AIChE J.*, **32**, 547 (1986)] and a related method due to Frantz and Van Brunt (AIChE National Meeting, Miami Beach, 1986). Thermodynamic continuation has also been used to find azeotropes in multicomponent systems by Fidkowski et al. [*Comput. Chem. Engng.,* **17,** 1141 (1993)]. Parametric continuation methods may be considered to be physical continuation methods. The reflux ratio or bottoms flow rate has been used in parametric solutions of the MESH equations [Jelinek et al., *Chem. Eng. Sci.*, **28,** 1555 (1973)].

Bryne and Baird [*Comput. Chem. Engng.,* **9,** 593 (1985)] describe the use of proprietary continuation methods. Woodman (Ph.D. thesis, University of Cambridge, 1989) has combined several continuation methods to solve problems that involved nonstandard specifications and multiple liquid phases.

For detailed descriptions of homotopy methods in chemical engineering, see Seader [*Computer Modeling of Chemical Processes*, AIChE Monograph Series 15, **81,** (1985)].

Other Methods *Relaxation techniques* differ from both tearing algorithms and simultaneous convergence methods in that the relaxation techniques do not solve steady-state problems. Rather, at least one set of the MESH equations is cast in an unsteady-state form. The equations are then integrated from some initial state (guess) until successive values of the variables do not change. The appeal of the relaxation methods lies in their extreme stability. A drawback is that convergence is generally a very slow process, slowing even more as the solution is approached. For this reason, the method is used (only) for problems which are very difficult to converge or for situations in which a knowledge of how the steady state is achieved is important. Key papers are by Rose, Sweeney, and Schrodt [*Ind. Eng. Chem.*, **50,** 737 (1958)]; Ball (AIChE National Meeting, New Orleans, 1961); Verneuil and Oleson (ACS National Mtg., Los Angeles, 1971); and Ketchum [*Chem. Eng. Sci.*, **34,** 387 (1979)].

Collocation methods are widely used for solving systems of partial differential equations. Despite their considerable potential for certain types of equilibrium-stage simulation problems, collocation methods have not become part of the mainstream of equilibrium-stage simulation. Key papers are by Stewart et al. [*Chem. Eng. Sci.*, **40,** 409 (1985)], Swartz and Stewart [*AIChE J.*, **32,** 1832 (1986)], Cho and Joseph [*AIChE J.*, **29,** 261, 270 (1983); *Comput. Chem. Engng.*, **8,** 81 (1984)], and Seferlis and Hrymak [*Chem. Eng. Sci.*, **49,** 1369 (1994); *AIChE J.*, **40,** 813 (1994)].

Methods that have been developed for finding the optimal solution(s) to engineering models have also been used to solve difficult equilibrium-stage separation process problems. An example of a method in this category is that of Lucia and Wang [*Comput. Chem. Engng.,* **28,** 2541 (2004)].

Examples In what follows we illustrate possible column specifications by considering four examples from Seader (*Perry's Chemical Engineers' Handbook,* 7th ed., 1997). They are a simple distillation column, a more complicated distillation column, an absorber, and a reboiled stripper. A simultaneous convergence method was used for the calculations reported below. The computer program that was used for these exercises automatically generated initial estimates of all the unknown variables (flows, temperatures, and mole fractions). In most cases the results here differ only very slightly from those obtained by Seader (almost certainly due to small differences in physical property constants).

Example 3: Simple Distillation Column Compute stage temperatures, interstage vapor and liquid flow rates and compositions, and reboiler and condenser duties for the butane-pentane splitter studied in Example 1. The specifications for this problem are summarized below and in Fig. 13-37.

The specifications made in this case are summarized below:

Variable	Number	Value
Number of stages	1	11
Feed stage location	1	6
Component flows in feed	$c = 5$	5, 15, 25, 20, 35 lb·mol/h
Feed pressure	1	120 psia
Feed vapor fraction	1	0
Pressure on each stage including condenser and reboiler	$N = 11$	$P_j = 120$ psia
Heat duty on each stage except reboilers and condensers	$N - 2 = 9$	$Q_j = 0$
Vapor flow to condenser (replaces heat duty of reboiler)	1	$V_2 = 175$ lb·mol/h
Distillate flow rate (replaces heat duty of condenser)	1	$D = 48.9$ lb·mol/h
Total	31	

In addition, we have assumed that the pressure of the reflux divider is the same as the pressure of the condenser, the heat loss from the reflux divider is zero, and the reflux temperature is the boiling point of the condensed overhead vapor.

The Peng-Robinson equation of state was used to estimate K values and enthalpy departures [as opposed to the De Priester charts used in Example 1 and by Seader (ibid.) who solved this problem by using the Thiele-Geddes (op. cit.) method].

With 11 stages and 5 components the equilibrium-stage model has 143 equations to be solved for 143 variables (the unknown flow rates, temperatures, and mole fractions). Convergence of the computer algorithm was obtained in just four iterations. Computed product flows are shown in Fig. 13-37.

A pseudobinary McCabe-Thiele diagram for this multicomponent system is shown in Fig. 13-38. For systems with more than two components, these diagrams can only be computed from the results of a computer simulation. The axes are defined by the relative mole fractions:

$$X = \frac{x_{lk}}{x_{lk} + x_{hk}} \qquad Y = \frac{y_{lk}}{y_{lk} + y_{hk}}$$

where the subscripts *lk* and *hk* refer to light and heavy key, respectively. The lines in the diagram have similar significance as would be expected from our knowledge of McCabe-Thiele diagrams for binary systems discussed earlier in this section; the triangles correspond to equilibrium stages. The operating lines are not straight because of heat effects and because the feed is not in the best location.

The fact that the staircase of triangles visible in Fig. 13-38 fails to come close to the corners of the diagram where $X = Y = 1$ and $X = Y = 0$ shows that the separation is not especially sharp. It is worth asking what can be done to improve the separation obtained with this column. The parameters that have a significant effect on the separation are the numbers of stages in the sections above and below the feed, the reflux ratio, and a product flow rate (or reflux flow). Figure 13-39 shows how the mole fraction of *i*-pentane in the overhead and of *n*-butane in the bottom product changes with the reflux ratio. For the base case considered above, the reflux ratio is 2.58 (calculated from the results of the simulation). It is clear that increasing the reflux ratio has the desired effect of improving product purity. This improvement in purity is, however, accompanied by an increase in both the operating cost, indicated in Fig. 13-39 by the increase in reboiler duty, and capital cost, because a larger column would be needed to accommodate the increased internal flow. Note, however, that the curves that represent the mole fractions of the keys in the overhead and bottoms appear to flatten, showing that product purity will not increase indefinitely as the reflux ratio increases. Further improvement in product purity can best be made by changing a different specification.

Figure 13-40 shows the tradeoff in product purities when we change the specified distillate flow rate, maintaining all other specifications at the values

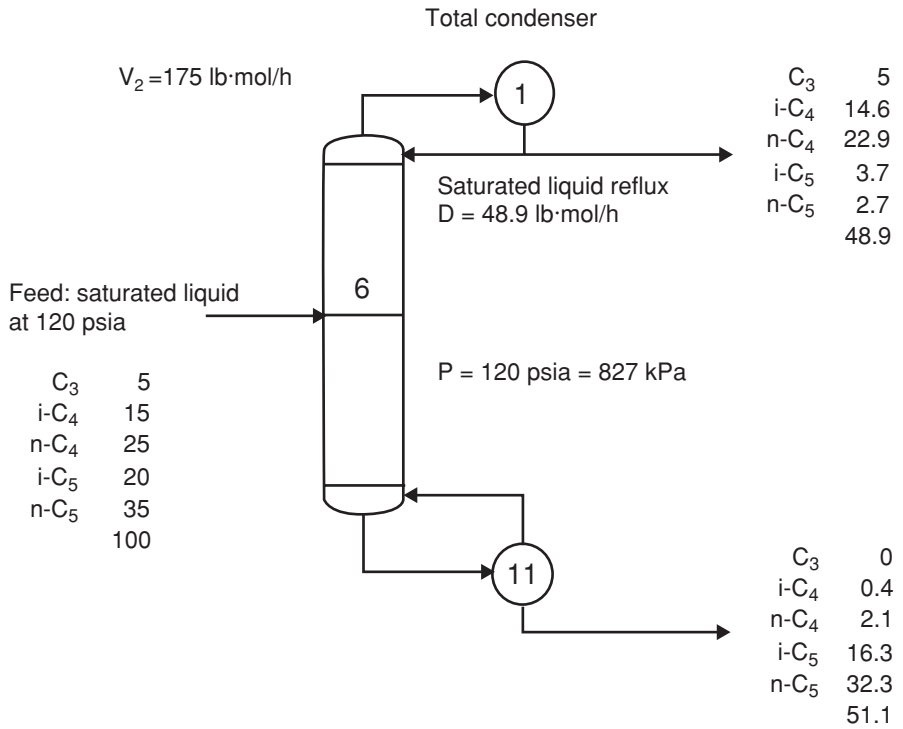

FIG. 13-37 Specifications and calculated product stream flows for butane-pentane splitter. Flows are in pound-moles per hour.

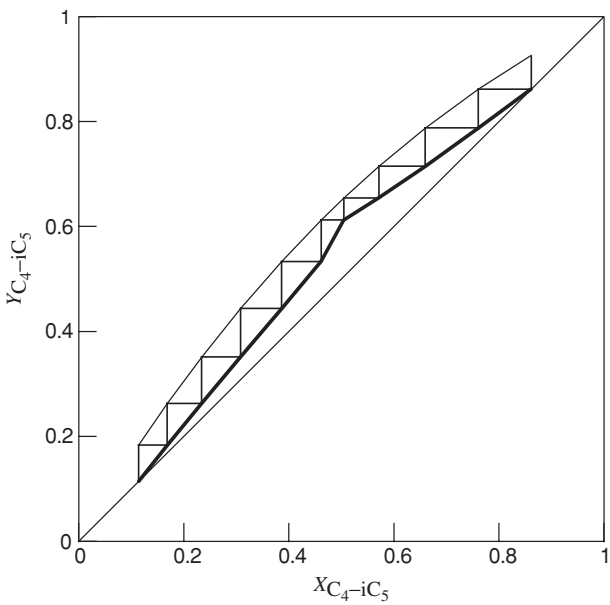

FIG. 13-38 Multicomponent McCabe-Thiele diagram for butane-pentane splitter in Fig. 13-37.

specified in the base case. At lower distillate flow rates the mole fraction of heavy key (*i*-C_5) in the distillate is small, and at higher distillate flow rates the mole fraction of light key (*n*-C_4) in the bottoms is small. Both cannot be small simultaneously. From this result we see that the "best" overall product purities are obtained when the distillate rate is in the vicinity of 45 lb·mol/h. On reflection this should not come as a surprise; the flow rate of the light key (*n*-butane) and all components with a higher volatility is 45 lb·mol/h. However, even with the distillate flow rate set to 45 lb·mol/h there remains room for improvement in the separation.

The other key design specifications here are the total number of stages and the location of the feed stage. In most cases, increasing the number of stages will improve the separation. On increasing the number of stages to 26, with the feed to stage 12, increasing the overhead vapor flow to 195 lb·mol/h, and decreasing the distillate rate to 45 lb· mol/h, we obtain the following products:

Mole flows, lb·mol/h	Feed	Top	Bottom
Propane	5.00	5.00	0.00
Isobutane	15.00	15.00	0.00
N-Butane	25.00	24.81	0.19
Isopentane	20.00	0.16	19.84
N-Pentane	35.00	0.03	34.97
Total	100.00	45.00	55.00

The McCabe-Thiele diagram for this configuration, shown in Fig. 13-41, shows that the product purities have improved significantly.

The temperature and liquid phase composition profiles for this final case are shown in Fig. 13-42. The temperature increases from top to bottom of the column. This is normally the case in distillation columns (exceptions may occur with cold feeds or feeds with boiling points significantly lower than that of the mixture on stages above the feed stage). The composition profiles also are as expected. The components more volatile than the light key (*n*-butane) are

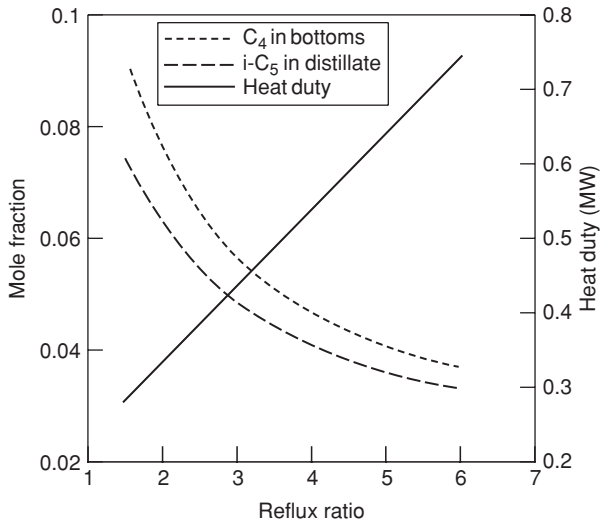

FIG. 13-39 Product mole fractions and reboiler heat duty as a function of the reflux ratio for butane-pentane splitter in Fig. 13-37.

concentrated above the feed; those compounds less volatile than the heavy key (*i*-pentane) are concentrated below the feed. The mole fractions of the two keys exhibit maxima, the light key above the feed stage and the heavy key below the feed stage. The decrease in the mole fraction of light key over the top few stages is necessary to accommodate the increase in the composition of the lighter compounds. Similar arguments pertain to the decrease in the mole fraction of the heavy key over the stages toward the bottom of the column.

Flow profiles are shown in Fig. 13-42*c*. Note the step change in the liquid flow rate around the feed stage. Had the feed been partially vaporized, we would have observed changes in both vapor and liquid flows around the feed stage, and a saturated vapor feed would significantly change only the vapor flow profile. The slight (in this case) curvature in the flow profiles is due to enthalpy changes.

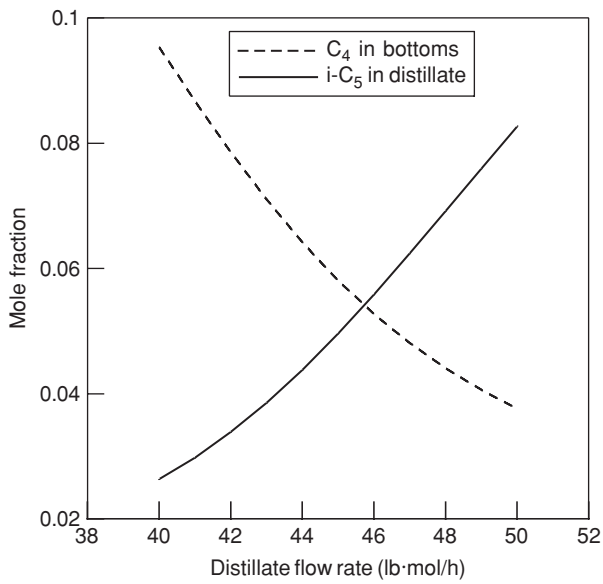

FIG. 13-40 Product mole fraction duty as a function of the distillate rate for butane-pentane splitter in Fig. 13-37.

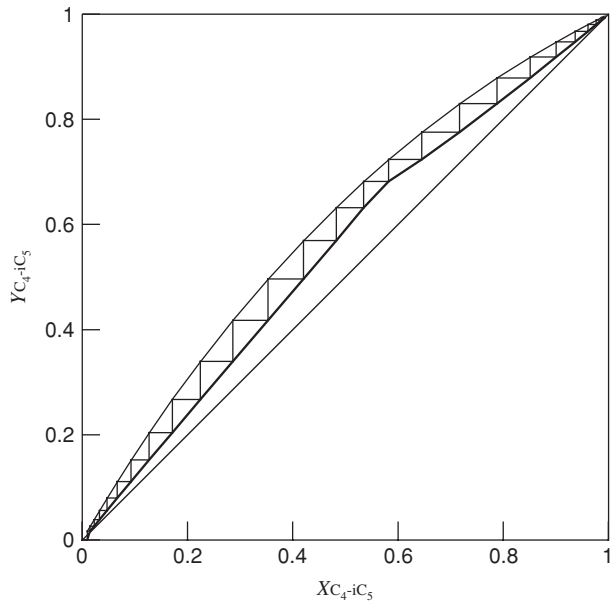

FIG. 13-41 Multicomponent McCabe-Thiele diagram for butane-pentane splitter after optimization to improve product purities.

Example 4: Light Hydrocarbon Distillation Compute stage temperatures, interstage vapor and liquid flow rates and compositions, and reboiler and condenser duties for the light hydrocarbon distillation column shown in Fig. 13-43. How might the separation be improved?

This more complicated example features a partial condenser (with vapor product) and a vapor sidestream withdrawn from the 13th stage. The SRK equation of state may be used for estimating the *K* values and enthalpy departures for thermodynamic properties.

The specifications made in this case are summarized below:

Variable	Number	Value
Number of stages	1	17
Feed stage location	1	9
Component flows in feed	$c = 5$	3, 20, 37, 35, 5 lb·mol/h
Feed pressure	1	260 psia
Feed vapor fraction	1	0
Pressure on each stage including condenser and reboiler	$N = 17$	$P_j = 250$ psia
Heat duty on each stage except reboilers and condensers	$N - 2 = 15$	$Q_j = 0$
Reflux rate (replaces heat duty of reboiler)	1	$L_1 = 150$ lb·mol/h
Distillate flow rate (replaces heat duty of condenser)	1	$D = 23$ lb·mol/h
Sidestream stage	1	13
Sidestream flow rate and phase	2	37 lb·mol/h vapor
Total	46	

As in Example 3, we have assumed that the pressure of the reflux divider is the same as the pressure of the condenser, the heat loss from the reflux divider is zero, and the reflux temperature is the boiling point of the condensed overhead vapor.

The specifications were selected to obtain three products: a vapor distillate rich in C_2 and C_3, a vapor sidestream rich in *n*-C_4, and a bottoms rich in *n*-C_5 and *n*-C_6, as summarized in the table below.

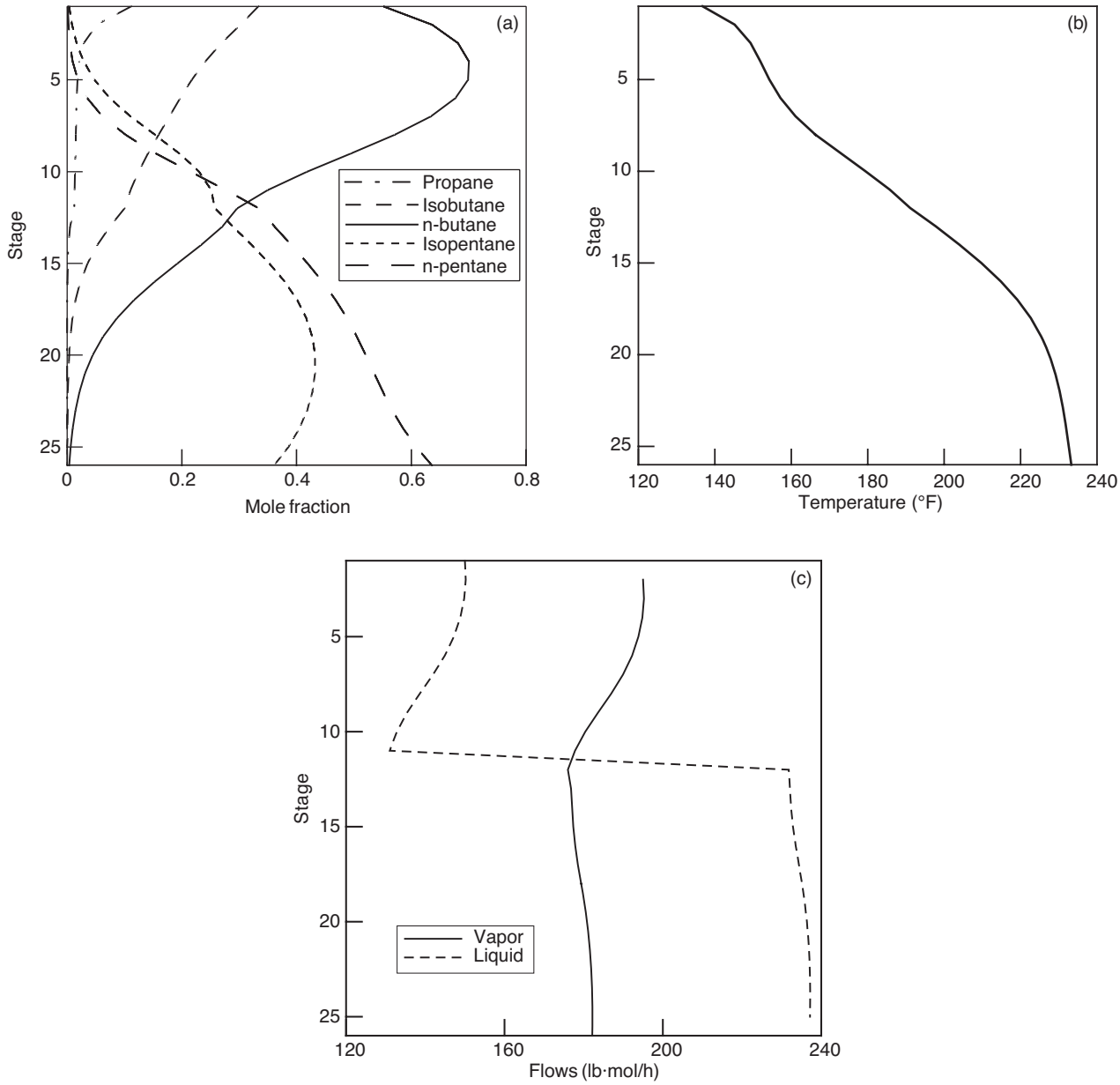

FIG. 13-42 (*a*) Composition, (*b*) temperature, and (*c*) flow profiles in butane-pentane splitter.

Mole flows, lb·mol/h	Feed	Top	Bottom	Sidestream
Ethane	3.00	3.00	0.0	0.0
Propane	20.00	18.3	0.0	1.6
N-Butane	37.00	1.7	9.6	25.7
N-Pentane	35.00	0.0	25.8	9.2
N-Hexane	5.00	0.0	4.5	0.5
Total molar flow	100.00	23.0	40.0	37.0

Convergence of the simultaneous convergence method was obtained in five iterations.

Further improvement in the purity of the sidestream as well as of the other two products could be obtained by increasing the reflux flow rate (or reflux ratio) and the number of stages in each section of the column. If, e.g., we increase the number of stages to 25 (including condenser and reboiler in this total), with the feed to stage 7 and the sidestream removed from stage 17, we obtain the following:

Mole flows, lb·mol/h	Feed	Top	Bottom	Sidestream
Ethane	3.00	3.00	0.00	0.00
Propane	20.00	19.46	0.00	0.54
N-Butane	37.00	0.54	7.46	29.00
N-Pentane	35.00	0.00	27.93	7.07
N-Hexane	5.00	0.00	4.61	0.39
Total	100.0	23.0	40.0	37.00

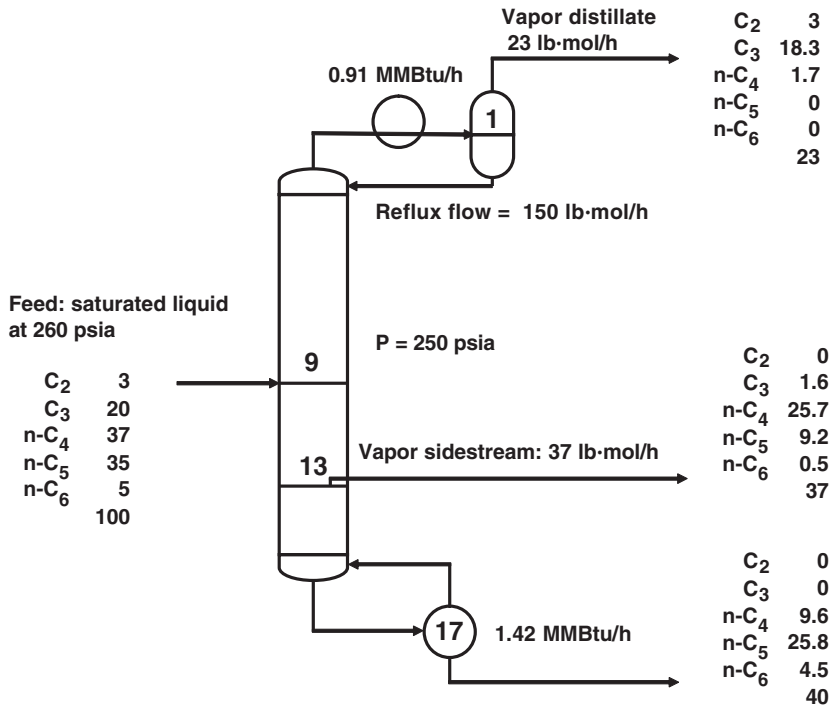

FIG. 13-43 Specifications and calculated product stream flows and heat duties for light hydrocarbon still. Flows are in pound-moles per hour.

The McCabe-Thiele diagram for this design, showing that the feed is to the optimum stage, is shown in Fig. 13-44. The flow profiles are shown in Fig. 13-45; note the step changes due to both the feed and the sidestream. As was the case in Example 3, the curvature in the flow profiles is due to enthalpy changes.

Example 5: Absorber Compute stage temperatures and interstage vapor and liquid flow rates and compositions for the absorber specifications shown in Fig. 13-46. Note that a second absorber oil feed is used in addition to the main absorber oil and that heat is withdrawn from the seventh theoretical stage. The oil may be taken to be *n*-dodecane.

The specifications made in this case are summarized below:

Variable	Number	Value(s)
Number of stages	1	8
Location of feed 1	1	1
Component flows in feed 1	$c = 6$	0, 0, 0, 0, 0, 250 lb·mol/h
Pressure of feed 1	1	400 psia
Temperature of feed 1	1	80°F
Location of feed 2	1	4
Component flows in feed 2	$c = 6$	13, 3, 4, 5, 5, 135 lb·mol/h
Pressure of feed 2	1	400 psia
Temperature of feed 2	1	80°F
Location of feed 3	1	8
Component flows in feed 3	$c = 6$	360, 40, 25, 15, 15, 10 lb·mol/h
Pressure of feed 3	1	400 psia
Temperature of feed 3	1	80°F
Pressure on each stage	$N = 8$	$P_j = 400$ psia; $j = 1, 2, \ldots, 8$
Heat duty on each stage	$N = 8$	$Q_j = 0, j = 1, 2, \ldots, 6, 8$; $Q_7 = 150{,}000$ Btu/h
Total	44	

The simultaneous solution method solved this example in four iterations. The Peng-Robinson equation of state was used to estimate *K* values and enthalpy departures and by Seader (*Perry's Chemical Engineers' Handbook,* 7th ed.) who solved this problem by using the SR method.

The computed product flows are summarized below:

Mole flows, lb·mol/h	Lean oil	Secondary oil	Rich gas	Lean gas	Rich oil
Methane	0.0	13.0	360.0	303.7	69.3
Ethane	0.0	3.0	40.0	10.7	32.3
Propane	0.0	4.0	25.0	0.2	28.8
N-Butane	0.0	4.0	15.0	0.0	19.0
N-Pentane	0.0	5.0	10.0	0.0	15.0
N-Dodecane	250.0	135.0	0.0	0.0	385.0
Total molar flow	250.0	164.0	450.0	314.6	549.4

The energy withdrawn from stage 7 has the effect of slightly increasing the absorption of the more volatile species in the rich oil leaving the bottom of the column. Temperature and flow profiles are shown in Fig. 13-47. The temperature profile shows the rise in temperature toward the bottom of the column that is typical of gas absorption processes. The bottom of the column is where the bulk of the absorption takes place, and the temperature rise is a measure of the heat of absorption. The liquid flow profile exhibits a step change due to the secondary oil feed at the midpoint of the column.

Example 6: Reboiled Stripper Compute stage temperatures and interstage vapor and liquid flow rates and compositions and reboiler heat duty for the reboiled stripper shown in Fig. 13-48. Thermodynamic properties may be estimated by using the Grayson-Streed modification of the Chao-Seader method.

The specifications made in this case are summarized in Fig. 13-48 and in the table below. The specified bottoms rate is equivalent to removing most of the *n*-C_5 and *n*-C_6 in the bottoms.

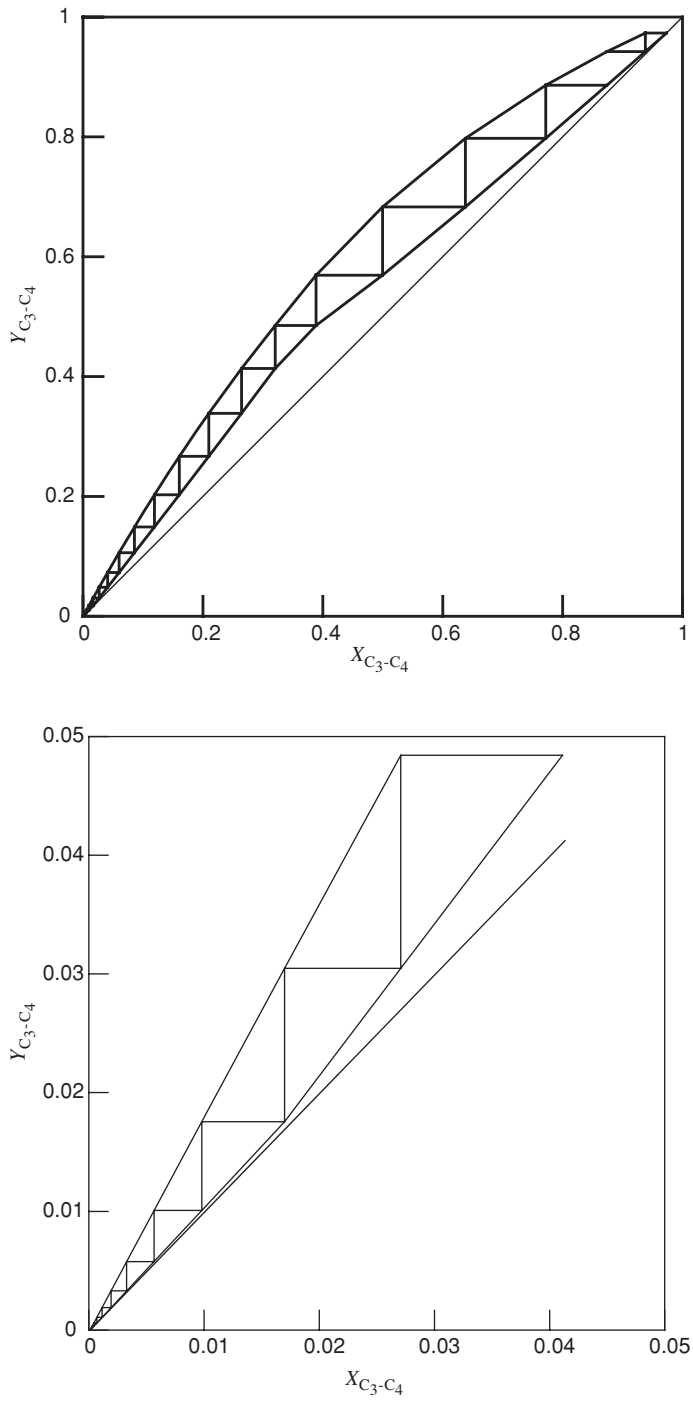

FIG. 13-44 Multicomponent McCabe-Thiele diagram for the hydrocarbon distillation in Fig. 13-43.

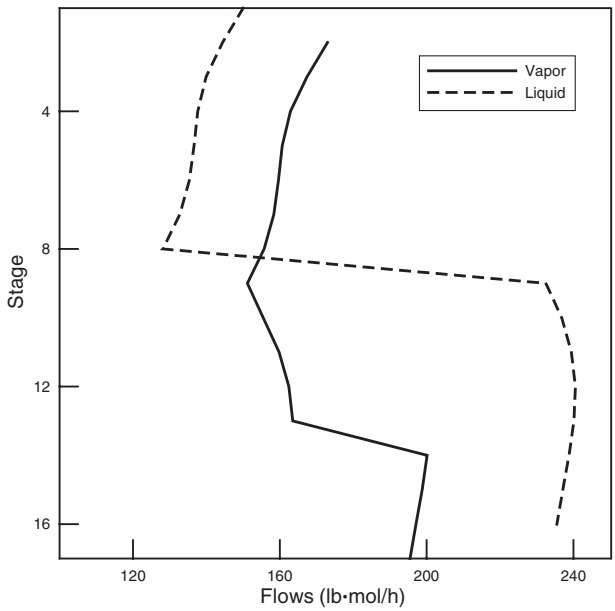

FIG. 13-45 Flow profiles in hydrocarbon distillation in Fig. 13-43.

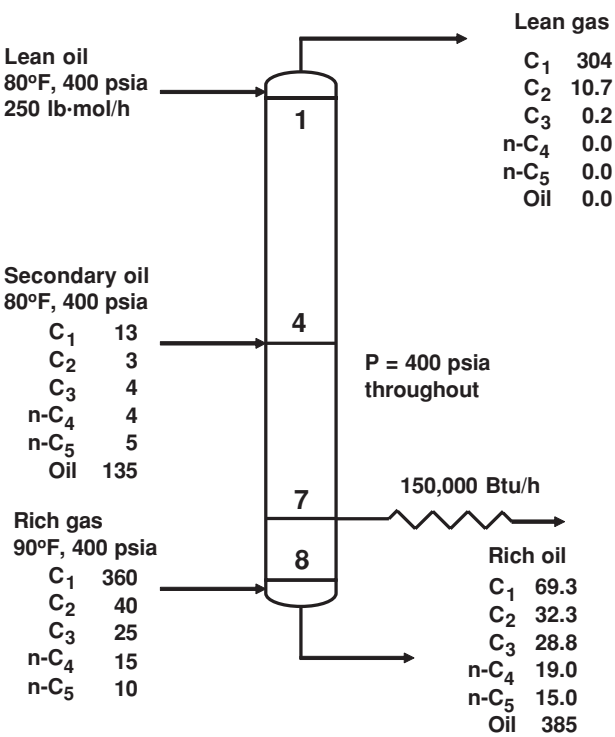

FIG. 13-46 Specifications and calculated product stream flows and heat duties for absorber. Flows are in pound-moles per hour.

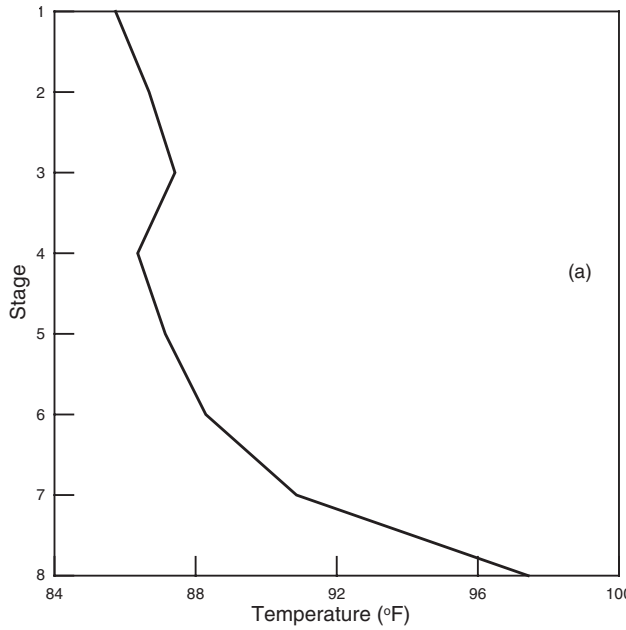

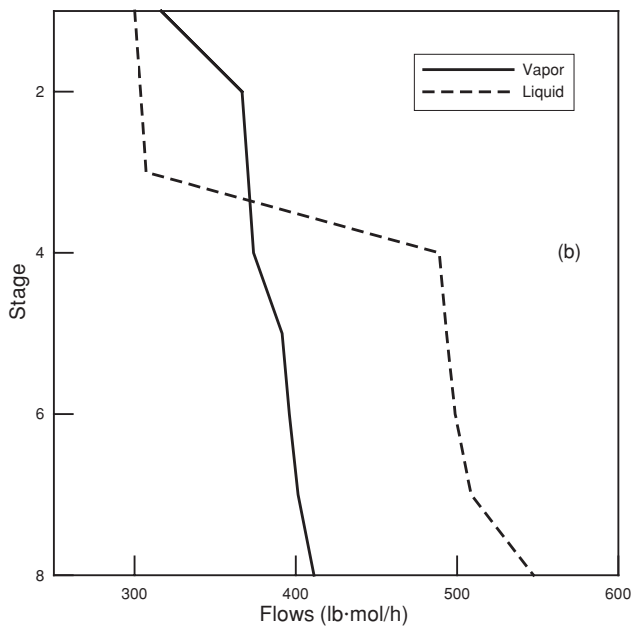

FIG. 13-47 (*a*) Temperature and (*b*) flow profiles in absorber in Fig. 13-46.

Variable	Number	Value(s)
Number of stages	1	8
Component flows in feed	$c = 7$	0.22, 59.51, 73.57, 153.2, 173.2, 58.22, 33.63 lb·mol/h
Pressure of feed	1	150 psia
Temperature of feed	1	40.8°F
Pressure on each stage	$N = 8$	$P_j = 150$ psia; $j = 1, \ldots, 8$
Heat duty on each stage (except reboiler)	$N - 1 = 7$	$Q_j = 0$, $j = 1, \ldots, 7$
Bottom product flow rate	1	99.33 lb·mol/h
Total	26	

Convergence in this case was obtained after four iterations. The computed product flows and reboiler duty are shown alongside the specifications in Fig. 13-48 and in the table below.

Mole flows, lb·mol/h	Feed	Overhead	Bottoms
Nitrogen	0.22	0.02	0.20
Methane	59.51	59.51	0.00
Ethane	73.57	73.57	0.00
Propane	153.22	153.16	0.06
N-Butane	173.22	150.09	23.13
N-Pentane	58.22	13.23	44.99
N-Hexane	33.63	2.69	30.94
Total	551.59	452.26	99.33

Computed temperature, flow rates, and vapor-phase mole fraction profiles, shown in Fig. 13-49, are not of the shapes that might have been expected. Vapor and liquid flow rates for n-C_4 change dramatically from stage to stage.

Example 7: An Industrial* i-*Butane/*n-*Butane Fractionator Klemola and Ilme [*Ind. Eng. Chem.*, **35**, 4579 (1996)] and Ilme (Ph.D. thesis, University of Lapeenranta, Finland, 1997) report data from an industrial *i*-butane/*n*-butane fractionator that is used here as the basis for this example.

The column has 74 valve trays, the design details of which can be found in Example 11. The feed was introduced onto tray 37.

To properly model an existing column, it is necessary to know all feed and product conditions (flow rate, temperature, pressure, and composition). Flows, temperatures, and pressures often are available from standard instrumentation. It may be necessary to obtain additional samples of these streams to determine their composition. Such sampling should be scheduled as part of a plant trial to ensure that measured data are consistent. Ideally, multiple sets of plant measurements should be obtained at different operating conditions, and care should be taken to ensure that operating data are obtained at steady state since a steady-state model can only be used to describe a column at steady state. Measurements should be taken over a time interval longer than the residence time in the column and time-averaged to avoid a possible mismatch between feed and product data. Condenser and reboiler heat duties should be known (or available from the appropriate energy balance) whenever possible.

The measured compositions and flow rates of the feed and products for the C_4 splitter are summarized in the table below.

Measured Feed and Product Flows and Compositions (Mass %) for *i*-Butane/*n*-Butane Fractionator (Ilme op. cit.)

Species	Feed	Top	Bottom
Propane	1.50	5.30	0.00
Isobutane	29.4	93.5	0.30
n-Butane	67.7	0.20	98.1
C_4 olefins	0.50	1.00	0.20
Neopentane	0.10	0.00	0.20
Isopentane	0.80	0.00	1.10
n-Pentane	0.10	0.00	0.10
Total flow, kg/h	26,234	8011	17,887

Other measured parameters are as follows:

Other Details of the *i*-Butane/*n*-Butane Fractionator

Reflux flow rate, kg/h	92,838
Reflux temperature, °C	18.5
Column top pressure, kPa	658.6
Pressure drop per tray, kPa	0.47
Feed pressure, kPa	892.67
Boiler duty, MW	10.24

Rarely, and this is a case in point, are plant data in exact material balance, and it will be necessary to reconcile errors in such measurements before continuing. The feed and product compositions, as adjusted by Ilme so that they satisfy material balance constraints, are provided below. Note how the C_4 olefins are assigned to isobutene and 1-butene.

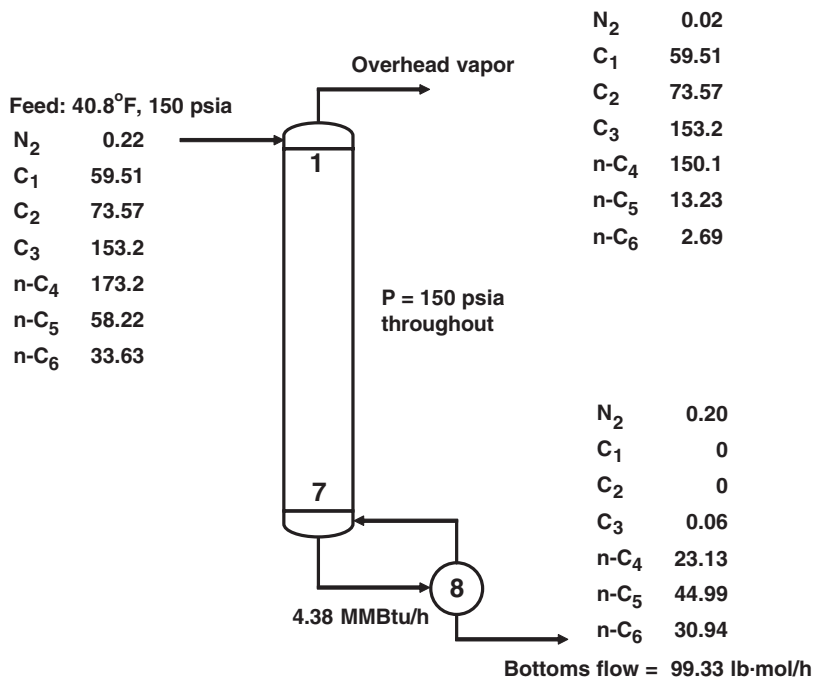

FIG. 13-48 Specifications and calculated product stream flows and reboiler heat duty for a reboiled stripper. Flows are in pound-moles per hour.

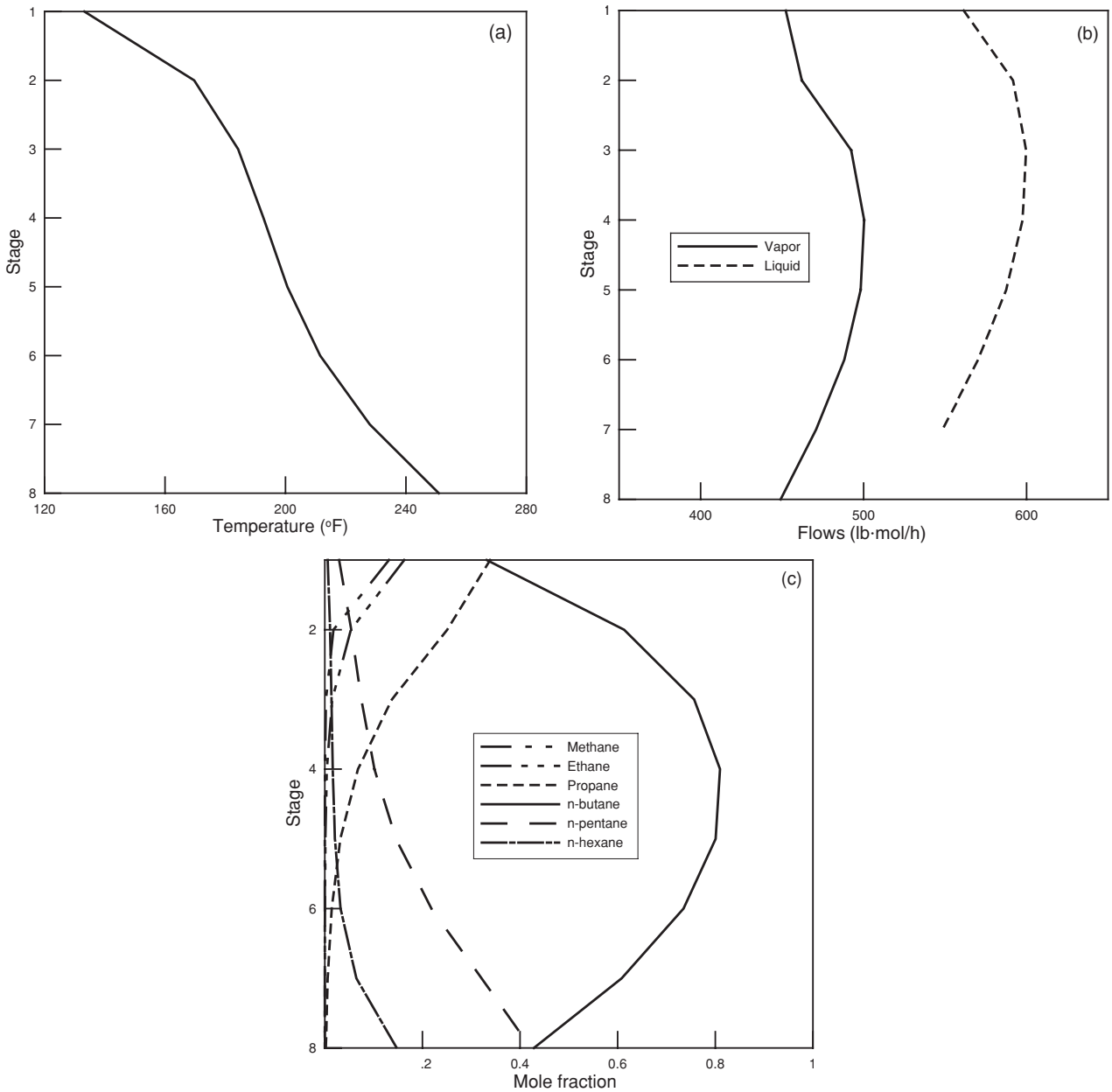

FIG. 13-49 (*a*) Temperature, (*b*) flow, and (*c*) vapor mole fraction profiles in reboiled stripper in Fig. 13-48.

Adjusted Feed and Product Compositions (Mass %) and Flows for *i*-Butane/*n*-Butane Fractionator (Ilme op. cit.)

Species	Feed	Top	Bottom
Propane	1.54	4.94	0.00
Isobutane	29.5	94.2	0.3
n-Butane	67.7	0.20	98.1
Isobutene	0.13	0.23	0.08
1-Butene	0.20	0.41	0.10
Neopentane	0.11	0.00	0.17
Isopentane	0.77	0.00	1.12
n-Pentane	0.08	0.00	0.11
Total flow, kg/h	26,122	8123	17,999

To proceed with building a model of this column, we specify the number of stages equal to the number of trays plus condenser and reboiler ($N = 76$). The common arrangement of locating the actual feed between stages may require modeling as two separate feeds, the liquid portion to the stage below and the vapor portion to the stage above. In this particular illustration the feed is (assumed to be) saturated liquid, and we provide just a single feed to stage 38.

Upon computing the bubble point of the overhead product, we find that the measured reflux temperature is well below the estimated boiling point. Thus, we choose the subcooled condenser model. The steady-state concept of the "subcooled" condenser often does not exist in practice. Instead, the condenser is in vapor-liquid equilibrium with the vapor augmented by a blanket of noncondensable gas (that has the effect of lowering the dew point of the overhead vapor). The subcooled condenser is a convenient work-around for steady-state models (as is needed here), but not for dynamic models. We assume a partial reboiler.

The pressure of the top stage is specified (at 658.6 kPa). The pressures of all trays below the top tray can then be fixed from the knowledge of the per-tray pressure drop (0.47 kPa). The pressure of the condenser is not known here. Thus, in the absence of further information, we make the condenser pressure equal to the top tray pressure (knowing that in practice it will be lower).

It is advisable to use the plant set points in building a model. For example, it is possible that a column simulation might involve the specification of the reflux ratio and bottoms flow rate because such specifications are (relatively) easy to converge. It is quite likely that the column may be controlled by using the temperature at some specific location (e.g., the temperature of tray 48). This specification should be used in building the model. In this case we do not know the set points used for controlling the column, but we do have sufficient information to allow us to compute the reflux ratio from plant flow data ($R = 11.6$). Finally, the bottom product flow is specified as equal to the adjusted value reported above (17,999 kg/h).

The specifications made to model this column are summarized below:

Variable	Number	Value
Number of stages	1	$N = 76$
Feed stage location	1	39
Component flows in feed	$c = 8$	See previous table
Feed pressure	1	120 psia
Feed vapor fraction	1	0
Pressure at the top of the column	1	658.6 kPa
Pressure drop per stage	$N - 1 = 75$	0.47 kPa
Heat duty on each stage except reboilers and condensers	$N - 2 = 74$	$Q_j = 0$
Reflux ratio (replaces heat duty of condenser)	1	$R = 11.588$
Bottoms flow rate (replaces heat duty of reboiler)	1	$B = 17{,}999$ kg/h
Temperature of reflux	1	291.65 K
Total	165	

Finally, we must select appropriate methods of estimating thermodynamic properties. Ilme (op. cit.) used the SRK equation of state to model this column, whereas Klemola and Ilme (op. cit.) had earlier used the UNIFAC model for liquid-phase activity coefficients, the Antoine equation for vapor pressures, and the SRK equation for vapor-phase fugacities only. For this exercise we used the Peng-Robinson equation of state. Computed product compositions and flow rates are shown in the table below.

Specified Feed and Computed Product Compositions (Mass %) and Flows for *i*-Butane/*n*-Butane Fractionator (Ilme op. cit.)

Compound	Feed	Top	Bottom
Propane	1.54	4.95	0.00
Isobutane	29.49	93.67	0.53
n-Butane	67.68	0.73	97.89
Isobutene	0.13	0.29	0.06
1-Butene	0.20	0.36	0.13
Neopentane	0.11	0.00	0.16
Isopentane	0.77	0.00	1.12
n-Pentane	0.08	0.00	0.12
Total flow, kg/h	26,122	8123.01	17,999

The agreement with the adjusted material balance (tabulated previously) appears to be quite good, and to a first approximation it seems that we have a good model of the column.

Note that although this column is distilling a mixture containing at least eight identifiable compounds, only two are present in significant amounts, and therefore this is essentially a binary separation. It is usually relatively straightforward to match product compositions in processes involving only two different species simply by adjusting the number of equilibrium stages. We return to this point later.

Efficiencies In actual operation the trays of a distillation column rarely, if ever, operate at equilibrium despite attempts to approach this condition by proper design and choice of operating conditions. The usual way of dealing with departures from equilibrium in multistage towers is through the use of stage and/or overall efficiencies.

The overall column efficiency is defined by

$$E_o = \frac{N_{\text{EQ}}}{N_{\text{actual}}} \tag{13-57}$$

where N_{EQ} is the number of equilibrium stages.

There are many different definitions of stage (or tray) efficiency, with that of Murphree [*Ind. Eng. Chem.*, **17,** 747–750, 960–964 (1925)] being by far the most widely used in separation process calculations:

$$E_i^{MV} = \frac{y_{i,j} - y_{i,j+1}}{y^*_{i,j} - y_{i,j+1}} \tag{13-58}$$

Here $E_{i,j}^{MV}$ is the Murphree vapor efficiency for component i on stage j, and $y^*_{i,j}$ is the composition of the vapor in equilibrium with the liquid. Other types of efficiency include that of Hausen [*Chemie Ingr. Tech.*, **25,** 595 (1953)], vaporization (see Holland, op. cit.), and generalized Hausen [Standart, *Chem. Eng. Sci.*, **20,** 611 (1965)]. There is by no means a consensus on which is best. Arguments for and against various types are presented by, among others, Standart [op. cit.; *Chem. Eng. Sci.*, **26,** 985 (1971)], Holland and McMahon [*Chem. Eng. Sci.*, **25,** 431 (1972)], and Medina et al. [*Chem. Eng. Sci.*, **33,** 331 (1978), **34,** 1105 (1979)]. Possibly the most soundly based definition, the generalized Hausen efficiency of Standart (op. cit.), is never used in industrial practice. Seader [*Chem. Eng. Progress*, **85**(10), 41 (1989)] summarizes the shortcomings of efficiencies.

The Murphree (and Hausen) efficiencies of both components in a binary mixture are equal; although they cannot be less than 0, they may be greater than 1. A table of typical values of Murphree tray efficiency can be found in Sec. 14. Also described in Sec. 14 are methods for estimating Murphree efficiencies when they are not known.

For multicomponent systems (i.e., those with more than two components) there are $c - 1$ independent component efficiencies, and there are sound theoretical reasons as well as experimental evidence for not assuming the individual component efficiencies to be alike; indeed, they may take values between plus and minus infinity. Component efficiencies are more likely to differ for strongly nonideal mixtures. While models exist for estimating efficiencies in multicomponent systems [see chapter 13 in Taylor and Krishna, (op. cit.) for a review of the literature], they are not widely used and have not (yet) been included in any of the more widely used commercial simulation programs.

The fact that component efficiencies in multicomponent systems are unbounded means that the arithmetic average of the component Murphree efficiencies is useless as a measure of the performance of a multicomponent distillation process. Taylor, Baur, and Krishna [*AIChE J.*, **50,** 3134 (2004)] proposed the following efficiency for multicomponent systems:

$$\varepsilon_j = \frac{\sqrt{\sum_{i=1}^{c} (\Delta y_{i,j})^2}}{\sqrt{\sum_{i=1}^{c} (\Delta y^*_{i,j})^2}} \tag{13-59}$$

This efficiency has a simple and appealing physical significance; it is the ratio of the length of the actual composition profile (in mole fraction space) to the length of the composition profile given by the equilibrium-stage model. The Taylor-Baur-Krishna (TBK) efficiency has just one value per stage regardless of the number of components in the mixture; it can never be negative. For binary systems in tray columns the TBK average efficiency simplifies to the Murphree efficiency [Taylor, Baur, and Krishna (op. cit.)].

Murphree efficiencies are easily incorporated within simultaneous convergence algorithms (something that is not always easy, or even possible, with some tearing methods). (As an aside, note that vaporization

efficiencies are very easily incorporated in all computer algorithms, a fact that has helped to prolong the use of these quantities in industrial practice despite the lack of any convenient way to relate them to the fundamental processes of heat and mass transfer. Unfortunately, it is not at all easy to include the more fundamentally sound TBK efficiencies in a computer method for equilibrium-stage simulations.)

The Murphree-stage efficiency also makes a good continuation parameter for cases that are hard to converge. For vanishingly small stage efficiencies the column performs no separation, and the streams leaving the stage have essentially the same flow rates, composition, and temperature as the combined feeds to the stage. This fact can be exploited in a simple continuation method for solving difficult equilibrium-stage separation process problems [Muller, Ph.D. Thesis in Chem. Engng., ETH Zurich, 1979; Sereno, Ph.D. Thesis in Chem. Engng., University of Porto, 1985; Vickery, Ferrari, and Taylor, *Comput. Chem. Engng.*, **12,** 99 (1988)]. These methods are very effective at solving difficult problems involving *standard specifications* (in which the reflux ratio and bottoms flow rate are specified); however, they cannot easily handle problems involving nonstandard specifications (e.g., when a product stream purity is specified).

Efficiencies are often used to fit actual operating data, along with the number of equilibrium stages in each section of the column (between feed and product takeoff points). The maximum number of these efficiencies is the number of independent efficiencies per stage ($c - 1$) times the number of stages—potentially a very large number, indeed. This many adjustable parameters may lead to a model that fits the data very well, but has no predictive ability (i.e., cannot describe how the column will behave when something changes). At the other extreme, the overall efficiency defined by Eq. (13-57) is just a single parameter that can improve the robustness of the model and speed of convergence, but it may be difficult to match actual temperature and/or composition profiles since there is unlikely to be a one-to-one correspondence between the model stages and actual trays. A compromise often used in practice is to use just one value for all components and all stages in a single section of a column. Efficiencies should not be used to model condensers and reboilers; it is usually safe to assume that they are equilibrium devices. It is also unwise to employ Murphree efficiencies for trays with a vapor product since any Murphree efficiency less than 1 will necessarily lead to the prediction of a subcooled vapor.

Example 8: The Industrial* i-*Butane/*n-*Butane Fractionator (Again) With the material on efficiencies in mind, we return to the model of the C_4 splitter that we developed in Example 7.

It is possible to estimate the overall efficiency for a column such as this one simply by adjusting the number of equilibrium stages in each section of the column that is needed to match the mass fractions of *i*-butane in the distillate and *n*-butane in the bottoms. Using the SRK equation of state for estimating thermodynamic properties, Ilme (op. cit.) found that 82 equilibrium stages (plus condenser and reboiler) and the feed to stage 38 were required. This corresponds to an overall column efficiency of 82/74 = 111 percent. Klemola and Ilme (op. cit.) used the UNIFAC model for liquid-phase activity coefficients, the Antoine equation for vapor pressures, and the SRK equation for vapor-phase fugacities only and found that 88 ideal stages were needed; this corresponded to an overall efficiency of 119 percent. With the Peng-Robinson equation of state for the estimation of thermodynamic properties, we find that 84 stages are needed (while maintaining the feed to the center stage as is the case here); the overall column efficiency for this model is 114 percent. The differences between these efficiencies are not large in this case, but the important point here is that efficiencies—all types—depend on the choice of model used to estimate the thermodynamic properties. Caution must therefore be exercised when one is using efficiencies determined in this way to predict column performance.

As an alternative to varying the number of stages, we may prefer to maintain a one-to-one correspondence between the number of stages and the number of actual trays, 74 in this case (plus condenser and reboiler), with the feed to tray 38. Using the Peng-Robinson equation of state and a Murphree stage efficiency of 116 percent, we find the product mass fractions that are in excellent agreement with the plant data. The McCabe-Thiele (Hengstebeck) diagram for this case, assembled from the results of the simulation, is shown in Fig. 13-50. Composition profiles computed from this model are shown in Fig. 13-51. Note that the mole fractions are shown on a logarithmic axis so that all the composition profiles can easily be seen.

It must be remembered that this is essentially a binary separation and that it is usually relatively straightforward to match product compositions in processes involving only two different species. In other cases involving a greater number of species with significant concentrations, it will likely be necessary to vary both the number of stages and the component efficiencies to match plant data. We do not recommend adjusting thermodynamic model parameters to fit plant data since this can have unfortunate consequences on the prediction of product distributions, process temperatures, and/or pressures.

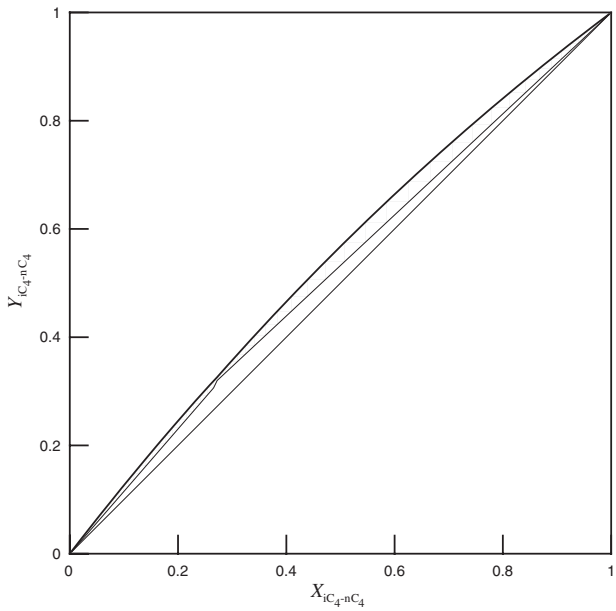

FIG. 13-50 McCabe-Thiele diagram for C_4 splitter.

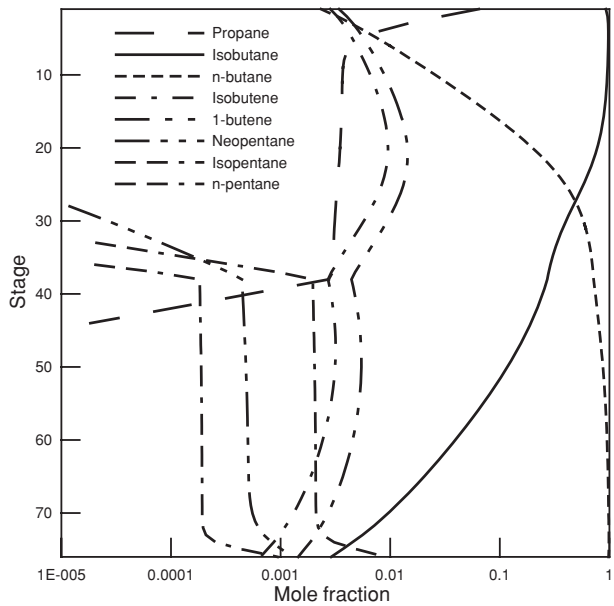

FIG. 13-51 Liquid-phase mole fraction profiles for *i*-butane/*n*-butane fractionator.

The performance of a packed column often is expressed in terms of the height equivalent to a theoretical plate (HETP) for packed columns. The HETP is related to the height of packing H by

$$\text{HETP} = \frac{H}{N_{EQ}} \tag{13-60}$$

In this case N_{EQ} is the number of equilibrium stages (theoretical plates) needed to accomplish the separation that is possible in a real packed column of height H.

Example 9: HETP of a Packed Absorber McDaniel, Bassyoni, and Holland [*Chem. Engng. Sci.*, **25,** 633 (1970)] presented the results of field tests on a packed absorber in a gas plant. The packed section was 23 ft in height, and the column was 3 ft in diameter and filled with 2-in metallic Pall rings. The measured feeds are summarized in the table below.

Stream	Lean oil	Rich gas
Pressure, psia	807	807
Temperature, °F	2.9	0
Mole flows, lb·mol/h		
Carbon dioxide	0.0	14.1
Nitrogen	0.0	5.5
Methane	0.0	2655.8
Ethane	0.0	199.9
Propane	0.0	83.2
Isobutane	0.0	19.1
n-Butane	0.0	10.9
Isopentane	0.2	3.5
n-Pentane	0.2	1.5
n-Hexane	4.5	0.4
n-Heptane	17.2	0.2
n-Octane	54.5	0.1
n-Nonane	50.5	0.0
n-Decane	61.7	0.0
Total molar flow	188.9	2994.2

Determine the number of equilibrium stages needed to match the lean gas product flow for this column (2721.1 lb·mol/h, 93.6% methane).

As a first step, we choose an appropriate thermodynamic model that will be used to estimate K values and enthalpies. Either the Chao-Seader method or the Peng-Robinson equation of state could be considered for this system. It turns out not to be possible to match the plant data with the Chao-Seader method since even one equilibrium stage overpredicts the separation by a very significant amount. It is not even possible to match the exit flows by using the Chao-Seader model combined with a stage efficiency as low as 0.00001. With the Peng-Robinson equation of state, however, it is possible to obtain reasonable agreement with the measured overall product flows by using precisely one equilibrium stage! This suggests that the HETP for this column is 23 ft, a value much higher than any HETP ever published by a packing vendor. In this case the reason for the unrealistic estimate of the HETP has nothing to do with the packing; it is the extreme sensitivity of the simulation to the thermodynamic model, emphasizing the need for caution when one is using efficiencies and HETPs to model some absorption (and distillation) processes.

Using a Simulator to Solve Distillation Problems Computer-based methods for solving distillation (and related) column simulation problems now are reasonably reliable. Nevertheless, at times such methods fail to converge. The principal cause of convergence failures is generally a poor initial estimate of the variables being computed. Below we discuss some of the reasons that a simulation might be difficult to converge, along with suggestions on what might make the problem more amenable to solution. The key idea is to modify the problem that is difficult to solve as posed into one that is easy to solve—essentially to provide an improved initial estimate that is more likely to lead to convergence. Note that most simulators allow a calculation to be restarted from an older converged solution. The solution to the "easy" problem may then be used as a starting point for the more difficult problem whose solution is desired. By doing this we are employing a form of continuation (albeit executed manually, at least in part) to solve those problems with which the algorithm at hand may have trouble.

As a rule, the degree of difficulty increases with increasing nonideality. Simultaneous convergence methods are often recommended for simulating strongly nonideal systems (as opposed to tearing or inside-out methods), but even SC methods can experience difficulties with strongly nonideal systems. A possible remedy is to make the system "less" nonideal. It is likely that an activity coefficient model is part of the model used to describe the thermodynamics of these systems, and the source of the convergence difficulties often encountered with such systems. First solving an equivalent ideal system that omits entirely the activity coefficient model (i.e., using Raoult's law) may provide a converged solution that may be an adequate starting point for the nonideal system of interest. However, since many simulators use ideal solution thermodynamic models in any self-initialization method, this technique may not be of sufficient help.

A measure of the nonideality of the system is given by the magnitude of the interaction parameters for the activity coefficient model. It is possible, therefore, to lessen the degree of nonideality by reducing the interaction parameters sufficiently to make the problem easy to solve. The parameters may then be increased in size in a series of steps until the desired values are reached, each time using the solution converged by using the previous set of parameter values as the starting point. It is essential that the parameters return to their correct values in the final step because intermediate solutions have no meaning, serving merely as an aid to convergence. Using the stage efficiency as a continuation parameter also is useful for such cases, provided that the simulation employs standard specifications (more on this topic below).

The most strongly nonideal systems are those that may exhibit two liquid phases. We have avoided detailed discussion of such systems in this section because special algorithms are needed for these cases; see, however, the section on azeotropic distillation and, for example, chapter 8 of Doherty and Malone (op. cit.) for entry points to the literature.

Large heat effects can lead to convergence difficulties. For such systems it is the enthalpies that are the source of the nonlinearity that leads to convergence failures. It is generally not straightforward to modify enthalpies in a simulator because no adjustable parameters exert their influence over the enthalpy in a way comparable to that of the interaction parameters in the activity coefficient model. Use of a constant-enthalpy model in distillation calculations, if available, will lead to constant molar flows from stage to stage (within each separate section of the column), a condition often approached in many real distillation (but not absorption) columns. Thus, if the simulator includes a constant-enthalpy model, then this can be used to obtain a converged solution that may provide a good starting point for the problem with a more realistic enthalpy model.

High pressure adds to the difficulties of converging simulation models. It is likely that an equation of state will be used to estimate fugacity coefficients and enthalpy departures in such systems. Mixtures become increasingly nonideal as the pressure is raised. In some cases the column may operate close to the critical point at which the densities of both phases approach each other. In other cases the iterations may take the estimates of temperature and composition into regions where the equation of state can provide only one mathematically real root for density or compressibility. Occurrences of this behavior often are a source of convergence difficulties. For such systems we suggest reducing the pressure until the problem becomes easy to solve. A converged solution obtained in this way may be used as the starting point for subsequent calculations at increasingly higher pressures (up to that desired).

Very large numbers of stages can pose their own kind of convergence difficulty. A possible remedy is to reduce the number of stages until a converged solution can be obtained. This solution can then be used as the starting point for a problem with more stages. Interpolation will have to be used to estimate values of the flows, temperatures, and mole fractions for any added stages, something not available in all programs.

Nonstandard specifications are very likely to be the source of convergence difficulties. It is all too easy to specify a desired product purity or component flow rate that simply cannot be attained with the specified column configuration. There is always (at least) one solution if the reflux ratio and bottoms flow rate are specified (the so-called standard specifications), which is likely to converge easily. Other specifications that can cause difficulties for similar reasons include specifying temperatures and compositions anywhere in the column and specifying condenser and/or reboiler heat duties. A way to circumvent this kind of difficulty is first to obtain a converged solution for a case involving standard specifications. Once the behavior of the column is

understood, it will be possible to make sensible nonstandard specifications, again using an old converged result as a starting point.

Columns in which temperature and/or compositions change over a wide range in a limited number of stages pose their own particular difficulties. Some highly nonideal systems exhibit this kind of behavior (see Example 11 below). For cases such as this, it is wise to limit periteration changes to temperature and composition. Most modern computer methods will do this as a matter or course, and problems with this cause are not the source of convergence difficulties that they once were.

This is by no means an exhaustive list of the reasons that computer-based simulations fail. Indeed, in many cases it is a combination of more than one of the above factors that leads to difficulty. In those cases it may be necessary to combine several of the strategies outlined above to solve the simulation problem. Often, however, there is no substitute for trial and error. Haas [chap. 4 in Kister (op. cit.), 1992] offers some additional insight on using simulators to solve distillation column models.

Example 10: Multiple Steady States in Distillation This example is one of the most famous in the entire literature on distillation column modeling, having been studied, in one form or another, by many investigators including Magnussen et al. [*I. Chem. E. Symp. Series*, **56** (1979)], Prokopakis and Seider [*AIChE J.*, **29,** 49 (1983)], and Venkataraman and Lucia [*Comput. Chem. Engng.*, **12,** 55 (1988)]. The column simulated here is adapted from the work of Prokopakis and Seider and shown in Fig. 13-52. The ethanol-benzene-water ternary system actually splits into two liquid phases when the overhead vapor is condensed and cooled below its bubble point. One liquid phase is sent to a second column, and the other is returned to the main column as (cold) reflux. Here, in common with others, this column is modeled by ignoring the condenser and decanter. Reflux is simulated by a feed of appropriate composition, temperature, and pressure to the top of the column. The UNIQUAC method was used for estimating the activity coefficients, with parameters given by Prokopakis and Seider. The numerical results are very sensitive to the choice of activity coefficient model and associated parameters; qualitatively, however, the behavior illustrated below is typical of many systems.

This system is considered difficult because convergence of the MESH equations can be difficult to obtain with any algorithm. In fact, for the specifications considered here, there are no less than three solutions; the composition profiles are shown in Fig. 13-53. The goal of the distillation is to recover high-purity ethanol in the bottom stream from the column by using benzene as a mass separating agent. The low-purity profile in Fig. 13-53*a*, containing a large amount of water in the bottom product, is easily obtained from an ideal solution starting point (but with severe restrictions on the maximum allowed temperature change per iteration). The intermediate profile in Fig. 13-53*b* is rather more difficult to obtain. We were able to find it by using, as a starting point, a profile that had been converged at a stage efficiency of 0.7. The high-purity solution in Fig. 13-53*c*, containing very little water in the bottom product, is also easily obtained from an initial profile calculated by assuming that the stage efficiency is quite low (0.3). Multiple solutions for this column have been reported by many authors (including the three cited above). In fact, with the parameters used here, the three solutions exist over a narrow range of ethanol feed flows. Taylor, Achuthan, and Lucia [*Comput. Chem. Engng.*, **20,** 93 (1996)] found complex-valued solutions to the MESH equations for values outside this range.

Multiple steady-state solutions of the MESH equations have been found for many systems, and the literature on this topic is quite extensive. An introduction to the literature is provided by Bekiaris, Guttinger, and Morari [*AIChE J.*, **46,** 955 (2000)]. Chavez, Seader, and Wayburn [*Ind. Eng. Chem. Fundam.*, **25,** 566 (1986)] used homotopy methods to find multiple solutions for some systems of interlinked columns. Parametric continuation has been used to detect multiple solutions of the MESH equations [Ellis et al., *Comput. Chem. Engng.*, **10,** 433 (1986); Kovach and Seider (op. cit.); Burton, Ph.D. Thesis in Chem. Engng., Cambridge University, 1986]. That real distillation columns can possess multiple steady states has been confirmed by the experimental work of Kienle et al. [*Chem. Engng. Sci.*, **50,** 2691 (1995)], Køggersbol et al. [*Comput. Chem. Engng.*, **20,** S835 (1996)], Gaubert et al. [*Ind. Eng. Chem. Res.*, **40,** 2914 (2001)], and others.

NONEQUILIBRIUM MODELING

Although the widely used equilibrium-stage models for distillation, described above, have proved to be quite adequate for binary and close-boiling, ideal and near-ideal multicomponent vapor-liquid mixtures,

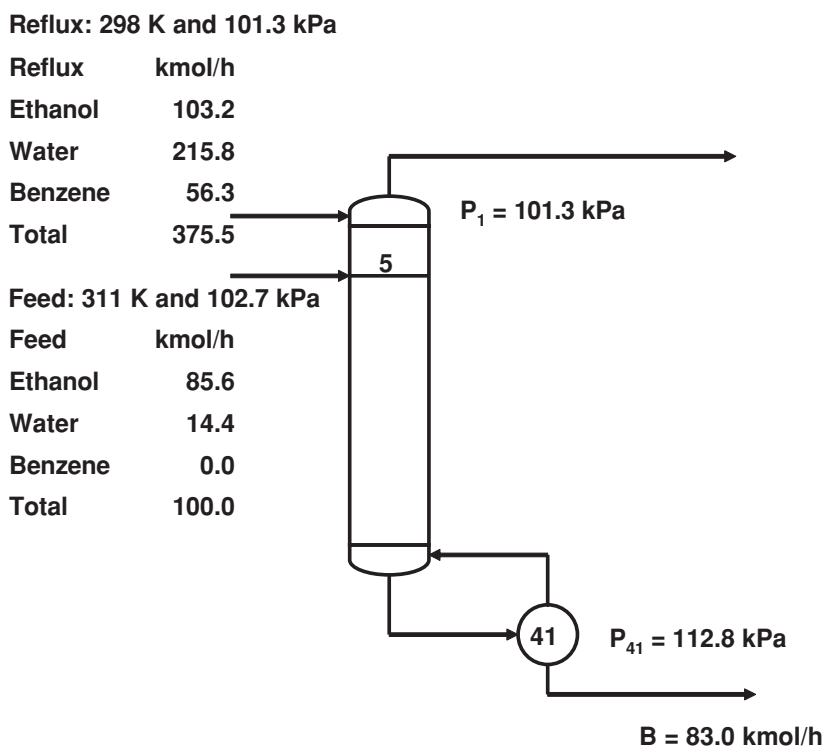

FIG. 13-52 Azeotropic distillation tower for distillation of an ethanol-water mixture using benzene as a mass separating agent. [*After Prokopakis and Seider (op. cit.).*]

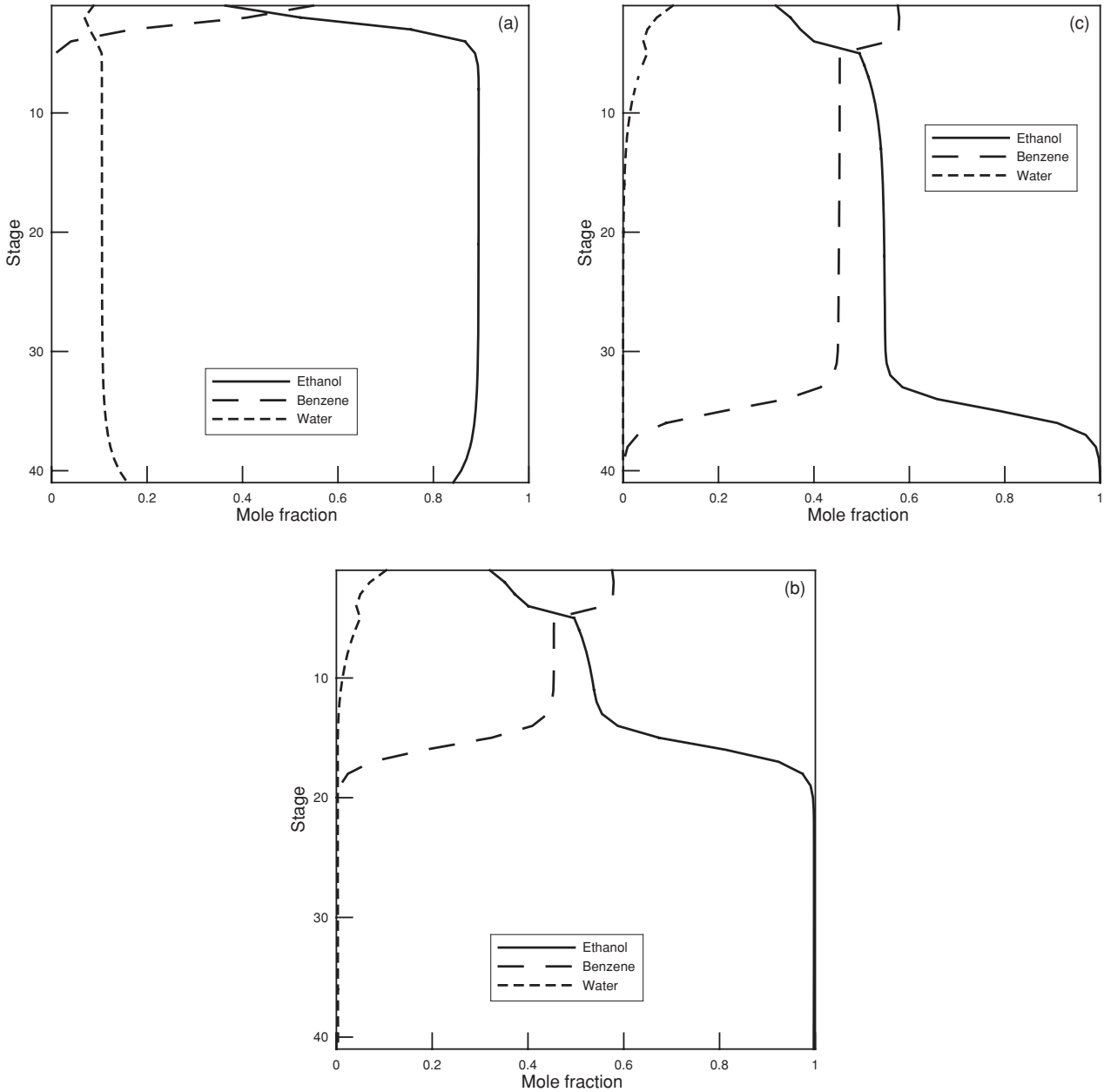

FIG. 13-53 Liquid-phase mole fraction profiles for ethanol-benzene-water distillation. (*a*) Low-purity profile. (*b*) Intermediate-purity profile. (*c*) High-purity profile.

their deficiencies for general multicomponent mixtures have long been recognized. Even Murphree (op. cit.), who formulated the widely used plate efficiencies that carry his name, pointed out clearly their deficiencies for multicomponent mixtures and when efficiencies are small. Walter and Sherwood [*Ind. Eng. Chem.*, **33,** 493 (1941)] showed that experimentally measured efficiencies could cover an enormous range, with some values less than 10 percent. Toor [*AIChE J.*, **3,** 198 (1957)] predicted that the Murphree vapor efficiencies in some multicomponent systems could cover the entire range of values from minus infinity to plus infinity, a result that was verified experimentally by others.

In recent years a new approach to the modeling of distillation and absorption processes has become available: the *nonequilibrium* or *rate-based* models. These models treat these classical separation processes as the mass-transfer rate governed processes that they really are, and avoid entirely the (a priori) use of concepts such as efficiency and HETP [Krishnamurthy and Taylor, *AIChE J.*, **31,** 449–465 (1985); Taylor, Kooijman, and Hung, *Comput. Chem. Engng.*, **18,** 205–217 (1994)].

A schematic diagram of a nonequilibrium (NEQ) stage is given in Fig. 13-54. This NEQ stage may represent (part of) the two phases on

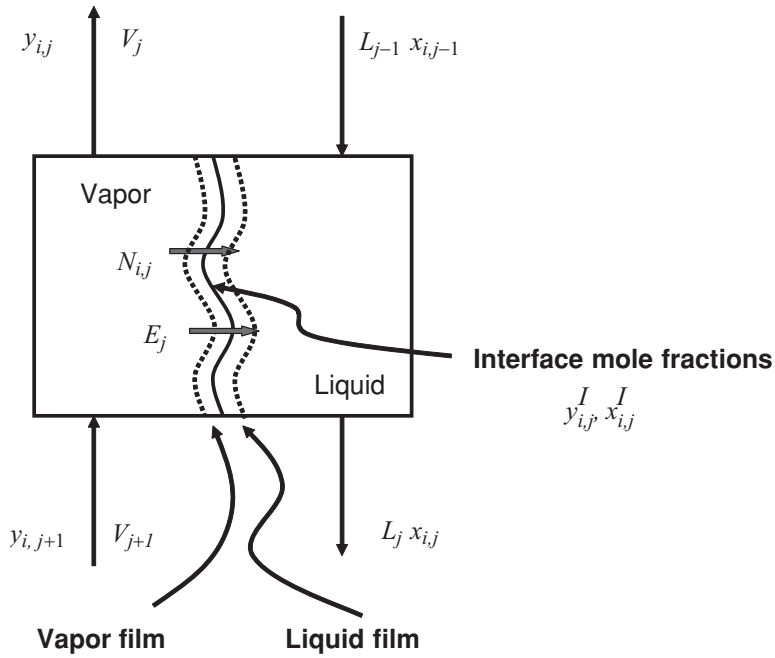

FIG. 13-54 Schematic diagram of a nonequilibrium stage.

a tray or within a section of a packed column. The wavy line in the middle of the box represents the phase interface. This illustration is intended only to aid in understanding the basic principles of nonequilibrium modeling; the actual flow patterns and the shape of the phase boundary are very complicated and depend upon, among other things, the equipment design, the column operation, and the physical properties of the system.

In a nonequilibrium model, separate balance equations are written for each distinct phase. The material balances for each species in the vapor and liquid phases on an arbitrary stage j are

$$(1 + r_j^V)V_j y_{i,j} - V_{j+1} y_{i,j+1} - f_{i,j}^V + \mathcal{N}_{i,j}^V = 0 \qquad (13\text{-}61)$$

$$(1 + r_j^L)L_j x_{i,j} - L_{j-1} x_{i,j-1} - f_{i,j}^L - \mathcal{N}_{i,j}^L = 0 \qquad (13\text{-}62)$$

where r_j^V and r_j^L are the ratios of sidestream to interstage flows and are defined by Eqs. (13-49); $f_{i,j}^p$ is the external feed flow rate of species i in phase p to stage j; and $\mathcal{N}_{i,j}$ is the rate of mass transfer across the phase interface (with units of moles per second or equivalent). Formally, we may write

$$\mathcal{N}_{i,j}^p = \int N_{i,j}^p \, da_j \qquad (13\text{-}63)$$

where $N_{i,j}^p$ is the molar flux in phase p [with units of mol/(m^2·s) or equivalent] at a particular point in the two-phase dispersion and da_j is the portion of interfacial area through which that flux passes. A material balance around the interface yields

$$\mathcal{N}_{i,j}^V = \mathcal{N}_{i,j}^L \qquad (13\text{-}64)$$

The sum of the phase and interface balances yields the component material balance for the stage as a whole, the equation used in the equilibrium-stage model.

The energy balance is treated in a similar way, split into two parts—one for each phase, each part containing a term for the rate of energy transfer across the phase interface.

$$(1 + r_j^V)V_j H_j^V - V_{j+1} H_{j+1}^V - F_j^V H_j^{VF} + \mathcal{E}_j^V + Q_j^V = 0 \qquad (13\text{-}65)$$

$$(1 + r_j^L)L_j H_j^L - L_{j-1} H_{j-1}^L - F_j^L H_j^{LF} - \mathcal{E}_j^L + Q_j^L = 0 \qquad (13\text{-}66)$$

where E_j^p is the rate of energy transfer across the phase interface in phase p and is defined by

$$\mathcal{E}_j^p = \int_a E_j^p \, da \qquad (13\text{-}67)$$

where a is the interfacial area and E_j^p is the energy flux across the interface from/to phase p. An energy balance at the phase interface yields

$$\mathcal{E}_j^V = \mathcal{E}_j^L \qquad (13\text{-}68)$$

In addition, we need summation equations for the mole fractions in the vapor and liquid phases.

A review of early applications of NEQ models is available in chapter 14 of Taylor and Krishna (op. cit.).

It is worth emphasizing that Eqs. (13-61) to (13-68) hold regardless of the models used to calculate the interphase transport rates $\mathcal{N}_{i,j}$ and $\mathcal{E}_j^p$. With a mechanistic model of sufficient complexity it is possible, at least in principle, to account for mass transfer from bubbles in the froth on a tray as well as to entrained droplets in a spray, as well as transport between the phases flowing over and through the elements of packing in a packed column. However, a completely comprehensive model for estimating mass-transfer rates in all the possible flow regimes does not exist at present, and simpler approaches are used.

The simplest approach is to say that the molar fluxes at a vapor-liquid interface may be expressed as

$$N_i^V = c_t^V k_i^V (y_i^V - y_i^I) + y_i^V N_t^V \qquad (13\text{-}69)$$

with a similar expression for the liquid phase.

$$N_i^L = c_t^L k_i^L (x_i^I - x_i^L) + x_i^L N_t^L \qquad (13\text{-}70)$$

In these equations c_t^V and c_t^L are the molar densities of the superscripted phases, y_i^V is the mole fraction in the bulk vapor phase, x_i^L is the mole fraction in the bulk liquid phase, and x_i^I and y_i^I are the mole fractions of species i at the phase interface. Also N_t^p is the total molar flux in phase p, and k_i^V and k_i^L are the mass-transfer coefficients for

the vapor and liquid phases (with units of velocity), respectively. Methods for estimating mass-transfer coefficients in distillation processes are discussed briefly below and at greater length in Section 5 of this handbook.

The second term on the right-hand sides of Eqs. (13-69) and (13-70) is not often important in distillation (its neglect is equivalent to the assumption of equimolar counterflows in the column), but can be quite significant in gas absorption.

The energy fluxes are related by

$$E^V = q^V + \sum_{i=1}^{c} N_i^V \overline{H}_i^V = E = q^L + \sum_{i=1}^{c} N_i^L \overline{H}_i^L = E^L \qquad (13\text{-}71)$$

with

$$q^V = h^V(T^V - T^I) \quad q^L = h^L(T^I - T^L) \qquad (13\text{-}72)$$

where h^V and h^L are the heat-transfer coefficients in the vapor and liquid phases, respectively.

The inclusion in the model of the mass and energy transport equations introduces the mole fractions and temperature at the interface. It is common in almost all treatments of mass transfer across a phase boundary to assume that the mole fractions in the vapor and liquid phases at the interface are in equilibrium with each other. We may, therefore, use the very familiar equations from phase equilibrium thermodynamics to relate the interface mole fractions

$$y_i^I = K_i x_i^I \qquad (13\text{-}73)$$

where the superscript I denotes the interface compositions and K_i is the vapor-liquid equilibrium ratio (or K value) for component i. In equilibrium-stage calculations, the equilibrium equations are used to relate the composition of the streams leaving the stage, and the K values are evaluated at the composition of the two exiting streams and the stage temperature (usually assumed to be the same for both phases). In nonequilibrium models the K values are evaluated at the interface composition and temperature by using exactly the same thermodynamic property models as that used in equilibrium-stage simulations. The interface composition and temperature must, therefore, be computed during a nonequilibrium column simulation. Strictly speaking, the composition and temperature at the interface vary with position in two-phase dispersion that exists on a tray or within the confines of a packed bed. In most NEQ models, the interface state is assumed uniform on the stage; thus, the model of a single stage includes one set of mass-transfer, heat-transfer, and phase equilibrium equations.

In equilibrium-stage models, the compositions of the leaving streams are related through the assumption that they are in equilibrium (or by use of an efficiency equation). It is important to recognize that efficiencies are not used in a nonequilibrium model; they may, however, be calculated from the results obtained by solving the model equations.

Degrees of Freedom Table 13-10 summarizes the equations for a single nonequilibrium stage. There are $6c + 5$ independent equations per stage. As with the equilibrium-stage model discussed above, we have not included the feed mole fraction summation equation, or those for the vapor and liquid streams coming from adjacent stages.

TABLE 13-10 Equations for a Nonequilibrium Stage

Equation	Equation no.	Number
Vapor-phase component balance	(13-61)	c
Liquid-phase component balance	(13-62)	c
Interface material balance	(13-64)	c
Vapor bulk mole fraction summation equation		1
Liquid bulk mole fraction summation equation		1
Vapor-phase energy balance	(13-65)	1
Liquid-phase energy balance	(13-66)	1
Equilibrium at the interface	(13-73)	c
Mass transfer in the vapor phase	(13-69)	$c - 1$
Mass transfer in the liquid phase	(13-70)	$c - 1$
Energy balance at phase interface	(13-71)	1
Summation equation for vapor mole fractions at phase interface		1
Summation equation for liquid mole fractions at phase interface		1
	Total	$6c + 5$

TABLE 13-11 Variables for a Nonequilibrium Stage

Variable	Symbol	Number	Specified
Vapor and liquid flow rates	V_j, L_j	2	
Sidestream flow rates	U_j, W_j	2	Yes
Vapor-phase bulk composition	$y_{i,j}$	c	
Liquid-phase bulk composition	$x_{i,j}$	c	
Vapor interface composition	$y_{i,j}^I$	c	
Liquid interface composition	$x_{i,j}^I$	c	
Component feed flow rates	$f_{i,j}^V$, $f_{i,j}^L$	$2c$	Yes
Feed pressure and temperature		2	Yes
Vapor-phase temperature	T_j^V	1	
Liquid-phase temperature	T_j^L	1	
Interface temperature	T_j^I	1	
Stage pressure	P_j	1	Yes
Heat loss from vapor phase	Q_j^V	1	Yes
Heat loss from liquid phase	Q_j^L	1	Yes
Mass-transfer rates in the vapor phase	$\mathcal{N}_{i,j}^V$	c	
Mass-transfer rates in the liquid phase	$\mathcal{N}_{i,j}^L$	c	
	Total	$8c + 12$	$2c + 7$

Degrees of Freedom Table 13-10 summarizes the equations for a single nonequilibrium stage. There are $6c + 5$ independent equations per stage. As with the equilibrium-stage model discussed above, we have not included the feed mole fraction summation equation, or those for the vapor and liquid streams coming from adjacent stages.

The variables appearing in these equations are summarized in Table 13-11.

It is important to recognize that we have not included mass- and heat-transfer coefficients in the table of variables. These quantities are considered analogous to the thermodynamic properties of the equilibrium-stage model and are functions of other variables (as discussed in greater detail below).

The $6c + 5$ variables for each stage determined during the solution of the nonequilibrium model equations are the vapor and liquid flow V_j and L_j, respectively; the bulk vapor mole fractions, $y_{i,j}$ (c in number); the bulk liquid mole fractions $x_{i,j}$ (c); the vapor and liquid temperatures T_j^V and T_j^L, respectively; the interface mole fractions and temperature $y_{i,j}^I$ (c), $x_{i,j}^I$ (c), and T_j^I; and the mass-transfer rates $\mathcal{N}_{i,j}^V$ (c) and $\mathcal{N}_{i,j}^L$ (c). Note that the interface material balance, Eq. (13-64), means that only one set of mass-transfer rates really needs to be counted in the set of variables for this stage, say, $\mathcal{N}_{i,j}$ (this reduces the number of variables being computed). The remaining variables, $2c + 7$ in number, that need to be specified, are identified in Table 13-11. It is important to recognize that the other flows and composition variables appearing in the nonequilibrium-stage model equations are associated with the equivalent equations for adjacent stages. Although it appears that the number of degrees of freedom is higher for this more complicated model, this is misleading. The additional variables that are specified here take into account that there is one additional heat duty (one per phase) and that the feed is split into vapor and liquid fractions. In practice, the overall feed flow, pressure, temperature (or vapor fraction), and composition would be specified, and the vapor and liquid component flows in the feed determined from an adiabatic flash.

Physical Properties The only physical properties needed for an equilibrium-stage simulation are those needed to estimate K values and enthalpies; these same properties are needed for nonequilibrium models as well. Enthalpies are required for the energy balance equations; vapor-liquid equilibrium ratios are needed for the calculation of driving forces for mass and heat transfer. The need for mass- (and heat-) transfer coefficients means that nonequilibrium models are rather more demanding of physical property data than are equilibrium-stage models. These coefficients may depend on a number of other physical properties, as summarized in Table 13-12.

Methods for estimating physical and transport properties are described in Sections 4 and 5 of this handbook [see also Poling et al., *The Properties of Gases and Liquids*, McGraw-Hill, 5th ed. (2001)].

Flow Models In a real column the composition of the vapor and liquid phases changes due to flow across a tray or over and around packing. Thus, the bulk phase mole fractions that appear in the rate equations (13-69) and (13-70) vary with position and should not automatically be assumed to be equal to the average exit mole

TABLE 13-12 Physical Property Needs of Equilibrium and Nonequilibrium Models

Property	EQ model	NEQ model	Used for
K values	Yes	Yes	Driving forces
Enthalpy	Yes	Yes	Energy balances
Activity coefficient	Yes	Yes	*K* values, enthalpies
Fugacity coefficients	Yes	Yes	*K* values, enthalpies
Vapor pressure	Yes	Yes	*K* values
Heat capacity	Yes	Yes	Enthalpies, heat-transfer coefficient
Mass-transfer coefficients		Yes	Mass-transfer rate equations
Heat-transfer coefficients		Yes	Energy-transfer rate equation
Density		Yes	Mass-transfer coefficients
Diffusion coefficients		Yes	Mass-transfer coefficients
Viscosity		Yes	Mass-transfer coefficients
Surface tension		Yes	Mass-transfer coefficients
Thermal conductivity		Yes	Heat-transfer coefficients

fractions that appear in the material balance equations. In practice, we assume a flow pattern for the vapor and liquid phases, and this allows us to determine appropriate average mole fractions for use in the rate equations. There are three flow models in general use: mixed flow, plug flow, and dispersion flow (Lockett, op. cit.). A flow model needs to be identified for each phase. If both phases are assumed well mixed, then the average mole fractions are indeed equal to the mole fractions in the exit streams. This is the simplest (and an often used) approach that leads to the most conservative simulation (lowest mass-transfer rates, tallest column); at the opposite extreme is plug flow. The most realistic model is dispersion flow (see Lockett, op. cit.), but this model is not included in most computer implementations of NEQ models as it is quite complicated. For further discussion of the importance of flow models and the equations used to estimate average compositions, see Taylor and Krishna (op. cit.) and Kooijman and Taylor [*Chem. Engng. J.*, **57,** 177 (1995)].

Mass-Transfer Coefficients Mass-transfer coefficients (and the equally important interfacial area, a parameter with which they frequently are combined) may be computed from empirical correlations or theoretical models.

The mass-transfer performance of trays often is expressed by way of a dimensionless group called the number of transfer units [see Lockett (op. cit.), Kister (op. cit.), and Sec. 14 for additional background]. These dimensionless numbers are defined by

$$\mathbb{N}^V = k^V a' t_V = \frac{k^V a h_f}{u_s^V} \tag{13-74}$$

$$\mathbb{N}^L = k^L \bar{a} t_L = \frac{k^L a h_f Z}{Q_L/W} \tag{13-75}$$

where h_f = froth height, m
Z = liquid flow path length, m
W = weir length, m
$Q_L = \dfrac{L}{c_t^L}$ = volumetric liquid flow rate, m^3/s
$u_s = \dfrac{V}{c_t^V A_{bub}}$ = superficial vapor velocity, m/s
A_{bub} = bubbling area of tray, m^2
h_L = clear liquid height on tray, m
a' = interfacial area per unit volume of vapor, m^2/m^3
$\bar{a}$ = interfacial area per unit volume of liquid, m^2/m^3

These areas are related to the interfacial area per unit volume of froth a by

$$a' = \frac{1}{1-a} \quad \bar{a} = \frac{a}{\alpha} \tag{13-76}$$

where $\alpha = h_L/h_f$ is the relative froth density. Also t_V and t_L are the vapor- and liquid-phase residence times, defined by

$$t_V = (1-\alpha) h_f u_s \tag{13-77}$$

$$t_L = \frac{Z}{u_L} = \frac{h_L Z W}{Q_L} \tag{13-78}$$

The *AIChE Bubble Tray Design Manual,* published in 1958 [see also Gerster et al., *Tray Efficiencies in Distillation Columns*, AIChE (1958)], presented the first comprehensive procedure for estimating the numbers of transfer units in distillation. For many years this work represented the only such procedure available in the open literature; the work of organizations such as Fractionation Research Incorporated (FRI) was available only to member companies. Other comprehensive procedures for trays appeared in the 1980s [Zuiderweg, *Chem. Engng. Sci.*, **37,** 1441 (1982); Chan and Fair, *Ind. Engng. Chem. Proc. Des. Dev.*, **23,** 814, 820 (1984)]. Readers are referred to Kister (op. cit.), Lockett (op. cit.), Klemola and Ilme (op. cit.), and Sec. 14 of this handbook for summaries and references to what is available in the open literature.

Example 11: Mass-Transfer Coefficient in a Tray Column Consider again the C_4 splitter that formed the basis of Examples 7 and 8. The key design parameters for the valve trays are given in the table below (from Klemola and Ilme, op. cit.).

Column height	51.8 m	Downcomer area center	0.86 m^2
Column diameter	2.9 m	Tray spacing	0.6 m
Number of trays	74	Hole diameter	39 mm
Weir length, side	1.859 m	Total hole area	0.922 m^2
Weir length, center	2.885 m	Outlet weir height	51 mm
Liquid flow path length	0.967 m per pass	Tray thickness	2 mm
Active area	4.9 m^2	Number of valves per tray	772
Downcomer area, side	0.86 m^2	Free fractional hole area	18.82%

Estimate the mass-transfer coefficients for tray 7 where the flow and physical properties are estimated to be as summarized below:

	Gas/vapor	Liquid
Flow, mol/s	590	550
Density, kg/m^3	16.8	520
Viscosity, N/m^2	8.6×10^{-6}	1.35×10^{-4}
Molecular weight, kmol/kg	58.0	58.0
Diffusivity, m^2/s	800×10^{-9}	1.0×10^{-9}
Surface tension, N/m	0.014	

We use the AIChE correlation to illustrate the general approach, noting that the correlation was not developed specifically for valve trays (few methods were). In this model the number of transfer units is given by

$$\mathbb{N}^V = \frac{0.776 + 4.57\, h_w - 0.238 F_s + 104.8 Q_L/W}{\sqrt{\mathrm{Sc}^V}} \tag{13-79}$$

$$\mathbb{N}^L = 19{,}700\sqrt{D^L}\,(0.4F_s + 0.17)t_L \tag{13-80}$$

In the expressions above h_w is the weir height (m). The vapor-phase Schmidt number Sc^V is defined by $\mathrm{Sc}^V = \mu^V/(\rho^V D^V)$, which here takes the value $\mathrm{Sc}^V = 0.640$.

The superficial velocity is computed next from $u_s^V = V/(c_t^V A_{bub}) = 0.42$ m/s. Here F_s is the so-called F factor and is $F_s = u_s^V\sqrt{\rho^V} = 1.7\ (kg/ms)^{1/2}$. The volumetric liquid flow is $Q_L = L/c_t^L = 0.061\ m^3/s$.

The froth height on the tray is estimated (by using the methods in Sec. 14 of this handbook—see also Lockett, 1986; Kister, 1992) to be $h_f = 0.143$ m. The liquid-phase residence time is $t_L = h_L Z W/Q_L = 4.67$ s.

The number of transfer units follows for the vapor phase from Eq. (13-79) as $\mathbb{N}^V = 2.45$ and for the liquid phase from Eq. (13-80) as $\mathbb{N}^L = 2.33$. The products of the vapor- and liquid-phase mass-transfer coefficients and the interfacial area follow directly from the second parts of the same equations. Note that it is not possible with these correlations to separate the mass-transfer coefficient from the interfacial area. In practice this is not a concern since it is the mass-transfer rates that are needed rather than the fluxes and the product suffices for NEQ model computations.

The diffusivities used in this example were for the light key–heavy key pair of components. For systems similar to this one, the diffusion coefficients of all binary pairs in the mixture would be expected to have similar values. This will not be the case for mixtures of components that differ sharply in their fundamental properties (e.g., size, polarity). For these more highly nonideal mixtures, it is necessary to estimate the mass-transfer coefficients for each of the binary pairs.

The number of transfer units for packed columns is defined by

$$\mathbb{N}^V = \frac{k^V a' H}{u_V} \tag{13-81}$$

$$\mathbb{N}^L = \frac{k^L a' H}{u_L} \tag{13-82}$$

where $u_V = V/(c_t^V A_c)$ and $u_L = L/(c_t^L A_c)$ are the superficial vapor and liquid velocities, with A_c the cross-sectional area of the column; a' is the interfacial area per unit volume. The height of a transfer unit (HTU) is defined as

$$\mathbb{H}^V = \frac{H}{\mathbb{N}^V} = \frac{u_V}{k^V a'} \tag{13-83}$$

$$\mathbb{H}^L = \frac{H}{\mathbb{N}^L} = \frac{u_L}{k^L a'} \tag{13-84}$$

Methods of estimating numbers and/or heights of transfer units and mass-transfer coefficients and interfacial areas in packed columns are reviewed by Ponter and Au Yeung (in *Handbook of Heat and Mass Transfer*, Gulf Pub., 1986), by Wang et al. [*Ind. Eng. Chem. Res.*, **44,** 8715 (2005)], and in Sec. 5 of this handbook; one such method is illustrated below.

Example 12: Mass-Transfer Coefficients in a Packed Column Estimate the mass-transfer coefficients at the top of the packed gas absorber in Example 9. The column has 23 ft of 2-in metallic Pall rings and is 3 ft in diameter. The specific surface area of this packing is 112 m^2/m^3. The flows and physical properties are estimated to be as summarized below.

	Gas/vapor	Liquid
Flow, mol/s	332	37
Temperature, K	267	266
Density, kg/m^3	51.2	705
Viscosity, N/m^2	1.17×10^{-5}	2.43×10^{-4}
Molecular weight, kmol/kg	16.8	87.9
Diffusivity, m^2/s	100×10^{-9}	4.6×10^{-9}
Surface tension, N/m	0.0085	

We will use the well-known correlation of Onda et al. (see Sec. 14) to estimate the mass-transfer coefficients. The vapor-phase coefficient is given by

$$\frac{k^V}{a_p D^V} = A\left(\frac{\rho^V u^V}{\mu^V a_p}\right)^{0.7}\left(\frac{\mu^V}{\rho^V D^V}\right)^{0.33}(a_p d_p)^{-2} \tag{13-85}$$

where d_p is the nominal packing size (2 in = 0.0508 m), and a_p is the specific surface area of the packing. Also A is a constant that has the value 2 if nominal packing size is less than 0.012 m, otherwise, $A = 5.23$.

The liquid-phase mass-transfer coefficient is given by

$$k^L = 0.0051\left(\frac{\rho^L}{\mu^L g}\right)^{-1/3}\left(\frac{u_L}{a'\mu^L}\right)^{2/3}\left(\frac{\mu^L}{\rho^L D^L}\right)^{1/2}(a_p d_p)^{0.4} \tag{13-86}$$

Finally, the interfacial area per unit volume is given by

$$a' = a_p\left\{1 - \exp\left[-1.45\left(\frac{\sigma_c}{\sigma^L}\right)^{0.75}\left(\frac{\rho^L u_L}{a_p \mu_L}\right)^{0.1}\left(\frac{a_p u_L^2}{g}\right)^{0.05}\left(\frac{u_L^2 \rho^L}{a_p \sigma^L}\right)^{0.2}\right]\right\} \tag{13-87}$$

The vapor and liquid velocities are calculated to be $u_V = V/(c_t^V A_t) = 0.42$ m/s and $u_L = L/(c_t^L A_t) = 0.0017$ m/s. Substituting the values provided above into Eqs. (13-85) to (13-87) gives $k^V = 0.0021$ m/s, $a' = 96.2$ m^2/m^3, and $k^L = 3.17 \times 10^{-4}$ m/s.

Solving the NEQ Model Equations In general, a nonequilibrium model of a column has many more equations than does an equivalent equilibrium-stage model. Nevertheless, we use may essentially the same computational approaches to solve the nonequilibrium model equations: simultaneous convergence (Krishnamurthy and Taylor, op. cit.) and continuation methods [Powers et al., *Comput. Chem. Engng.*, **12,** 1229 (1988)]. Convergence of a nonequilibrium model is likely to be slower than that of the equilibrium model because of the greater number of model equations and the associated overhead in evaluating a greater number of physical properties. Finally, we note that the strategies outlined above for helping to converge equilibrium-stage simulation may prove equally useful when simulating distillation operations using the nonequilibrium models described here.

Equipment Design As we have already seen, the estimation of mass-transfer coefficients and interfacial areas from empirical correlations nearly always requires us to know something about the column design. At the very least we need to know the diameter and type of internal column (although usually we need to know more than that since most empirical correlations for mass-transfer coefficients have some dependency on equipment design parameters, e.g., weir height of trays). This need for more or less complete equipment design details suggests that nonequilibrium models cannot be used in preliminary process design (before any actual equipment design has been carried out). This is not true, however. Column design methods are available in the literature as well in most process simulation programs, and it is straightforward to carry out equipment sizing calculations at the same time as the stage equations are being solved (Taylor et al., op. cit.). This does not add significantly to the difficulty of the calculation, while providing the very significant advantage of allowing nonequilibrium or rate-based models to be used at all stages of process simulation.

Example 13: A Nonequilibrium Model of a C_4 Splitter Consider, again the C_4 splitter that formed the basis of Examples 7, 8, and 11.

When we create a nonequilibrium model of this—or any—column, we do not need to guess how many stages to use in each section of the column. The real column had 74 valve trays; the model column includes 74 model trays with the feed to tray 38 [plus a (subcooled) condenser and a reboiler, both of which are modeled as equilibrium stages, as described above]. All operating specifications are the same as for the corresponding equilibrium-stage model and are given in Examples 7 and 8. It is necessary to choose models that allow for the estimation of the rates of interphase mass transfer; that means selecting vapor and liquid flow models and correlations to estimate the mass-transfer coefficients in each phase, as discussed above. In this case the AIChE correlations were used. It is known that this method is more conservative than others (i.e., the predicted efficiencies are lower). The importance of the flow model is clear from the simulation results tabulated below. The predicted component Murphree efficiencies computed with Eq. (13-58) vary more widely from stage to stage and from component to component than might be expected for a system such as this. The TBK efficiency, on the other hand, does not change by more than a few percentage points over the height of the column; the value in the table below is an average of that computed for each tray from the simulation results using Eq. (13-59).

Vapor flow model	Liquid flow model	i-C_4 in distillate, %	n-C_4 in bottoms, %	TBK efficiency, %
Mixed	Mixed	90.2	96.3	63
Plug	Mixed	92.2	97.2	78
Plug	Dispersion	93.9	98.0	106

Internal vapor and/or liquid composition data rarely are available, but such data are the best possible for model discrimination and validation. It is often relatively easy to match even a simple model only to product compositions. In the absence of composition profiles, the internal temperature profile can often be as useful provided that it is known to which phase a measured temperature pertains. The table below compares the few available measured tray temperatures with those computed during the simulation. The agreement is quite good.

	Temperature, °C	
Tray	Measured	Predicted
9	47.5	48.6
65	62.2	62.5
74	63.2	63.1

A portion of the McCabe-Thiele diagram for the simulation involving plug flow of vapor and dispersion flow of the liquid is shown in Fig. 13-55. For a nonequilibrium column these diagrams can only be constructed from the results of a computer simulation. Note that the triangles that represent the stages extend beyond the curve that represents the equilibrium line; this is so because the efficiencies are greater than 100 percent.

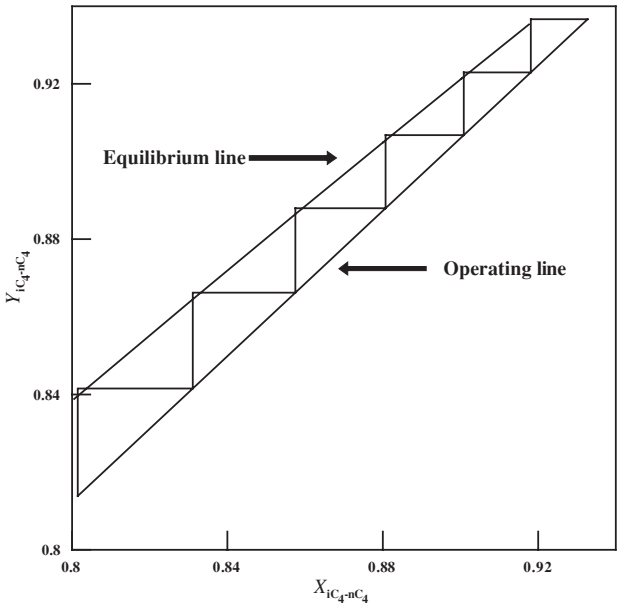

FIG. 13-55 Expanded view near upper right corner of McCabe-Thiele diagram for C_4 splitter.

In this particular case the converged composition and temperature profiles have the same shape as those obtained with the equilibrium-stage model (with specified efficiency) and, therefore, are not shown. The reason for the similarity is that, as noted above, this is basically a binary separation of very similar compounds. The important point here is that, unlike the equilibrium-stage model simulations, the nonequilibrium model predicted how the column would perform; *no parameters were adjusted to provide a better fit to the plant data.* That is not to say, of course, that NEQ models cannot be used to fit plant data. In principle, the mass-transfer coefficients and interfacial area (or parameters in the equations used to estimate them) can be tuned to help the model better fit plant data.

MAXWELL-STEFAN APPROACH

Strictly speaking, Eqs. (13-69) and (13-70) are valid only for describing mass transfer in binary systems under conditions where the rates of mass transfer are low. Most industrial distillation and absorption processes, however, involve more than two different chemical species. The most fundamentally sound way to model mass transfer in multicomponent systems is to use the Maxwell-Stefan (MS) approach (Taylor and Krishna, op. cit.).

The MS equation for diffusion in a mixture with any number of different species can be written as

$$d_i = -\sum_{k=1}^{c} \frac{x_i x_k (u_i - u_k)}{Đ_{ik}} \tag{13-88}$$

where $Đ_{ik}$ is the Maxwell-Stefan diffusion coefficient for the binary *i-k* pair of components. Methods for estimating these coefficients are discussed by Taylor and Krishna (op. cit.) (see also Section 5 of this handbook and Poling et al., op. cit.).

In Eq. (13-88), d_i is termed the generalized driving force. For an ideal gas mixture the driving force is related to the partial pressure gradient and the mole fraction gradient as follows:

$$d_i = \frac{1}{P}\frac{dp_i}{dz} = \frac{dx_i}{dz} \tag{13-89}$$

For a nonideal fluid, the driving force is related to the chemical potential gradient

$$d_i = \frac{x_i}{RT}\frac{d\mu_i}{dz} \tag{13-90}$$

Equations (13-88) for ideal gas mixtures may be derived by using nothing more complicated than Newton's second law: *The sum of the forces acting on the molecules of a particular species is directly proportional to the rate of change of momentum.* The rate of change of momentum between different species is proportional to the concentrations (mole fractions) of the different species and to their relative velocity [see also Taylor and Krishna (op. cit.) for a more complete derivation]. Equation (13-88) is more familiar in the form

$$d_i = -\sum_{k=1}^{c} \frac{x_i N_k - x_k N_i}{c_t Đ_{ik}} \tag{13-91}$$

where we have replaced the velocities by the molar fluxes $N_i = c_i u_i$ (see Section 5). Only $c - 1$ of Eqs. (13-91) are independent; the mole fraction of the last component is obtained by the mole fraction summation equations for both phases.

Solving the MS equations can be quite involved (see Taylor and Krishna, op. cit.). Most often a simple film model solution of Eqs. (13-91) is used, leading to a simple difference approximation to the MS equations

$$\Delta x_i = -\sum_{k=1}^{c} \frac{\bar{x}_i N_k - \bar{x}_k N_i}{c_t \kappa_{i,k}} \tag{13-92}$$

where $\kappa_{i,k}$ is the mass-transfer coefficient for the binary *i-k* pair of components. The Maxwell-Stefan mass-transfer coefficients can be estimated from existing correlations for mass-transfer coefficients using the binary MS diffusion coefficients.

For a nonideal fluid the driving force is related to the chemical potential gradient

$$d_i = \frac{x_i}{RT}\frac{d\mu_i}{dz} \tag{13-93}$$

The difference approximation of this expression is somewhat more involved since we have to include the derivative of the activity (or fugacity) coefficient in the approximation. If, as often is assumed to be the case (not always with justification), the resistance to mass transfer in the liquid phase is negligible, then the MS equations for the liquid phase can safely be replaced by

$$\Delta x_i = x_i^I - x_i^L = 0 \tag{13-94}$$

The use of the MS equations in place of the simpler Eqs. (13-69) and (13-70) does not change the number of independent model equations or the number of degrees of freedom.

Example 14: The Need for Rigorous Maxwell-Stefan-Based NEQ Models Design a distillation column to separate a feed of 20 mol/s methanol, 10 mol/s isopropanol, and 20 mol/s water. The bottom product is to contain no more than 0.5 mol % methanol, and the distillate is to contain at least 99 mol % methanol but no more than 50 ppm water.

As a first step we attempt to design the column by using the equilibrium-stage model. Following Doherty and Malone (op. cit.), the NRTL model was used for the activity coefficients and the Antoine equation for the vapor pressures. Doherty and Malone estimate the minimum reflux as 5; we used a value 50 percent higher in this example and specified the bottoms product rate at 30 mol/s; this choice provides a consistent basis for the comparison of different models. The number of stages and the location of the feed were varied until a column configuration was obtained that met the desired product purity: 80 total stages (including total condenser and partial reboiler) with the feed to stage 16.

Efficiencies of alcohol-water and alcohol-alcohol systems obtained experimentally in sieve tray columns vary from 60 to 100 percent (Sec. 14 in the seventh

edition of this handbook). After specifying an average efficiency of 80 percent, we find that 99 total stages with the feed to stage 21 were needed to get the distillate product below 50 ppm water.

If we use the nonequilibrium model to design a sieve tray column, it is found that a column with 84 trays (plus condenser and reboiler) and with the feed to tray 21 (stage 22) will produce an overhead product of the desired purity. The reflux ratio and bottoms flows were maintained at the values employed for the equilibrium-stage design. The AIChE method was used for estimating the mass-transfer coefficient–interfacial area products, and the vapor and liquid phases were assumed to be in plug flow. The pressure was assumed constant in the column (an assumption that would need to be relaxed at a later stage of the design exercise). The computer simulation also provided a preliminary tray design; that for the trays above the feed is summarized in the table below.

Column diameter, m	1.76
Total tray area, m^2	2.43
Number of flow passes	2
Tray spacing, m	0.6
Liquid flow path length, m	0.75
Active area, % total	91.4
Total hole area, % active	14
Downcomer area, % total	4.3
Hole diameter, mm	5
Hole pitch, mm	12
Weir type	Segmental
Combined weir length, m	1.55
Weir height, mm	50

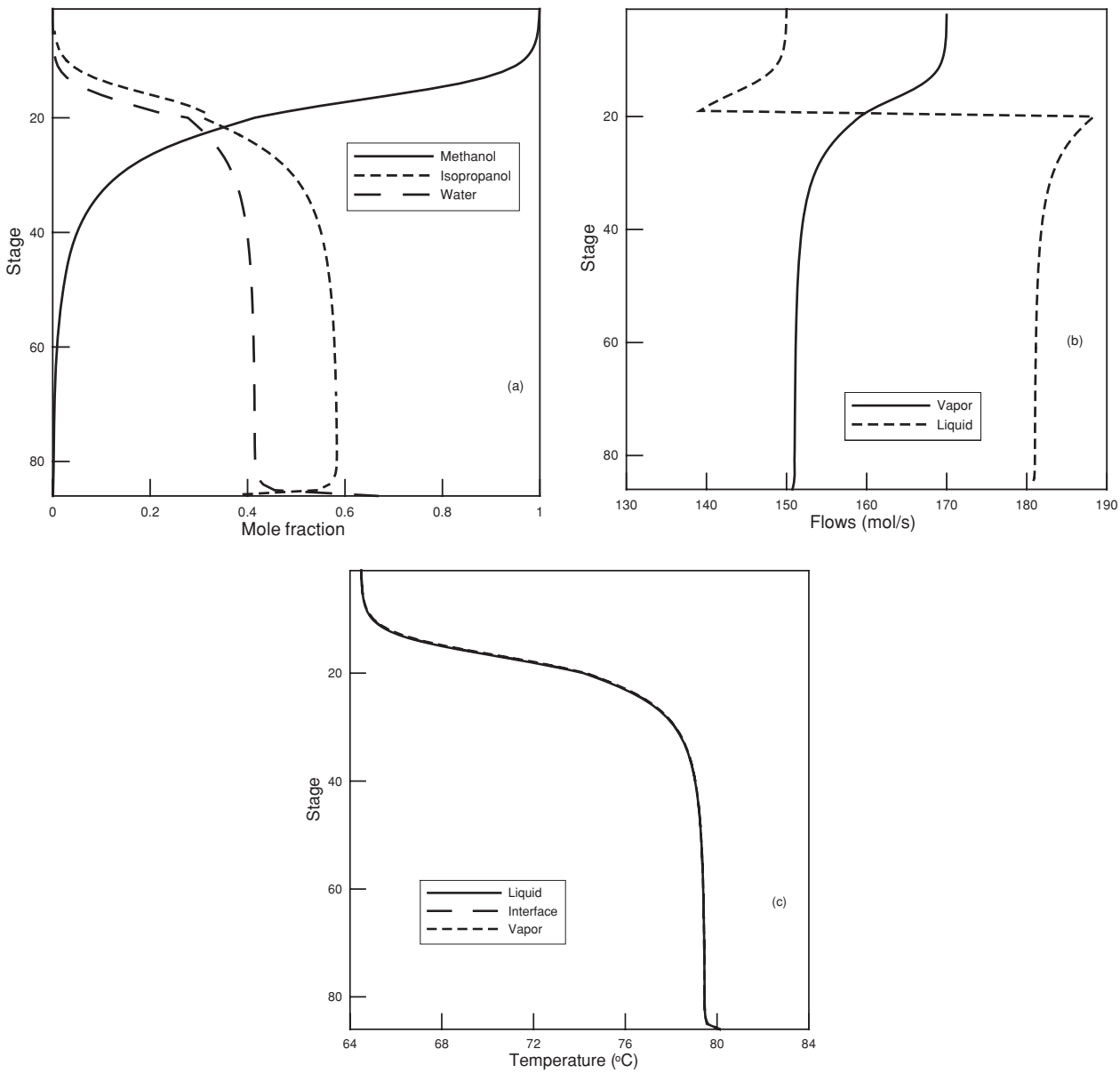

FIG. 13-56 Composition, flow, and temperature profiles in nonideal distillation process.

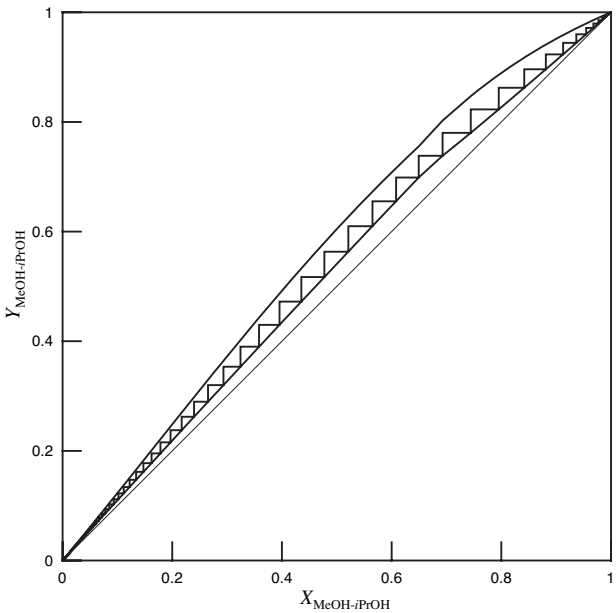

FIG. 13-57 McCabe-Thiele diagram for nonideal distillation column.

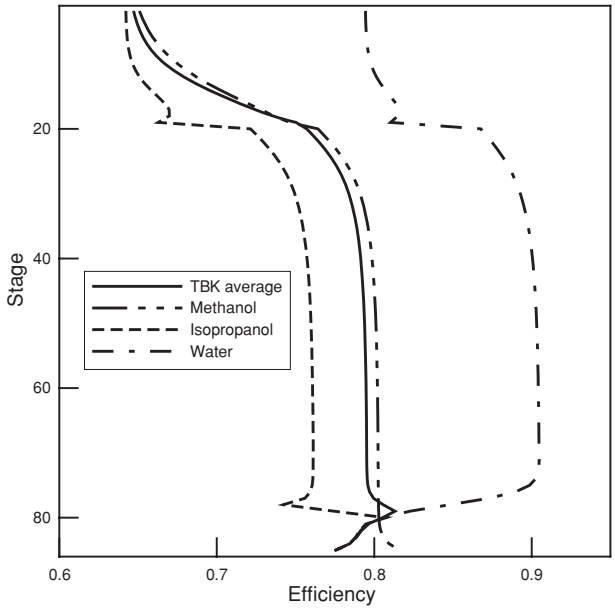

FIG. 13-58 Component Murphree efficiencies and TBK average efficiency [defined by Eq. (13-59)] for nonideal distillation.

To converge the nonequilibrium model at the specified reflux ratio, it was necessary first to solve the problem at a much lower reflux ratio $R = 2$ and then increase R in steps until the desired value of 7.5 was reached.

The liquid composition, flow, and temperature profiles are shown in Fig. 13-56. In this particular system the vapor and liquid temperatures estimated by the rate-based model are quite close (as often is the case in distillation operations).

The McCabe-Thiele diagram for this column is shown in Fig. 13-57. Note that in this case the triangles that represent the stages do not touch the equilibrium line. The length of the vertical section of each step in Fig. 13-57 is a measure of the efficiency of that tray. The component Murphree efficiencies calculated from the simulation results and Eq. (13-58), as well as the TBK average efficiency defined by Eq. (13-59), are shown in Fig. 13-58. The efficiency of methanol in the stripping section is seen to be around 80 percent, that of isopropanol to be approximately 75 percent, while that of water is close to 90 percent in the bulk of the column before falling off on the bottom few trays. All component efficiencies are found to be lower in the rectifying section. The TBK average efficiency, also shown in Fig. 13-58, is close to the Murphree efficiency of methanol and varies from 60 percent in the top of the column to 78 percent. Thus, the constant value of 80 percent used above appears to be appropriate, and yet, the column designed with the constant-efficiency model required no less than 99 stages (97 trays)!

With 84 trays as opposed to 78 equilibrium stages (not counting condenser and reboiler in either case), we find an overall efficiency of 93 percent, a figure that is quite at odds with the values of the individual component efficiencies seen in Fig. 13-58. How, then, is it possible that the nonequilibrium model suggests that the column needs only 6 trays more than the number of equilibrium stages? It is, in fact, because the efficiency of water is so much higher than that of the alcohols that leads to a column design that can produce high-purity methanol while producing the 50-ppm methanol bottom product in so few extra stages. Note that nonequilibrium models will not always lead to a design with fewer trays than might be suggested by a constant-efficiency model; it is just as likely for the mass-transfer rate-based model to predict that more stages will be needed—it all depends on the differences between the component efficiencies.

Individual component efficiencies can vary as much as they do in this example only when the diffusion coefficients of the three binary pairs that exist in this system differ significantly. For ideal or nearly ideal systems, all models lead to essentially the same results. This example demonstrates the importance of mass-transfer models for nonideal systems, especially when trace components are a concern. For further discussion of this example, see Doherty and Malone (op. cit.) and Baur et al. [*AIChE J.* **51,** 854 (2005)]. It is worth noting that there exists extensive experimental evidence for mass-transfer effects for this system, and it is known that nonequilibrium models accurately describe the behavior of this system, whereas equilibrium models (and equal-efficiency models) sometime predict completely erroneous product compositions [Pelkonen et al., *Ind. Engng. Chem. Res.*, **36,** 5392 (1997) and *Chem. Eng. Process*, **40,** 235 (2001); Baur et al., *Trans. I. Chem. E.*, **77,** 561 (1999)].

Nonequilibrium models should be preferred to equilibrium models when efficiencies are unknown, cannot be reliably predicted, and are low and/or highly variable; in nonideal systems and in processes where trace components are a concern.

There is a rapidly growing body of literature on nonequilibrium modeling of distillation and absorption processes. An extended bibliography is available at www.chemsep.org/publications. A brief review of other applications follows.

Simulation methods currently in use for three-phase systems and systems involving chemical reaction employ the equilibrium-stage model [Doherty and Malone (op. cit.)]. Three-phase distillation remains relatively poorly understood compared to conventional distillation operations involving just a single liquid phase. It is important to be able to correctly predict the location of the stages where a second liquid phase can form (e.g., to determine the appropriate location for a sidestream decanter). The limited experimental data available suggest that efficiencies are low and highly variable with between 25 percent and 50 percent being not uncommon. Clearly, a model based on the assumption of equilibrium on every stage cannot hope to be able to *predict* column performance. Cairns and Furzer [*Ind. Engng. Chem. Res.*, **29,** 5392 (1997)] explicitly warn against incorporating Murphree efficiencies into the equilibrium-stage model for three-phase systems, although Müller and Marquardt [*Ind. Engng. Chem. Res.*, **36,** 5410 (1997)] find that an efficiency modified EQ stage model to be perfectly adequate for their column for the dehydration of ethanol using cyclohexane.

It is possible to develop nonequilibrium models for systems with more than two phases, as shown by Lao and Taylor [*Ind. Engng. Chem. Res.*, **33,** 2367 (1994)], Eckert and Vaněk [*Comput. Chem. Eng.*, **25,** 603 (2001)], and Higler et al. [*Comput. Chem. Eng.*, **28,** 2021 (2004)]. Experimental work that can be used to evaluate these models is scarce; see, however, Cairns and Furzer (op. cit.) and Springer et al. [*Chem. Eng. Res. Design*, **81,** 413 (2003)].

There is now an extensive literature on using nonequilibrium models for reactive distillation; see, e.g., Taylor and Krishna [*Chem. Eng.*

TABLE 13-13 Selected List of Suppliers of Column Simulation Software

Supplier	Website	EQ model	NEQ model
Aspen Tech	www.aspentech.com	Yes	Yes
Bryan Research & Engineering	www.bre.com	Yes	
ChemSep	www.chemsep.com	Yes	Yes
Chemstations	www.chemstations.net	Yes	Yes
Deerhaven Technical Software	www.deerhaventech.com	Yes	
Honeywell	www.honeywell.com	Yes	Yes
Process Systems Engineering	www.psenterprise.com	Yes	Yes
ProSim	www.prosim.net	Yes	
SimSci-ESSCOR	www.simsci-esscor.com	Yes	Yes
VMG	virtualmaterials.com	Yes	

Sci., **55,** 6139 (2000)], Sundmacher and Kienle (*Reactive Distillation: Status and Future Directions*, Wiley-VCH, 2003), Noeres et al. [*Chem. Engng. Processing*, **42,** 157 (2003)], and Klöcker et al. [*Chem. Engng. Processing*, **44,** 617 (2005)]. Gas absorption accompanied by chemical reaction for a long time has been modeled by using mass-transfer rate-based concepts; see, e.g., Cornelisse et al. [*Chem. Eng. Sci.*, **35,** 1245 (1980)], Pacheco and Rochelle [*Ind. Eng. Chem. Res.*, **37,** 4107 (1998)], and a review by Kenig et al. [*Chem. Eng. Technol.*, **26,** 631 (2003)]. For such systems the chemical reaction influences the efficiencies to such an extent that the concept loses its meaning.

Even at steady state, efficiencies vary from component to component and with position in a column. Thus, if the column is not at steady state, then efficiencies also must vary with time as a result of changes to flow rates and composition inside the column. Thus, equilibrium-stage models with efficiencies should not be used to model the dynamic behavior of distillation and absorption columns. Nonequilibrium models for studying column dynamics are described by, e.g., Kooijman and Taylor [*AIChE J.*, **41,** 1852 (1995)], Baur et al. [*Chem. Eng. Sci.,* **56,** 2085 (2001)], Gunaseelan and Wankat [*Ind. Eng. Chem. Res.*, **41,** 5775 (2002)], Peng et al. [*Chem. Eng. Sci.*, **58,** 2671 (2003)], and Kenig et al. [*Chem. Eng. Sci.*, **54,** 5195 (1999)].

SOFTWARE FOR DISTILLATION COLUMN SIMULATIONS

Computer software for equilibrium-stage and nonequilibrium column models is available from a number of suppliers. Many other models have been implemented primarily for research purposes and are not available commercially.

In Table 13-13 we list several suppliers of column simulation models that are available commercially, without in any way claiming that this list is exhaustive or providing an endorsement of any particular package. We recommend that users interested in any of these (or other) packages carry out an independent evaluation that focuses on the ability of the package to tackle the simulation problems of direct interest. The simulations described in this subsection were carried out with *ChemSep*.

DEGREES OF FREEDOM AND DESIGN VARIABLES

DEFINITIONS

In the models described in previous subsections, we have determined the degrees of freedom on a case-by-case basis. We now develop a general approach to the topic.

For separation processes, a design solution is possible if the number of independent equations equals the number of unknowns

$$N_i = N_v - N_c \tag{13-95}$$

where N_v is the total number of variables (unknowns) involved in the process under consideration, N_c is the number of restricting relationships among the unknowns (independent equations), and N_i is the degrees of freedom that must be specified for there to be exactly the same number of unknowns as there are independent equations in the model. The concept of degrees of freedom in this context is similar to the same concept that appears in the Gibbs phase rule. The degrees of freedom is the number of design variables that must be specified to define one unique operation (solution) of the process.

The variables N_i with which the designer of a separation process must be concerned are

1. Stream concentrations (e.g., mole fractions)
2. Temperatures
3. Pressures
4. Stream flow rates
5. Repetition variables N_r

The first three are intensive variables. The fourth is an extensive variable that is not considered in the usual phase rule analysis. The fifth is neither an intensive nor an extensive variable but is a single degree of freedom that the designer uses in specifying how often a particular element is repeated in a unit. For example, a distillation column section is composed of a series of equilibrium stages, and when the designer specifies the number of stages that the section contains, he or she uses the single degree of freedom represented by the repetition variable ($N_r = 1.0$). If the distillation column contains more than one section (such as above and below a feed stage), the number of stages in each section must be specified, and as many repetition variables exist as there are sections, that is, $N_r = 2$.

The various restricting relationships N_c can be classified as

1. Inherent
2. Mass balance
3. Energy balance
4. Phase distribution
5. Chemical equilibrium

The inherent restrictions are usually the result of definitions and take the form of identities. For example, the concept of the equilibrium stage involves the inherent restrictions that $T^V = T^L$ and $P^V = P^L$ where the superscripts V and L refer to the equilibrium exit streams.

The mass balance restrictions are the C balances written for the C components present in the system. (Since we will deal with only nonreactive mixtures, each chemical compound present is a phase rule component.) An alternative is to write $C - 1$ component balances and one overall mass balance.

The phase distribution restrictions reflect the requirement that $f_i^V = f_i^L$ at equilibrium where f is the fugacity. This may be expressed by Eq. (13-1). In vapor-liquid systems, it should always be recognized that all components appear in both phases to some extent and there will be such a restriction for each component in the system. In vapor-liquid-liquid systems, each component will have three such restrictions, but only two are independent. In general, when all components exist in all phases, the number of restricting relationships due to the distribution phenomenon will be $C\,(N_p - 1)$, where N_p is the number of phases present.

For the analysis here, the forms in which the restricting relationships are expressed are unimportant. Only the number of such restrictions is important.

ANALYSIS OF ELEMENTS

An *element* is defined as part of a more complex *unit.* The unit may be all or only part of an operation or the entire *process.* Our strategy will be to analyze all elements that appear in a separation process and to determine the number of design variables associated with each. The appropriate elements can then be quickly combined to form the desired units and the various units combined to form the entire process. Of course allowance must be made for the connecting streams *(interstreams)* whose variables are counted twice when elements or units are joined.

The simplest element is a *single homogeneous stream.* The variables necessary to define it are

	N_v^e
Compositions	$C-1$
Temperature	1
Pressure	1
Flow rate	1
	$C+2$

There are no restricting relationships when the stream is considered only at a point. Henley and Seader *(Equilibrium-Stage Separation Operations in Chemical Engineering,* Wiley, New York, 1981) count all C compositions as variables, but then have to include as a restriction.

$$\sum_i x_i = 1 \quad \text{or} \quad \sum_i y_i = 1 \tag{13-96}$$

A stream divider simply splits a stream into two or more streams of the same composition. Consider Fig. 13-59, which shows the division of the condensed overhead liquid L_c into distillate D and reflux L_{N+1}. The divider is permitted to operate nonadiabatically if desired.

Three mass streams and one possible "energy stream" are involved, so

$$N_v^e = 3(C+2) + 1 = 3C + 7 \tag{13-97}$$

Each mass stream contributes $C+2$ variables, but an energy stream has only its rate q as a variable. The independent restrictions are as follows:

	N_c^e
T and P identities between L_{N+1} and D	2
Composition identities between L_{N+1} and D	$C-1$
Mass balances	C
Energy balance	1
	$2C+2$

The number of design variables for the element is given by

$$N_i^e = N_v^e - N_c^e = (3C+7) - (2C+2) = C+5 \tag{13-98}$$

Specification of the feed stream L_c ($C+2$ variables), the ratio L_{N+1}/D, the "heat leak" q, and the pressure of either stream leaving the divider uses these design variables and defines one unique operation of the divider.

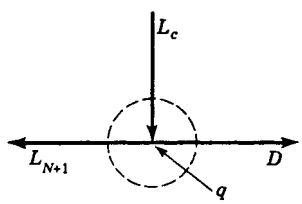

FIG. 13-59 Stream divider.

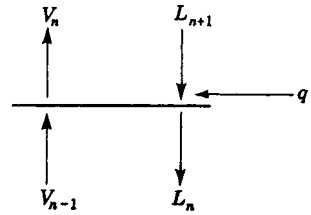

FIG. 13-60 Simple equilibrium stage.

A simple equilibrium stage (no feed or sidestreams) is depicted in Fig. 13-60. Four mass streams and a heat leak (or heat addition) stream provide the following number of variables:

$$N_v^e = 4(C+2) + 1 = 4C + 9 \tag{13-99}$$

Vapor and liquid streams V_n and L_n, respectively, are in equilibrium with each other by definition and therefore are at the same T and P. These two inherent identities when added to C-component balances, one energy balance, and the C phase distribution relationships give

$$N_v^e = 2C + 3 \tag{13-100}$$

Then

$$N_i^e = N_v^e - N_c^e \tag{13-101}$$

$$= (4C+9) - (2C+3) = 2C + 6 \tag{13-102}$$

These design variables can be used as follows:

Specifications	N_i^e
Specification of L_{n+1} stream	$C+2$
Specification of V_{n-1} stream	$C+2$
Pressure of either leaving stream	1
Heat leak q	1
	$2C+6$

The results of the analyses for all the various elements commonly encountered in distillation processes are summarized in Table 13-14. Details of the analyses are given by Smith (*Design of Equilibrium Stage Processes,* McGraw-Hill, New York, 1967) and in a somewhat different form by Henley and Seader (op. cit.).

ANALYSIS OF UNITS

A *unit* is defined as a combination of elements and may or may not constitute the entire process. By definition

$$N_v^u = N_r + \sum_i N_i^e \tag{13-103}$$

and

$$N_i^u = N_v^u - N_c^u \tag{13-104}$$

TABLE 13-14 Design Variables N_i^e for Various Elements

Element	N_v^e	N_c^e	N_f^e
Homogeneous stream	$C+2$	0	$C+2$
Stream divider	$3C+7$	$2C+2$	$C+5$
Stream mixer	$3C+7$	$C+1$	$2C+6$
Pump	$2C+5$	$C+1$	$C+4$
Heater	$2C+5$	$C+1$	$C+4$
Cooler	$2C+5$	$C+1$	$C+4$
Total condenser	$2C+5$	$C+1$	$C+4$
Total reboiler	$2C+5$	$C+1$	$C+4$
Partial condenser	$3C+7$	$2C+3$	$C+4$
Partial reboiler	$3C+7$	$2C+3$	$C+4$
Simple equilibrium stage	$4C+9$	$2C+3$	$2C+6$
Feed stage	$5C+11$	$2C+3$	$3C+8$
Sidestream stage	$5C+11$	$3C+4$	$2C+7$
Adiabatic equilibrium flash	$3C+6$	$2C+3$	$C+3$
Nonadiabatic equilibrium flash	$3C+7$	$2C+3$	$C+4$

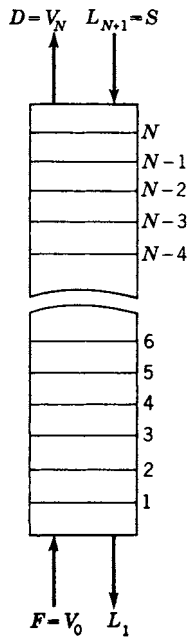

FIG. 13-61 Simple absorption column.

where N_c^u refers to *new* restricting relationships (identities) that may arise when elements are combined. Here N_c^u does not include any of the restrictions considered in calculating the N_i^e's for the various elements. It includes only the stream identities that exist in each interstream between two elements. The interstream variables $(C + 2)$ were counted in each of the two elements when their respective N_i^e's were calculated. Therefore, $C + 2$ new restricting relationships must be counted for each interstream in the combination of elements to prevent redundancy.

The simple absorber column shown in Fig. 13-61 is analyzed here to illustrate the procedure. This unit consists of a series of simple equilibrium stages of the type in Fig. 13-60. Specification of the number of stages N uses the single repetition variable and

$$N_c^u = N_r + \sum_i N_i^e = 1 + N(2C + 6) \tag{13-105}$$

since $N_i^e = 2C + 6$ for a simple equilibrium stage in Table 13-14. There are $2(N - 1)$ interstreams, and therefore $2(N - 1)(C + 2)$ new identities (not previously counted) come into existence when elements are combined. Subtraction of these restrictions from N_v^u gives N_i^u, the design variables that must be specified.

$$N_i^u = N_v^u - N_c^u = N_r + \sum_i N_i^e - N_c^u \tag{13-106}$$

$$= [1 + N(2C + 6)] - 2[(N - 1)(C + 2)] \tag{13-107}$$

$$= 2C + 2N + 5 \tag{13-108}$$

These might be used as follows:

Specifications	N_i^u
Two feed streams	$2C + 4$
Number of stages N	1
Pressure of either stream leaving each stage	N
Heat leak for each stage	N
	$2C + 2N + 5$

A more complex unit is shown in Fig. 13-62, which is a schematic diagram of a distillation column with one feed, a total condenser, and a partial reboiler. Dotted lines encircle the six connected elements (or units) that constitute the distillation operation. The variables N_v^u that must be considered in the analysis of the entire process are just the sum of the N_i^e's for these six elements since here $N_r = 0$. Using Table 13-14, we get the following:

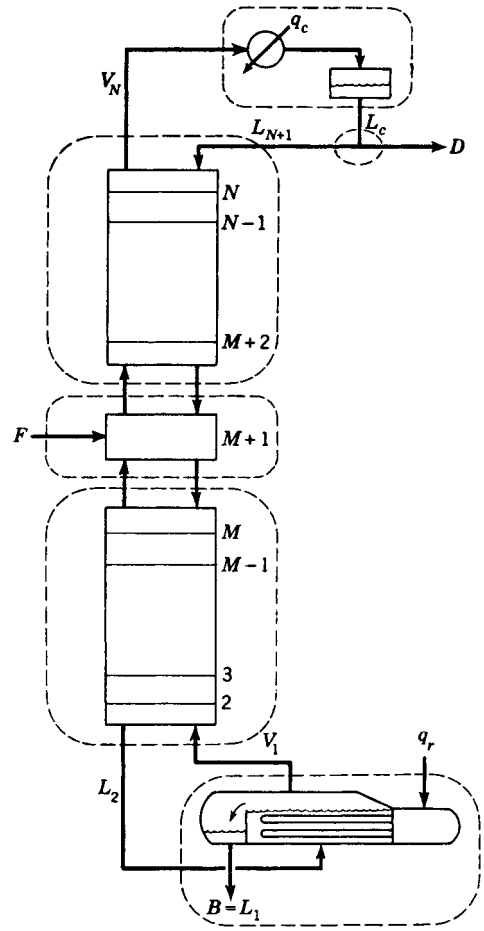

FIG. 13-62 Distillation column with one feed, a total condenser, and a partial reboiler.

Element (or unit)	$N_v^u = \sum_i N_i^e$
Total condenser	$C + 4$
Reflux divider	$C + 5$
$N - (M + 1)$ equilibrium stages	$2C + 2(N - M - 1) + 5$
Feed stage	$3C + 8$
$M - 1$ equilibrium stages	$2C + 2(M - 1) + 5$
Partial reboiler	$C + 4$
	$10C + 2N + 27$

Here, the two units of $N - (M + 1)$ and $M - 1$ stages are treated just as elements. Nine interstreams are created by the combination of elements, so

$$N_c^u = 9(C + 2) = 9C + 18 \tag{13-109}$$

The number of design variables is

$$N_i^u = C + 2N + 9N_v^u = (10C + 2N + 27) - (9C + 18) \tag{13-110}$$

$$= C + 2N + 9 \tag{13-111}$$

One set of specifications that is particularly convenient for computer solutions is the following:

Specifications	N_i^u
Pressure of either stream leaving each stage (including reboiler)	N
Pressure of stream leaving condenser	1
Pressure of either stream leaving reflux divider	1
Heat leak for each stage (excluding reboiler)	$N-1$
Heat leak for reflux divider	1
Feed stream	$C+2$
Reflux temperature	1
Total number of stages N	1
Number of stages below feed M	1
Distillate rate D/F	1
Reflux ratio L_{N+1}/D	1
	$C+2N+9$

Other specifications often used in place of one or more of the last four listed are the fractional recovery of one component in either D or B and/or the composition of one component in either D or B.

OTHER UNITS AND COMPLEX PROCESSES

In Table 13-15, the number of design variables is summarized for several distillation-type separation operations, most of which are shown in Fig. 13-2. For columns not shown in Figs. 13-1 or 13-2 that involve additional feeds and/or sidestreams, add $C+3$ degrees of freedom for each additional feed ($C+2$ to define the feed and 1 to designate the feed stage) and 2 degrees of freedom for each sidestream (1 for the sidestream flow rate and 1 to designate the sidestream-stage location). Any number of elements or units can be combined to form complex processes. No new rules beyond those developed earlier are necessary for the analysis. Further examples are given in Henley and Seader (op. cit.). An alternative method for determining the degrees of freedom for equipment and processes is given by Pham [*Chem. Eng. Sci.*, **49,** 2507 (1994)].

TABLE 13-15 Design Variables N_i^u for Separation Units

Unit	N_i^u*
Distillation (partial reboiler-total condenser)	$C+2N+9$
Distillation (partial reboiler-partial condenser)	$C+2N+6$
Absorption	$2C+2N+5$
Rectification (partial condenser)	$C+2N+3$
Stripping	$2C+2N+5$
Reboiled stripping (partial reboiler)	$C+2N+3$
Reboiled absorption (partial reboiler)	$2C+2N+6$
Refluxed stripping (total condenser)	$2C+2N+9$
Extractive distillation (partial reboiler–total condenser)	$2C+2N+12$

*N includes reboiler, but not condenser.

DISTILLATION SYSTEMS

Distillation systems for the separation of nonazeotropic mixtures are discussed in this subsection. Many of the results extend also to azeotropic mixtures when the desired splits do not attempt to break azeotropes or cross a distillation boundary.

Whenever we desire to separate a mixture into multiple products, various combinatorial possibilities of column arrangements are feasible and the optimal (usually the least expensive) column configurations are sought. For example, there are at least two possible ways of separating a ternary mixture of components A, B, and C into pure-product streams (where A is the most volatile and C the least volatile component):

1. *Direct split*, where component A is separated from BC first (A/BC split) and then mixture BC is distilled to separate B from C
2. *Indirect split*, where C is removed first (AB/C) and then mixture AB is distilled

The difference in energy required for these splits can be assessed by simply comparing the total minimum vapor flows (summed over all the columns) for each column sequence. Example calculations were performed for a mixture with relative volatilities $\alpha_A = 4$, $\alpha_B = 2$, and $\alpha_C = 1$ containing 90 percent of A, 5 percent of B, and 5 percent of C in the feed stream. The indirect split requires 58 percent more energy than the direct split, assuming that columns are connected by a liquid stream in both cases. Moreover, the system using more energy requires bigger heat exchangers and larger column diameters, which increase the capital investment costs. Therefore, the direct split configuration would clearly be a better choice in this case.

One of the most important factors that determines the column configuration is the formulation (or goals) of the separation task with respect to the total flow sheet. Although a mixture may consist of C components, it does not mean that all C products are necessary. The components contained in streams recycled into the process (e.g., unreacted reactants recycled to the reactor) usually do not have to be separated from each other. Also separation of streams that are later mixed (blended) should be avoided, if possible. The separation system needs to be optimized together with the entire plant, either simultaneously or in a hierarchical approach, as described by Douglas (*The Conceptual Design of Chemical Processes,* McGraw-Hill, New York, 1988).

Heuristic methods have been widely used for synthesis of distillation sequences to avoid lengthy calculations. Many heuristics are intuitive, e.g., "Remove corrosive components first," "Remove most plentiful components first," or "Remove the lightest component first." Since heuristics are just rules of thumb, they sometimes conflict with one another and may provide wrong answers even if they are not in conflict among themselves [Malone, Glinos, Marques, and Douglas, *AIChE J.*, **31,** 683 (1985)]. More exact, algorithmic synthesis methods and cost optimization should be used in practice. The total energy of separation has been identified as the major component of the total separation system cost and energy-saving distillation schemes for light hydrocarbons with high levels of flexibility and operability, were discussed by Petterson and Wells [*Chem. Engng.*, **84,** (20), 78, 1977]. Tedder and Rudd presented a three-part paper [*AIChE J.*, **24,** 303 (1978)], where they compared eight distillation systems for the separation of ternary mixtures and determined the regions of economic optimality (with respect to feed compositions and relative volatilities). They proposed several heuristics to compare various configurations. They evaluated several rank order functions that allow for comparison of various configurations without detailed cost calculations. Interestingly, one of the rank order functions used successfully to compare various systems was the total minimum vapor flow. Minimum vapor flow will also be used to compare various distillation systems presented here. Finally, in the third part of their paper, Tedder and Rudd proposed a design method for various column networks.

In other approaches, Gomez-Munoz and Seader [*Comp. & Chem. Eng*, **9,** 311 (1985)] proposed an optimization algorithm based on maximum thermodynamic efficiency. However, Smith and Linhoff [*Chem. Eng. Res. Des.*, **66,** 195 (1988)] pointed out the importance of a simultaneous design of the separation network and the rest of the process. They developed a pinch method based on the temperature–heat duty diagram to accomplish this task. Nishida, Stephanopoulos, and Westerberg [*AIChE J.*, **27,** 321 (1981)] presented a comprehensive review of process synthesis, including distillation. Westerberg [*Comp. & Chem. Eng.*, **9,** 421 (1985)] discussed methods for synthesis of distillation systems that include sharp splits, nonsharp splits, thermal linking, and heat integration. More recently, Agrawal [*AIChE J.*, **49,** 379 (2003)] presented a method for systematic generation of distillation configurations, including conventional and complex columns—a detailed discussion of these systems is given below. Sorting through the alternatives and selecting the low-cost systems can be quite tedious and are best done with computer-aided optimization strategies such as those proposed by Caballero and Grossmann [*Ind. Eng. Chem. Res.*, **40,** 2260 (2001)].

POSSIBLE CONFIGURATIONS OF DISTILLATION COLUMNS

This subsection describes how to generate the feasible combinatorial possibilities of distillation column configurations for separation of mixtures that do not form azeotropes. Components are named A, B, C, D, . . . and they are listed in the order of decreasing volatility (or increasing boiling temperature). We limit our considerations to splits where the most volatile (lightest) component and the least volatile (heaviest) component do not distribute between the top and bottom product. For simplicity, we consider only separations where final products are relatively pure components. Systems containing simultaneously simple and complex distillation columns are considered. Simple columns are the conventional columns with one feed stream and two product streams; complex columns have multiple feeds and/or multiple product streams.

The combinatorial possibilities for separating a three-component mixture ABC into two product streams in which the most volatile component and the least volatile component do not distribute between the top and bottom product are

1. A/BC—Top product A is separated from bottom product BC.
2. AB/BC—Component B distributes between both product streams.
3. AB/C—Top product AB is separated from bottoms C.

These separations are also frequently referred to as splits; sharp splits (none of the components distribute) in cases (1) and (3), and a nonsharp split in case (2). When we add binary separations, the column configuration corresponding to split (1) is known as the direct split; the column configuration corresponding to split (2) is called the prefractionator system, and configuration (3) is called the indirect split (see Fig. 13-63). In the prefractionator system the binary columns separating components AB and BC may be stacked together, forming one column with three products A, B, and C as indicated by the dashed envelope in Fig. 13-63*b*. These systems are called the *basic column configurations*. Basic column configurations are configurations in which the types of interconnecting streams are not defined. The arrows on the flow sheets symbolize the net material flow, but the types of streams connecting the columns (liquid, vapor, two-phase, multiple streams) are not specified. Reboilers and condensers are deliberately not shown in Fig. 13-63, because for some types of interconnecting streams they are not necessary.

Symbolic-network representations of these separation systems, called *state-task networks* (STNs), are shown in Fig. 13-64. In this representation, the states (feeds, intermediate mixtures, and products) are represented by the nodes (ABC, AB, BC, A, B, C) in the network, and the tasks (separations) are depicted as lines (1, 2, . . . , 6) connecting the nodes, where arrows denote the net flow of material. This STN representation was used by Sargent to represent distillation systems [*Comp. & Chem. Eng.*, **22,** 31 (1998)] and has been widely used ever since. Originally STNs were introduced by Kondili, Pantelides, and Sargent [*Comp. & Chem. Eng.*, **17,** 211 (1993)] for representing batch processes.

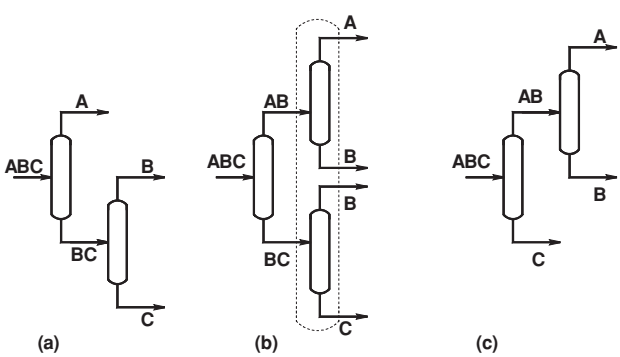

FIG. 13-63 Basic column configurations. (*a*) Direct split. (*b*) Prefractionator system. (*c*) Indirect split.

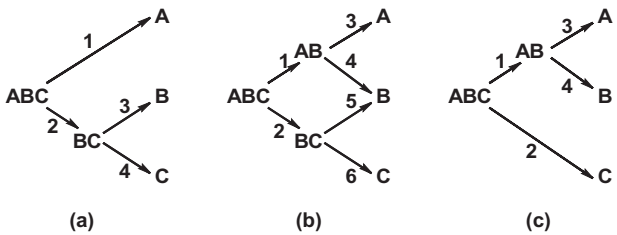

FIG. 13-64 State-task networks. (*a*) Direct split. (*b*) Prefractionator system. (*c*) Indirect split.

Interconnecting streams may be liquids, vapors, or two-phase mixtures. The total energy of separation can be minimized for the direct split if the two columns have a liquid connection; for the indirect split it is minimized if the columns have a vapor connection, and for the prefractionator system if the top connection is vapor and the bottom connection is liquid. See Fidkowski and Krolikowski [*AIChE J.*, **33,** 643 (1987); **36,** 1275 (1990)].

A complete direct split configuration, including reboilers and condensers, is shown in Fig. 13-65*a*. The numbers used to represent the column sections in this figure correspond to the numbers used to represent the tasks in the STN (Fig. 13-64*a*). By eliminating the reboiler from the first column in Fig. 13-65*a* and supplying the boil-up from the second column, we obtain the side rectifier arrangement, shown in Fig. 13-65*b*. An alternative side rectifier arrangement is seen more clearly in Fig. 13-65*c*, where the stripping section of the binary BC column (section 4) has been moved and lumped with the first column. Note that all these three configurations can be represented by one state-task network, shown in Fig. 13-64*a*. In each configuration in Fig. 13-65, feed ABC is separated in section 1 to get component A and in section 2 to get mixture BC. Then mixture BC is further separated in section 3 to give component B and in section 4 to produce C. Therefore, all these three systems are topologically equivalent to the same basic column configuration represented by the STN in Fig. 13-64*a* and the column arrangement in Fig. 13-63*a*. However, if we take into account reboilers and condensers, we see that only the two side rectifier configurations (Fig. 13-65*b* and *c*) are topologically equivalent. Side stripper configurations can be obtained from the indirect split in an analogous way (Fig. 13-66*a*, *b*, and *c*).

By eliminating the reboiler and condenser in the prefractionator column in Fig. 13-67*a* (the column containing sections 1 and 2) we obtain a *thermally coupled system*, also known as a Petlyuk system, shown in Fig. 13-67*b* [Petlyuk, Platonov, and Slavinskii, *Int. Chem. Eng.*, **5,** 555 (1965)]. Side stripper, side rectifier, and Petlyuk systems can also be built as divided wall columns, as explained in detail in the subsection below on thermally coupled systems.

There are many other possible ternary column systems that have different interconnecting streams between the columns. For example, if we eliminate only the reboiler (or only the condenser) from the prefractionator column in Fig. 13-67*a*, we obtain a partially thermally coupled system [Agrawal and Fidkowski, *AIChE J.*, **45,** 485 (1999), U.S. Patent 5,970,742]. In other instances, one may significantly increase the thermodynamic efficiency of the direct split and the indirect split if a portion of the interconnecting stream is vaporized and fed to the second column below the liquid connection [Agrawal and Fidkowski, *Ind. Eng. Chem. Res.*, **38,** 2065 (1999)].

There are six possible types of splits for a quaternary mixture. The ternary mixtures resulting from these splits may be separated in one of the three possible ternary splits, as described above. Table 13-16 summarizes the resulting number of possible basic column configurations. This number does not account for the various possible types of interconnecting streams.

This method of generating various column configurations [Fidkowski, *AIChE J.*, **52,** 2098 (2006)] is very similar to the methods

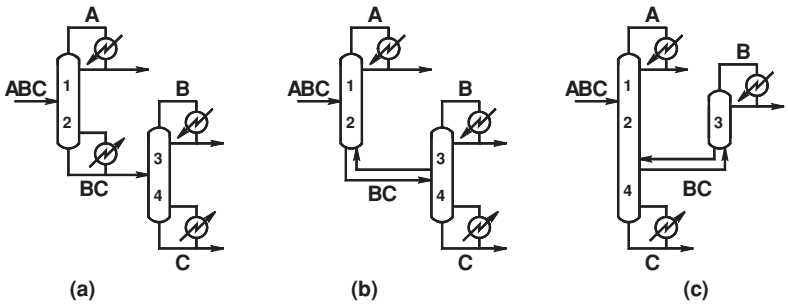

FIG. 13-65 (*a*) Direct split configuration. (*b*), (*c*) Side rectifier configurations.

used previously for conventional systems; see, e.g., Rathore, Van Wormer, and Powers [*AIChE J.*, **20,** 491 (1974); **20,** 940 (1974)]. The only difference is that in addition to sharp splits, the nonsharp splits are included here, which leads to unconventional systems. Similar methods were proposed by Rong et al. [Rong, Kraslawski, and Turunen, *Ind. Eng. Chem. Res.*, **42,** 1204 (2003)] to generate all the possible quaternary thermally coupled configurations.

The basic column configurations for all 22 quaternary distillation systems are shown in Fig. 13-68. Five of these configurations consist of only sharp splits; hence each species appears in only one product stream. Seventeen of the configurations have at least one nonsharp split, which results in each distributing component appearing in product streams from two different locations. Again, the interconnecting streams could be liquid, vapor, two-phase, or two-way liquid and vapor, as in thermally linked columns. There might also be several alternatives for column stacking, which increases the number of possible configurations even further. Subsequently, one can analyze possible splits for a five-component mixture, etc. These splits create quaternary and ternary products that can be further separated by one of the column configurations discussed above.

THERMALLY COUPLED SYSTEMS AND DIVIDING WALL COLUMNS

In recent years there has been significant interest in thermally coupled systems and dividing wall columns for ternary mixtures. In this subsection we discuss such column arrangements, their energy requirements, design and optimization methods, controllability and operability, experimental and industrial experience, and extension to more than three components.

Two columns are thermally coupled if a vapor (liquid) stream is sent from the first column to the second column and then a return liquid (vapor) stream is implemented between the same locations. These streams, when introduced at the top or bottom of a column, provide (at least partial) reflux or boil-up to this column.

The development of thermally coupled systems started with attempts to find energy-saving schemes for the separation of ternary mixtures into three products. One of the first industrial applications was the side rectifier configuration for air separation. The side stripper configuration followed naturally. By combining the two we obtain the fully thermally coupled system of Petlyuk, Platonov, and Slavinskii [*Int. Chem. Eng.*, **5,** 555 (1965)]; see Fig. 13-67*b*. It consists of the prefractionator which accepts the ternary feed stream followed by the main column that produces the products (product column).

The dividing wall column was invented as a way of producing three pure products from a single column [Monro, U.S. Patent 2,134,882 (1933); Wright, U.S. Patent 2,471,134 (1949)]. In some cases it is possible to achieve high purity of the intermediate component in the sidestream of a distillation column. This is possible when the sidestream is withdrawn above the feed as a liquid or below the feed as a vapor and when relative volatilities of components differ significantly. In many applications, however, a sidestream is contaminated to an appreciable extent by either the light or the heavy component. For example, if a sidestream is withdrawn from the rectifying section, it must contain not only the intermediate component but also some of the most volatile component. This contamination problem can be eliminated by adding a dividing wall that prevents the most volatile component (and the heaviest component) from entering the zone where the intermediate component is withdrawn; see Fig. 13-69.

The dividing wall column is topologically equivalent to the fully thermally coupled system (Fig. 13-67*b*). The prefractionator and the main product column are built in one shell, separated by a dividing wall (Fig. 13-69*c*). Similarly, the side rectifier (Fig. 13-65*c*) and side stripper (Fig. 13-66*c*) configurations can be built in one shell as dividing wall columns [Agrawal, *Ind. Eng. Chem. Res.*, **40,** 4258 (2001)]. The corresponding dividing wall columns are shown in Fig. 13-69*a*

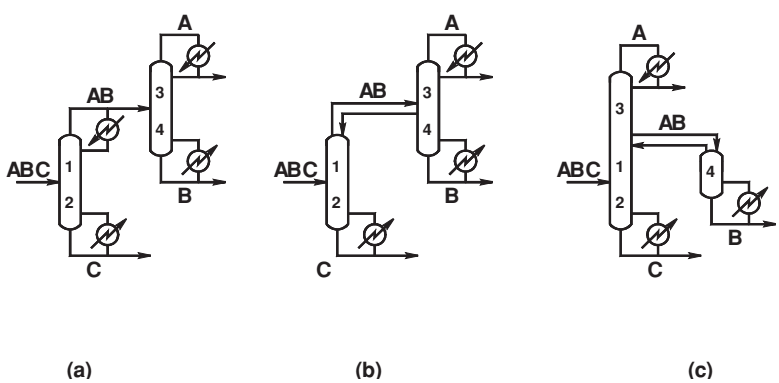

FIG. 13-66 (*a*) Indirect split configuration. (*b*), (*c*) Side stripper configurations.

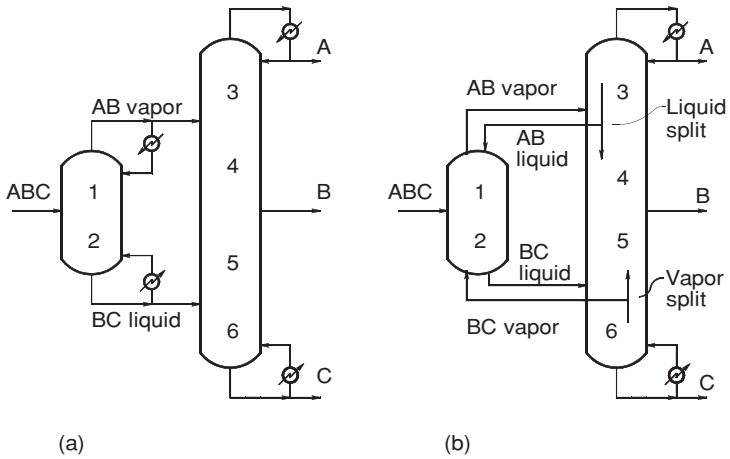

FIG. 13-67 (*a*) Prefractionator system. (*b*) Thermally coupled system.

and *b,* respectively. The corresponding sections in the thermally coupled systems and the dividing wall columns have exactly the same numbers and perform exactly the same separation tasks, indicating that the column arrangements are topologically equivalent.

Various design, simulation, and evaluation methods have been developed for the distillation systems shown in Figs. 13-65 to 13-67. These include those by Stupin and Lockhart [*Chem. Eng. Prog.*, **68** (10), 71 (1972)]; Fidkowski and Krolikowski [*AIChE J.*, **32,** 537 (1986)]; Nikolaides and Malone [*Ind. Eng. Chem. Res.*, **27,** 811, (1988)]; Rudd [Distillation Supplement to the Chemical Engineer, S14, (1992)]; Triantafyllou and Smith [*Trans. Inst. Chem. Eng.*, **70,** Part A, 118 (1992)]; Finn [*Gas Sep. Purif.*, **10,** 169 (1996)]; Annakou and Mizsey [*Ind. Eng. Chem. Eng.*, **35,** 1877 (1996)]; Hernandez and Jimenez [*Comp. & Chem. Eng.*, **23,** 1005 (1999)]; Dunnebier and Pantelides [*Ind. Eng. Chem. Res.*, **38**, 162 (1999)]; Watzdorf, Bausa, and Marquardt [*AIChE J.*, **45,** 1615 (1999)]; Kim [*J. Chem. Eng. Japan*, **34,** 236 (2001)]. The fully thermally coupled system uses less energy than any other ternary column configuration [Fidkowski and Krolikowski, *AIChE J.*, **33,** 643–653 (1987)]. The energy savings may be on the order of 30 to 50 percent, depending on the feed composition and volatilities of the components. Similar energy savings are possible in partially thermally coupled columns, where only one connection (top or bottom) between the columns is thermally coupled and the other is just a single liquid or vapor stream together with an associated condenser or reboiler, respectively [Agrawal and Fidkowski, *AIChE J.*, **45,** 485 (1999)]. Fidkowski and Krolikowski [*AIChE J.*, **32,** 537 (1986)]

TABLE 13-16 Number of Basic Column Configurations for Separation of a Four-Component Mixture

Split	Distillate/bottoms	Number of configurations
1	A/BCD	3
2	AB/BCD	3
3	AB/CD	1
4	ABC/BCD	$3 \times 3 = 9$
5	ABC/CD	3
6	ABC/D	3
	Total	22

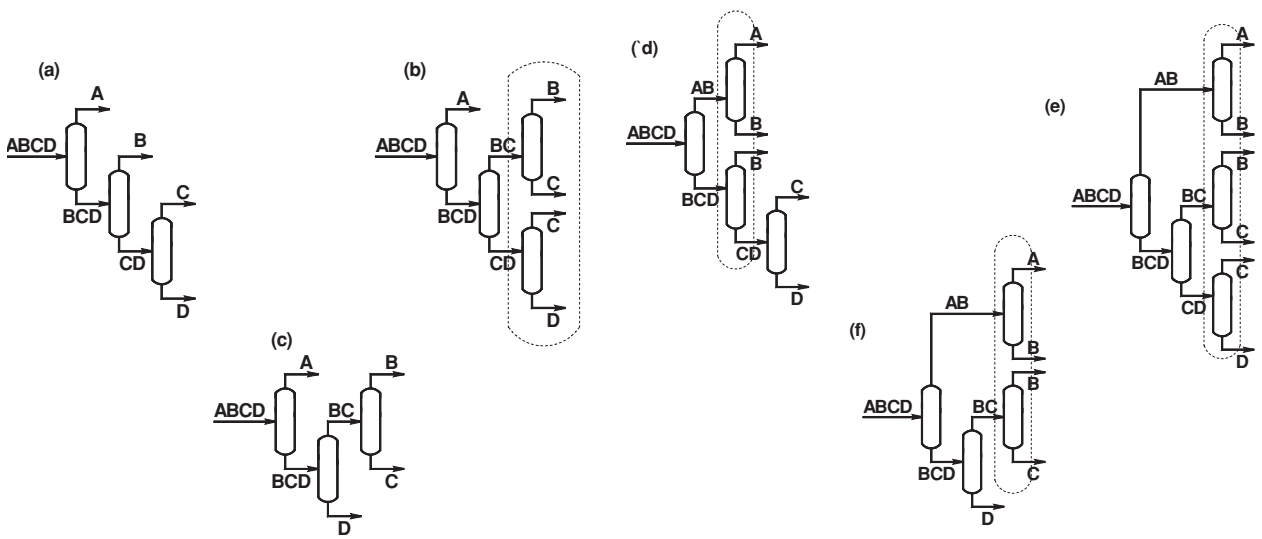

FIG. 13-68 Basic column configurations for separation of a four-component mixture.

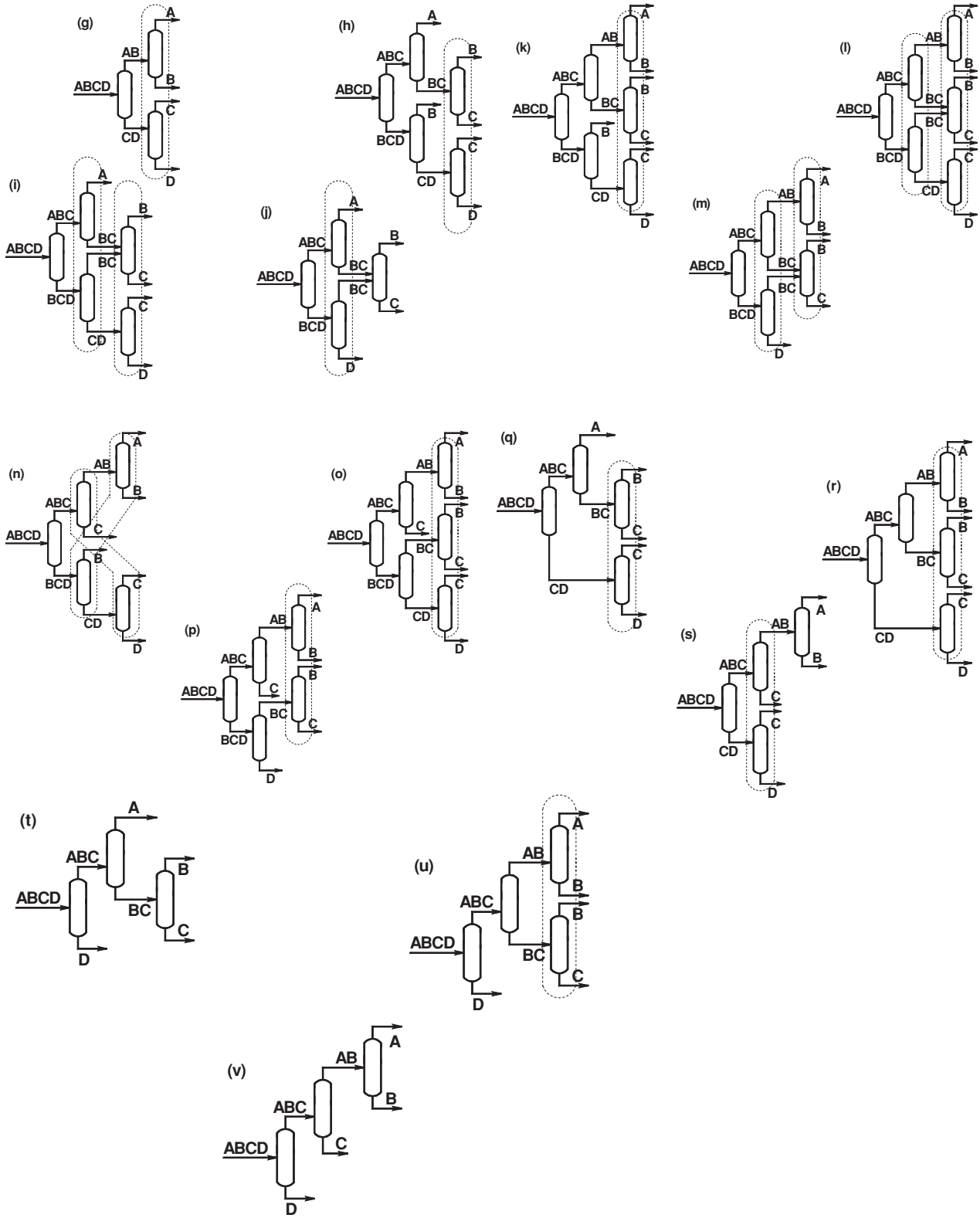

FIG. 13-68 (*Continued*)

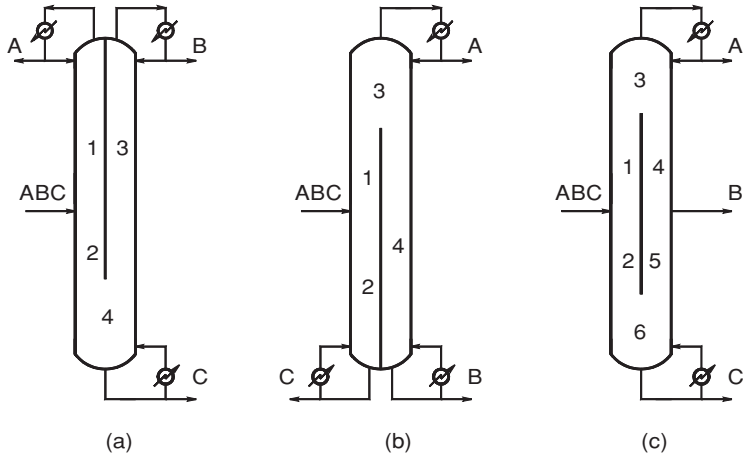

FIG. 13-69 Dividing wall columns equivalent to (*a*) side rectifier configuration, (*b*) side stripper configuration, (*c*) thermally coupled system.

solved analytically the optimization problem for the minimum vapor boil-up rate from the reboiler in the main column for the fully thermally coupled system (shown in Fig. 13-67*b*), assuming constant molar overflow and constant relative volatilities among the components. The solution depends on the splits of vapor and liquid between the main product column and the prefractionator [or between both sides of the dividing wall (Fig. 13-69*c*)]. The minimum vapor flow for each column in the system is shown in Fig. 13-70 as a function of β, where the parameter β is defined as the fractional recovery of the distributing component B in the top product of the prefractionator

$$\beta = \frac{V_1 y_B - L_1 x_B}{f_B} \tag{13-112}$$

where V_1 and L_1 are the vapor and liquid flows at the top of the prefractionator (section 1), y_B and x_B are corresponding mole fractions of component B, and f_B denotes the molar flow of component B in the feed stream. The lower line in Fig. 13-70 is the minimum vapor flow in the first column, the prefractionator. At $\beta = 0$ it corresponds to the A/BC split and at $\beta = 1$ to the AB/C split. There is a minimum in the minimum vapor flow in the prefractionator for $\beta = \beta_P$, the so-called transition split; β_P can be calculated as

$$\beta_P = \frac{\alpha_B - \alpha_C}{\alpha_A - \alpha_C} \tag{13-113}$$

where the α's are relative to any reference component.

The transition split divides direct-type splits from indirect-type splits as discussed by Doherty and Malone (*Conceptual Design of Distillation Systems*, 2001, chaps. 4 and 5); also see Fidkowski, Doherty, and Malone [*AIChE J.*, **39,** 1301(1993)]. The upper line in Fig. 13-70 is the minimum vapor flow leaving the reboiler of the main column, which also corresponds to the minimum vapor flow for the entire system since all the vapor for the total system is generated by this reboiler. For $\beta = 0$ the minimum vapor flow for the entire thermally coupled system (i.e., main column) becomes equal to the minimum vapor flow for the side rectifier system (i.e., main column of the side-rectifier system; see Fig. 13-65*b* or *c*) $(V_{SR})_{min}$; for $\beta = 1$ it is equal to the minimum vapor flow of the entire side stripper system $(V_{SS})_{min}$ (which is the sum of the vapor flows from both the reboilers in this system; see Fig. 13-66*b* or *c*). Coincidentally, the values of these two minimum vapor flows are always the same: $(V_{SR})_{min} = (V_{SS})_{min}$. For $\beta = \beta_R$ the main column is pinched at both feed locations; i.e., the minimum vapor flows for separations A/B and B/C are equal.

The minimum vapor flow for the entire thermally coupled system is flat over a wide range of β: $\beta_P \le \beta \le \beta_R$. This is the reason why dividing wall columns usually work well without tight control of the vapor or liquid split between both sides of the partition. The optimally designed fully thermally coupled system should operate with a fractional recovery of B in the top product of the prefractionator placed somewhere between points *P* and *R*. The transition split *P* is located at one end of the optimal section *PR*, and it is not a recommended design point for normal operation because process disturbances may move the operating point outside the optimal section *PR* shown in Fig. 13-70.

Although invented long ago, dividing wall columns and fully thermally coupled distillation systems were not implemented in practice until the late 1980s. The major objections concerned controllability and operability. Recently, however, several papers have shown that control of these systems is possible; see, e.g., Hernandez and Jimenez [*Ind. Eng. Chem. Res.*, **38,** 3957 (1999)]; Mutalib, Zeglam, and Smith [*Trans. Inst. Chem. Eng.*, **76,** 319 (1998)]; Halvorsen and Skogestad [*Comp. Chem. Eng.*, **21,** Suppl., S249 (1997)]. A major control problem was attributed to inability to set the vapor split between the main column and prefractionator due to conflicting pressure drop requirements between sections 6 and 2, as well as sections 1 and 3 in Fig. 13-67*b*. For the BC vapor to flow from section 6 to section 2, the pressure in the main column at the top of section 6 must be *higher* than the pressure in the prefractionator at the bottom of section 2. But the pressure at the bottom of section 3 in the main column must be *lower* than the pressure at the top of section 1 in the prefractionator, or else the AB vapor stream will not flow from the prefractionator to the main column. Liquid split control is easier to realize in practice, by using liquid collectors, overflows, or pumps. How much vapor flows straight up the main column and how much vapor splits off to the prefractionator depends on the pressure drops in the middle sections of the main column (sections 4 and 5 in Fig. 13-67*b*, between the interconnecting streams) and in the prefractionator. These pressure drops depend on the height of these sections, type of packing or stages, and liquid flows. Therefore, these pressure drops cannot be easily controlled in the configuration shown in Fig. 13-67*b;* moreover, they may even be such that vapor flows in the wrong direction.

Agrawal and Fidkowski [*AIChE J.*, **44,** 2565 (1998); U.S. Patent 6,106,674] proposed robustly operable two-column configurations that cleverly overcome this design and control problem. One is shown in Fig. 13-71. This new configuration is topologically equivalent to the original thermally coupled configuration in Fig. 13-67*b* and retains its energy advantage. In the new Agrawal and Fidkowski configuration, column section 6 is just shifted from the product column to the

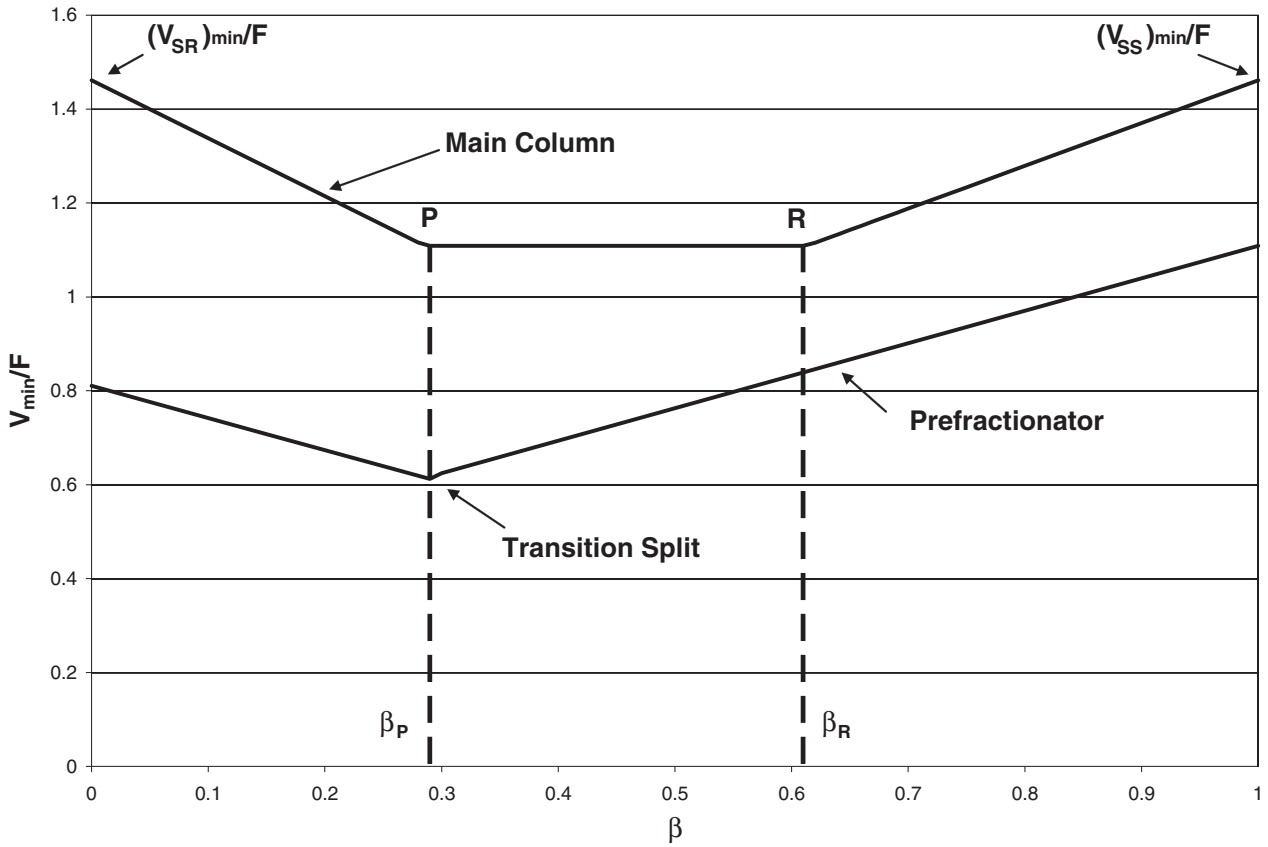

FIG. 13-70 Minimum vapor flows in the thermally coupled system; bottom curve, minimum vapor flow in prefractionator; top curve, minimum vapor flow from the reboiler of the main column (total minimum vapor flow for entire system) for $\alpha_A = 6.25$, $\alpha_B = 2.5$, $\alpha_C = 1.0$ and feed mole fractions $z_A = 0.33$, $z_B = 0.33$, and $z_C = 0.34$.

bottom of prefractionator; thus the two interconnecting vapor streams flow in the *same direction*. The first column (with sections 1, 2, and 6) in Fig. 13-71 operates at a slightly higher pressure than the second column, and the relative flows of the vapor streams can be changed by using a valve on one of them, as shown in the figure. The Agrawal and Fidkowski thermally coupled systems are expected to have higher investment cost than dividing wall columns, and the same investment cost as a Petlyuk thermally coupled system. However, for certain feed compositions and volatilities, the energy optimum in Fig. 13-70 may be narrow (i.e., the interval *PR* may be short) and dividing wall columns may not be able to operate at the optimum. On the other hand, the Agrawal and Fidkowski configurations are able to operate at the optimum because of better control. Also the Agrawal and Fidkowski configurations are useful in cases where high-purity products (especially B) are required. This is so because the two columns are built in separate shells which may contain more stages in one of the shells than could be accommodated in the corresponding side of the dividing wall column.

Experimental tests of dividing wall columns were carried out by Mutalib, Zeglam, and Smith [*Trans. Inst. Chem. Eng.* **76,** 319 (1998)]. Today there are about 60 dividing wall columns in operation; 42 are owned by BASF (*Parkinson*, CEP, p. 10, July 2005).

Thermally coupled systems can also be devised for multicomponent mixtures. Sargent and Gaminibandara (*Optimization in Action*, L. W. C. Dixon, ed., Academic Press, London, 1976, p. 267) presented a natural extension of the Petlyuk column sequence to multicomponent systems. Agrawal [*Ind. Eng. Chem. Res.*, **35,** 1059 (1996); *Trans. Inst. Chem. Eng.*, **78,** 454 (2000)] presented a method for generating an even more complete superstructure from which all the known column configurations (including thermally coupled systems) can be derived. Fidkowski and Agrawal [*AIChE J.*, **47,** 2713 (2001)] presented a method for calculating the minimum vapor flows in multicomponent thermally coupled systems. They analyzed the quaternary fully thermally coupled system in detail (there are many equivalent column configurations, all with the minimum number of column sections, which is 10, as well as one reboiler and one condenser; one of the configurations is shown in Fig. 13-72). They showed that one of the optimum solutions (with the minimum value of the total minimum vapor flow rate from the single reboiler in the system) occurs when the quaternary feed column (far left column in Fig. 13-72) and both ternary columns (the two middle columns in Fig. 13-72) perform transition splits. They also concluded that the optimized quaternary fully coupled system always requires less energy than the five sharp-split conventional systems (where each column performs a sharp split and has one feed, two products, one reboiler, and one condenser). The basic configurations for these five sharp-split systems are shown in Fig. 13-68*a, c, g, t,* and *v*. Selecting the best thermally coupled column configuration can be tedious without computer-aided tools such as the disjunctive programming approach developed by Caballero and Grossmann [*Ind. Eng. Chem. Res.*, **40,** 2260 (2001)].

All the multicomponent thermally coupled configurations have a corresponding dividing wall column equivalent. Keibel [*Chem. Eng. Technol.*, **10,** 92 (1987)] has shown examples of columns with multiple dividing walls, separating three, four, and six components. Agrawal [*Ind. Eng. Chem. Res.*, **40,** 4258 (2001)] presented several examples of quaternary columns with partitions and multiple reboilers and condensers. One of these examples is shown in Fig. 13-73.

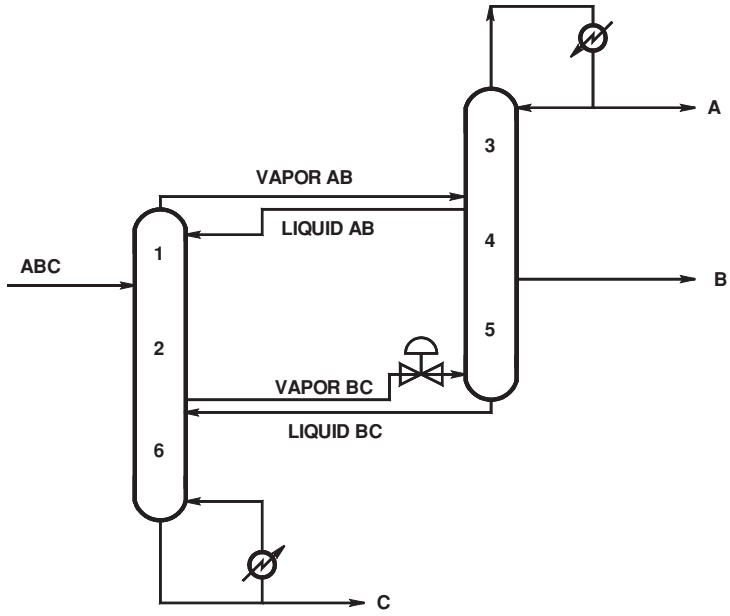

FIG. 13-71 Agrawal and Fidkowski thermally coupled system (topologically equivalent to the Petlyuk system shown in Fig. 13-67*b*).

THERMODYNAMIC EFFICIENCY

Thermodynamic efficiency can be a useful figure of merit (in place of total cost, or total vapor rate) for comparing alternative column configurations. This is especially true for cryogenic distillations where very low temperatures are needed and highly efficient "cold box" designs are needed for achieving them. Thermodynamic efficiency of thermally coupled and other distillation systems for the separation of ternary mixtures was analyzed by Agrawal and Fidkowski [*Ind. Eng. Chem. Res.*, **37,** 3444 (1998)]. Feed composition regions for column configurations with the highest thermodynamic efficiency are shown in Fig. 13-74. Often, the efficiency of the direct split or the indirect split is better than the efficiency of thermally coupled systems. This is primarily due to the ability of these configurations to accept or reject heat at the intermediate boiling or condensing temperatures of the binary submixtures. The fully thermally coupled system can only accept heat at the temperature of the highest-boiling component (boiling point of C) and reject heat at the lowest temperature (condensation temperature of A). This conclusion gave rise to new, more thermodynamically efficient thermally coupled configurations, as discussed by Agrawal and Fidkowski [*Ind. Eng. Chem. Res.*, **38,** 2065 (1999); U.S. Patent 6,116,051].

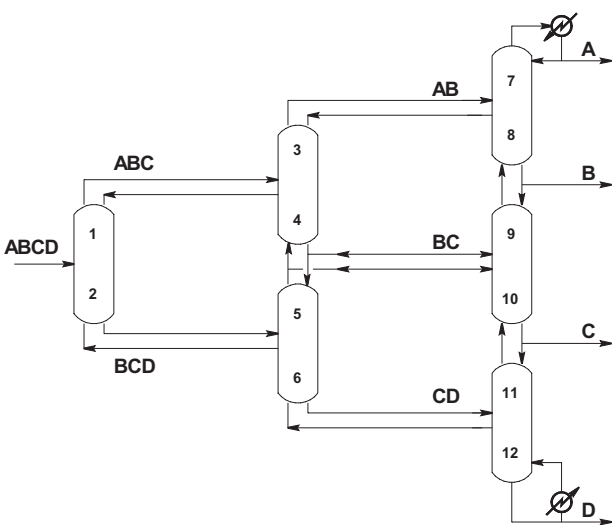

FIG. 13-72 One configuration of a fully thermally coupled system for separation of a quaternary mixture.

HEAT INTEGRATION

In this subsection we describe heat pumps, multieffect distillation of binary mixtures, synthesis of multicomponent distillation systems with heat integration, and multieffect distillation for thermally coupled configurations.

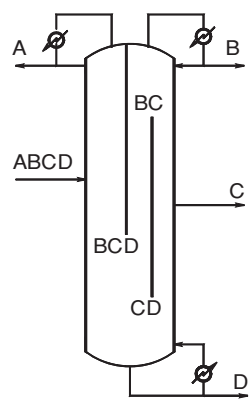

FIG. 13-73 One possible dividing wall column for separation of a quaternary mixture.

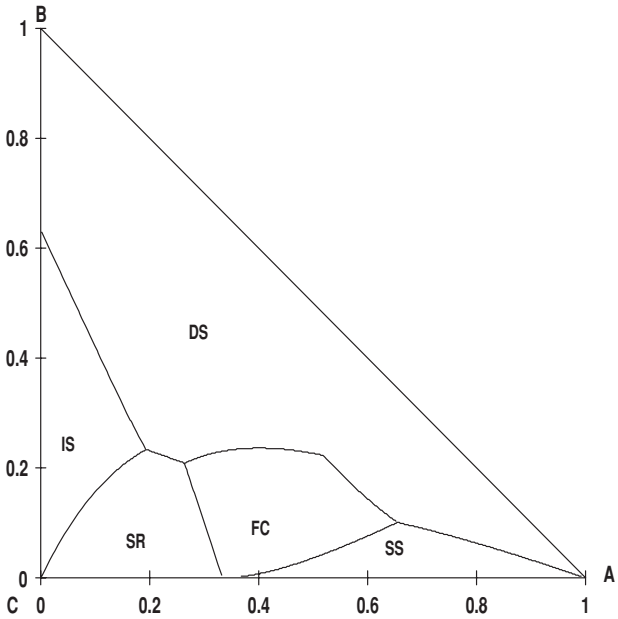

FIG. 13-74 Feed composition regions of column configurations with highest thermodynamic efficiency; DS—direct split, IS—indirect split, SR—side rectifier, SS—side stripper, FC—fully thermally coupled. Example for $\alpha_A = 4.0$, $\alpha_B = 2.0$, and $\alpha_C = 1.0$.

Two columns are heat-integrated when they exchange heat indirectly through a heat exchanger. This is different than in thermally linked configurations, where the heat exchange between columns is direct, through the material stream connecting the columns. The objective of heat integration in distillation systems is to save energy. Heat integration is realized by matching heat sources (usually condensers) with heat sinks (usually reboilers). The other heat exchangers considered for heat integration might be feed preheaters and product coolers. Typical examples of heat integration schemes are heat transfer from a condenser to a reboiler, or heat exchange between a (hot) column feed and a reboiler. If the temperature of the heat source (condenser) is sufficiently higher than the temperature of the heat sink (reboiler), the opportunity for the match is straightforward. If the condenser temperature is too low, one may increase the condensing pressure or use a heat pump.

For example, the reboiler and condenser from the same column may be heat-integrated by using a heat pump, as discussed by Null [*Chem. Eng. Prog.*, **72**(7), 58 (1976)]. A heat pump may use an external fluid which is vaporized in the condenser, then compressed and condensed in the column reboiler (Fig. 13-75*a*). Another heat pump (Fig. 13-75*b*) uses column overhead vapor, which is compressed and condensed in the reboiler and then returned to the top of the column as reflux. A third possibility is to use the column bottoms, which is let down in pressure and vaporized in the condenser, then compressed and fed back to the bottom of the column as boil-up (Fig. 13-75*c*).

The entire rectifying section can be pressurized, and the heat can be transferred between any desired stages of the rectifying and stripping sections. This is called *secondary reflux and vaporization* (SRV) distillation. It reduces the consumption of both hot and cold utilities, and the sizes of the reboiler and condenser. However, capital cost is increased by additional intermediate heat exchangers; moreover, since the process is more thermodynamically reversible, it requires more stages to achieve the desired separation.

In multiple-column systems, possibilities for heat integration may be created by increasing the pressure in one of the columns, to increase the temperature of the condenser. When the temperature of the condenser becomes higher than the temperature of some other column reboiler, it is possible to heat-integrate these streams via a heat exchanger and reuse the heat rejected from the condenser. However, there are several drawbacks to this procedure. The required heat-transfer area in the integrated exchangers needs to be increased due to smaller temperature differences between the process streams than would normally exist when hot and cold external utilities are used to provide boil-up and condensation. Higher-pressure columns need hotter external heating utilities that are more expensive. Separation in higher-pressure columns is more difficult (because relative volatilities tend to decrease with increasing pressure), and more stages and energy may be required. Finally, higher-pressure column shells and piping may be more expensive, although this is not always certain, since the overall dimensions decrease with pressure.

One of the first industrial applications of heat-integrated distillation was a double column for air separation, developed by Linde in the beginning of the 20th century (Fig. 13-76). Air is compressed (typically to about 6 bar) and fed in the bottom of the high-pressure column. Nitrogen is condensed at the top of the high-pressure column.

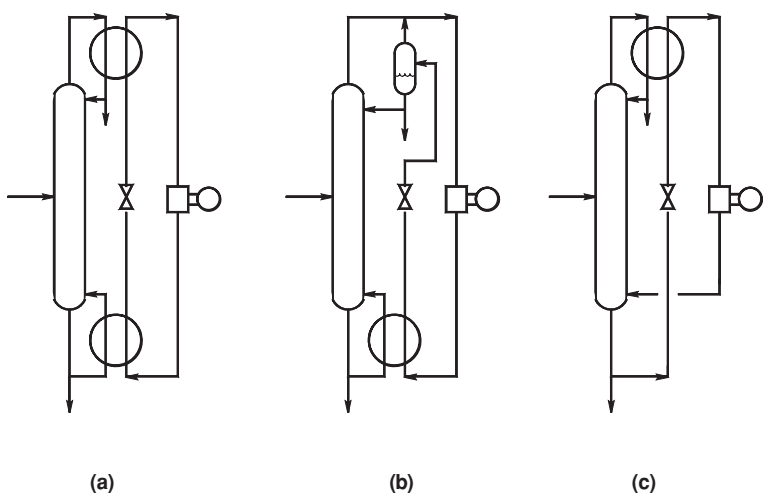

FIG. 13-75 Heat pumps transfer heat from the top to the bottom of the column. (*a*) External fluid heat pump. (*b*) Heat pump using column overhead. (*c*) Heat pump using column bottoms.

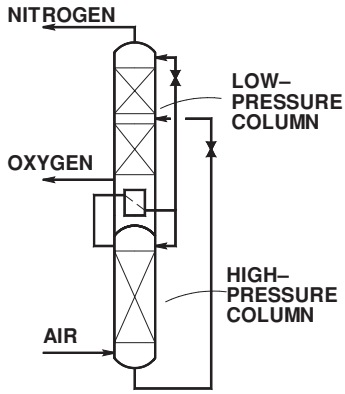

FIG. 13-76 Double-column arrangement for air separation.

The heat of condensation provides boil-up to the low-pressure column, by vaporizing oxygen in the sump located above the nitrogen condenser. Another industrial example of heat integration occurs in the large-scale methanol-water separation in the production of methanol from synthesis gas; see Siirola [*Adv. Chem. Engng*., **23,** 1 (1996)]. Several alternative designs were evaluated, and the regions of superior cost were developed on volatility-feed composition diagrams. Three heat-integrated designs were better than a single column:

1. *Split feed configuration*, in which the feed is split between the high-pressure and the low-pressure columns
2. *Sloppy first bottom split, second column pressurized*, in which the bottoms from the first column is further separated in the high-pressure column
3. *Sloppy first bottom split, first column pressurized*, in which the bottoms from the first, high-pressure column is further separated in the low-pressure column

These heat-integrated systems were economically advantageous because of the large feed flow rate. The last configuration was built.

Design heuristics and computer-aided design methods for heat-integrated distillation systems have been developed in numerous publications. Wankat [*Ind. Eng. Chem. Res*., **32,** 894 (1993)] analyzed 23 different multieffect distillation systems obtained by dividing a single column into two or three columns and operating them at various pressures or compositions, to obtain the temperatures necessary for heat integration. He developed heuristics to devise a feasible system. Rathore, Van Wormer, and Powers [*AIChE J*., **20,** 491 (1974) and **20,** 940 (1974)] presented an algorithmic synthesis method for multicomponent separation systems with energy integration. The five-component separation problem was solved by decomposing it into all the sharp splits and then examining all the possible integrations of heat exchangers. Thermally coupled systems, however, were not considered. Umeda, Niida, and Shiriko [*AIChE J*., **25,** 423 (1979)] published a thermodynamic approach to heat integration in distillation systems based on pinching heat source and heat sink curves on the temperature–heat duty diagram. Linhoff and coworkers (*A User Guide on Process Integration for the Efficient Use of Energy*, Institution of Chemical Engineers, Rugby, U.K., 1982) developed the very successful *pinch technology* approach, commonly used for heat exchanger synthesis and heat integration of entire plants. But, most successfully, Andrechowich and Westerberg [*AIChE J*., **31,** 1461 (1985)] presented a simple conceptual design approach wherein temperature-enthalpy diagrams are used to select the best column stacking. This design method is the recommended starting point for heat integration studies.

Even thermally coupled systems can be heat-integrated, as discovered by Agrawal [*AIChE J*., **46,** 2211 (2000)]. To achieve heat integration without compressors, the vapor connections between the columns must be eliminated. This is shown in Fig. 13-77*a*. The configuration is constructed by extending the prefractionator to a full column with a reboiler and condenser, and adding sections 3x and 6x (analogous to sections 3 and 6 in the product column). By balancing heat duties, only liquid interconnecting streams remain, and the configuration is still thermodynamically equivalent to the original thermally coupled system (Fig. 13-67*b*). It is now possible to heat-integrate the columns by pressurizing one of them and allowing heat transfer from the high-pressure condenser to the low-pressure reboiler (Fig. 13-77*b*). The thermally coupled system and dividing wall column are equally energy-efficient. Therefore, the thermally coupled system with heat integration is even more energy-efficient than the dividing wall column.

There is a significant cost associated with heat integration (e.g., for heat pump compressors, taller columns with more stages, thicker walls of high-pressure equipment, higher cost of high-temperature utilities) which is why such configurations are not widely used. The operational flexibility of a heat-integrated system also becomes more constrained. However, heat-integrated systems can be quite economical for some applications. Typical applications where heat-integrated systems are preferred include

- Cryogenic separation, where very low-temperature cooling utilities do not exist and need to be created, which is very expensive. Therefore, it makes sense to reuse the expensive refrigeration.
- Very large-scale processes, with large feed and product flow rates. Because of the large feed rate, multiple columns may be required to process a given feed anyway. These cases have the potential to save a lot of energy due to heat integration. Also, pressurizing some equipment in these large-scale processes allows for decreased equipment sizes or increased production rate at a fixed equipment size.

IMBALANCED FEEDS

In many practical cases, feed compositions are far from equimolar, with some components present in very small amount (e.g., less than 2 percent). In these cases the top or bottom product flow rate is less than 2 percent of the feed flow rate. The design for imbalanced feeds may include

- Various column diameters
- Intermittent pumping of heavies from the reboiler
- Intermittent firing up a specially devoted column to purify the dirty product made at a small rate
- In a continuous operation an overrefluxed section (to keep the column diameter the same over the height of the column)
- Producing an impure product to be purified later or discarded

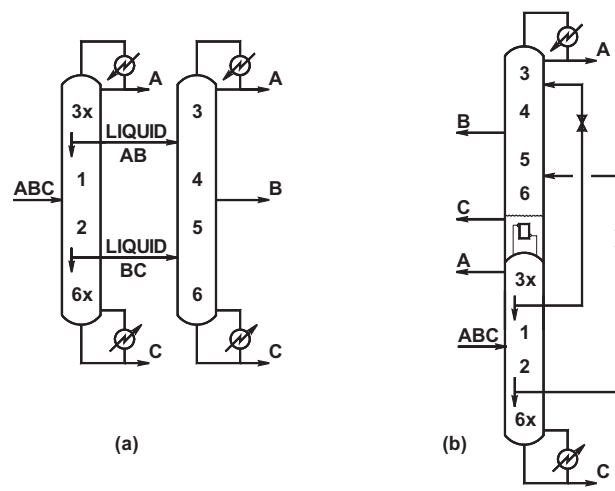

FIG. 13-77 (*a*) Configuration equivalent to thermally coupled system, but without vapor interconnecting streams. (*b*) Heat-integrated thermally coupled system.

ENHANCED DISTILLATION

In distillation operations, separation results from differences in vapor- and liquid-phase compositions arising from the partial vaporization of a liquid mixture or the partial condensation of a vapor mixture. The vapor phase becomes enriched in the more volatile components while the liquid phase is depleted of those same components. In many situations, however, the change in composition between the vapor and liquid phases in equilibrium becomes small (so-called pinched condition), and a large number of successive partial vaporizations and partial condensations are required to achieve the desired separation. Alternatively, the vapor and liquid phases may have identical compositions, because of the formation of an azeotrope, and no separation by simple distillation is possible.

Several enhanced distillation-based separation techniques have been developed for close-boiling or low-relative-volatility systems, and for systems exhibiting azeotropic behavior. All these special techniques are ultimately based on the same differences in the vapor and liquid compositions as ordinary distillation; but, in addition, they rely on some additional mechanism to further modify the vapor-liquid behavior of the key components. These enhanced techniques can be classified according to their effect on the relationship between the vapor and liquid compositions:

1. *Azeotropic distillation and pressure-swing distillation.* Methods that cause or exploit azeotrope formation or behavior to alter the boiling characteristics and separability of the mixture.
2. *Extractive distillation and salt distillation.* Methods that primarily modify liquid-phase behavior to alter the relative volatility of the components of the mixture.
3. *Reactive distillation.* Methods that use chemical reaction to modify the composition of the mixture or, alternatively, use existing vapor-liquid differences between reaction products and reactants to enhance the performance of a reaction.

AZEOTROPY

At low to moderate pressure ranges typical of most industrial applications, the fundamental composition relationship between the vapor and liquid phases in equilibrium can be expressed as a function of the total system pressure, the vapor pressure of each pure component, and the liquid-phase activity coefficient of each component i in the mixture:

$$y_i P = x_i \gamma_i P_i^{\text{sat}} \tag{13-114}$$

In systems that exhibit ideal liquid-phase behavior, the activity coefficients γ_i are equal to unity and Eq. (13-114) simplifies to Raoult's law. For nonideal liquid-phase behavior, a system is said to show negative deviations from Raoult's law if $\gamma_i < 1$ and, conversely, positive deviations from Raoult's law if $\gamma_i > 1$. In sufficiently nonideal systems, the deviations may be so large that the temperature-composition phase diagrams exhibit extrema, as shown in Figs. 13-6, 13-7, and 13-8. At such maxima or minima, the equilibrium vapor and liquid compositions are identical. Thus,

$$y_i = x_i \qquad \text{for all } i = 1, \ldots, c \tag{13-115}$$

and the system is said to form an azeotrope (from the Greek word meaning "to boil unchanged"). Azeotropic systems show a minimum in the T vs. x, y diagram when the deviations from Raoult's law are positive (Fig. 13-6) and a maximum in the T vs. x, y diagram when the deviations from Raoult's law are negative (Fig. 13-7). If, at these two conditions, a single liquid phase is in equilibrium with the vapor phase, the azeotrope is homogeneous. If multiple-liquid-phase behavior is exhibited at the azeotropic condition, the azeotrope is heterogeneous. For heterogeneous azeotropes, the vapor-phase composition is equal to the *overall* composition of the two (or more) liquid phases (Fig. 13-8). These conditions are consequences of the general definition of an azeotrope in any kind of mixture (i.e., homogeneous, heterogeneous, reactive, or in any combination), which is as follows: An *azeotropic state* is one in which mass transfer occurs between phases in a closed system while the composition of each phase remains constant, but not necessarily equal (see Prigogine and Defay, *Chemical Thermodynamics*, 4th ed., Longmans Green and Co., London, 1967; Rowlinson, *Liquids and Liquid Mixtures*, 2d ed., Butterworths, London, 1969; Doherty and Malone, *Conceptual Design of Distillation Systems*, McGraw-Hill, 2001, chaps. 5, 8, App. C).

Mixtures with only small deviations from Raoult's law (i.e., ideal or nearly ideal mixtures) may form an azeotrope but only if the saturated vapor pressure curves of the two pure components cross each other (such a point is called a Bancroft point). In such a situation, the azeotrope occurs at the temperature and pressure where the curves cross, and perhaps also in the vicinity close to the Bancroft point [e.g., cyclohexane (n.b.p. 80.7°C) and benzene (n.b.p. 80.1°C) form an almost ideal mixture yet exhibit a minimum-boiling azeotrope with roughly equal proportions of each component]. As the boiling point difference between the components increases, the composition of the azeotrope shifts closer to one of the pure components (toward the lower-boiling pure component for minimum-boiling azeotropes, and toward the higher-boiling pure component for maximum-boiling azeotropes). For example, the minimum-boiling azeotrope between methanol (n.b.p. 64.5°C) and toluene (n.b.p. 110.6°C) occurs at ≈ 90 mol % methanol, and the minimum-boiling azeotrope between methyl acetate (n.b.p. 56.9°C) and water (n.b.p. 100°C) occurs at ≈ 90 mol % methyl acetate. Mixtures of components whose boiling points differ by more than about 50°C generally do not exhibit azeotropes distinguishable from the pure components even if large deviations from Raoult's law are present. As a qualitative guide to liquid-phase activity coefficient behavior, Robbins [*Chem. Eng. Prog.*, **76**(10), 58 (1980)] developed a matrix of chemical families, shown in Table 13-17, which indicates expected deviations from Raoult's law.

The formation of two liquid phases within some boiling temperature range is generally an indication that the system will also exhibit a minimum-boiling azeotrope, since two liquid phases may form when deviations from Raoult's law are large and positive. The fact that immiscibility does occur, however, does not guarantee that the azeotrope will be heterogeneous since the azeotropic composition may not necessarily fall within the composition range of the two-liquid phase region, as is the case for the methyl acetate–water and tetrahydrofuran-water systems. Since strong positive deviations from Raoult's law are required for liquid-liquid phase splitting, maximum-boiling azeotropes ($\gamma_i < 1$) are never heterogeneous.

Additional general information on the thermodynamics of phase equilibria and azeotropy is available in Malesinski (*Azeotropy and Other Theoretical Problems of Vapour-Liquid Equilibrium*, Interscience, London, 1965), Swietoslawski (*Azeotropy and Polyazeotropy*, Pergamon, London, 1963), Van Winkle (*Distillation*, McGraw-Hill, New York, 1967), Smith and Van Ness (*Introduction to Chemical Engineering Thermodynamics*, McGraw-Hill, New York, 1975), Wizniak [*Chem. Eng. Sci.*, **38,** 969 (1983)], and Walas (*Phase Equilibria in Chemical Engineering*, Butterworths, Boston, 1985). Horsley (*Azeotropic Data-III*, American Chemical Society, Washington, 1983) compiled an extensive list of experimental azeotropic boiling point and composition data for binary and some multicomponent mixtures. Another source for azeotropic data and activity coefficient model parameters is the multivolume *Vapor-Liquid Equilibrium Data Collection* (DECHEMA, Frankfort, 1977), a compendium of published experimental VLE data. Most of the data have been tested for thermodynamic consistency and have been fitted to the Wilson, UNIQUAC, Van Laar, Margules, and NRTL equations. An extensive two-volume compilation of azeotropic data for 18,800 systems involving 1700 compounds, entitled *Azeotropic Data* by Gmehling et al., was published in 1994 by VCH Publishers, Deerfield Beach, Fla. A computational method for determining the temperatures and compositions of all homogeneous azeotropes of a multicomponent mixture, from liquid-phase activity coefficient correlations, by a differential arclength homotopy continuation method is given by Fidkowski, Malone, and Doherty [*Computers and Chem. Eng.*, **17,** 1141 (1993)]. The method was generalized to determine all homogeneous and heterogeneous azeotropes by Wasylkiewicz, Doherty, and Malone [*Ind. Eng. Chem. Res.*, **38,** 4901 (1999)].

RESIDUE CURVE MAPS AND DISTILLATION REGION DIAGRAMS

The simplest form of distillation involves boiling a multicomponent liquid mixture in an open evaporation from a single-stage batch still. As the liquid is boiled, the vapor generated is removed from contact with the liquid as soon as it is formed. Because the vapor is richer in the more volatile components than the liquid, the composition and boiling temperature of the liquid remaining in the still change continuously over time and move progressively toward less volatile compositions and higher temperatures until the last drop is vaporized. This last composition may be a pure-component species, or a maximum-boiling azeotrope, and it may depend on the initial composition of the mixture charged to the still.

The trajectory of liquid compositions starting from some initial composition is called a residue curve, the collection of all such curves for a given mixture is called a residue curve map. Arrows are usually added to these curves, pointing in the direction of increasing time, which corresponds to increasing temperature, and decreasing volatility. If the liquid is well mixed and the vaporization is slow, such that the escaping vapor is in phase equilibrium with the residual liquid, then residue curve maps contain exactly the same information as the corresponding phase equilibrium diagram for the mixture, but they represent it in a way that is much more useful for understanding distillation systems. Composition changes taking place in simple batch distillation can be described mathematically by the following ordinary differential equation

$$\frac{dx_i}{d\xi} = x_i - y_i \qquad \text{for all } i = 1, \ldots, c \tag{13-116}$$

where ξ is a dimensionless nonlinear time scale. Normally, y_i and x_i are related by an isobaric VLE model. Integrating these equations forward in time leads to the less volatile final compositions; integrating them backward in time leads to the more volatile compositions which would produce a residue curve passing through the specified initial composition. A *residue curve map* (RCM) is generated by varying the initial composition and integrating Eq. (13-116) both forward and backward in time [Doherty and Perkins, *Chem. Eng. Sci.,* **33,** 281 (1978); Doherty and Malone, op. cit., chap. 5]. Unlike a binary y-x plot, relative-volatility information is not represented on an RCM. Therefore, it is difficult to determine the ease of separation from a residue curve map alone. The steady states of Eq. (13-116) are the constant-composition trajectories corresponding to $dx_i/d\xi = 0$ for all $i = 1, \ldots, c$. The steady states therefore correspond to *all* the pure components and *all* the azeotropes in the mixture.

Residue curve maps can be constructed for mixtures of any number of components, but can be pictured graphically only up to four components. For binary mixtures, a T vs. x, y diagram or a y-x diagram suffices; the system is simple enough that vapor-phase information can be included with liquid-phase information without confusion. For ternary mixtures, liquid-phase compositions are plotted on a triangular diagram, similar to that used in liquid-liquid extraction. Four-component systems can be plotted in a three-dimensional tetrahedron. The vertices of the triangular diagram or tetrahedron represent the pure components. Any binary, ternary, and quaternary azeotropes are placed at the appropriate compositions on the edges and/or interior of the triangle and tetrahedron.

The simplest form of ternary RCM, as exemplified for the ideal normal-paraffin system of pentane-hexane-heptane, is illustrated in Fig. 13-78*a*, using a right-triangle diagram. Maps for all other nonazeotropic ternary mixtures are qualitatively similar. Each of the infinite number of possible residue curves originates at the pentane vertex, travels toward and then away from the hexane vertex, and terminates at the heptane vertex. The family of all residue curves that originate at one composition and terminate at another composition defines a *distillation region*. Systems that do not involve azeotropes have only one region—the entire composition space. However, for many systems, not all residue curves originate or terminate at the same two compositions. Such systems will have more than one distillation region. The residue curve that divides two distillation regions in which adjacent residue curves originate from different compositions or terminate at different compositions is called a *simple batch distillation boundary* or *separatrix.* Distillation boundaries are related to the existence of azeotropes. In the composition space for a binary system, the distillation boundary is a point (the azeotropic composition). For three components, the distillation boundary is a curve; for four components, the boundary is a surface; and so on.

TABLE 13-17 Solute-Solvent Group Interactions

Solute class	Group	Solvent class 1	2	3	4	5	6	7	8	9	10	11	12
	H-donor												
1	Phenol	0	0	–	0	–	–	–	–	–	–	–	–
2	Acid, thiol	0	0	–	0	–	–	0	0	0	0	–	–
3	Alcohol, water	–	–	0	+	+	0	–	–	–	–	–	–
4	Active-H on multihalo paraffin	0	0	+	0	–	–	–	–	–	–	0	–
	H-acceptor												
5	Ketone, amide with no H on N, sulfone, phosphine oxide	–	–	+	–	0	+	–	–	–	+	–	–
6	Tertamine	–	–	0	–	+	0	–	–	0	+	0	0
7	Secamine	–	0	–	–	+	+	0	0	0	0	0	–
8	Priamine, ammonia, amide with 2H on N	–	0	–	–	+	+	0	0	–	+	–	–
9	Ether, oxide, sulfoxide	–	0	+	–	+	0	0	–	0	+	0	–
10	Ester, aldehyde, carbonate, phosphate, nitrate, nitrite, nitrile, intramolecular bonding, e.g., *o*-nitro phenol	–	0	+	–	+	+	0	–	–	0	–	–
11	Aromatic, olefin, halogen aromatic, multihalo paraffin without active H, monohalo paraffin	+	+	+	0	+	0	0	–	0	+	0	0
	Non-H-bonding												
12	Paraffin, carbon disulfide	+	+	+	+	+	0	+	+	+	+	0	0

SOURCE: Robbins, L. A., *Chem. Eng. Prog.,* **76**(10), 58–61 (1980), by permission.

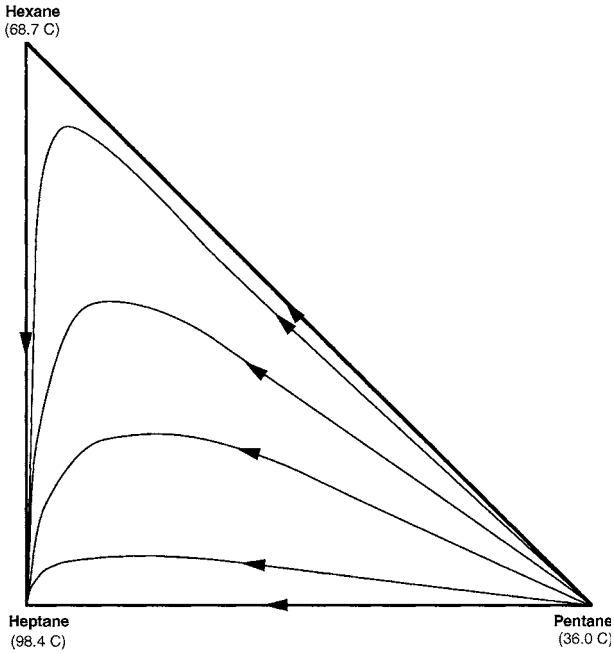

FIG. 13-78*a* Residue curve map: Nonazeotropic pentane-hexane-heptane system at 1 atm.

The boundaries of the composition diagram (e.g., the edges of a composition triangle) also form region boundaries since they divide physically realistic residue curves with positive compositions from unrealistic curves with negative compositions. All pure components and azeotropes in a system lie on region boundaries. Within each region, the most volatile composition on the boundary (either a pure component or a minimum-boiling azeotrope, and the origin of all residue curves in that region) is called the *low-boiling node.* The least-volatile composition on the boundary (either a pure component or a maximum-boiling azeotrope, and the terminus of all residue curves in that region) is called the *high-boiling node.* All other pure components and azeotropes are called *intermediate-boiling saddles*. Adjacent regions may share some (but not all) nodes and saddles. Pure components and azeotropes are labeled as nodes and saddles as a result of the boiling points of all the components and azeotropes in a system. If one species is removed, the labeling of all remaining pure components and azeotropes, particularly those that were saddles, may change. Distillation boundaries always originate or terminate at saddle azeotropes, but never at pure component saddles—distillation boundaries can be calculated by using the method proposed by Lucia and Taylor [*AIChE J.*, **52,** 582 (2006)]. Ternary saddle azeotropes are particularly interesting because they are more difficult to detect experimentally (being neither minimum-boiling nor maximum-boiling). However, their presence in a mixture implies the existence of distillation boundaries which may have an important impact on the design of a separation system. The first ternary saddle azeotrope to be detected experimentally was reported by Ewell and Welch [*Ind. Eng. Chem.*, **37,** 1224 (1945)], and a particularly comprehensive set of experimental residue curves were reported by Bushmakin and Kish [*J. Appl. Chem. USSR (Engl. Trans.)*, **30,** 205 (1957)] for a ternary mixture with a ternary saddle azeotrope (reproduced as fig. 5.9 in Doherty and Malone, op. cit.). More ternary saddle azeotropes are reported in Gmehling et al. (*Azeotropic Data*, 1994).

Both methylethylketone (MEK) and methylisopropylketone (MIPK) form minimum-boiling homogeneous azeotropes with water (Fig. 13-78*b*). In this ternary system, a distillation boundary connects the binary azeotropes and divides the RCM into two distillation regions, I and II. The high-boiling node of region I is pure water, while the low-boiling node is the MEK-water azeotrope. In region II, the high- and low-boiling nodes are MIPK and the MEK-water azeotrope, respectively. These two regions, however, have a different number of saddles—one in region I and two in region II. This leads to region I having three sides, while region II has four sides. The more complicated cyclohexane-ethanol-water system (Fig. 13-78*c*) has three boundaries and three regions, all of which are four-sided and share the ternary azeotrope as the low-boiling node.

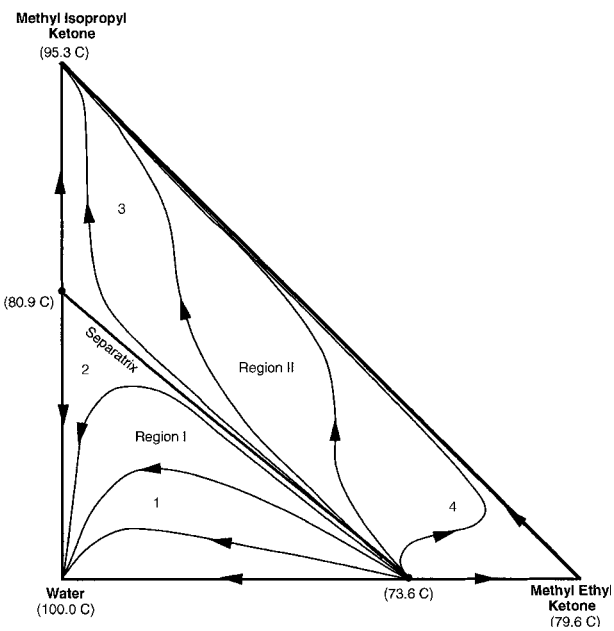

FIG. 13-78*b* Residue curve map: MEK-MIPK-water system at 1 atm containing two minumum-boiling binary azeotropes.

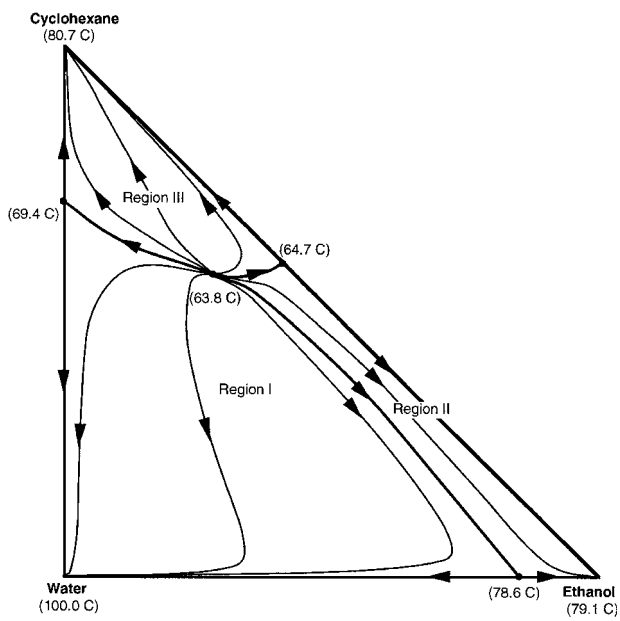

FIG. 13-78*c* Residue curve map: Ethanol-cyclohexane-water system at 1 atm containing four minimum-boiling azeotropes (three binary and one ternary) and three distillation regions.

The liquid composition profiles in continuous staged or packed distillation columns operating at infinite reflux and boil-up are closely approximated by simple distillation residue curves [Van Dongen and Doherty, *Ind. Eng. Chem. Fundam.*, **24,** 454 (1985)]. Residue curves are also indicative of many aspects of the general behavior of continuous columns operating at more practical reflux ratios. For example, to a first approximation, the stage-to-stage liquid compositions (along with the distillate and bottoms compositions) of a single-feed, two-product, continuous distillation column lie on the same residue curve. Therefore, for systems with distillation boundaries and multiple regions, distillation composition profiles are constrained to lie in specific regions. The precise boundaries of these distillation regions are a function of reflux ratio, but they are closely approximated by the RCM distillation boundaries. If a RCM distillation boundary exists in a system, a corresponding continuous distillation boundary will also exist. Both types of boundaries correspond exactly at all pure components and azeotropes.

Residue curves can be constructed from experimental data or can be calculated by integrating Eq. (13-116) if equation-of-state or activity-coefficient expressions are available (e.g., Wilson binary-interaction parameters, UNIFAC groups). However, considerable information on system behavior can still be deduced from a simple qualitative sketch of the RCM distillation boundaries based only on pure-component and azeotrope boiling point data and approximate azeotrope compositions. Rules for constructing such qualitative *distillation region diagrams* (DRDs) are given by Foucher et al. [*Ind. Eng. Chem. Res.*, **30,** 760, 2364 (1991)]. For ternary systems containing no more than one ternary azeotrope and no more than one binary azeotrope between each pair of components, 125 such DRDs are mathematically possible [Matsuyama and Nishimura, *J. Chem. Eng. Japan*, **10,** 181 (1977); Doherty and Caldarola, *Ind. Eng. Chem. Fundam.*, **24,** 474 (1985); Peterson and Partin, *Ind. Eng. Chem. Res.*, **36,** 1799 (1997)], although only a dozen or so represent most systems commonly encountered in practice.

Figure 13-79 illustrates all the 125 possible DRDs for ternary systems [see Peterson and Partin, *Ind. Eng. Chem. Res.*, **36,** 1799 (1997)]. Azeotropes are schematically depicted generally to have equimolar composition, distillation boundaries are shown as straight lines, and the arrows on the distillation boundaries indicate increasing temperature. These DRDs are indexed in Table 13-18 according to a temperature profile sequence of position numbers, defined in a keyed triangular diagram at the bottom of the table, arranged by increasing boiling point. Positions 1, 3, and 5 are the pure components in order of decreasing volatility. Positions 2, 4, and 6 are binary azeotropes at the positions shown in the keyed triangle, and position 7 is the ternary azeotrope. Azeotrope position numbers are deleted from the temperature profile if the corresponding azeotrope is known not to exist. Note that not every conceivable temperature profile corresponds to a thermodynamically consistent system, and such combinations have been excluded from the index. As is evident from the index, some DRDs are consistent with more than one temperature profile. Also some temperature profiles are consistent with more than one DRD. In such cases, the correct diagram for a system must be determined from residue curves obtained from experimental or calculated data.

Schematic DRDs are particularly useful in determining the implications of possibly unknown ternary saddle azeotropes by postulating position 7 at interior positions in the temperature profile. Also note that some combinations of binary azeotropes require the existence of a ternary saddle azeotrope. As an example, consider the system acetone (56.4°C), chloroform (61.2°C), and methanol (64.7°C) at 1-atm pressure. Methanol forms minimum-boiling azeotropes with both acetone (54.6°C) and chloroform (53.5°C), and acetone-chloroform forms a maximum-boiling azeotrope (64.5°C). Experimentally there are no data for maximum- or minimum-boiling ternary azeotropes for this mixture. Assuming no ternary azeotrope, the temperature profile for this system is 461325, which from Table 13-18 is consistent with DRD 040 and DRD 042. However, Table 13-18 also indicates that the pure-component and binary azeotrope data are consistent with three temperature profiles involving a ternary saddle azeotrope, namely, 4671325, 4617325, and 4613725. All three of these temperature profiles correspond to DRD 107. Calculated residue curve trajectories for the acetone-chloroform-methanol system at 1-atm pressure, as shown in Fig. 13-80, suggest the existence of a ternary saddle azeotrope and DRD 107 as the correct approximation of the distillation regions. Ewell and Welch [*Ind. Eng. Chem.*, **37,** 1224 (1945)] confirmed experimentally such a ternary saddle at 57.5°C.

APPLICATIONS OF RCM AND DRD

Residue curve maps and distillation region diagrams are very powerful tools for understanding all types of batch and continuous distillation operations, particularly when combined with other information such as liquid-liquid binodal curves. Applications include

1. *System visualization.* Location of distillation boundaries, azeotropes, distillation regions, feasible products, and liquid-liquid regions.
2. *Evaluation of laboratory data.* Location and confirmation of saddle ternary azeotropes and a thermodynamic consistency check of data.
3. *Process synthesis.* Concept development, construction of flow sheets for new processes, and redesign or modification of existing process flow sheets.
4. *Process modeling.* Identification of infeasible or problematic column specifications that could cause simulation convergence difficulties or failure, and determination of initial estimates of column parameters including feed-stage location, number of stages in the stripping and enriching sections, reflux ratio, and product compositions.
5. *Control analysis/design.* Analysis of column balances and profiles to aid in control system design and operation.
6. *Process trouble shooting.* Analysis of separation system operation and malfunction, examination of composition profiles, and tracking of trace impurities with implications for corrosion and process specifications.

Material balances for mixing or continuous separation operations are represented graphically on triangular composition diagrams such as residue curve maps or distillation region diagrams by straight lines connecting pertinent compositions. The straight lines are exact representations of the compositions due to the lever rule. Overall flow rates are found by the inverse-lever-arm rule. Distillation material balance lines are governed by two constraints:

1. The bottoms, distillate, and overall feed compositions must lie on the same straight line.
2. The bottoms and distillate compositions must lie (to a very close approximation) on the same residue curve.

Since residue curves do not cross simple batch distillation boundaries, the distillate and bottoms compositions must be in the same distillation region with the mass balance line intersecting a residue curve in two places. Mass balance lines for mixing and for other separations not involving vapor-liquid equilibria, such as extraction and decantation, are of course not limited by distillation boundaries.

For a given multicomponent mixture, a single-feed, two-product distillation column (simple column) can be designed with sufficient stages, reflux, and material balance control to produce separations ranging from the *direct-split* mode of operation (low-boiling node taken as distillate) to the *indirect-split* mode (high-boiling node taken as bottoms). The bow tie shaped set of reachable product compositions for a simple distillation column is roughly bounded by the (straight) material balance lines connecting the feed composition to the sharpest direct separation and the sharpest indirect separation possible (see Fig. 13-81). A more accurate approximation involves replacing two of the straight-line segments of the bow tie with the residue curve through the feed composition [Stichlmair and Herguijuela, *AIChE J.*, **38,** 1523 (1992)]. The exact shape of the reachable product composition regions involves replacing two of the straight-line segments of the bow tie with a locus of pinch points, as explained by Wahnschafft et al. [*Ind. Eng. Chem. Res.*, **31,** 2345 (1992)] and Fidkowski, Doherty, and Malone [*AIChE J.*, **39,** 1303 (1993)]. Since residue curves are deflected by saddles, it is generally not possible to obtain a saddle product (pure component or azeotrope) from a simple distillation column.

Consider the recovery of MIPK from an MEK-MIPK-water mixture. The approximate bow tie regions of product compositions for three different feeds are shown in Fig 13-81. From feed F3, which is situated in a different distillation region than the desired product, pure MIPK cannot be obtained at all. Feed F2 is more favorable, with the upper edge of the bow tie region along the MEK-MIPK (water-free) face of the composition triangle and part of the lower

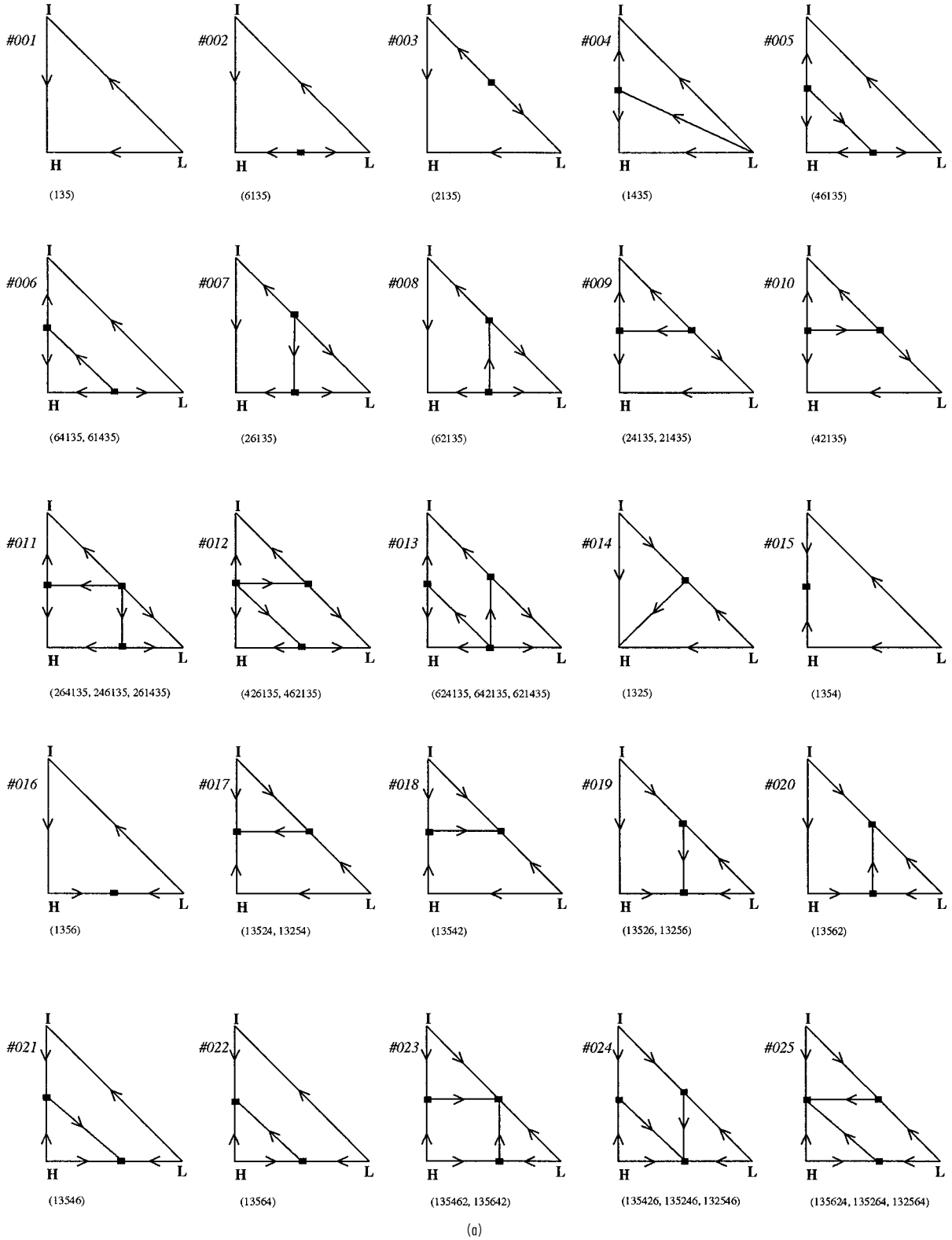

(a)

FIG. 13-79 Distillation region diagrams for ternary mixtures.

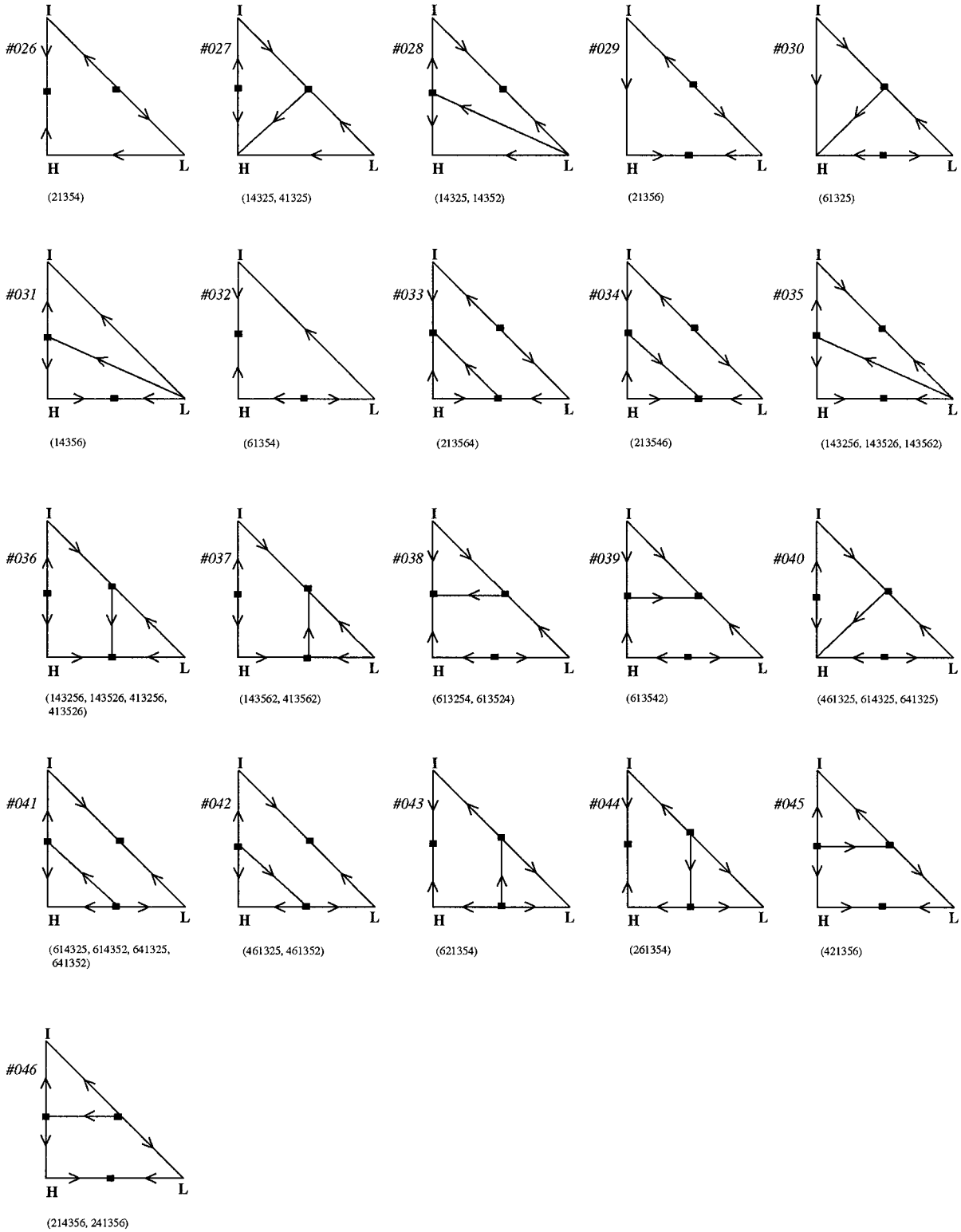

(b)

FIG. 13-79 (*Continued*)

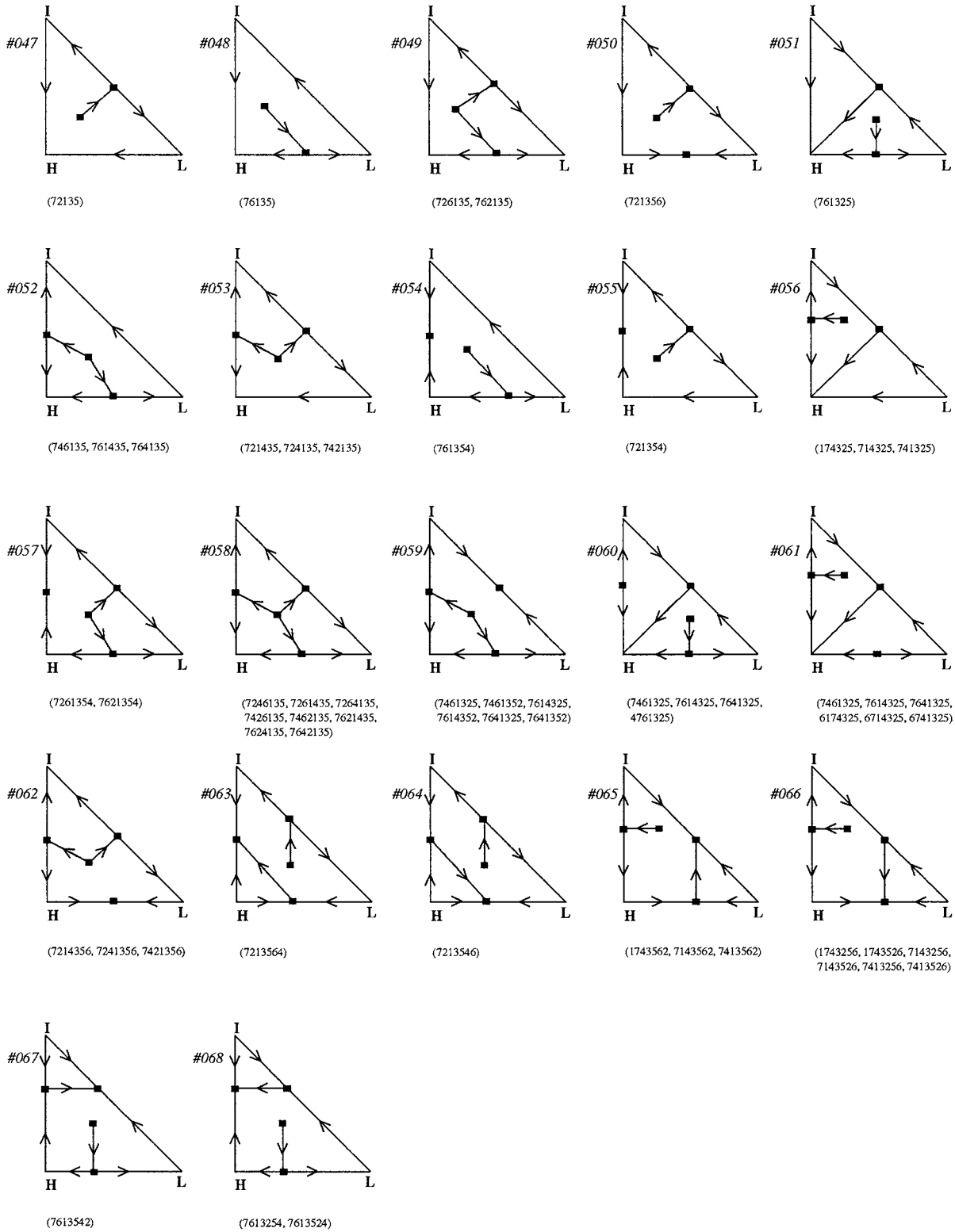

(c)

FIG. 13-79 (*Continued*)

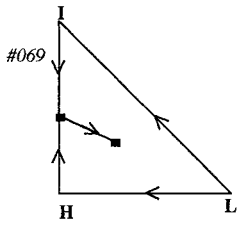

(13547)

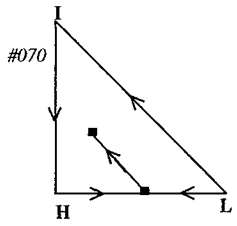

(13567)

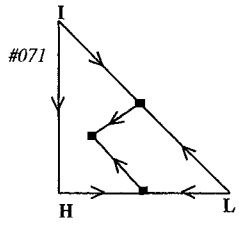

(132567,135267, 135627)

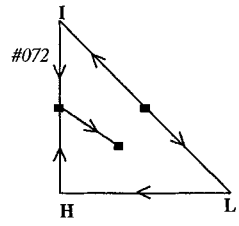

(213547)

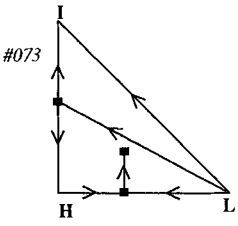

(143567)

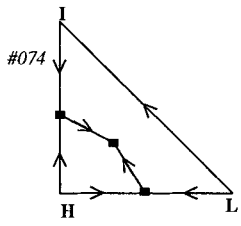

(135467, 135647)

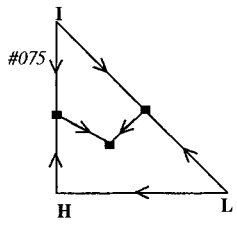

(132547, 135247, 135427)

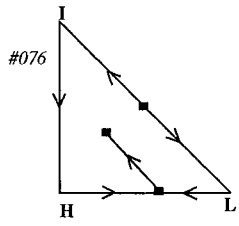

(213567)

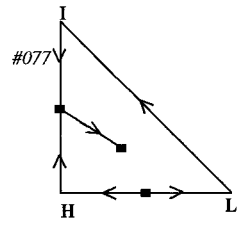

(613547)

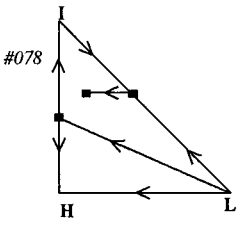

(143257, 143275, 143527)

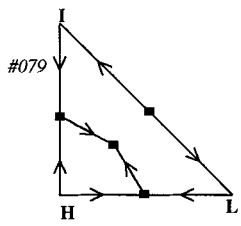

(2135467, 2135647)

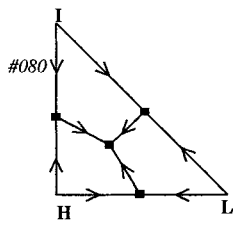

(1325467, 1325647, 1352467, 1352647, 1354267, 1354627, 1356247,1356427)

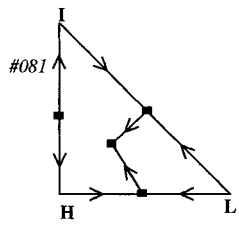

(1432567, 1435267, 1435627 4132567, 4135267, 4135627)

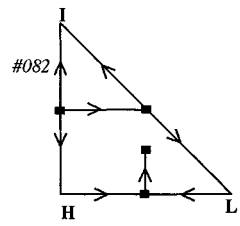

(4213567)

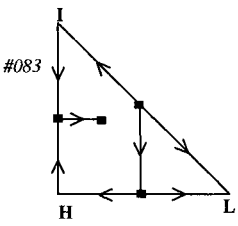

(2613547)

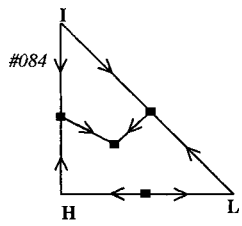

(6132547, 6135247, 6135427)

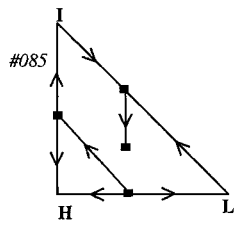

(6143257, 6143275, 6143527, 6413257, 6413275, 6413527)

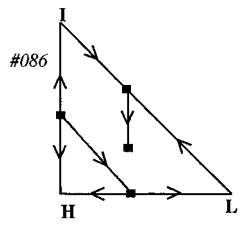

(4613257, 4613275, 4613527)

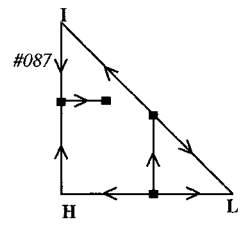

(6213547)

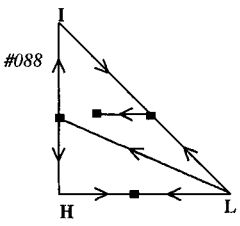

(1432567, 1432576, 1432756, 1435267, 1435276, 1435627)

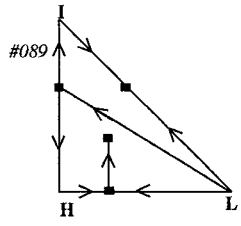

(1432567, 1435267, 1435627, 1435672)

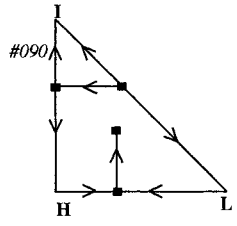

(2143567, 2413567)

(d)

FIG. 13-79 (*Continued*)

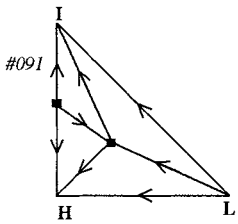

(14735, 41735)

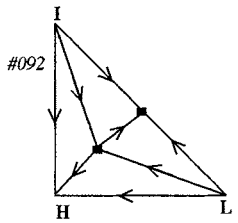

(13725, 13752)

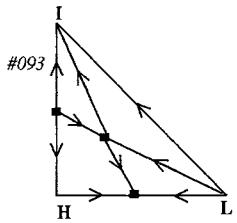

(147356, 417356)

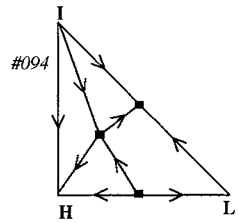

(613725, 613752)

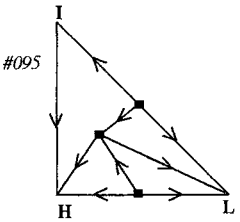

(267135, 627135)

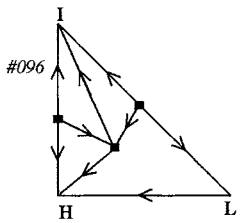

(214735, 241735, 247135, 421735, 427135)

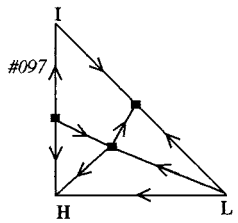

(143725, 143752, 147325, 147352, 413725, 413752, 417325, 417352)

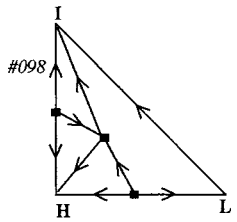

(461735, 467135, 614735, 641735, 647135)

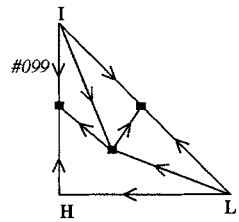

(135724, 135742, 137254, 137524, 137542)

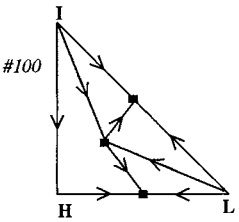

(135726, 135762, 137256, 137526, 13756)

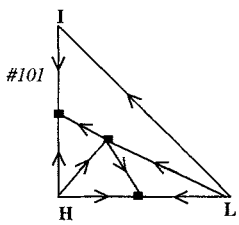

(135746, 135764)

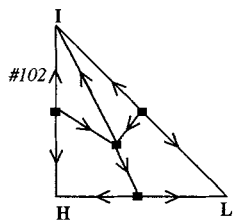

(2476135, 4276135)

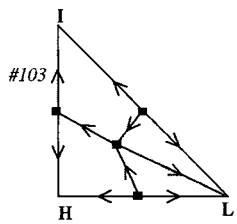

(2671435, 2674135, 6271435, 6274135)

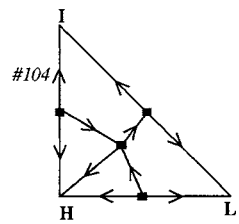

(4672135, 6472135)

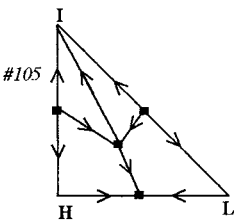

(2147356, 2417356, 2471356, 4217356, 4271356)

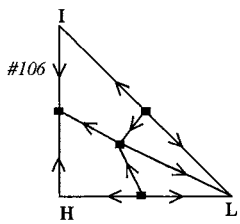

(2671354, 6271354)

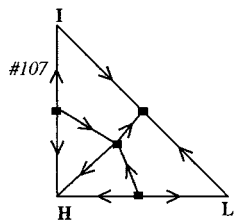

(4613752, 4613725,4617352, 4617325, 4671325, 4671352, 6143725, 6143752, 6147325, 6147352, 6413725, 6413752, 6417325, 6417352, 6471325, 6471352)

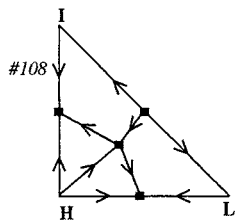

(2135746, 2135764)

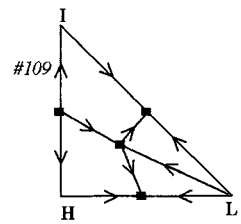

(1435726, 1435762, 1437256, 1437526, 1437562, 1473256, 1473526, 1473562, 4135726, 4135762, 4137256, 4137526, 4137562, 4173256, 4173526, 4173562)

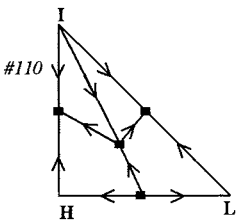

(6135724, 6135742, 6137254, 6137524, 6137542)

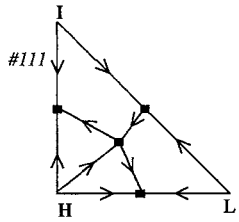

(1325746, 1325764, 1352746, 1352764)

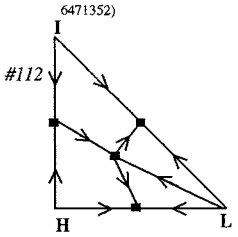

(1354726, 1354762)

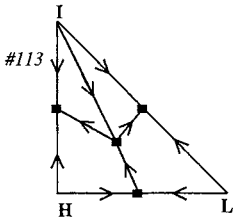

(1356724, 1356742)

(e)

FIG. 13-79 (*Continued*)

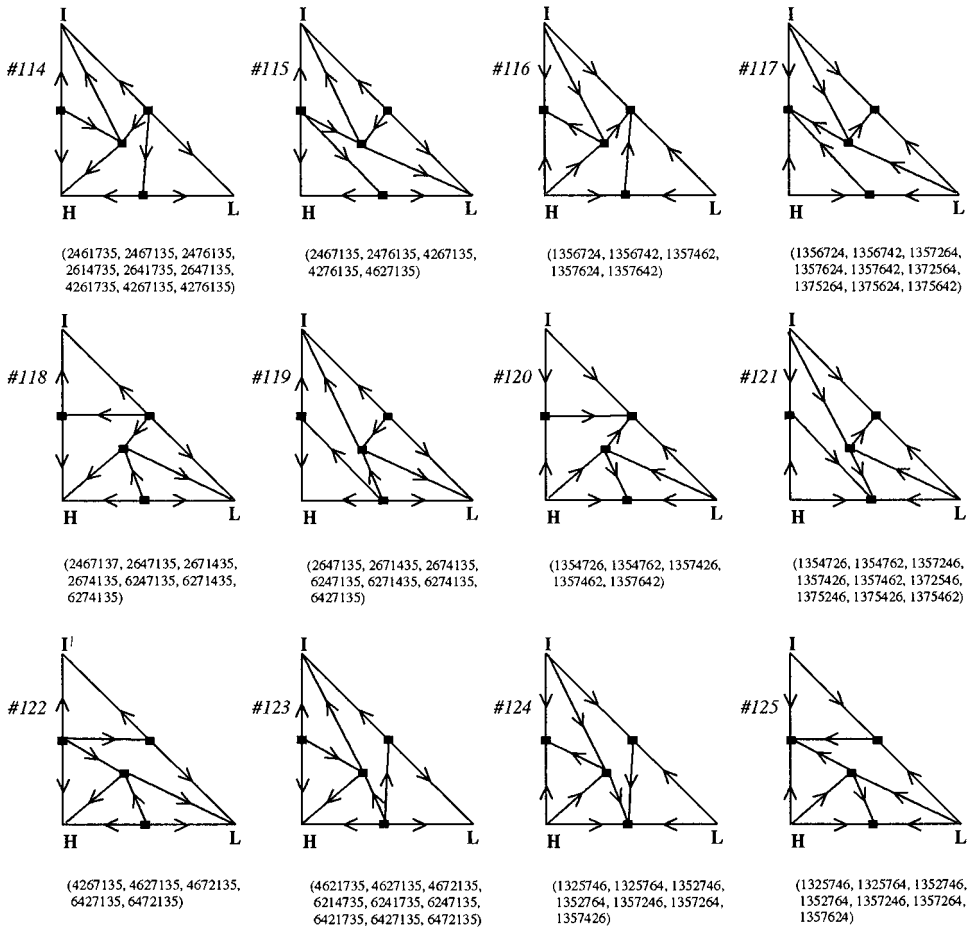

(f)

FIG. 13-79 (*Continued*)

edge along the MEK-water (MIPK-free) face. There are conditions under which both the water in the MIPK bottoms product can be driven to low levels (high-product purity) and MIPK in the distillate can be driven to low levels (high-product recovery), although achieving such an operation depends on having an adequate number of stages and reflux ratio.

Although feed F2 lies in the same distillation region as F1, the bow tie region for feed F2 is significantly different than that for F1, with the upper edge along the water-MIPK (MEK-free) face of the triangle and the lower edge along the distillation boundary. From this feed it is not possible to simultaneously achieve a high-purity MIPK specification while obtaining high MIPK recovery. If the column is operated to get a high purity of MIPK, then the material balance line runs into the distillation boundary. Alternatively, if the column is operated to obtain a high recovery of MIPK (by removing the MEK-water azeotrope as distillate), the material balance requires the bottoms to lie on the water-MIPK face of the triangle.

The number of saddles in a particular distillation region can have significant impact on column profile behavior, process stability, and convergence behavior in process simulation of the system. Referring to the MIPK-MEK-water system in Fig. 13-78*b*, region I contains one saddle (MIPK-water azeotrope), while region II contains two saddles (pure MEK and the MIPK-water azeotrope). These are three- and four-sided regions, respectively. In a three-sided region, all residue curves track toward the solitary saddle. However, in a four- (or more) sided region with saddles on either side of a node, some residue curves will tend to track toward one saddle, while others track toward another saddle. For example, residue curve 1 in region I originates from the MEK-water azeotrope low-boiling node and travels first toward the single saddle of the region (MIPK-water azeotrope) before ending at the water high-boiling node. Likewise, residue curve 2 and all other residue curves in region I follow the same general path.

In region II, residue curve 3 originates from the MEK-water azeotrope, travels toward the MIPK-water saddle azeotrope, and ends at pure MIPK. However, residue curve 4 follows a completely different path, traveling toward the pure MEK saddle before ending at pure MIPK. Some multicomponent columns have been designed for operation in four-sided regions with the feed composition adjusted so that both the high-boiling and low-boiling nodes can be obtained simultaneously as products. However, small perturbations in feed composition or reflux can result in feasible operation on many different residue curves that originate and terminate at these product compositions. Multiple steady states and composition profiles that shift dramatically from tracking toward one saddle to the other are possible [Kovach and Seider, *AIChE J.*, **33,** 1300 (1987); Pham, Ryan, and Doherty, *AIChE J.*, **35,** 1585 (1989)]. Consider a column operating in region II of the MIPK-MEK-water diagram. Figure 13-82 shows the composition and temperature profiles for the column operating at three different sets of

TABLE 13-18 Temperature Profile—DRD # Table*

Temp. Profile	DRD #	Temp. Profile	DRD #	Temp. Profile	DRD #	Temp. Profile	DRD #	Temp. Profile	DRD #	Temp. Profile	DRD #
135	001	137524	099	624135	013	1357462	120	2671435	103	6247135	118
1325	014	137526	100	627135	095		121		119		119
1354	015	137542	099	641325	041		116		118		123
1356	016	137562	100		040	1357624	117	2674135	118	6271354	106
1435	004	143256	035	641352	041		116		119	6271435	118
2135	003		036	641735	098		125		103		103
6135	002	143257	078	642135	013	1357642	120	4132567	081		119
13254	017	143275	078	647135	098		117	4135267	081	6274135	103
13256	019	143526	036	714325	056		116	4135627	081		118
13524	017		035	721354	055	1372546	121	4135726	109		119
13526	019	143527	078	721356	050	1372564	117	4135762	109	6413257	085
13542	018	143562	035	721435	053	1375246	121	4137256	109	6413275	085
13546	021		037	724135	053	1375264	117	4137526	109	6413527	085
13547	069	143567	073	726135	049	1375426	121	4137562	109	6413725	107
13562	020	143725	097	741325	056	1375462	121	4173256	109	6413752	107
13564	022	143752	097	742135	053	1375624	117	4173526	109	6417325	107
13567	070	147325	097	746135	052	1375642	117	4173562	109	6417352	107
13725	092	147352	097	761325	051	1432567	089	4213567	082	6421735	123
13752	092	147356	093	761354	054		088	4217356	105	6427135	122
14325	028	174325	056	761435	052		081	4261735	114		123
027		213546	034	762135	049	1432576	088	4267135	122		119
14352	028	213547	072	764135	052	1432756	088		115	6471325	107
14356	031	213564	033	1325467	080	1435267	081		114	6471352	107
14735	091	213567	076	1325647	080		089	4271356	105	6472135	104
21354	026	214356	046	1325746	111		088	4276135	114		122
21356	029	214735	096		124	1435276	088		102		123
21435	009	241356	046		125	1435627	089		115	6714325	061
24135	009	241735	096	1325764	111		081	4613257	086	6741325	061
26135	007	246135	011		124		088	4613275	086	7143256	066
41325	027	247135	096		125	1435672	089	4613527	086	7143526	066
41735	091	261354	044	1352467	080	1435726	109	4613725	107	7143562	065
42135	010	261435	011	1352647	080	1435762	109	4613752	107	7213546	064
46135	005	264135	011	1352746	125	1437256	109	4617325	107	7213564	063
61325	030	267135	095		111	1437526	109	4617352	107	7214356	062
61354	032	413256	036		124	1437562	109	4621735	123	7241356	062
61435	006	413526	036	1352764	124	1473256	109	4627135	123	7246135	058
62135	008	413562	037		111	1473526	109		115	7261354	057
64135	006	413725	097		125	1473562	109		122	7261435	058
72135	047	413752	097	1354267	080	1743256	066	4671325	107	7264135	058
76135	048	417325	097	1354627	080	1743526	066	4671352	107	7413256	066
132546	024	417352	097	1354726	120	1743562	065	4672135	104	7413526	066
132547	075	417356	093		121	2135467	079		122	7413562	065
132564	025	421356	045		112	2135647	079		123	7421356	062
132567	071	421735	096	1354762	121	2135746	108	4761325	060	7426135	058
135246	024	426135	012		120	2135764	108	6132547	084	7461325	060
135247	075	427135	096		112	2143567	090	6135247	084		059
135264	025	461325	040	1356247	080	2147356	105	6135427	084		061
135267	071		042	1356427	080	2413567	090	6135724	110	7461352	059
135426	024	461352	042	1356724	113	2417356	105	6135742	110	7462135	058
135427	075	461735	098		117	2461735	114	6137254	110	7613254	068
135462	023	462135	012		116	2467135	114	6137524	110	7613524	068
135467	074	467135	098	1356742	116		115	6137542	110	7613542	067
135624	025	613254	038		117		118	6143257	085	7614325	061
135627	071	613524	038		113	2471356	105	6143275	085		060
135642	023	613542	039	1357246	121	2476135	115	6143527	085		059
135647	074	613547	077		125		114	6143725	107	7614352	059
135724	099	613725	094		124		102	6143752	107	7621354	057
135726	100	613752	094	1357264	117	2613547	083	6147325	107	7621435	058
135742	099	614325	041		125	2614735	114	6147352	107	7624135	058
135746	101		040		124	2641735	114	6174325	061	7641325	061
135762	100	614735	098	1357426	121	2647135	118	6213547	087		060
135764	101	621354	043		120		119	6214735	123		059
137254	099	614352	041		124		114	6214735	123	7641352	059
137256	100	621435	013			2671354	106	6241735	123	7642135	058

Ternary DRD table lookup procedure:

1. Classify a system by writing down each position number in ascending order of boiling points.
   - A position number is not written down if there is no azeotrope at that position.
   - The resulting sequence of numbers is known as the *temperature profile.*
   - Each temperature profile will have a minimum of three numbers and a maximum of seven numbers.
   - List multiple temperature profiles when you have incomplete azeotropic data.
   - All seven position numbers are shown on the diagram.
2. Using the table, look up the temperature profile(s) to find the corresponding DRD #.

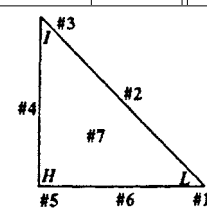

*Table 13-18 and Fig. 13-79 developed by Eric J. Peterson, Eastman Chemical Co.

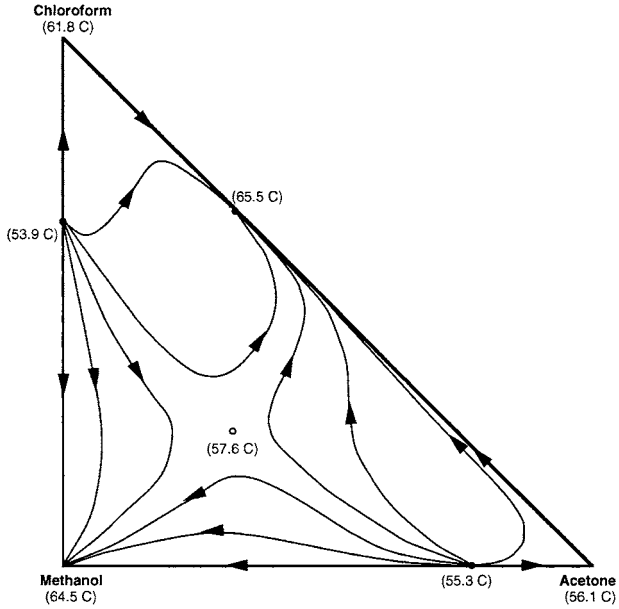

FIG. 13-80 Residue curves for acetone-chloroform-methanol system at 1-atm pressure suggesting a ternary saddle azeotrope.

operating conditions and two feed locations, as given in Table 13-19. The desired product specification is 97 mol % MIPK, no more than 3 mol % MEK, and less than 10 ppm residual water. For case A (Fig. 13-82*a*), the column profile tracks up the water-free side of the diagram. A pinched zone (i.e., section of little change in tray temperature and composition) occurs above the feed between the feed tray (tray 4) and tray 18. The temperature remains constant at about 93°C throughout the pinch zone. Product specifications are met.

When the feed composition becomes slightly enriched in water, as with case B, the column profile changes drastically (Fig. 13-82*b*). At the same reflux and boil-up, the column no longer meets specifications. The MIPK product is lean in MIPK and too rich in water. The profile now tracks generally up the left side of region II. Note also the dramatic change in the temperature profile. A pinched zone still exists above the feed between trays 4 and 18, but the tray temperature in the zone has dropped to 80°C (from 93°C). Most of the trays are required to move through the vicinity of the saddle. Typically, pinches (if they exist) occur close to saddles and nodes.

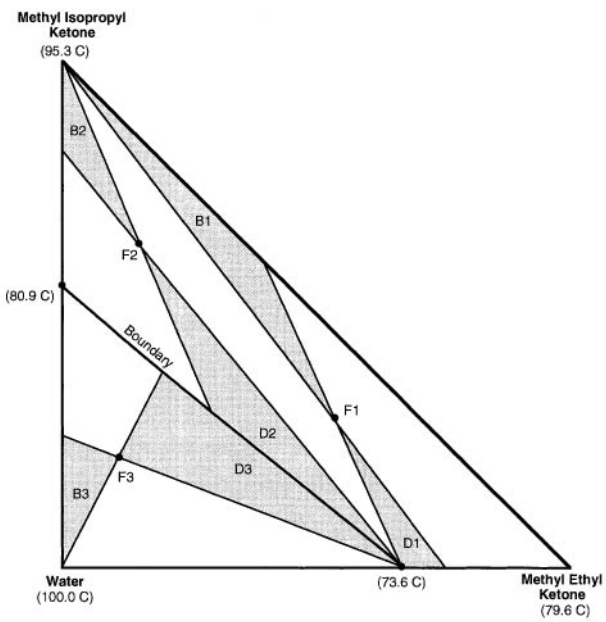

FIG. 13-81 MEK-MIPK-water system. Approximate product compositions regions for a simple distillation column.

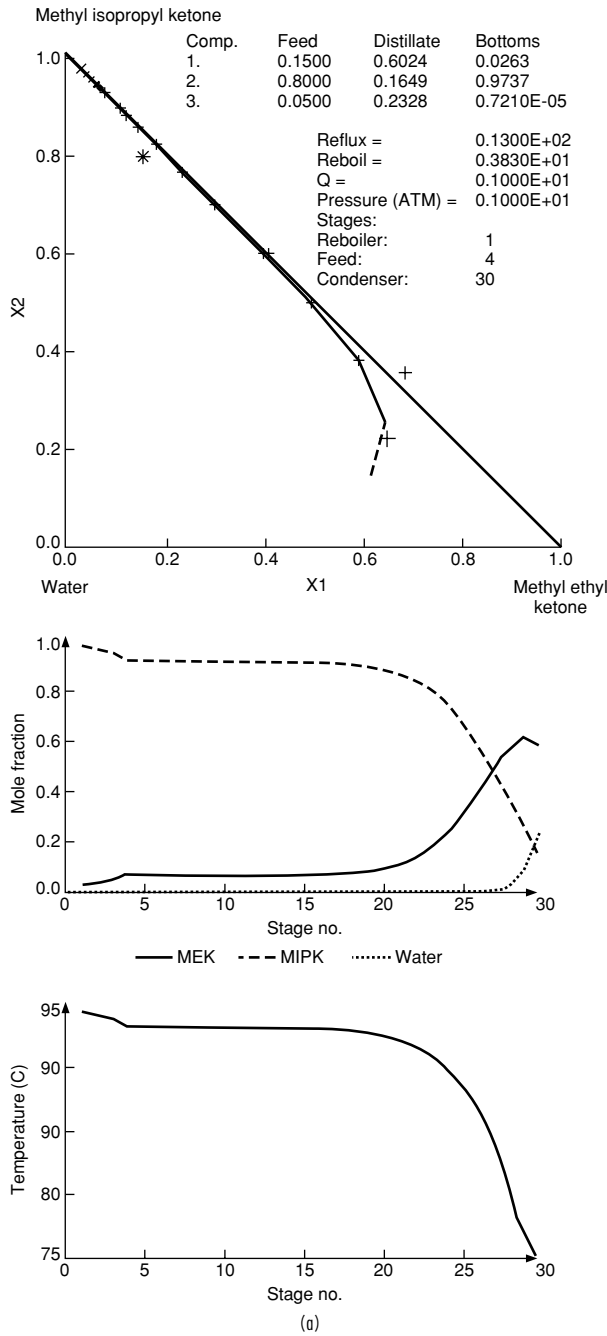

FIG. 13-82 Sensitivity of composition and temperature profiles for MEK-MIPK-water system at 1 atm.

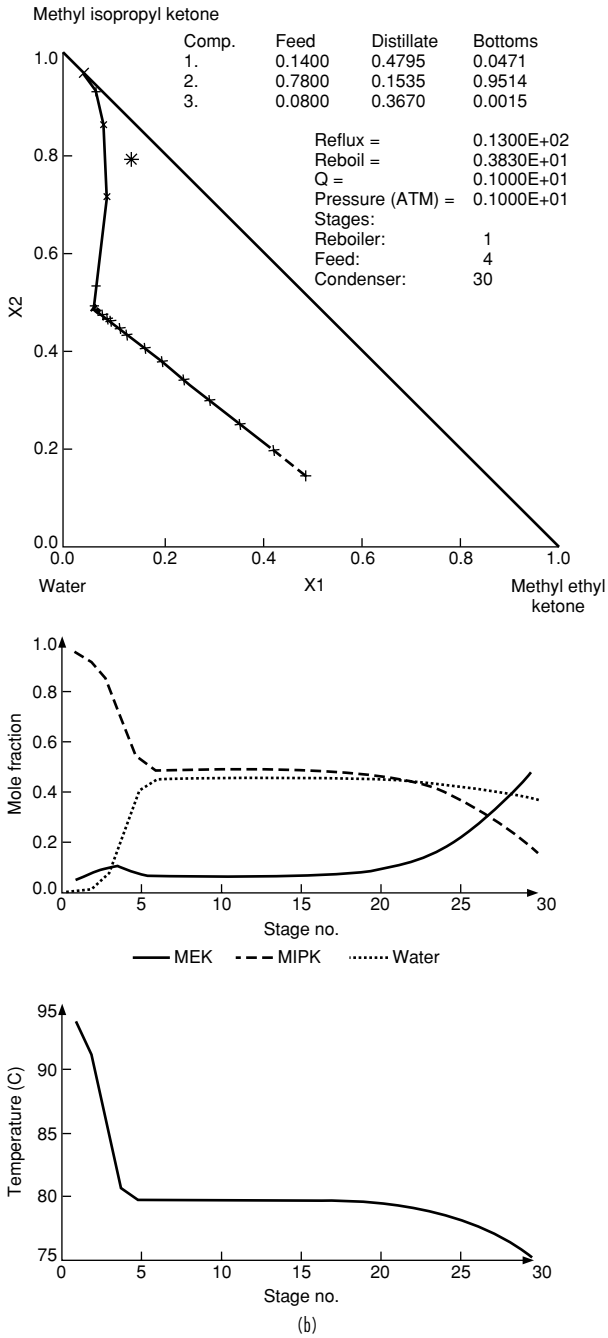

FIG. 13-82 (*Continued*)

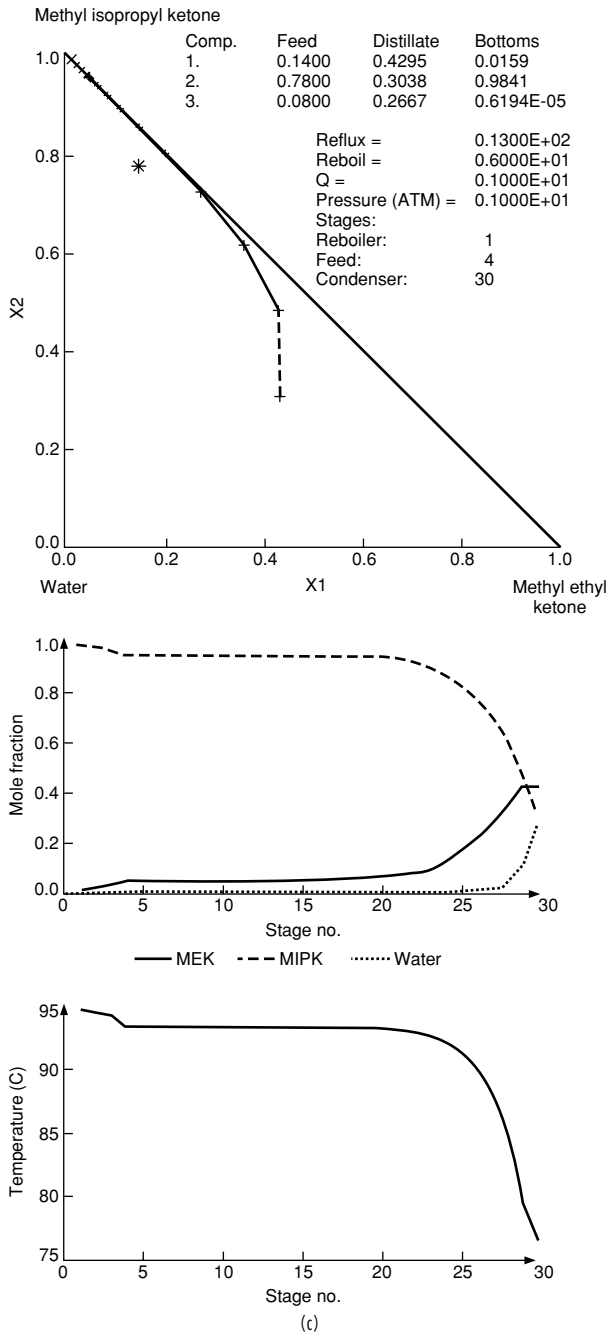

FIG. 13-82 (*Continued*)

In case C (Fig. 13-82*c*), increasing the boil-up ratio to 6 brings the MIPK product back within specifications, but the production rate and recovery have dropped off. In addition, the profile has switched back to the right side of the region; and the temperatures on trays in the pinched zone (trays 4 through 18) are back to 93°C. Such a drastic fluctuation in tray temperature with a relatively minor adjustment of the manipulated variable (boil-up in this case) can make control difficult. This is especially true if the control strategy involves maintaining a constant temperature on one of the trays between trays 4 and 18. If a tray is selected that exhibits wide temperature swings, the control system may have a difficult time compensating for disturbances. Such columns are also often difficult to model with a process simulator. Design algorithms often rely on perturbation of a variable (such as reflux or reboil) while checking for convergence of column heat and

TABLE 13-19 Sets of Operating Conditions for Fig. 13-82

Case	Reflux ratio	Reboil ratio		Feed composition	Distillate composition	Bottoms composition
A	13	3.8	MEK	0.15	0.60	0.03
			MIPK	0.80	0.16	0.97
			water	0.05	0.24	7 ppm
B	13	3.8	MEK	0.14	0.48	0.05
			MIPK	0.78	0.15	0.95
			water	0.08	0.37	20,000 ppm
C	13	6	MEK	0.14	0.43	0.02
			MIPK	0.78	0.30	0.98
			water	0.08	0.27	6.5 ppm

material balances. In situations where the column profile is altered drastically by minor changes in the perturbed variable, the simulator may be close to a feasible solution, but successive iterations may appear to be very far apart. The convergence routine may continue to oscillate between column profiles and never reach a solution. Likewise, when an attempt is made to design a column to obtain product compositions in different distillation regions, the simulation will never converge.

AZEOTROPIC DISTILLATION

The term *azeotropic distillation* has been applied to a broad class of fractional distillation-based separation techniques when specific azeotropic behavior is exploited to effect a separation. The agent that causes the specific azeotropic behavior, often called the *entrainer,* may already be present in the feed mixture (a self-entraining mixture) or may be an added mass separation agent. Azeotropic distillation techniques are used throughout the petrochemical and chemical processing industries for the separation of close-boiling, pinched, or azeotropic systems for which simple distillation is either too expensive or impossible. With an azeotropic feed mixture, presence of the azeotroping agent results in the formation of a more favorable azeotropic pattern for the desired separation. For a close-boiling or pinched feed mixture, the azeotroping agent changes the dimensionality of the system and allows separation to occur along a less pinched path. Within the general heading of azeotropic distillation techniques, several approaches have been followed in devising azeotropic distillation flow sheets including

1. Choosing an entrainer to give a residue curve map with specific distillation regions and node temperatures
2. Exploiting changes in azeotropic composition with total system pressure
3. Exploiting curvature of distillation region boundaries
4. Choosing an entrainer to cause azeotrope formation in combination with liquid-liquid immiscibility

The first three of these are solely VLE-based approaches, involving a series of simple distillation column operations and recycles. The final approach relies on distillation (VLE), but also exploits another physical phenomenon, liquid-liquid phase formation (phase splitting), to assist in entrainer recovery. This approach is the most powerful and versatile. Examples of industrial uses of azeotropic distillation grouped by method are given in Table 13-20.

The choice of the appropriate azeotropic distillation method and the resulting flow sheet for the separation of a particular mixture are strong functions of the separation objective. For example, it may be desirable to recover all constituents of the original feed mixture as pure components, or only some as pure components and others as azeotropic mixtures suitable for recycle. Not every objective may be obtainable by azeotropic distillation for a given mixture and portfolio of candidate entrainers.

Exploiting Homogeneous Azeotropes Homogeneous azeotropic distillation refers to a flow sheet structure in which azeotrope formation is exploited or avoided in order to accomplish the desired separation in one or more distillation columns. Either the azeotropes in the system do not exhibit two-liquid-phase behavior, or the liquid-phase behavior is not or cannot be exploited in the separation sequence. The structure of a particular sequence will depend on the geometry of the residue curve map or distillation region diagram for the feed mixture-entrainer system. Two approaches are possible:

1. Selection of an entrainer such that the desired products all lie within the *same* distillation region (the products may be pure components or azeotropic mixtures)
2. Selection of an entrainer such that some type of distillation boundary-crossing mechanism is employed to separate desired products that lie in *different* regions.

As mentioned previously, ternary mixtures can be represented by 125 different residue curve maps or distillation region diagrams. However, feasible distillation sequences using the first approach can be developed for breaking homogeneous binary azeotropes by the addition of a third component only for those more restricted systems that do not have a distillation boundary connected to the azeotrope and for which one of the original components is a node. For example, from Fig. 13-79, the following eight residue curve maps are suitable for breaking homogeneous minimum-boiling azeotropes: DRD 002, 027, 030, 040, 051, 056, 060, and 061 as collected in Fig. 13-83. To produce the necessary distillation region diagrams, an entrainer must be found that is either: (1) an intermediate boiler that forms no azeotropes (DRD 002), or (2) lowest-boiling or intermediate-boiling and forms a maximum-boiling azeotrope with the lower-boiling original component (A). In these cases, the entrainer may also optionally form a minimum-boiling azeotrope with the higher boiling of the original components or a minimum-boiling ternary azeotrope. In all cases, after the addition of the entrainer, the higher-boiling original component (B) is a high-boiling node and is removed as bottoms product from a first column operated in the indirect-split mode with the lower-boiling original component recovered as distillate in a second column; see flow sheet in Fig. 13-83.

The seven residue curve maps suitable for breaking homogeneous maximum-boiling binary azeotropes (DRD 028, 031, 035, 073, 078, 088, 089) are shown in Fig. 13-84. In this case, the entrainer must form a minimum-boiling azeotrope with the higher-boiling original component and either a maximum-boiling azeotrope or no azeotrope with the lower-boiling original component. In all cases, after the addition of the entrainer, the lower-boiling original component is a low-boiling node and is removed as distillate from a first column operated in the direct-split mode with the higher-boiling original component recovered as bottoms product in a second column; see flow sheet in Fig. 13-84.

The restrictions on the boiling point and azeotrope formation of the entrainer act as efficient screening criteria for entrainer selection. Entrainers that do not show appropriate boiling point characteristics can be discarded without detailed analysis. However, the entrainers in Fig. 13-83 do suffer from serious drawbacks that limit their practical application. DRD 002 requires that the entrainer be an intermediate-boiling component that forms no azeotropes. Unfortunately these are often difficult criteria to meet, as any intermediate boiler will be closer-boiling to both of the original components and, therefore, will be more likely to be at least pinched or even form azeotropes. The remaining feasible distillation region diagrams require that the entrainer form a maximum-boiling azeotrope with the lower-boiling original component. Because maximum-boiling azeotropes are relatively rare, finding a suitable entrainer may be difficult.

For example, the dehydration of organics that form homogeneous azeotropes with water is a common industrial problem. It is extremely difficult to find an intermediate-boiling entrainer that also does not form an azeotrope with water. Furthermore, the resulting separation is likely to be close-boiling or pinched throughout most of the column, requiring a large number of stages. For example, consider the separation of valeric acid (187.0°C) and water. This system exhibits a minimum-boiling azeotrope (99.8°C) with a composition and boiling point close to those of pure water. Ignoring for the moment potentially severe corrosion problems, formic acid (100.7°C), which is an intermediate boiler and which forms a maximum-boiling azeotrope with water (107.1°C), is a candidate entrainer (DRD 030, Fig. 13-85*a*). In the conceptual sequence shown in Fig. 13-85*b*, a recycle of the formic acid–water maximum-boiling azeotrope is added to the

TABLE 13-20 Examples of Azeotropic Distillation

System	Type	Entrainer(s)	Remark
Exploitation of homogeneous azeotropes			
No known industrial examples			
Exploitation of pressure sensitivity			
THF-water	Minimum-boiling azeotrope	None	Alternative to extractive distillation
Methyl acetate-methanol	Minimum-boiling azeotrope	None	Element of recovery system for alternative to production of methyl acetate by reactive distillation; alternative to azeotropic, extractive distillation
Alcohol-ketone systems	Minimum-boiling azeotropes	None	
Ethanol-water	Minimum-boiling azeotrope	None	Alternative to extractive distillation, salt extractive distillation, heterogeneous azeotropic distillation; must reduce pressure to less than 11.5 kPa for azeotrope to disappear
Exploitation of boundary curvature			
Hydrochloric acid-water	Maximum-boiling azeotrope	Sulfuric acid	Alternative to salt extractive distillation
Nitric acid-water	Maximum-boiling azeotrope	Sulfuric acid	Alternative to salt extractive distillation
Exploitation of azeotropy and liquid phase immiscibility			
Ethanol-water	Minimum-boiling azeotrope	Cyclohexane, benzene, heptane, hexane, toluene, gasolene, diethyl ether	Alternative to extractive distillation, pressure-swing distillation
Acetic acid-water	Pinched system	Ethyl acetate, propyl acetate, diethyl ether, dichloroethane, butyl acetate	
Butanol-water	Minimum-boiling azeotrope	Self-entraining	
Acetic acid-water-vinyl acetate	Pinched, azeotropic system	Self-entraining	
Methyl acetate-methanol	Minimum-boiling azeotrope	Toluene, methyl isobutyl ketone	Element of recovery system for alternative to production of methyl acetate by reactive distillation; alternative to extractive pressure-swing distillation
Diethoxymethanol-water-ethanol	Minimum-boiling azeotropes	Self-entraining	
Pyridine-water	Minimum-boiling azeotrope	Benzene	Alternative to extractive distillation
Hydrocarbon-water	Minimum-boiling azeotrope	Self-entraining	

original valeric acid–water feed, which may be of any composition. Using the indirect-split mode of operation, the high-boiling node valeric acid is removed in high purity and high recovery as bottoms in a first column, which by mass balance produces a formic acid–water distillate. This binary mixture is fed to a second column that produces pure water as distillate and the formic acid–water azeotrope as bottoms for recycle to the first column. The inventory of formic acid is an important optimization variable in this theoretically feasible but difficult separation scheme.

Exploiting Pressure Sensitivity Breaking a homogeneous azeotrope that is part of a distillation boundary (i.e., the desired products lie in different distillation regions on either side of the boundary) requires that the boundary be "crossed" by the separation system. This may be done by mixing some external stream with the original feed stream in one region such that the resulting composition is in another region for further processing. However, the external stream must be completely regenerated, and mass balance must be preserved. For example, it is not possible to break a homogeneous binary azeotrope simply by adding one of the products to cross the azeotropic composition.

The composition of many azeotropes varies with the system pressure (Horsley, *Azeotropic Data-III,* American Chemical Society, Washington, 1983; Gmehling et al., *Azeotropic Data,* VCH Publishers, Deerfield Beach, Fla., 1994). This effect can be exploited to separate azeotropic mixtures by so-called pressure-swing distillation if at some pressure the azeotrope simply disappears, such as does the ethanol-water azeotrope at pressures below 11.5 kPa. However, pressure sensitivity can still be exploited if the azeotropic composition and related distillation boundary change sufficiently over a moderate change in total system pressure. A composition in one distillation region under one set of conditions could be in a different region under a different set of conditions. A two-column sequence for separating a binary maximum-boiling azeotrope is shown in Fig. 13-86 for a system in which the azeotropic composition at pressure P1 is richer in component B than the azeotropic composition at pressure P2. The first column, operating at pressure P1, is fed a mixture of fresh feed plus recycle stream from the second column such that the overall composition lies on the A-rich side of the azeotropic composition at P1. Pure component A is recovered as distillate, and a mixture near the azeotropic composition is produced as bottoms. The pressure of this bottoms stream is changed to P2 and fed to the second column. This feed is on the B-rich side of the azeotropic composition at P2. Pure component B is now recovered as the distillate, and the azeotropic bottoms composition is recycled to the first column. An analogous flow sheet can be used for separating binary homogeneous minimum-boiling azeotropes. In this case the pure components are recovered as bottoms in both columns, and the distillate from each column is recycled to the other column.

For pressure-swing distillation to be practical, the azeotropic composition must vary at least 5 percent (preferably 10 percent or more) over a moderate pressure range (not more than 10 atm between the two pressures). With a very large pressure range, refrigeration may be required for condensation of the low-pressure distillate, or an impractically high reboiler temperature may result in the high-pressure column. The smaller the variation of azeotrope composition over the pressure range, the larger the recycle flow rates between the two columns. In particular, for minimum-boiling azeotropes, the pressure-swing distillation approach requires high energy usage and high capital

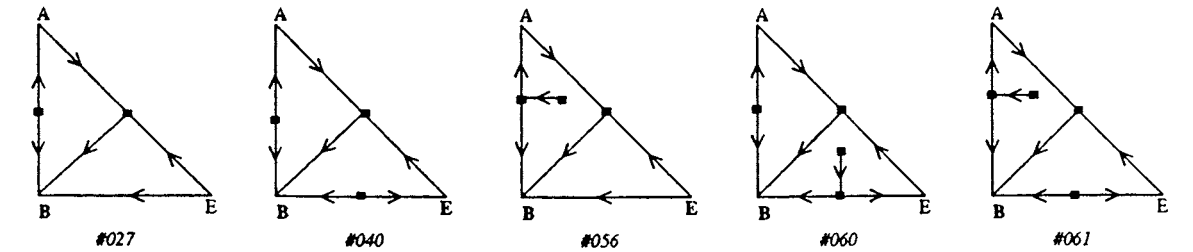

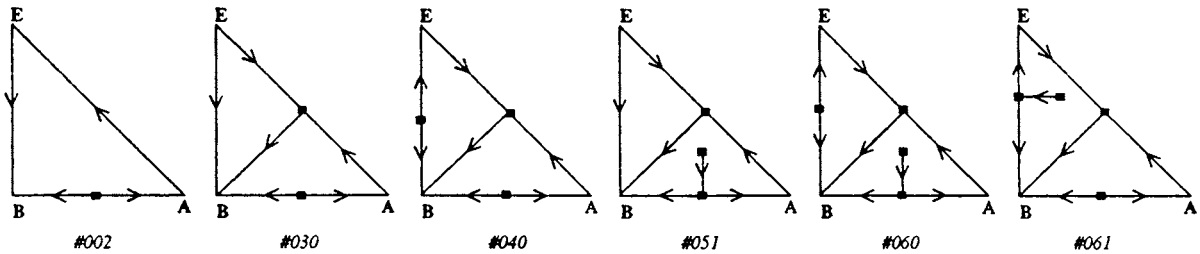

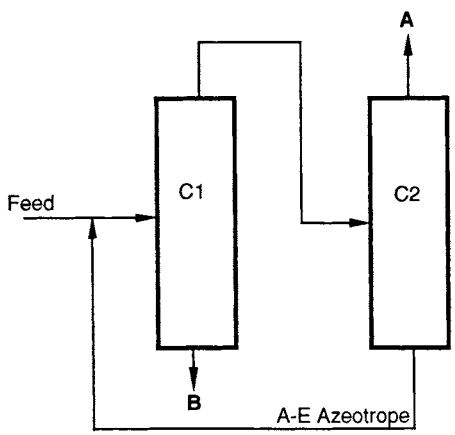

FIG. 13-83 Feasible distillation region diagrams and associated distillation system for breaking a homogeneous minimum-boiling binary azeotrope A-B. Component B boils at a higher temperature than does A.

costs (large-diameter columns) because both recycled azeotropic compositions must be taken overhead. Moreover, one lobe of an azeotropic VLE diagram is often pinched regardless of pressure; and, therefore, one of the columns will require a large number of stages to produce the corresponding pure-component product.

General information on pressure-swing distillation can be found in Van Winkle (*Distillation,* McGraw-Hill, New York, 1967), Wankat (*Equilibrium-Staged Separations,* Elsevier, New York, 1988), and Knapp and Doherty [*Ind. Eng. Chem. Res.,* **31,** 346 (1992)]. Only a relatively small fraction of azeotropes are sufficiently pressure-sensitive for a pressure-swing process to be economical. Some applications include the minimum-boiling azeotrope tetrahydrofuran-water [Tanabe et al.; U.S. Patent 4,093,633 (1978)], and maximum-boiling azeotropes of hydrogen chloride–water and formic acid–water (Horsley, *Azeotropic Data-III,* American Chemical Society, Washington, 1983). Since distillation boundaries move with pressure-sensitive azeotropes, the pressure-swing principle can also be used for overcoming distillation boundaries in multicomponent azeotropic mixtures.

Exploiting Boundary Curvature A second approach to boundary crossing exploits boundary curvature to produce compositions in different distillation regions. When distillation boundaries exhibit extreme curvature, it may be possible to design a column such that the distillate and bottoms compositions are on the same residue curve in one distillation region, while the feed composition (which is not

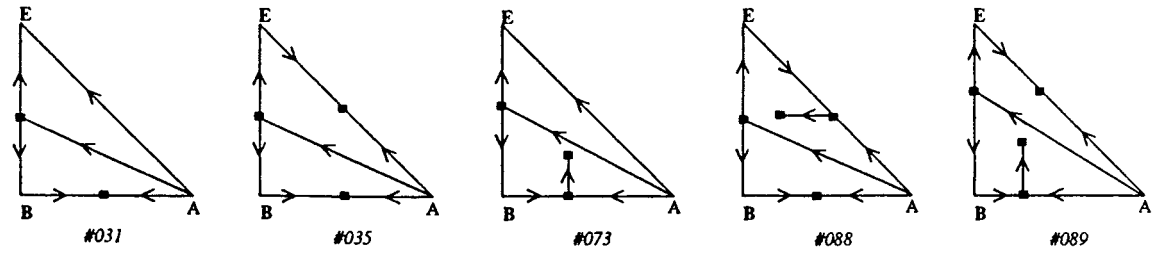

INTERMEDIATE-BOILING ENTRAINER.

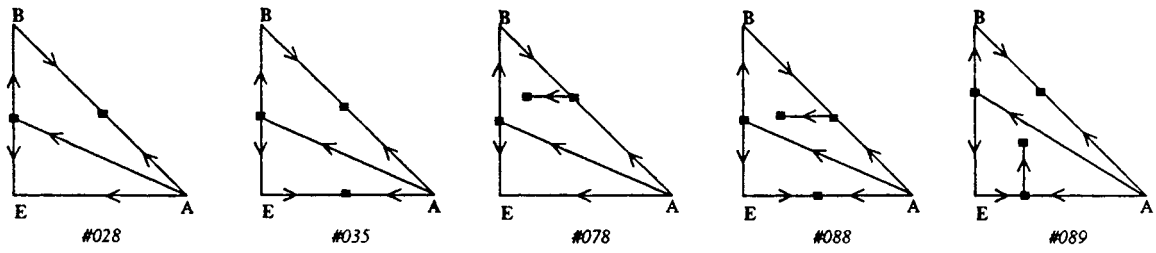

HIGH-BOILING ENTRAINER.

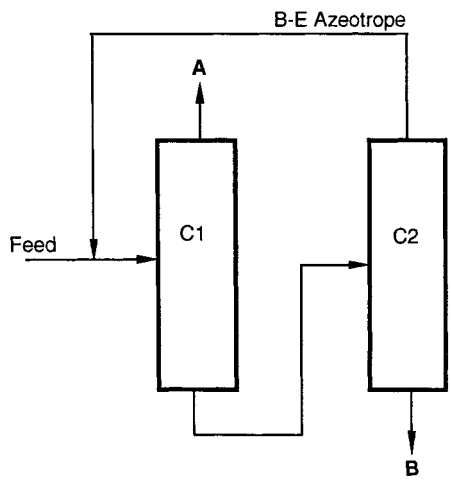

FIG. 13-84 Feasible distillation region diagrams and associated distillation system for breaking a homogeneous maximum-boiling binary azeotrope A-B. Component B boils at a higher temperature than does A.

required to lie on the column composition profile) is in another distillation region. For such a column to meet material balance constraints (i.e., bottom, distillate, feed compositions on a straight line), the feed must be located in a region where the boundary is concave.

As an example, Van Dongen (Ph.D. Thesis, University of Massachusetts, 1983) considered the separation of a methanol–methyl acetate mixture, which forms a homogeneous azeotrope, using *n*-hexane as an entrainer. The distillation boundaries for this system (Fig. 13-87*a*) are somewhat curved. A separation sequence that exploits this boundary curvature is shown in Fig. 13-87*b*. Recycled methanol–methyl acetate binary azeotrope and methanol–methyl acetate–hexane ternary azeotrope are added to the original feed F0 to produce a net feed composition F1 for column C1 designed to lie on a line between pure methanol and the curved part of the boundary between regions I and II. Column C1 is operated in the indirect-split mode, producing the high-boiling node methanol as a bottoms product, and by mass balance, a distillate near the curved boundary. The distillate, although in region I, becomes feed F2 to column C2 which is operated in the direct-split mode entirely in region II, producing the low-boiling node ternary azeotrope as distillate and by mass balance, a methanol–methyl acetate mixture as bottoms (B2). This bottoms mixture is on the opposite side of the methanol–methyl acetate azeotrope than the original feed F0. The bottoms from C2 is finally fed to binary distillation column C3, which produces pure methyl acetate as bottoms product (B3)

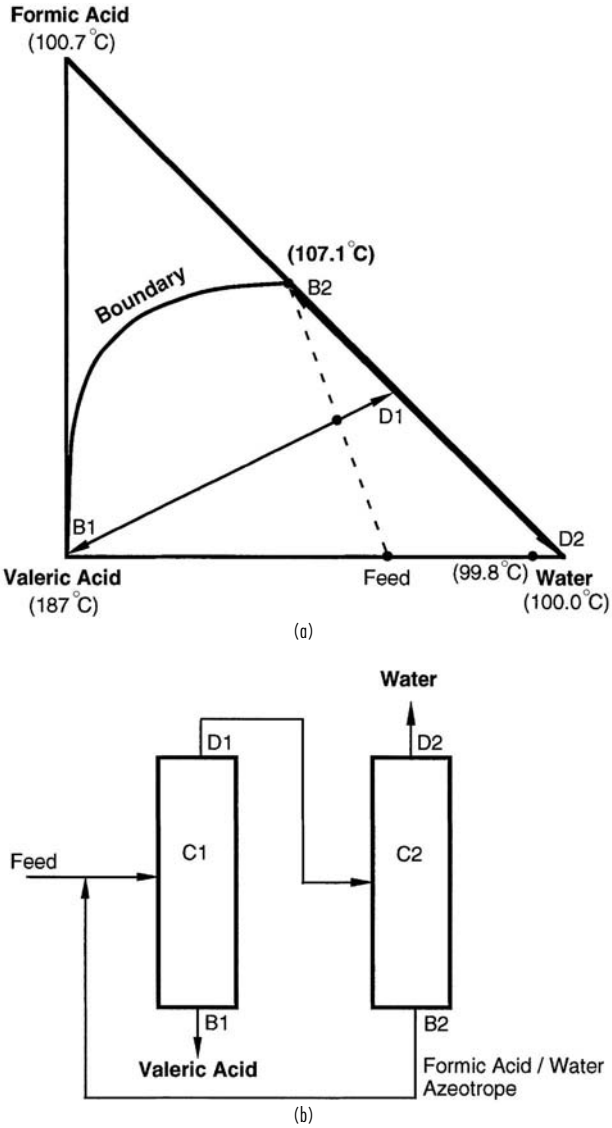

FIG. 13-85 Valeric acid-water separation with formic acid. (*a*) Mass balances on distillation region diagram. (*b*) Conceptual sequence.

and the methanol–methyl acetate azeotrope as distillate (D3). The distillates from columns C2 and C3 are recycled to column C1. The distillate and bottoms compositions for column C2 lie on the same residue curve, and the composition profile lies entirely within region II, even though its feed composition is in region I. Additional information on exploiting boundary curvature, including the useful concept of a *pitchfork distillation boundary*, can be found in Doherty and Malone (*Conceptual Design of Distillation Systems*, McGraw-Hill, 2001, sec. 5.4).

Exploiting boundary curvature for breaking azeotropes is very similar to exploiting pressure sensitivity from a mass balance point of view, and suffers from the same disadvantages. Separation schemes have large recycle flows, and in the case of minimum-boiling azeotropes, the recycle streams are distillates. However, in the case of maximum-boiling azeotropes, these recycles are bottoms products, and the economics are improved. One such application, illustrated in Fig. 13-88, is the separation of the maximum-boiling nitric acid–water azeotrope by adding sulfuric acid. Recycled sulfuric acid is added to a

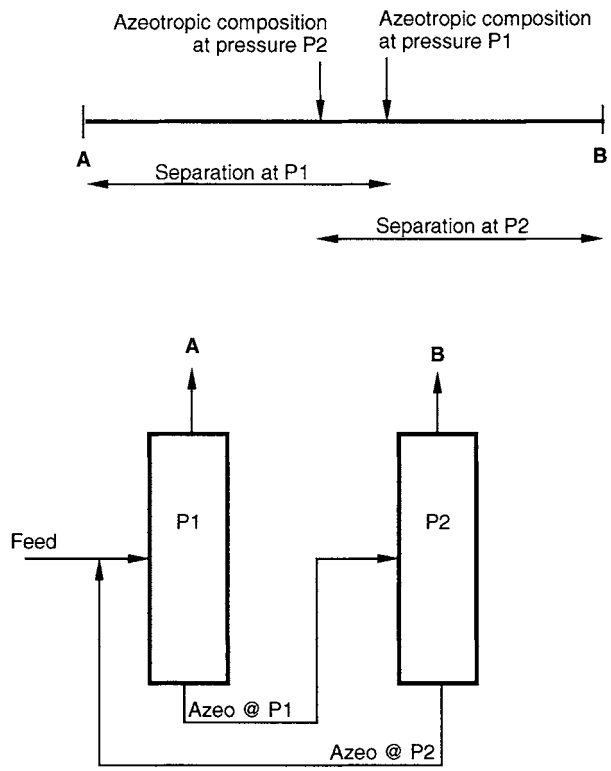

FIG. 13-86 Conceptual sequence for separating maximum-boiling binary azeotrope with pressure-swing distillation.

nitric acid–water mixture near the azeotropic composition to produce a net feed F1 in region II. The first column, operated in the direct-split mode, produces a nitric acid distillate and a bottoms product, by mass balance, near the distillation boundary. In this case, sulfuric acid associates with water so strongly and the distillation boundary is so curved and nearly tangent to the water–sulfuric acid edge of the composition diagram that the second column operating in the indirect-split mode in region I, producing sulfuric acid as bottoms product, also produces a distillate close enough to the water specification that a third column is not required [Thiemann et al., in *Ullmann's Encyclopedia of Industrial Chemistry*, 5th ed., vol. **A17,** VCH Verlagsgesellschaft mbH, Weinheim, (1991)].

Exploiting Azeotropy and Liquid-Phase Immiscibility One powerful and versatile separation approach exploits several physical phenomena simultaneously including nonideal vapor-liquid behavior, where possible, and liquid-liquid behavior to bypass difficult distillation separations. For example, the overall separation of close-boiling mixtures can be made easier by the addition of an entrainer that introduces liquid-liquid immiscibility and forms a heterogeneous minimum-boiling azeotrope with one (generally the lower-boiling) of the key components. Two-liquid-phase formation provides a means of breaking this azeotrope, thus simplifying the entrainer recovery and recycle process. Moreover, since liquid-liquid tie lines are unaffected by distillation boundaries (and the separate liquid phases are often located in different distillation regions), liquid-liquid phase splitting is a powerful mechanism for crossing distillation boundaries. The phase separator is usually a simple decanter, but sometimes a multistage extractor is substituted. The decanter or extractor can also be replaced by some other non-VLE-based separation technique such as membrane permeation, chromatography, adsorption, or crystallization. Also sequences may include additional separation operations (distillations or other methods) for preconcentration of the feed mixture, entrainer recovery, and final-product purification.

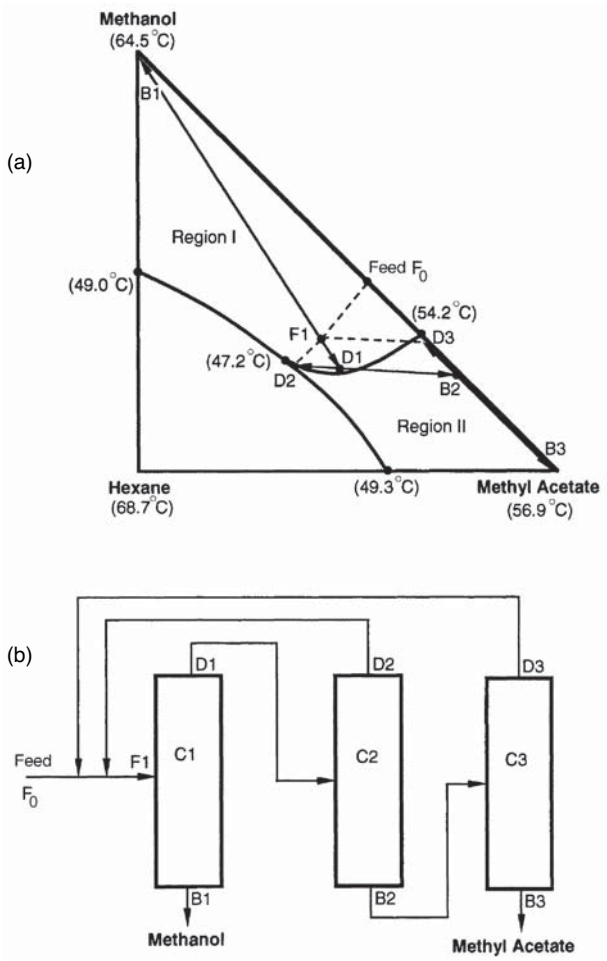

FIG. 13-87 Separation of methanol–methyl acetate by exploitation of distillation boundary curvature.

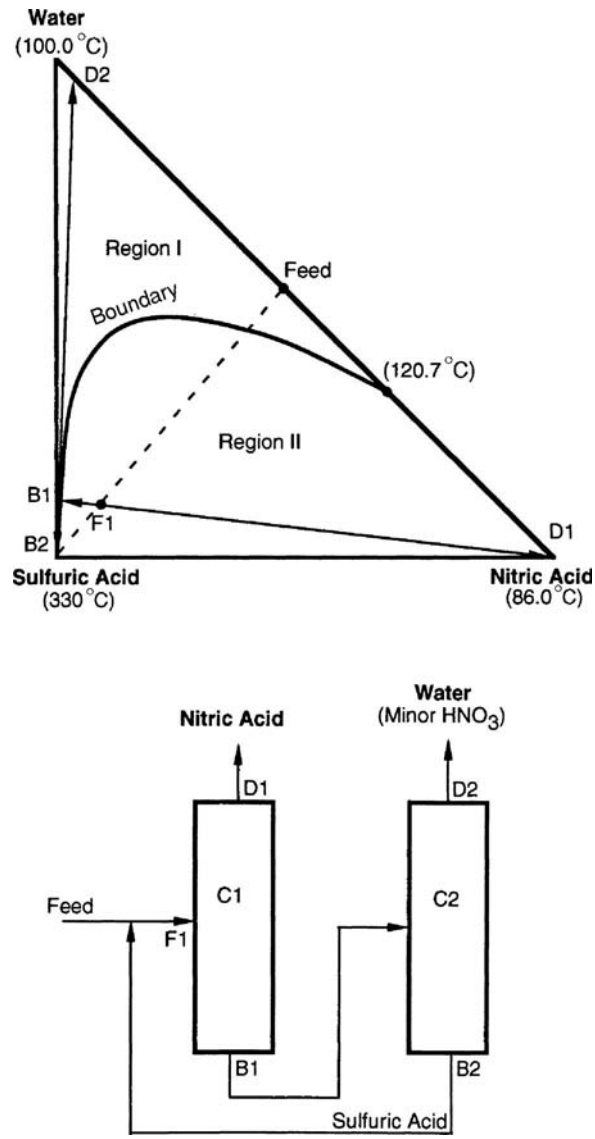

FIG. 13-88 Separation of nitric acid–water system with sulfuric acid in a two-column sequence exploiting extreme boundary curvature.

The simplest case of combining VLE and LLE is the separation of a binary heterogeneous azeotropic mixture. One example is the dehydration of 1-butanol, a self-entraining system, in which butanol (117.7°C) and water form a minimum-boiling heterogeneous azeotrope (93.0°C). As shown in Fig. 13-89, the fresh feed may be added to either column C1 or C2, depending on whether the feed is on the organic-rich side or the water-rich side of the azeotrope. The feed may also be added into the decanter directly if it does not move the overall composition of the decanter outside of the two-liquid phase region. Column C1 produces anhydrous butanol as a bottoms product and a composition close to the butanol-water azeotrope as the distillate. After condensation, the azeotrope rapidly phase-separates in the decanter. The upper layer, consisting of 78 wt % butanol, is refluxed totally to column C1 for further butanol recovery. The water layer, consisting of 92 wt % water, is fed to column C2. This column produces pure water as a bottoms product and, again, a composition close to the azeotrope as distillate for recycle to the decanter. Sparged steam may be used in C2, saving the cost of a reboiler. A similar flow sheet can be used for dehydration of hydrocarbons and other species that are largely immiscible with water.

A second example of the use of liquid-liquid immiscibilities in an azeotropic distillation sequence is the separation of the ethanol-water minimum-boiling homogeneous azeotrope. For this separation, a number of entrainers have been proposed, which are usually chosen to be immiscible with water and form a ternary minimum-boiling (preferably heterogeneous) azeotrope with ethanol and water (and, therefore, usually also binary minimum-boiling azeotropes with both ethanol and water). All such systems correspond to DRD 058, although the labeling of the vertices depends on whether the entrainer is lower-boiling than ethanol, intermediate-boiling, or higher-boiling than water. The residue curve map for the case of cyclohexane as entrainer was illustrated in Fig. 13-78*c*. One three-column distillation sequence is shown in Fig. 13-90. Other two-, three-, or four-column sequences have been described by Knapp and Doherty (*Kirk-Othmer Encyclopedia of Chemical Technology,* 5th ed., vol. 8, p. 786, Wiley, New York, 2004).

Fresh aqueous ethanol feed is first preconcentrated to nearly the azeotropic composition in column C3, while producing a water bottoms product. The distillate from C3 is sent to column C1, which is refluxed with the entire organic (entrainer-rich) layer, recycled from a decanter. Mixing of these two streams is the key to this sequence as it allows the overall feed composition to cross the distillation boundary

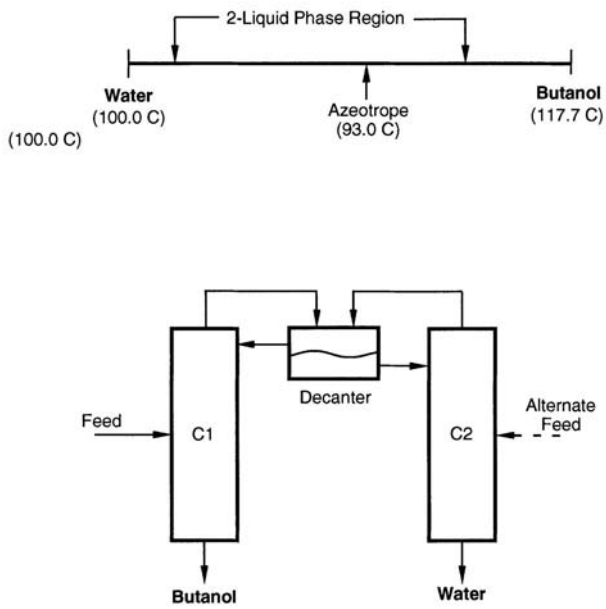

FIG. 13-89 Separation of butanol-water with heterogeneous azeotropic distillation.

into region II. Column C1 is operated to recover pure high-boiling node ethanol as a bottoms product and to produce a distillate close to the ternary azeotrope. If the ternary azeotrope is heterogeneous (as it is in this case), it is sent to the decanter for phase separation. If the ternary azeotrope is homogeneous (as it is in the alternative case of ethyl acetate as the entrainer), the distillate is first mixed with water before being sent to the decanter. The inventory of entrainer is adjusted to allow column C1 to operate essentially between two nodes, although such practice, as discussed previously, is relatively susceptible to instabilities from minor feed or reflux perturbations. Refluxing a fraction of the water-rich decanter layer results in an additional degree of freedom to mitigate against variability in the feed composition. The remaining portion of the water layer from the decanter is stripped of residual cyclohexane in column C2, which may be operated either in the direct-split mode (producing low-boiling node ternary azeotrope as distillate and, by mass balance, an ethanol-water bottoms for recycle to C3) or in the indirect-split mode (producing high-boiling node water as bottoms and, by mass balance, a ternary distillate near the distillation boundary). (The distillate may be recycled to the decanter, the top of column C1, or the C1 feed.) The indirect-split mode alternatives are discussed in greater detail by Knapp and Doherty (*Kirk-Othmer Encyclopedia of Chemical Technology*, 5th ed., vol. 8, p. 786, Wiley, New York, 2004).

Design and Operation of Azeotropic Distillation Columns Simulation and design of azeotropic distillation columns are a difficult computational problem, but one that is readily handled, in most cases, by widely available commercial computer process simulation packages [Glasscock and Hale, *Chem. Eng.*, **101**(11), 82 (1994)]. Most simulators are capable of modeling the steady-state and dynamic behavior of both homogeneous azeotropic distillation systems and those systems involving two-liquid phase behavior within the column, if accurate thermodynamic data and activity coefficient or equation-of-state models are available. However, VLE and VLLE estimated or extrapolated from binary data or predicted from such methods as UNIFAC may not be able to accurately locate boundaries and predict the extent of liquid immiscibilities. Moreover, different activity coefficient models fit to the same experimental data often give very different results for the shape of distillation boundaries and liquid-liquid regions. Therefore the design of separation schemes relying on boundary curvature should not be attempted unless accurate, reliable experimental equilibrium data are available.

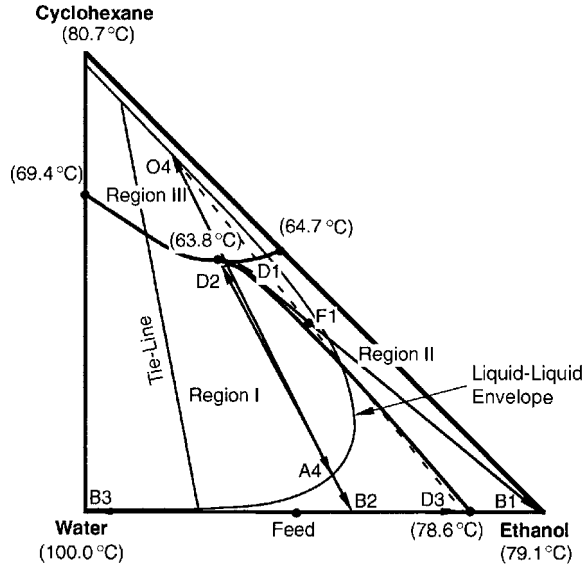

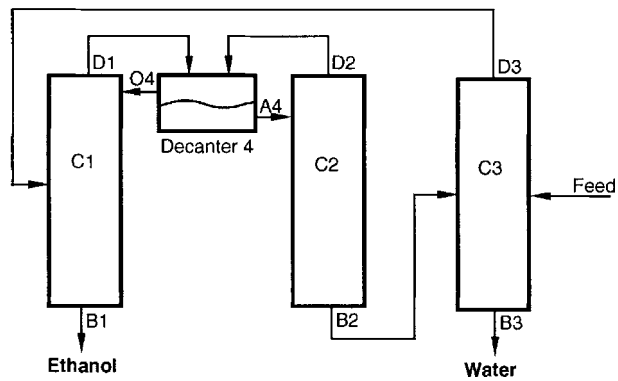

FIG. 13-90 Three-column sequence for ethanol dehydration with cyclohexane (operating column C2 in the direct-split mode).

Two liquid phases can occur within a column in the distillation of heterogeneous systems. Older references, e.g., Robinson and Gilliland (*Elements of Fractional Distillation*, McGraw-Hill, New York, 1950), state that the presence of two liquid phases in a column should be avoided as much as possible because performance may be reduced. However, more recent studies indicate that problems with two-phase flow have been overstated [Herron et al., *AIChE J.*, **34,** 1267 (1988); and Harrison, *Chem. Eng. Prog.*, **86**(11), 80 (1990)]. Based on case history data and experimental evidence, there is no reason to expect unusual capacity or pressure-drop limitations, and standard correlations for these parameters should give acceptable results. Because of the intense nature of the gas-liquid-liquid mixing on trays, mass-transfer efficiencies are relatively unaffected by liquid-liquid phase behavior. The falling-film nature of gas-liquid-liquid contact in packing, however, makes that situation more uncertain. Reduced efficiencies may be expected in systems where one of the keys distributes between the phases.

EXTRACTIVE DISTILLATION

Extractive distillation is a partial vaporization process in the presence of a miscible, high-boiling, nonvolatile mass separation agent, normally

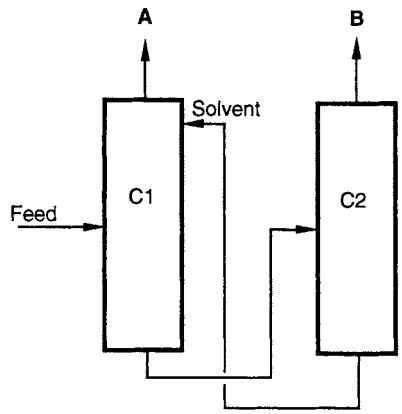

FIG. 13-91 Typical extractive distillation sequence. Component A is less associated with the solvent.

called the *solvent,* which is added to an azeotropic or nonazeotropic feed mixture to alter the volatilities of the key components without the formation of any additional azeotropes. Extractive distillation is used throughout the petrochemical and chemical processing industries for the separation of close-boiling, pinched, or azeotropic systems for which simple single-feed distillation is either too expensive or impossible. It can also be used to obtain products which are residue curve saddles, a task not generally possible with single-feed distillation.

Figure 13-91 illustrates the classical implementation of an extractive distillation process for the separation of a binary mixture. The configuration consists of a double-feed extractive column (C1) and a solvent recovery column (C2). The components A and B may have a low relative volatility or form a minimum-boiling azeotrope. The solvent is introduced into the extractive column at a high concentration a few stages below the condenser, but above the primary-feed stage. Since the solvent is chosen to be nonvolatile, it remains at a relatively high concentration in the liquid phase throughout the sections of the column below the solvent-feed stage.

One of the components, A (not necessarily the most volatile species of the original mixture), is withdrawn as an essentially pure distillate stream. Because the solvent is nonvolatile, at most a few stages above the solvent-feed stage are sufficient to rectify the solvent from the distillate. The bottoms product, consisting of B and the solvent, is sent to the recovery column. The distillate from the recovery column is pure B, and the solvent-bottoms product is recycled to the extractive column.

Extractive distillation works by the exploitation of the selective solvent-induced enhancements or moderations of the liquid-phase nonidealities of the original components to be separated. The solvent selectively alters the activity coefficients of the components being separated. To do this, a high concentration of solvent is necessary. Several features are essential:

1. The solvent must be chosen to affect the liquid-phase behavior of the key components differently; otherwise, no enhancement in separability will occur.
2. The solvent must be higher-boiling than the key components of the separation and must be relatively nonvolatile in the extractive column, in order to remain largely in the liquid phase.
3. The solvent should not form additional azeotropes with the components in the mixture to be separated.
4. The extractive column *must* be a double-feed column, with the solvent feed above the primary feed. The column must have an extractive section (middle section) between the rectifying section and the stripping section.

As a consequence of these restrictions, separation of binary mixtures by extractive distillation corresponds to only two possible three-component distillation region diagrams, depending on whether the binary mixture is pinched or close-boiling (DRD 001), or forms a minimum-boiling azeotrope (DRD 003). The addition of high-boiling solvents can also facilitate the breaking of maximum-boiling azeotropes (DRD 014), for example, splitting the nitric acid–water azeotrope with sulfuric acid. However, as explained in the subsection on azeotropic distillation, this type of separation might better be characterized as exploiting extreme boundary curvature rather than extractive distillation, as the important liquid-phase activity coefficient modification occurs in the bottom of the column. Although many references show sulfuric acid being introduced high in the column, in fact two separate feeds are not required.

Examples of industrial uses of extractive distillation grouped by distillation region diagram type are given in Table 13-21. Achievable product compositions in double-feed extractive distillation columns are very different from the bow tie regions for single-feed columns. For a given solvent, only one of the pure components in the original binary mixture can be obtained as distillate from the extractive column (the higher-boiling of which is a saddle for close-boiling systems, and both of which are saddles for minimum-boiling azeotropic systems). However, different solvents are capable of selecting either A or B as distillate (but not both). Simple tests are available for determining which component is the distillate, as discussed below.

Extractive distillation is generally only applicable to systems in which the components to be separated contain one or more different functional groups. Extractive distillation is usually uneconomical for separating stereoisomers, homologs, or structural isomers containing the same functional groups, unless the differences in structure also contribute to significantly different polarity, dipole moment, or hydrophobic character. One such counterexample is the separation of ethanol from isopropanol, where the addition of methyl benzoate raises the relative volatility from 1.09 to 1.27 [Berg et al., *Chem. Eng. Comm.*, **66,** 1 (1988)].

Solvent Effects in Extractive Distillation In the ordinary distillation of ideal or nonazeotropic mixtures, the component with the lowest pure-component boiling point is always recovered primarily in the distillate, while the highest boiler is recovered primarily in the bottoms. The situation is not as straightforward for an extractive distillation operation. With some solvents, the key component with the lower pure-component boiling point in the original mixture will be recovered in the distillate as in ordinary distillation. For another solvent, the expected order is reversed, and the component with the higher pure-component boiling point will be recovered in the distillate. The possibility that the expected relative volatility may be reversed by the addition of solvent is entirely a function of the way the solvent interacts with and modifies the activity coefficients and, thus, the volatility of the components in the mixture.

In normal applications of extractive distillation (i.e., pinched, close-boiling, or azeotropic systems), the relative volatilities between the light and heavy key components will be unity or close to unity. Assuming an ideal vapor phase and subcritical components, the relative volatility between the light and heavy keys of the desired separation can be written as the product of the ratios of the pure-component vapor pressures and activity coefficients whether the solvent is present or not:

$$\alpha_{L,H} = \left(\frac{P_L^{\text{sat}}}{P_H^{\text{sat}}}\right)\left(\frac{\gamma_L}{\gamma_H}\right) \tag{13-117}$$

where L and H denote the lower-boiling and higher-boiling key pure component, respectively.

The addition of the solvent has an indirect effect on the vapor-pressure ratio. Because the solvent is high-boiling and is generally added at a relatively high mole ratio to the primary-feed mixture, the temperature of an extractive distillation process tends to increase over that of a simple distillation of the original mixture (unless the system pressure is lowered). The result is a corresponding increase in the vapor pressure of both key components. However, the rise in operating temperature generally *does not* result in a significant modification of the relative volatility, because the ratio of vapor pressures often remains approximately constant, unless the slopes of the vapor-pressure curves differ significantly. The ratio of the vapor pressures typically remains greater than unity, following the "natural" volatility of the system.

TABLE 13-21 Examples of Extractive Distillation, Salt Extractive Distillation

System	Type	Solvent(s)	Remark
Ethanol-water	Minimum-boiling azeotrope	Ethylene glycol, acetate salts for salt process	Alternative to azeotropic distillation, pressure swing distillation
Benzene-cyclohexane	Minimum-boiling azeotrope	Aniline	
Ethyl acetate-ethanol	Minimum-boiling azeotrope	Higher esters or alcohols, aromatics	Process similar for other alcohol-ester systems
THF-water	Minimum-boiling azeotrope	Propylene glycol	Alternative to pressure swing distillation
Acetone-methanol	Minimum-boiling azeotrope	Water, aniline, ethylene glycol	
Isoprene-pentane	Minimum-boiling azeotrope	Furfural, DMF, acetonitrile	
Pyridine-water	Minimum-boiling azeotrope	Bisphenol	
Methyl acetate-methanol	Minimum-boiling azeotrope	Ethylene glycol monomethyl ether	Element of recovery system for alternative to production of methyl acetate by reactive distillation; alternative to azeotropic, pressure, swing distillation
C4 alkenes/C4 alkanes/ C4 dienes	Close-boiling and minimum-boiling azeotropes	Furfural, DMF, acetonitrile, *n*-methylpyrolidone	
C5 alkenes/C5 alkanes/ C5 dienes	Close-boiling and minimum-boiling azeotropes	Furfural, DMF, acetonitrile, *n*-methylpyrolidone	
Heptane isomers-cyclohexane	Close-boiling	Aniline, phenol	
Heptane isomers-toluene	Close-boiling and minimum-boiling azeotropes	Aniline, phenol	
Vinyl acetate-ethyl acetate	Close-boiling	Phenol, aromatics	Alternative to simple distillation
Propane-propylene	Close-boiling	Acrylonitrile	Alternative to simple distillation, adsorption
Ethanol-isopropanol	Close-boiling	Methyl benzoate	Alternative to simple distillation
Hydrochloric acid-water	Maximum-boiling azeotrope	Sulfuric acid, calcium chloride for salt process	Sulfuric acid process relies heavily on boundary curvature
Nitric acid-water	Maximum-boiling azeotrope	Sulfuric acid, magnesium nitrate for salt process	Sulfuric acid process relies heavily on boundary curvature

Since activity coefficients have a strong dependence on composition, the effect of the solvent on the activity coefficients is generally more pronounced. However, the magnitude and direction of change are highly dependent on the solvent concentration as well as on the liquid-phase interactions between the solvent and the key components. The solvent acts to lessen the nonidealities of the key component whose liquid-phase behavior is similar to that of the solvent, while enhancing the nonideal behavior of the dissimilar key. The solvent and the key component that show most similar liquid-phase behavior tend to exhibit weak molecular interactions. These components form an ideal or nearly ideal liquid solution. The activity coefficient of this key approaches unity, or may even show negative deviations from Raoult's law if solvating or complexing interactions occur. On the other hand, the dissimilar key and the solvent demonstrate unfavorable molecular interactions, and the activity coefficient of this key increases. The positive deviations from Raoult's law are further enhanced by the diluting effect of the high-solvent concentration, and the value of the activity coefficient of this key may approach the infinite dilution value, often a very large number.

The natural relative volatility of the system is enhanced when the activity coefficient of the lower-boiling pure component is increased by the solvent addition (γ_L/γ_H increases and $P_L^{\text{sat}}/P_H^{\text{sat}} > 1$). In this case, the lower-boiling pure component will be recovered in the distillate as expected. For the higher-boiling pure component to be recovered in the distillate, the addition of the solvent must decrease the ratio γ_L/γ_H such that the product of γ_L/γ_H and $P_L^{\text{sat}}/P_H^{\text{sat}}$ (that is, α_{LH}) in the presence of the solvent is less than unity. Generally, the latter is more difficult to achieve and requires higher solvent-to-feed ratios. It is normally better to select a solvent that forces the lower-boiling component overhead.

The effect of solvent concentration on the activity coefficients of the key components is shown in Fig. 13-92 for the system methanol-acetone with either water or methylisopropylketone (MIPK) as solvent. For an initial feed mixture of 50 mol % methanol and 50 mol % acetone (no solvent present), the ratio of activity coefficients of methanol and acetone is close to unity. With water as the solvent, the activity coefficient of the similar key (methanol) rises slightly as the solvent concentration increases, while the coefficient of acetone approaches the relatively large infinite dilution value. With methylisopropylketone as the solvent, acetone is the similar key and its activity coefficient drops toward unity as the solvent concentration increases, while the activity coefficient of the methanol increases.

Several methods are available for determining whether the lower- or higher-boiling pure component will be recovered in the distillate. For a series of solvent concentrations, the binary *y-x* phase diagram for the low-boiling and high-boiling keys can be plotted on a solvent-free basis. At a particular solvent concentration (dependent on the selected solvent and keys), the azeotropic point in the binary plot disappears at one of the pure-component corners. The component corresponding to the corner where the azeotrope disappears is recovered in the distillate (Knapp and Doherty, *Kirk-Othmer Encyclopedia of Chemical Technology,* 5th ed., vol. 8, p. 786, Wiley, New York, 2004). LaRoche et al. [*Can. J. Chem. Eng.,* **69,** 1302 (1991)] present a related method in which the $\alpha_{LH} = 1$ line is plotted on the ternary composition diagram. If this line intersects the lower-boiling pure component + solvent binary face, then the lower-boiling component will be recovered in the distillate, and vice versa if the $\alpha_{LH} = 1$ line intersects the higher-boiling pure component + solvent face. A very simple method, if a rigorous residue curve map is available, is to examine the shape and inflection of the residue curves as they approach the pure solvent vertex. Whichever solvent-key component face the residue curves predominantly tend toward as they approach the solvent vertex is the key component that will be recovered in the bottoms with the solvent (see property 6, p. 193, in Doherty and Malone, *op. cit.*). In Fig. 13-93*a,* all residue curves approaching the water (solvent) vertex are inflected toward the methanol-water face, with the result that methanol will be recovered in the bottoms and acetone in the distillate. Alternatively, with MIPK as the solvent, all residue curves show inflection toward the acetone-MIPK face (Fig. 13-93*b*), indicating that acetone will be recovered in the bottoms and methanol in the distillate.

Extractive Distillation Design and Optimization Extractive distillation column composition profiles have a very characteristic

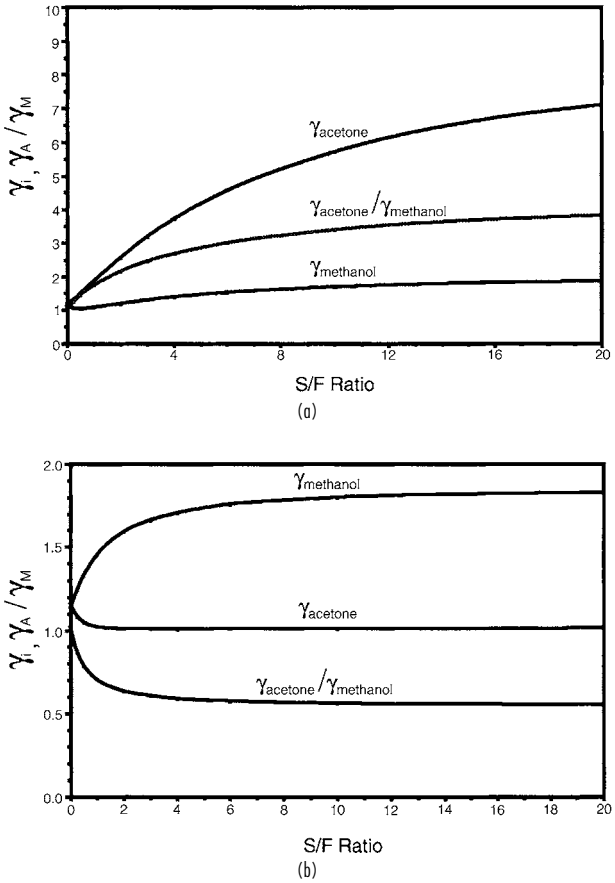

FIG. 13-92 Effect of solvent concentration on activity coefficients for acetone-methanol system. (*a*) Water solvent. (*b*) MIPK solvent.

shape on a ternary diagram. The composition profile for the separation of methanol-acetone with water is given in Fig. 13-94. Stripping and rectifying profiles start at the bottoms and distillate compositions, respectively, track generally along the faces of the composition triangle, and then turn toward the high-boiling (solvent) node and low-boiling node, respectively. For a feasible single-feed design, these profiles must cross at some point. However, in an extractive distillation they cannot cross. The extractive section profile acts at the bridge between these two sections. Most of the key component separation occurs in this section in the presence of high-solvent composition.

The variable that has the most significant impact on the economics of an extractive distillation is the solvent-to-feed flow rate ratio *S/F*. For close-boiling or pinched nonazeotropic mixtures, no minimum-solvent flow rate is required to effect the separation, as the separation is always theoretically possible (if not economical) in the absence of the solvent. However, the extent of enhancement of the relative volatility is largely determined by the solvent composition in the lower column sections and hence the *S/F* ratio. The relative volatility tends to increase as the *S/F* ratio increases. Thus, a given separation can be accomplished in fewer equilibrium stages. As an illustration, the total number of theoretical stages required as a function of *S/F* ratio is plotted in Fig. 13-95*a* for the separation of the nonazeotropic mixture of vinyl acetate and ethyl acetate using phenol as the solvent.

For the separation of a minimum-boiling binary azeotrope by extractive distillation, there is clearly a minimum-solvent flow rate below which the separation is impossible (due to the azeotrope). For azeotropic separations, the number of equilibrium stages is infinite at or below $(S/F)_{min}$ and decreases rapidly with increasing solvent feed

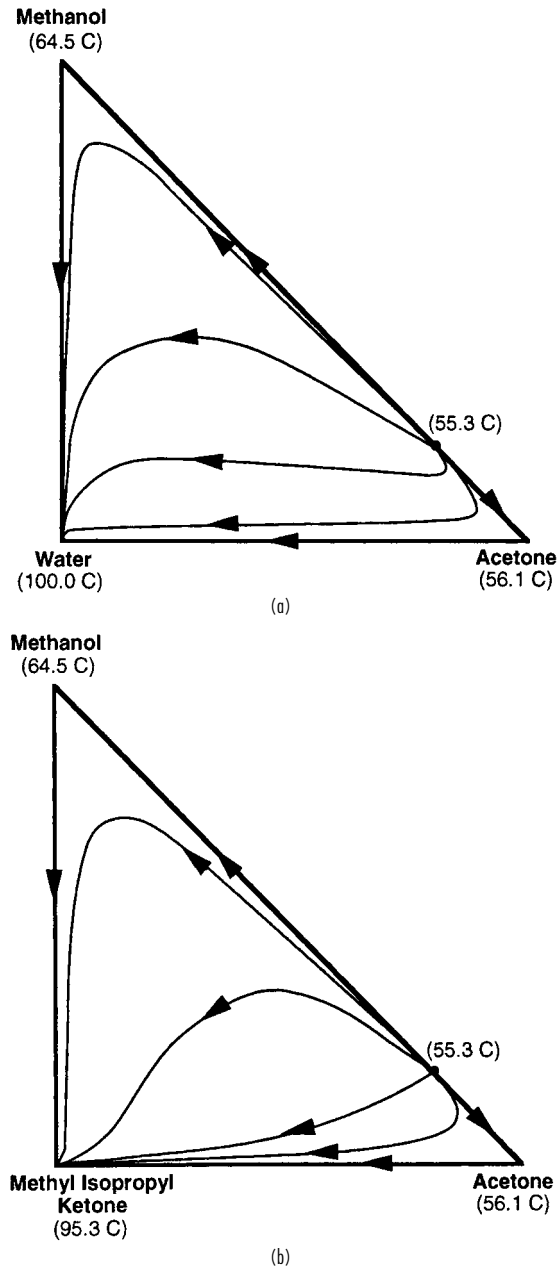

FIG. 13-93 Residue curve maps for acetone-methanol systems. (*a*) With water. (*b*) With MIPK.

flow, and then may asymptote, or rise slowly. The relationship between the total number of stages and the *S/F* ratio for a given purity and recovery for the azeotropic acetone-methanol system with water as solvent is shown in Fig 13-95*b*. A rough idea of $(S/F)_{min}$ can be determined from a pseudobinary diagram or by plotting the $\alpha_{L,H} = 1$ line on a ternary diagram. The solvent composition at which the azeotrope disappears in a corner of the pseudobinary diagram is an indication of $(S/F)_{min}$ [LaRoche et al., *Can. J. Chem. Eng.*, **69,** 1302 (1991)]. An exact method for calculating $(S/F)_{min}$ is given by Knapp and Doherty [*AIChE J.*, **40,** 243 (1994)]. Typically, operating *S/F* ratios for economically acceptable solvents are between 2 and 5. Higher

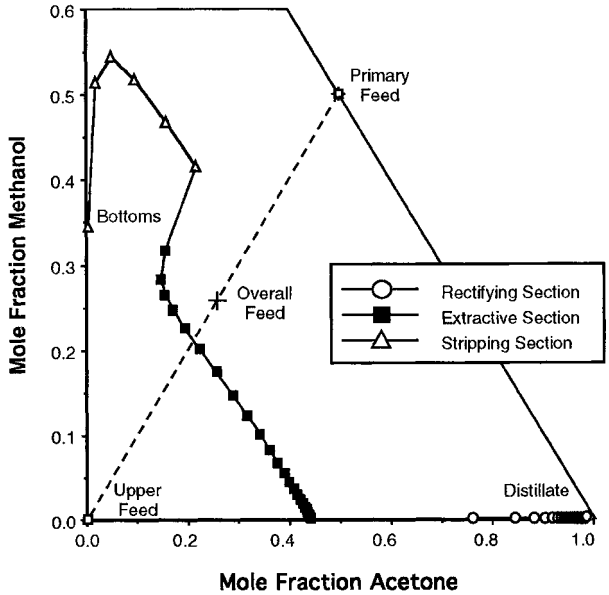

FIG. 13-94 Extractive distillation column composition profile for the separation of acetone-methanol with water.

S/F ratios tend to increase the diameter of both the extractive column and the solvent recovery columns, but reduce the required number of equilibrium stages and minimum reflux ratio. Moreover, higher *S/F* ratios lead to higher reboiler temperatures, resulting in the use of higher-cost utilities, higher utility usages, and greater risk of degradation.

Knight and Doherty [*Ind. Eng. Chem. Fundam.,* **28,** 564 (1989)] have published rigorous methods for computing minimum reflux for extractive distillation; they found that an operating reflux ratio of 1.2 to 1.5 times the minimum value is usually acceptable. Interestingly, unlike other forms of distillation, in extractive distillation the distillate purity or recovery does not increase monotonically with increasing reflux ratio for a given number of stages. Above a maximum reflux ratio the separation can no longer be achieved, and the distillate purity actually decreases for a given number of stages [LaRoche et al., *AIChE J.,* **38,** 1309 (1992)]. The difference between R_{min} and R_{max} increases as the *S/F* ratio increases. Large amounts of reflux lowers the solvent composition in the upper section of the column, degrading rather than enhancing column performance. Because the reflux ratio goes through a maximum, the conventional control strategy of increasing reflux to maintain purity can be detrimental rather than beneficial. However, R_{max} generally occurs at impractically high reflux ratios and is typically not of major concern.

The thermal quality of the solvent feed has no effect on the value of S/F_{min}, but does affect the minimum reflux to some extent, especially as the *S/F* ratio increases. The maximum reflux ratio R_{max} occurs at higher values of the reflux ratio as the upper-feed quality decreases; a subcooled upper feed provides additional refluxing capacity and less external reflux is required for the same separation. It is also sometimes advantageous to introduce the primary feed to the extractive distillation column as a vapor to help maintain a higher solvent composition on the feed tray and the trays immediately below.

Robinson and Gilliland (*Elements of Fractional Distillation,* McGraw-Hill, New York, 1950), Smith (*Design of Equilibrium Stage Processes,* McGraw-Hill, New York, 1963), Van Winkle (*Distillation,* McGraw-Hill, New York, 1967), and Walas (*Chemical Process Equipment,* Butterworths, Boston, 1988) discuss rigorous stage-to-stage design techniques as well as shortcut and graphical methods for determining minimum stages, $(S/F)_{min}$, minimum reflux, and the optimum locations of the solvent and primary feed points. Knapp and Doherty [*AIChE J.,* **40,** 243 (1994)] have published column design methods

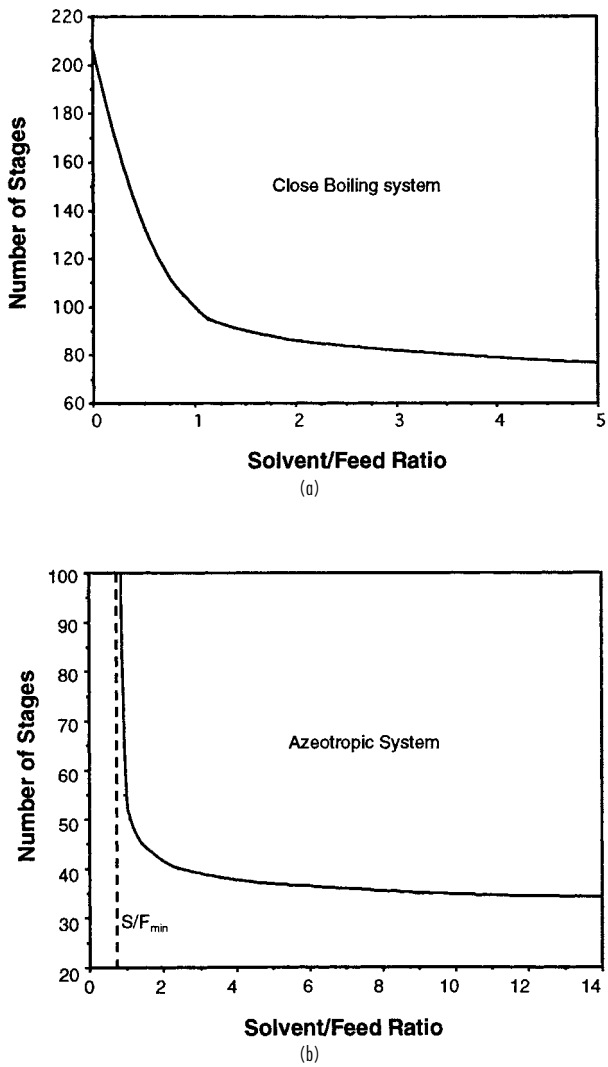

FIG. 13-95 Number of theoretical stages versus solvent-to-feed ratio for extractive distillation. (*a*) Close-boiling vinyl acetate–ethyl acetate system with phenol solvent. (*b*) Azeotropic acetone-methanol system with water solvent.

based on geometric arguments and fixed-point analysis that are capable of calculating $(S/F)_{min}$, as well as the minimum and maximum reflux ratio. Most commercial simulators are capable of solving multiple-feed extractive distillation heat and material balances, but do not include straightforward techniques for calculating $(S/F)_{min}$, or the minimum and maximum reflux ratio.

Solvent Screening and Selection Choosing an effective solvent can have the most profound effect on the economics of an extractive distillation process. The approach most often adopted is to first generate a short list of potential solvents by using simple qualitative screening and selection methods. Experimental verification is best undertaken only after a list of promising candidate solvents has been generated and some chance at economic viability has been demonstrated via preliminary process modeling.

Solvent selection and screening approaches can be divided into two levels of analysis. The first level focuses on identification of functional groups or chemical families that are likely to give favorable solvent–key component molecular interactions. The second level of analysis identifies and compares individual candidate solvents. The

various methods of analysis are described briefly and illustrated with an example of choosing a solvent for the methanol-acetone separation.

First Level: Broad Screening by Functional Group or Chemical Family

Homologous series. Select candidate solvents from the high-boiling homologous series of both light and heavy key components. Favor homologs of the heavy key, as this tends to enhance the natural relative volatility of the system. Homologous components tend to form ideal solutions and are unlikely to form azeotropes [Scheibel, *Chem. Eng. Prog.*, **44**(12), 927 (1948)].

Robbins chart. Select candidate solvents from groups in the Robbins chart (Table 13-17) that tend to give positive (or no) deviations from Raoult's law for the key component desired in the distillate and negative (or no) deviations for the other key.

Hydrogen-bonding characteristics. Select candidate solvents from groups that are likely to cause the formation of hydrogen bonds with the key component to be removed in the bottoms, or disruption of hydrogen bonds with the key to be removed in the distillate. Formation and disruption of hydrogen bonds are often associated with strong negative and positive deviations, respectively, from Raoult's law. Several authors have developed charts indicating expected hydrogen bonding interactions between families of compounds [Ewell et al., *Ind. Eng. Chem.*, **36,** 871 (1944); Gilmont et al., *Ind. Eng. Chem.*, **53,** 223 (1961); and Berg, *Chem. Eng. Prog.*, **65**(9), 52 (1969)]. Table 13-22 presents a hydrogen bonding classification of chemical families and a summary of deviations from Raoult's law.

Polarity characteristics. Select candidate solvents from chemical groups that tend to show higher polarity than one key component or lower polarity than the other key. Polarity effects are often cited as a factor in causing deviations from Raoult's law [Hopkins and Fritsch, *Chem. Eng. Prog.*, **51**(8), (1954); Carlson et al., *Ind. Eng. Chem.*, **46,** 350 (1954); and Prausnitz and Anderson, *AIChE J.*, **7**, 96 (1961)]. The general trend in polarity based on the functional group of a molecule is given in Table 13-23. The chart is best for molecules of similar size. A more quantitative measure of the polarity of a molecule is the polarity contribution to the three-term Hansen solubility parameter. A tabulation of calculated three-term solubility parameters is provided by Barton (*CRC Handbook of Solubility Parameters and Other Cohesion Parameters*, CRC Press, Boca Raton, Fla., 1991), along with a group contribution method for calculating the three-term solubility parameters of compounds not listed in the reference.

Second Level: Identification of Individual Candidate Solvents

Boiling point characteristics. Select only candidate solvents that boil at least 30 to 40°C above the key components to ensure that the solvent is relatively nonvolatile and remains largely in the liquid phase. With this boiling point difference, the solvent should also not form azeotropes with the other components.

Selectivity at infinite dilution. Rank candidate solvents according to their selectivity at infinite dilution. The selectivity at infinite

TABLE 13-22 Hydrogen Bonding Classification of Chemical Families

Class	Chemical family			
H-Bonding, Strongly Associative (HBSA)	Water Primary amides Secondary amides	Polyacids Dicarboxylic acids Monohydroxy acids	Polyphenols Oximes Hydroxylamines	Amino alcohols Polyols
H-Bond Acceptor-Donor (HBAD)	Phenols Aromatic acids Aromatic amines Alpha H nitriles	Imines Monocarboxylic acids Other monoacids Peracids	Alpha H nitros Azines Primary amines Secondary amines	*n*-alcohols Other alcohols Ether alcohols
H-Bond Acceptor (HBA)	Acyl chlorides Acyl fluorides Hetero nitrogen aromatics Hetero oxygen aromatics	Tertiary amides Tertiary amines Other nitriles Other nitros Isocyanates Peroxides	Aldehydes Anhydrides Cyclo ketones Aliphatic ketones Esters Ethers	Aromatic esters Aromatic nitriles Aromatic ethers Sulfones Sulfolanes
π-Bonding Acceptor (π-HBA)	Alkynes Alkenes	Aromatics Unsaturated esters		
H-Bond Donor (HBD)	Inorganic acids Active H chlorides	Active H fluorides Active H iodides	Active H bromides	
Non-Bonding (NB)	Paraffins Nonactive H chlorides	Nonactive H fluorides Sulfides	Nonactive H iodides Disulfides	Nonactive H bromides Thiols

Deviations from Raoult's Law

H-Bonding classes	Type of deviations	Comments
HBSA + NB HBAD + NB	Alway positive dev., HBSA + NB often limited miscibility	H-bonds broken by interactions
HBA + HBD	Always negative dev.	H-bonds formed by interactions
HBSA + HBD HBAD + HBD	Always positive deviations, HBSA + HBD often limited miscibility	H-bonds broken and formed; dissociation of HBSA or HBAD liquid most important effect
HBSA + HBSA HBSA + HBAD HBSA + HBA HBAD + HBAD HBAD + HBA	Usually positive deviations; some give maximum-boiling azeotropes	H-bonds broken and formed
HBA + HBA HBA + NB HBD + HBD HBD + NB NB + NB	Ideal, quasi-ideal systems; always positive or no deviations; azeotropes, if any, minimum-boiling	No H-bonding involved

NOTE: π-HBA is *enhanced* version of HBA.

TABLE 13-23 Relative Polarities of Functional Groups

MOST POLAR	Water
	Organic acids
	Amines
	Polyols
	Alcohols
	Esters
	Ketones
	Aldehydes
	Ethers
	Aromatics
	Olefins
LEAST POLAR	Paraffins
Effect of branching	
MOST POLAR	Normal
	Secondary
LEAST POLAR	Tertiary

TABLE 13-24 Comparison of Candidate Solvents for Methanol/Acetone Extractive Distillation

Solvent	Boiling pt. (°C)	Azeotrope formation	$\gamma^{\infty}_{Acetone}$	γ^{∞}_{MeOH}	$\gamma^{\infty}_{Acetone}/\gamma^{\infty}_{MeOH}$
MEK	79.6	With MeOH	1.01	1.88	0.537
MIPK	102.0	No	1.01	1.89	0.534
MIBK	115.9	No	1.06	2.05	0.517
Ethanol	78.3	No	1.85	1.04	1.78
1-Propanol	97.2	No	1.90	1.20	1.58
1-Butanol	117.8	No	1.93	1.33	1.45
Water	100.0	No	11.77	2.34	5.03
EG	197.2	No	3.71	1.25	2.97

$\gamma^{\infty}_{Acetone} = 1.79$ (in MeOH)
$\gamma^{\infty}_{MeOH} = 1.81$ (in acetone)

dilution is defined as the ratio of the activity coefficients at infinite dilution of the two key components in the solvent. Since solvent effects tend to increase as solvent concentration increases, the infinite-dilution selectivity gives an upper bound on the efficacy of a solvent. Infinite-dilution activity coefficients can be predicted by using such methods as UNIFAC, ASOG, MOSCED (Reid et al., *Properties of Gases and Liquids,* 4th ed., McGraw-Hill, New York, 1987). They can be found experimentally by using a rapid gas-liquid chromatography method based on relative retention times in candidate solvents (Tassios, in *Extractive and Azeotropic Distillation,* Advances in Chemistry Series 115, American Chemical Society, Washington, 1972), and they can be correlated to bubble point data [Kojima and Ochi, *J. Chem. Eng. Japan,* **7**(2), 71 (1974)]. DECHEMA (*Vapor-Liquid Equilibrium Data Collection,* Frankfort, 1977) has also published a compilation of experimental infinite-dilution activity coefficients.

Experimental measurement of relative volatility. Rank candidate solvents by the increase in relative volatility caused by the addition of the solvent. One technique is to experimentally measure the relative volatility of a fixed-composition, key component + solvent mixture (often a 1/1 ratio of each key, with a 1/1 to 3/1 solvent/key ratio) for various solvents [Carlson et al., *Ind. Eng. Chem.,* **46,** 350 (1954)]. The Othmer equilibrium still is the apparatus of choice for these measurements [Zudkevitch, *Chem. Eng. Comm.,* **116,** 41 (1992)].

At atmospheric pressure, methanol and acetone boil at 64.5 and 56.1°C, respectively, and form a minimum-boiling azeotrope at 55.3°C. The natural volatility of the system is acetone > methanol, so the favored solvents most likely will be those that cause acetone to be recovered in the distillate. However, for the purposes of the example, a solvent that reverses the natural volatility will also be identified. First, by examining the polarity of ketones and alcohols (Table 13-23), solvents favored for the recovery of methanol in the bottoms would come from groups more polar than methanol, such as acids, water, and polyols. Turning to the Robbins chart (Table 13-17), we see favorable groups are amines, alcohols, polyols, and water since these show expected positive deviations for acetone and zero or negative deviations for methanol. For reversing the natural volatility, solvents should be chosen that are less polar than acetone, such as ethers, hydrocarbons, and aromatics. Unfortunately, both ethers and hydrocarbons are expected to give positive deviations for both acetone and methanol, so should be discarded. Halohydrocarbons and ketones are expected to give positive deviations for methanol and either negative or no deviations for acetone. The other qualitative indicators show that both homologous series (ketones and alcohols) look promising. Thus, after discounting halohydrocarbons for environmental reasons, the best solvents will probably come from alcohols, polyols, and water for recovering methanol in the bottoms and ketones for recovering acetone in the bottoms. Table 13-24 shows the boiling points and experimental or estimated infinite-dilution activity coefficients for several candidate solvents from the aforementioned groups. Methylethylketone boils too low, as does ethanol, and also forms an azeotrope with methanol. These two candidates can be discarded. Other members of the homologous series, along with water and ethylene glycol, have acceptable boiling points (at least 30°C higher than those of the keys). Of these, water (the solvent used industrially) clearly has the largest effect on the activity coefficients, followed by ethylene glycol. Although inferior to water or ethylene glycol, both MIPK and MIBK would probably be acceptable for reversing the natural volatility of the system.

Extractive Distillation by Salt Effects A second method of modifying the liquid-phase behavior (and thus the relative volatility) of a mixture to effect a separation is by the addition of a nonvolatile, soluble, ionic salt. The process is analogous to extractive distillation with a high-boiling liquid. In the simplest case, for the separation of a binary mixture, the salt is fed at the top of the column by dissolving it in the hot reflux stream before introduction into the column. To function effectively, the salt must be adequately soluble in both components throughout the range of compositions encountered in the column. Since the salt is completely nonvolatile, it remains in the liquid phase on each tray and alters the relative volatility throughout the length of the column. No rectification section is needed above the salt feed. The bottoms product is recovered from the salt solution by evaporation or drying, and the salt is recycled. The ions of a salt are typically capable of causing much larger and more selective effects on liquid-phase behavior than the molecules of a liquid solvent. As a result, salt-to-feed ratios of less than 0.1 are typical.

The use of a salting agent presents a number of problems not associated with a liquid solvent, such as the difficulty of transporting and metering a solid or saturated salt solution, slow mixing or dissolution rate of the salt, limits to solubility in the feed components, and potential for corrosion. However, in the limited number of systems for which an effective salt can be found, the energy usage, equipment size, capital investment, and ultimate separation cost can be significantly reduced compared to that for extractive distillation using a liquid solvent [Furter, *Chem. Eng. Commun.,* **116,** 35 (1992)]. Applications of salt extractive distillation include acetate salts to produce absolute ethanol, magnesium nitrate for the production of concentrated nitric acid as an alternative to the sulfuric acid solvent process, and calcium chloride to produce anhydrous hydrogen chloride. Other examples are noted by Furter [*Can. J. Chem. Eng.,* **55,** 229 (1977)].

One problem limiting the consideration of salt extractive distillation is the fact that the performance and solubility of a salt in a particular system are difficult to predict without experimental data. Some recent advances have been made in modeling the VLE behavior of organic aqueous salt solutions using modified UNIFAC, NRTL, UNIQUAC, and other approaches [Kumar, *Sep. Sci. Tech.,* **28**(1), 799 (1993)].

REACTIVE DISTILLATION

Reactive distillation is a unit operation in which chemical reaction and distillation are carried out simultaneously within a fractional distillation apparatus. Reactive distillation may be advantageous for liquid-phase reaction systems when the reaction must be carried out with a large excess of one or more of the reactants, when a reaction

can be driven to completion by removal of one or more of the products as they are formed, or when the product recovery or by-product recycle scheme is complicated or made infeasible by azeotrope formation.

For consecutive reactions in which the desired product is formed in an intermediate step, excess reactant can be used to suppress additional series reactions by keeping the intermediate-species concentration low. A reactive distillation can achieve the same result by removing the desired intermediate from the reaction zone as it is formed. Similarly, if the equilibrium constant of a reversible reaction is small, high conversions of one reactant can be achieved by use of a large excess of the other reactant. Alternatively, by Le Chatelier's principle, the reaction can be driven to completion by removal of one or more of the products as they are formed. Typically, reactants can be kept much closer to stoichiometric proportions in a reactive distillation.

When a reaction mixture exhibits azeotropes, the recovery of products and recycle of excess reagents can be quite complicated and expensive. Reactive distillation can provide a means of breaking azeotropes by altering or eliminating the condition for azeotrope formation in the reaction zone through the combined effects of vaporization-condensation and consumption-production of the species in the mixture. Alternatively, a reaction may be used to convert the species to components that are more easily distilled. In each of these situations, the conversion and selectivity often can be improved markedly, with much lower reactant inventories and recycle rates, and much simpler recovery schemes. The capital savings can be quite dramatic. A list of applications of reactive distillation appearing in the literature is given in Table 13-25. Additional industrial applications are described by Sharma and Mahajani (chap. 1 in Sundmacher and Kienle, eds., *Reactive Distillation*, Wiley-VCH, 2003).

Although reactive distillation has many potential applications, it is not appropriate for all situations. Since it is in essence a distillation process, it has the same range of applicability as other distillation operations. Distillation-based equipment is not designed to effectively handle solids, supercritical components (where no separate vapor and liquid phases exist), gas-phase reactions, or high-temperature or high-pressure reactions such as hydrogenation, steam reforming, gasification, and hydrodealkylation.

Simulation, Modeling, and Design Feasibility Because reaction and separation phenomena are closely coupled in a reactive distillation process, simulation and design are significantly more complex than those of sequential reaction and separation processes. In spite of the complexity, however, most commercial computer process modeling packages offer reliable and flexible routines for simulating steady-state reactive distillation columns, with either equilibrium or kinetically controlled reaction models [Venkataraman et al., *Chem. Eng. Prog.,* **86**(6), 45 (1990)]. As with other enhanced distillation processes, the results are very sensitive to the thermodynamic models chosen and the accuracy of the VLE data used to generate model parameters. Of equal, if not greater significance is the accuracy of data and models for reaction rate as a function of catalyst concentration, temperature, and composition. Very different conclusions can be drawn about the feasibility of a reactive distillation if the reaction is assumed to reach chemical equilibrium on each stage of the column or if the reaction is assumed to be kinetically controlled [Barbosa and Doherty, *Chem. Eng. Sci.,* **43,** 541 (1988); Chadda, Malone, and Doherty, *AIChE J.,* 47, 590 (2001)]. Tray holdup and stage requirements are two important variables directly affected by the reaction time relative to the residence time inside the column. Unlike distillation without reaction, product feasibility can be quite sensitive to changes in tray holdup and production rate.

When an equilibrium reaction occurs in a vapor-liquid system, the phase compositions depend not only on the relative volatility of the components in the mixture, but also on the consumption (and production) of species. Thus, the condition for azeotropy in a nonreactive system ($y_i = x_i$ for all i) no longer holds true in a reactive system and must be modified to include reaction stoichiometry:

$$\frac{y_1 - x_1}{v_1 - v_T x_1} = \frac{y_i - x_i}{v_i - v_T x_i} \qquad \text{for all } i = 1, \ldots, c \qquad (13\text{-}118)$$

where

$$v_T = \sum_{i=1}^{c} v_i$$

and v_i represents the stoichiometric coefficient of component i (negative for reactants, positive for products).

Phase compositions that satisfy Eq. (13-118) are stationary points on a phase diagram and have been labeled *reactive azeotropes* by Barbosa and Doherty [*Chem. Eng. Sci.,* **43,** 529 (1988)]. At a reactive azeotrope the mass exchange between the vapor and liquid phases and the generation (or consumption) of each species are balanced such that the composition of neither phase changes. Reactive azeotropes show the same distillation properties as ordinary azeotropes and therefore affect the achievable products. Reactive azeotropes are predicted to exist in numerous reacting mixtures and have been confirmed experimentally in the reactive boiling mixture of acetic acid + isopropanol + isopropyl acetate + water [Song et al., *Nature,* **388,** 561 (1997); Huang et al., *Chem. Eng. Sci.,* **60,** 3363 (2005)].

Reactive azeotropes are not easily visualized in conventional y-x coordinates but become apparent upon a transformation of coordinates which depends on the number of reactions, the order of each reaction (for example, $A + B \rightleftharpoons C$ or $A + B \rightleftharpoons C + D$), and the presence of nonreacting components. The general vector-matrix form of

TABLE 13-25 Applications of Reactive Distillation

Process	Reaction type	Reference
Methyl acetate from methanol and acetic acid	Esterification	Agreda et al., *Chem. Eng. Prog.,* **86**(2), 40 (1990)
General process for ester formation	Esterification	Simons, "Esterification" in *Encyclopedia of Chemical Processing and Design*, Vol 19, Dekker, New York, 1983
Diphenyl carbonate from dimethyl carbonate and phenol	Esterification	Oyevaar et al., U.S. Patent 6,093,842 (2000)
Dibutyl phthalate from butanol and phthalic acid	Esterification	Berman et al., *Ind. Eng. Chem.,* **40,** 2139 (1948)
Ethyl acetate from ethanol and butyl acetate	Transesterification	Davies and Jeffreys, *Trans. Inst. Chem. Eng.,* **51,** 275 (1973)
Recovery of acetic acid and methanol from methyl acetate by-product of vinyl acetate production	Hydrolysis	Fuchigami, *J. Chem. Eng. Jap.,* **23,** 354 (1990)
Nylon 6,6 prepolymer from adipic acid and hexamethylenediamine	Amidation	Jaswal and Pugi, U.S. Patent 3,900,450 (1975)
MTBE from isobutene and methanol	Etherification	DeGarmo et al., *Chem. Eng. Prog.,* **88**(3), 43 (1992)
TAME from pentenes and methanol	Etherification	Brockwell et al., *Hyd. Proc.,* **70**(9), 133 (1991)
Separation of close boiling 3- and 4-picoline by complexation with organic acids	Acid-base	Duprat and Gau, *Can. J. Chem. Eng.,* **69,** 1320 (1991)
Separation of close-boiling meta and para xylenes by formation of tert-butyl meta-xyxlene	Transalkylation	Saito et al., *J. Chem. Eng. Jap.,* **4,** 37 (1971)
Cumene from propylene and benzene	Alkylation	Shoemaker and Jones, *Hyd. Proc.,* **67**(6), 57 (1987)
General process for the alkylation of aromatics with olefins	Alkylation	Crossland, U.S. Patent 5,043,506 (1991)
Production of specific higher and lower alkenes from butenes	Diproportionation	Jung et al., U.S. Patent 4,709,115 (1987)
4-Nitrochlorobenzene from chlorobenzene and nitric acid	Nitration	Belson, *Ind. Eng. Chem. Res.,* **29,** 1562 (1990)
Production of methylal and high purity formaldehyde		Masamoto and Matsuzaki, *J. Chem. Eng. Jap.,* **27,** 1 (1994)

the transform for c reacting components, with R reactions, and I nonreacting components, has been derived by Ung and Doherty [*Chem. Eng. Sci.*, **50,** 23 (1995)]. For the transformed mole fraction of component i in the liquid phase X_i, they give

$$X_i = \left[\frac{x_i - \mathbf{v}_i^T(\boldsymbol{\nu}_{\text{Ref}})^{-1}\,\mathbf{x}_{\text{Ref}}}{1 - \mathbf{v}_{\text{TOT}}^T(\boldsymbol{\nu}_{\text{Ref}})^{-1}\mathbf{x}_{\text{Ref}}} \right] \qquad i = 1, \ldots, c - R \qquad (13\text{-}119)$$

where $\mathbf{v}_i^T$ = row vector of stoichiometric coefficients of component i for each reaction
$\boldsymbol{\nu}_{\text{Ref}}$ = square matrix of stoichiometric coefficients for R reference components in R reactions
$\mathbf{x}_{\text{Ref}}$ = column vector of mole fractions for R reference components in liquid phase
$\mathbf{v}_{\text{TOT}}^T$ = row vector composed of sum of stoichiometric coefficients for each reaction

An equation identical to (13-119) defines the transformed mole fraction of component i in the vapor phase Y_i, where the terms in x are replaced by terms in y.

The transformed variables describe the system composition with or without reaction and sum to unity as do x_i and y_i. The condition for reactive azeotropy becomes $X_i = Y_i$. Barbosa and Doherty have shown that phase diagrams and distillation diagrams constructed by using the transformed composition coordinates have the same properties as phase and distillation diagrams for nonreactive systems and similarly can be used to assist in design feasibility and operability studies [*Chem. Eng. Sci.*, **43,** 529, 541, 1523, and 2377 (1988)]. Residue curve maps in transformed coordinates for the reactive system methanol–acetic acid–methyl acetate–water are shown in Fig. 13-96. Note that the nonreactive azeotrope between water and methyl acetate has disappeared, while the methyl acetate–methanol azeotrope remains intact. Only those azeotropes containing all the reactants or products will be altered by the reaction (water and methyl acetate can back-react to form acetic acid and methanol, whereas methanol and methyl acetate cannot further react in the absence of either water or acetic acid). This reactive system consists of only one distillation region in which the methanol–methyl acetate azeotrope is the low-boiling node and acetic acid is the high-boiling node.

The situation becomes more complicated when the reaction is kinetically controlled and does not come to complete chemical equilibrium under the conditions of temperature, liquid holdup, and rate of vaporization in the column reactor. Venimadhavan et al. [*AIChE J.*, **40,** 1814 (1994); **45,** 546 (1999)] and Rev [*Ind. Eng. Chem. Res.*, **33,** 2174 (1994)] show that the concept of a reactive azeotrope generalizes to the concept of a *reactive fixed point*, whose existence and location are a function of approach to equilibrium as well as the evaporation rate [see also Frey and Stichlmair, *Trans IChemE,* **77,** Part A, 613 (1999); Chadda, Malone, and Doherty, *AIChE J.*, 47, 590 (2001); Chiplunkar et al., *AIChE J.*, **51,** 464 (2005)]. In the limit of simultaneous phase and reaction equilibrium, a reactive fixed point becomes identical to the thermodynamic concept of a reactive azeotrope.

These ideas have been extended to reacting systems with (1) multiple chemical reactions [Ung and Doherty, *Ind. Eng. Chem. Res.*, **34,** 3195, 2555 (1995)], (2) multiple liquid phases [Ung and Doherty, *Chem. Eng. Sci.*, **50,** 3201 (1995); Qi, Kolah, and Sundmacher, *Chem. Eng. Sci.*, **57,** 163 (2002); Qi and Sundmacher, *Comp. Chem. Eng.*, **26,** 1459 (2002)], (3) membrane separations [Huang et al., *Chem. Eng. Sci.*, **59,** 2863 (2004)], (4) finite rates of vapor-liquid mass transfer [Baur, Taylor, and Krishna, *Chem. Eng. Sci.*, **56,** 2085 (2001); Nisoli, Doherty, and Malone, *AIChE J.*, **50,** 1795 (2004)], (5) column design and multiple steady-states (Guttinger, Dorn, and Morari, *Ind. Eng. Chem. Res.*, **36,** 794 (1997); Hauan, Hertzberg, and Lien, *Comput. Chem. Eng.*, **21,** 1117 (1997); Sneesby et al., *Ind. Eng. Chem. Res.*, **36,** 1855 (1997); Bessling et al., *Chem. Eng. Technol.*, **21,** 393 (1998); Okasinski and Doherty, *Ind. Eng. Chem. Res.*, **37,** 2821 (1998); Sneesby, Tade, and Smith, *Trans IChemE,* **76,** Part A, 525 (1998); Guttinger and Morari, *Ind. Eng. Chem. Res.*, **38,** 1633, 1649 (1999); Higler, Taylor, and Krishna, *Chem. Eng. Sci.*, **54,** 1389 (1999); Mohl et al., *Chem. Eng. Sci.*, **54,** 1029 (1999); Chen et al., *Comput. Chem. Eng.*, **26,** 81 (2002)]. Much useful information is available in Taylor and Krishna [*Chem. Eng. Sci*., **55,** 5183 (2000)] and Sundmacher and Kienle (*Reactive Distillation*, Wiley-VCH, 2003).

Mechanical Design and Implementation Issues The choice of catalyst has a significant impact on the mechanical design and operation of the reactive column. The catalyst must allow the reaction to occur at reasonable rates at the relatively low temperatures and pressures common in distillation operations (typically less than 10 atm and between 50 and 250°C). Selection of a homogeneous catalyst, such as a high-boiling mineral acid, allows the use of more traditional tray designs and internals (albeit designed with exotic materials of construction to avoid corrosion, and allowance for high-liquid holdups to achieve suitable reaction contact times). With a homogeneous catalyst, lifetime is not a problem, as it is added (and withdrawn) continuously. Alternatively, heterogeneous solid catalysts

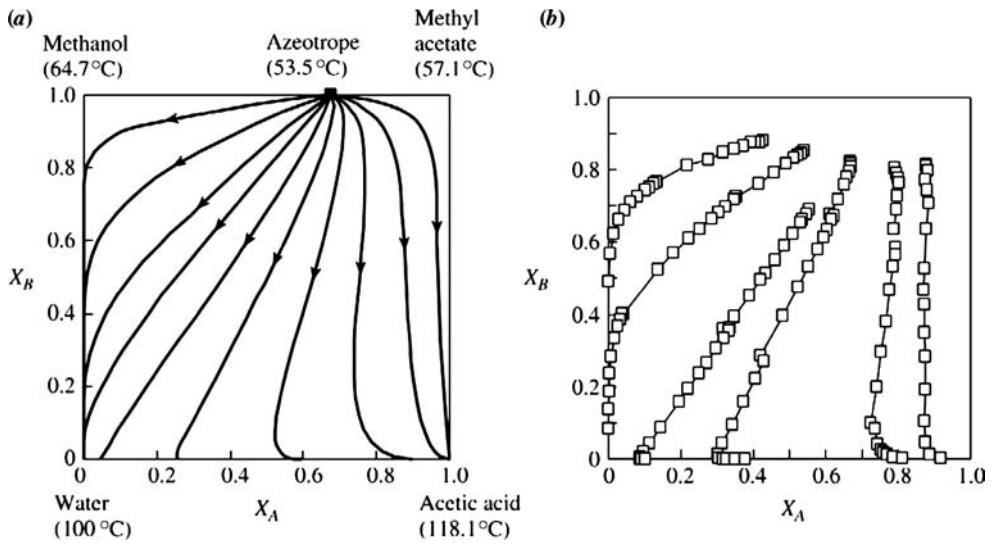

FIG. 13-96 Residue curve maps for the reactive system methanol–acetic acid–methyl acetate–water in phase and chemical equilibrium at 1-atm pressure. (*a*) Calculated by Barbosa and Doherty [*Chem. Eng. Sci.*, **43,** 1523 (1988)]. (*b*) Measured by Song et al. [*Ind. Eng. Chem. Res.*, **37,** 1917 (1998)].

TABLE 13-26 Catalyst Systems for Reactive Distillation

Description	Application	Reference
	Homogeneous catalysis	
Liquid-phase mineral-acid catalyst added to column or reboiler	Esterifications Dibutyl phlalate Methyl acetate	Keyes, *Ind. Eng. Chem.*, **24,** 1096 (1932) Berman et al., *Ind. Eng. Chem.,* **40,** 2139 (1948) Agreda et al., U.S. Patent 4,435,595 (1984)
	Heterogeneous catalysis	
Catalyst-resin beads placed in cloth bags attached to fiberglass strip. Strip wound around helical stainless steel mesh spacer	Etherifications Cumene	Smith et al., U.S. Patent 4,443,559 (1981) Shoemaker and Jones, *Hyd.* **57**(6), 57 (1987)
Ion exchange resin beads used as column packing	Hydrolysis of methyl acetate	Fuchigami, *J. Chem. Eng. Jap.,* **23,** 354 (1990)
Molecular sieves placed in bags or porous containers	Alkylation of aromatics	Crossland, U.S. Patent 5,043,506 (1991)
Ion exchange resins formed into Raschig rings	MTBE	Flato and Hoffman, *Chem. Eng. Tech.,* **15,** 193 (1992)
Granular catalyst resin loaded in corrugated sheet casings	Dimethyl acetals of formaldehyde	Zhang et al., Chinese Patent 1,065,412 (1992)
Trays modified to hold catalyst bed	MTBE	Sanfilippo et al., Eur. Pat. Appl. EP 470,625 (1992)
Distillation trays constructed of porous catalytically active material and reinforcing resins	None specified	Wang et al., Chinese Patent 1,060,228 (1992)
Method described for removing or replacing catalyst on trays as a liquid slurry	None specified	Jones, U.S. Patent, 5,133,942 (1992)
Catalyst bed placed in downcomer, designed to prevent vapor flow through bed	Etherifications, alkylations	Asselineau, Eur. Pat. Appl. EP 547,939 (1993)
Slotted plate for catalyst support designed with openings for vapor flow	None specified	Evans and Stark, Eur. Pat. Appl. EP 571,163 (1993)
Ion exchanger fibers (reinforced ion exchange polymer) used as solid-acid catalyst	Hydrolysis of methyl acetate	Hirata et al., Jap. Patent 05,212,290 (1993)
High-liquid holdup trays designed with catalyst bed extending below tray level, perforated for vapor-liquid contact	None specified	Yeoman et al., Int. Pat. Appl., WO 9408679 (1994)
Catalyst bed placed in downcomer, in-line withdrawal/addition system	None specified	Carland, U.S. Patent, 5,308,451 (1994)

require either complicated mechanical means for continuous replenishment or relatively long lifetimes to avoid constant maintenance. As with other multiphase reactors, use of a solid catalyst adds an additional resistance to mass transfer from the bulk liquid (or vapor) to the catalyst surface, which may be the limiting resistance. The catalyst containment system must be designed to ensure adequate liquid-solid contacting and minimize bypassing. A number of specialized column internal designs, catalyst containment methods, and catalyst replenishment systems have been proposed for both homogeneous and heterogeneous catalysts. A partial list of these methods is given in Table 13-26; see also the useful ideas presented by Krishna [*Chem. Eng. Sci.*, **57,** 1491 (2002); and chap. 7 in Sundmacher and Kienle, eds., *Reactive Distillation*, Wiley-VCH, 2003].

Heat management is another important consideration in the implementation of a reactive distillation process. Conventional reactors for highly exothermic or endothermic reactions are often designed as modified shell-and-tube heat exchangers for efficient heat transfer. However, a trayed or packed distillation column is a rather poor mechanical design for the management of the heat of reaction. Although heat can be removed or added in the condenser or reboiler easily, the only mechanism for heat transfer in the column proper is through vaporization (or condensation). For highly exothermic reactions, a large excess of reactants may be required as a heat sink, necessitating high-reflux rates and larger-diameter columns to return the vaporized reactants back to the reaction zone. Often a prereactor of conventional design is used to accomplish most of the reaction and heat removal before feeding to the reactive column for final conversion, as exemplified in most processes for the production of tertiary amyl methyl ether (TAME) [Brockwell et al., *Hyd. Proc.,* **70**(9), 133 (1991)]. Highly endothermic reactions may require intermediate reboilers. None of these heat management issues preclude the use of reactive distillation, but must be taken into account during the design phase. Comparison of heat of reaction and average heat of vaporization data for a system, as in Fig. 13-97, gives some indication of potential heat imbalances [Sundmacher, Rihko, and Hoffmann, *Chem. Eng. Comm.*, **127,** 151 (1994)]. The heat-neutral systems [$-\Delta H_{react} \approx \Delta H_{vap}$ (avg)]

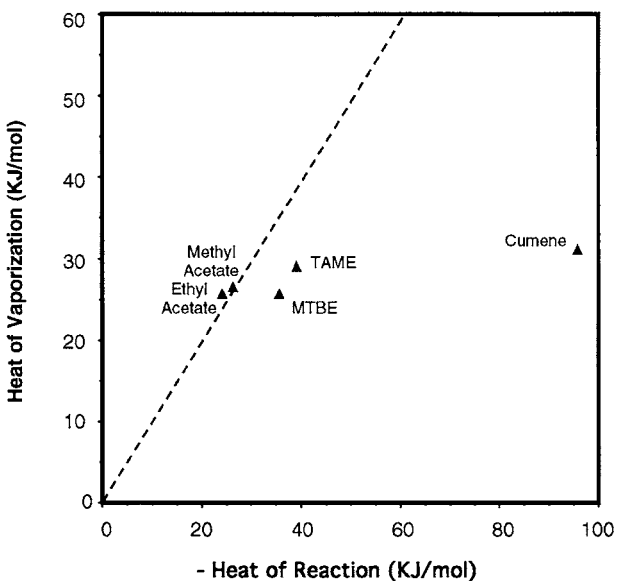

FIG. 13-97 Similarity of heats of reaction and vaporization for compounds made by reactive distillation.

such as methyl acetate and other esters can be accomplished in one reactive column, whereas the MTBE and TAME processes, with higher heats of reaction than that of vaporization, often include an additional prereactor. One exception is the catalytic distillation process for cumene production, which is accomplished without a prereactor. Three moles of benzene reactant are vaporized (and refluxed) for every mole of cumene produced. The relatively high heat of reaction is advantageous in this case as it reduces the overall

heat duty of the process by about 30 percent [Shoemaker and Jones, *Hyd. Proc.*, **57**(6), 57 (1987)].

Distillation columns with multiple conventional side reactors were first suggested by Schoenmakers and Buehler [*German Chem. Eng.*, **5,** 292 (1982)] and have the potential to accommodate gas-phase reactions, highly exo- or endothermic reactions, catalyst deactivation, and operating conditions outside the normal range suitable for distillation (e.g., short contact times, high temperature and pressure, etc). Krishna (chap. 7 in Sundmacher and Kienle, eds., *Reactive Distillation*, Wiley-VCH, 2003).

Process Applications The production of esters from alcohols and carboxylic acids illustrates many of the principles of reactive distillation as applied to equilibrium-limited systems. The true thermodynamic equilibrium constants for esterification reactions are usually in the range of 5 to 20. Large excesses of alcohols must be used to obtain acceptable yields, resulting in large recycle flow rates. In a reactive distillation scheme, the reaction is driven to completion by removal of the water of esterification. The method used for removal of the water depends on the boiling points, compositions, and liquid-phase behavior of any azeotropes formed between the products and reactants and largely dictates the structure of the reactive distillation flow sheet.

When the ester forms a binary low-boiling azeotrope with water or a ternary alcohol-ester-water azeotrope and that azeotrope is heterogeneous (or can be moved into the two-liquid phase region), the flow sheet illustrated in Fig. 13-98 can be used. Such a flow sheet works for the production of ethyl acetate and higher homologs. In this process scheme, acetic acid and the alcohol are continuously fed to the reboiler of the esterification column, along with a homogeneous strong-acid catalyst. Since the catalyst is largely nonvolatile, the reboiler acts as the primary reaction section. The alcohol is usually fed in slight excess to ensure complete reaction of the acid and to compensate for alcohol losses through distillation of the water-ester-(alcohol) azeotrope. The esterification column is operated such that the low-boiling, water-laden azeotrope is taken as the distillation product. Upon cooling, the distillate separates into two liquid phases. The aqueous layer is steam-stripped, with the organics recycled to the decanter or reactor. The ester layer from the decanter contains some water and possibly alcohol. Part of this layer may be refluxed to the esterification column. The remainder is fed to a low-boiler column where the water-ester and alcohol-ester azeotropes are removed overhead and recycled to the decanter or reactor. The dry, alcohol-free ester is then optionally taken overhead in a final refining column. Additional literature on the application of reactive distillation to ester production includes papers by Hanika, Kolena, and Smejkal [*Chem. Eng. Sci.*, **54,** 5205 (1999)], Schwarzer and Hoffmann [*Chem. Eng. Technol.*, **25,** 975 (2002)], Steinigeweg and Gmehling [*Ind. Eng. Chem. Res.*, **41,** 5483 (2002)], and Omata, Dimian, and Bliek [*Chem. Eng. Sci.*, **58,** 3159, 3175 (2003)].

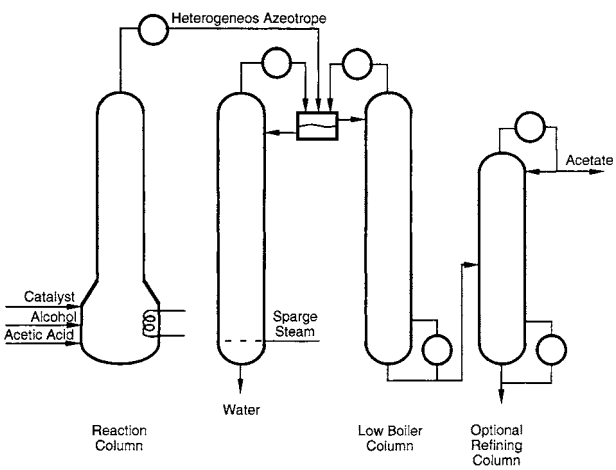

FIG. 13-98 Flow sheet for making esters which form a heterogeneous minimum-boiling azeotrope with water.

Methyl acetate cannot be produced in high purity by using the simple esterification scheme described above. The methyl acetate–methanol–water system does not exhibit a ternary minimum-boiling azeotrope, the methyl acetate–methanol azeotrope is lower-boiling than the water–methyl acetate azeotrope, a distillation boundary extends between these two binary azeotropes, and the heterogeneous region does not include either azeotrope, nor does it cross the distillation boundary. Consequently, the water of esterification cannot be removed effectively, and methyl acetate cannot be separated from the methanol and water azeotropes by a simple decantation in the same manner as outlined above. Conventional sequential reaction-separation processes rely on large excesses of acetic acid to drive the reaction to higher conversion to methyl acetate, necessitating a capital- and energy-intensive acetic acid–water separation and large recycle streams. The crude methyl acetate product, contaminated with water and methanol, can be purified by a number of enhanced distillation techniques such as pressure-swing distillation (Harrison, U.S. Patent 2,704,271, 1955), extractive distillation with ethylene glycol monomethylether as the solvent (Kumerle, German Patent 1,070,165, 1959), or azeotropic distillation with an aromatic or ketone entrainer (Yeomans, Eur. Patent Appl. 060717 and 060719, 1982). The end result is a capital- and energy-intensive process typically requiring multiple reactors and distillation columns.

The reactive distillation process in Fig. 13-99 provides a mechanism for overcoming both the limitations on conversion due to chemical

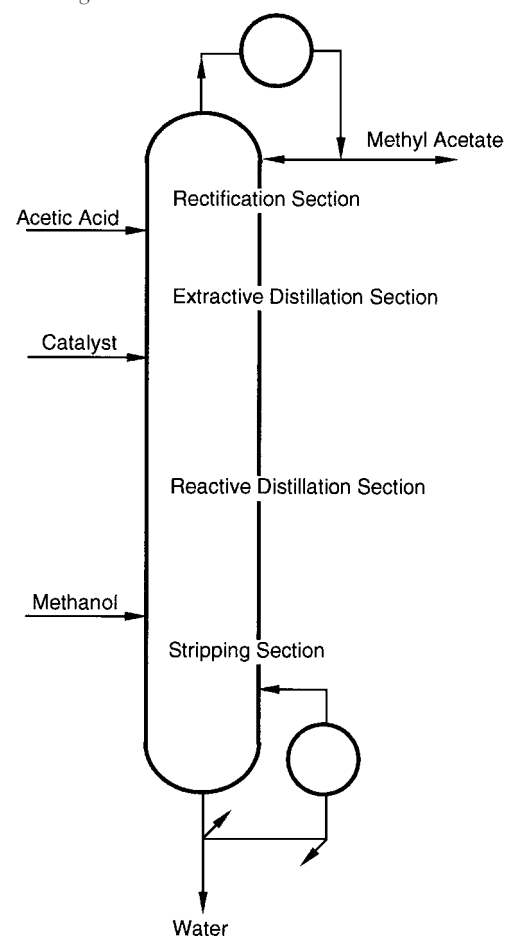

FIG. 13-99 Integrated reactive-extractive distillation column for the production of methyl acetate.

equilibrium as well as the difficulties in purification imposed by the water–methyl acetate and methanol–methyl acetate azeotropes [Agreda and Partin, U.S. Patent 4,435,595, 1984; Agreda, Partin, and Heise, *Chem. Eng. Prog.*, **86**(2), 40 (1990)]. Conceptually, this flow sheet can be thought of as four heat-integrated distillation columns (one of which is also a reactor) stacked on top of each other. The primary reaction zone consists of a series of countercurrent flashing stages in the middle of the column. Adequate residence time for the reaction is provided by high-liquid-holdup bubble cap trays with specially designed downcomer sumps to further increase tray holdup. A nonvolatile homogeneous catalyst is fed at the top of the reactive section and exits with the underflow water by-product. The extractive distillation section, immediately above the reactive section, is critical in achieving high methyl acetate purity. As shown in Fig. 13-96, simultaneous reaction and distillation eliminates the water–methyl acetate azeotrope (and the distillation boundary of the nonreactive system). However, pure methyl acetate remains a saddle in the reactive system and cannot be obtained as a pure component by simple reactive distillation. The acetic acid feed acts as a solvent in an extractive-distillation section placed above the reaction section, breaking the methanol-methyl acetate azeotrope, and yielding a pure methyl acetate distillate product. The uppermost rectification stages serve to remove any acetic acid from the methyl acetate product, and the bottommost stripping section removes any methanol and methyl acetate from the water by-product. The countercurrent flow of the reactants results in high local excesses at each end of the reactive section, even though the overall feed to the reactive column is stoichiometric. Therefore, the large excess of acetic acid at the top of the reactive section prevents methanol from reaching the distillate; similarly, methanol at the bottom of the reactive section keeps acetic acid from the water bottoms. Temperature and composition profiles for this reactive extractive distillation column are shown in Fig. 13-100*a* and *b*, respectively.

Much has been written about this reactive distillation scheme, including works by Bessling et al. [*Chem. Eng. Tech.*, **21,** 393 (1998)], Song et al., [*Ind. Eng. Chem. Res.*, **37,** 1917 (1998)], Huss et al. [*Comput. Chem. Eng.*, **27,** 1855 (2003)], Siirola ("An Industrial Perspective on Process Synthesis," pp. 222–233 in Biegler and Doherty, eds., *Foundations of Computer-Aided Process Design*, AIChE, New York, 1995), and Krishna (chap. 7 in Sundmacher and Kienle, eds., *Reactive Distillation*, Wiley-VCH, 2003).

SYNTHESIS OF MULTICOMPONENT SEPARATION SYSTEMS

The sequencing of distillation columns and other types of equipment for the separation of multicomponent mixtures has received much attention in recent years. Although one separator of complex design can sometimes be devised to produce more than two products, more often a sequence of two-product separators is preferable. Often, the sequence includes simple distillation columns. A summary of sequencing methods, prior to 1977, that can lead to optimal or near-optimal designs, is given by Henley and Seader (op. cit.). Modern methods for distillation column sequencing are reviewed by Modi and Westerberg [*Ind. Eng. Chem. Res.*, **31,** 839 (1992)], who also present a more generally applicable method based on a marginal price that is the change in price of a separation operation when the separation is carried out in the absence of nonkey components. The synthesis of sequences that consider a wide range of separation operations in a knowledge-based approach is given by Barnicki and Fair for liquid mixtures [*Ind. Eng. Chem. Res.*, **29,** 421 (1990)] and for gas/vapor mixtures [*Ind. Eng. Chem. Res.*, **31,** 1679 (1992)]. The problem decomposition approach of Wahnschafft, Le Rudulier, and Westerberg [*Ind. Eng. Chem. Res.*, **32,** 1121 (1993)] is directed to the synthesis of complex separation sequences that involve nonsharp splits and recycle, including azeotropic distillation. The method is applied by using a computer-aided separation process designer called *SPLIT.* An expert system, called *EXSEP,* for the synthesis of solvent-based separation trains is presented by Brunet and Liu [*Ind. Eng. Chem. Res.*, **32,** 315 (1993)]. The use of ternary composition diagrams and residue curve maps is reviewed and evaluated for application to the synthesis of complex separation sequences by Fien and Liu [*Ind. Eng. Chem. Res.*, **33,** 2506 (1994)]. In recent years many optimization-based process synthesis schemes have been proposed for distillation systems. The key research groups are led by Grossmann at Carnegie Mellon University, Manousiouthakis at UCLA, and Pistikopoulos at Imperial College, London. Further information about their methods and availability of computer programs can be obtained from the principals.

Synthesis schemes for reactive distillation have been proposed by Ismail, Proios, and Pistikopoulos [*AIChE J.*, **47,** 629 (2001)], Jackson and Grossmann [*Comput. Chem. Eng.*, **25,** 1661 (2001)], Schembecker and Tlatlik [*Chem. Eng. Process.*, **42,** 179 (2003)], and Burri and Manousiouthakis [*Comput. Chem. Eng.*, **28,** 2509 (2004)].

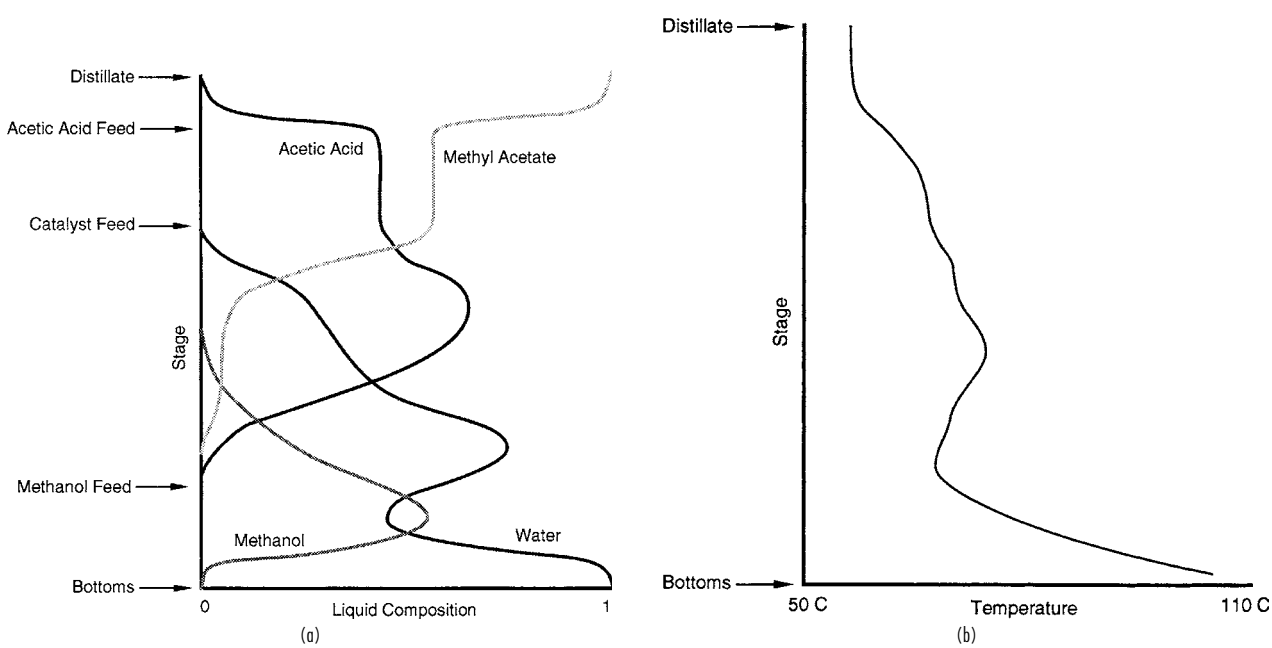

FIG. 13-100 Reactive extractive distillation for methyl acetate production. (*a*) Composition profile. (*b*) Temperature profile.

PETROLEUM AND COMPLEX-MIXTURE DISTILLATION

Although the principles of multicomponent distillation apply to petroleum, synthetic crude oil, and other complex mixtures, this subject warrants special consideration for the following reasons:

1. Such feedstocks are of exceedingly complex composition, consisting of, in the case of petroleum, many different types of hydrocarbons and perhaps of inorganic and other organic compounds. The number of carbon atoms in the components may range from 1 to more than 50, so that the compounds may exhibit atmospheric-pressure boiling points from −162°C (−259°F) to more than 538°C (1000°F). In a given boiling range, the number of different compounds that exhibit only small differences in volatility multiplies rapidly with increasing boiling point. For example, 16 of the 18 octane isomers boil within a range of only 12°C (22°F).

2. Products from the distillation of complex mixtures are in themselves complex mixtures. The character and yields of these products vary widely, depending upon the source of the feedstock. Even crude oils from the same locality may exhibit marked variations.

3. The scale of petroleum-distillation operations is generally large, and as discussed in detail by Nelson (*Petroleum Refinery Engineering,* 4th ed., McGraw-Hill, New York, 1958) and Watkins (*Petroleum Refinery Distillation,* 2d ed., Gulf, Houston, 1979), such operations are common in several petroleum refinery processes including atmospheric distillation of crude oil, vacuum distillation of bottoms residuum obtained from atmospheric distillation, main fractionation of gaseous effluent from catalytic cracking of various petroleum fractions, and main fractionation of effluent from thermal coking of various petroleum fractions. These distillation operations are conducted in large pieces of equipment that can consume large quantities of energy. Therefore, optimization of design and operation is very important and frequently leads to a relatively complex equipment configuration.

CHARACTERIZATION OF PETROLEUM AND PETROLEUM FRACTIONS

Although much progress has been made in identifying the chemical species present in petroleum, it is generally sufficient for purposes of design and analysis of plant operation of distillation to characterize petroleum and petroleum fractions by gravity, laboratory distillation curves, component analysis of light ends, and hydrocarbon-type analysis of middle and heavy ends. From such data, as discussed in the *Technical Data Book—Petroleum Refining* [American Petroleum Institute (API), Washington], five different average boiling points and an index of paraffinicity can be determined. These are then used to predict the physical properties of complex mixtures by a number of well-accepted correlations, whose use will be explained in detail and illustrated with examples. Many other characterizing properties or attributes such as sulfur content, pour point, water and sediment content, salt content, metals content, Reid vapor pressure, Saybolt Universal viscosity, aniline point, octane number, freezing point, cloud point, smoke point, diesel index, refractive index, cetane index, neutralization number, wax content, carbon content, and penetration are generally measured for a crude oil or certain of its fractions according to well-specified ASTM tests. But these attributes are of much less interest here even though feedstocks and products may be required to meet certain specified values of the attributes.

Gravity of a crude oil or petroleum fraction is generally measured by the ASTM D 287 test or the equivalent ASTM D 1298 test and may be reported as specific gravity (SG) 60/60°F [measured at 60°F (15.6°C) and referred to water at 60°F (15.6°C)] or, more commonly, as API gravity, which is defined as

$$\text{API gravity} = 141.5/(\text{SG } 60/60°\text{F}) - 131.5 \qquad (13\text{-}120)$$

Water, thus, has an API gravity of 10.0, and most crude oils and petroleum fractions have values of API gravity in the range of 10 to 80. Light hydrocarbons (*n*-pentane and lighter) have values of API gravity ranging upward from 92.8.

The volatility of crude oil and petroleum fractions is characterized in terms of one or more laboratory distillation tests that are summarized in Table 13-27. The ASTM D 86 and D 1160 tests are reasonably rapid batch laboratory distillations involving the equivalent of approximately one equilibrium stage and no reflux except for that caused by heat losses. Apparatus typical of the D 86 test is shown in Fig. 13-101 and consists of a heated 100-mL or 125-mL Engler flask containing a calibrated thermometer of suitable range to measure the temperature of the vapor at the inlet to the condensing tube, an inclined brass condenser in a cooling bath using a suitable coolant, and a graduated cylinder for collecting the distillate. A stem correction is not applied to the temperature reading. Related tests using similar apparatus are the D 216 test for natural gasoline and the Engler distillation.

In the widely used ASTM D 86 test, 100 mL of sample is charged to the flask and heated at a sufficient rate to produce the first drop of distillate from the lower end of the condenser tube in 5 to 15 min, depending on the nature of the sample. The temperature of the vapor at that instant is recorded as the initial boiling point (IBP). Heating is continued at a rate such that the time from the IBP to 5 vol % recovered of the sample in the cylinder is 60 to 75 s. Again, vapor temperature is recorded. Then successive vapor temperatures are recorded for 10 to 90 percent recovered in intervals of 10, and at 95 percent recovered, with the heating rate adjusted so that 4 to 5 mL is collected per minute. At 95 percent recovered, the burner flame is increased if necessary to achieve a maximum vapor temperature, referred to as the endpoint (EP) in 3 to 5 additional min. The percent recovery is reported as the maximum percent recovered in the cylinder. Any residue remaining in the flask is reported as percent residue, and percent loss is reported as the difference between 100 mL and the sum of the percent recovery and percent residue. If the atmosphere test pressure P is other than 101.3 kPa (760 torr), temperature readings may be adjusted to that pressure by the Sidney Young equation, which for degrees Fahrenheit is

$$T_{760} = T_P + 0.00012(760 - P)(460 + T_P) \qquad (13\text{-}121)$$

Another pressure correction for percent loss can also be applied, as described in the ASTM test method.

TABLE 13-27 Laboratory Distillation Tests

Test name	Reference	Main applicability
ASTM (atmospheric)	ASTM D 86	Petroleum fractions or products, including gasolines, turbine fuels, naphthas, kerosines, gas oils, distillate fuel oils, and solvents that do not tend to decompose when vaporized at 760 mmHg
ASTM [vacuum, often 10 torr (1.3 kPa)]	ASTM D 1160	Heavy petroleum fractions or products that tend to decompose in the ASTM D 86 test but can be partially or completely vaporized at a maximum liquid temperature of 750°F (400°C) at pressures down to 1 torr (0.13 kPa)
TBP [atmospheric or 10 torr (1.3 kPa)]	Nelson,* ASTM D 2892	Crude oil and petroleum fractions
Simulated TBP (gas chromatography)	ASTM D 2887	Crude oil and petroleum fractions
EFV (atmospheric, superatmospheric, or subatmospheric)	Nelson†	Crude oil and petroleum fractions

*Nelson, *Petroleum Refinery Engineering,* 4th ed., McGraw-Hill, New York, 1958, pp. 95–99.
†Ibid., pp. 104–105.

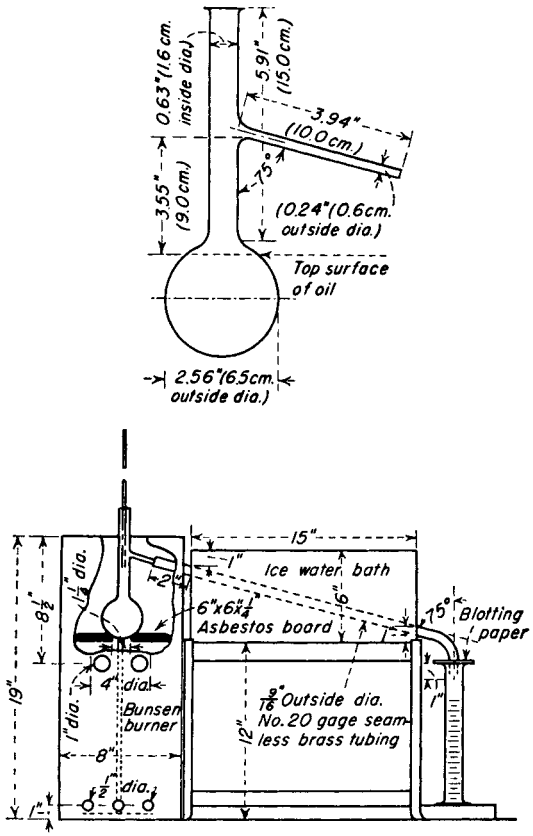

FIG. 13-101 ASTM distillation apparatus; detail of distilling flask is shown in the upper figure.

Results of a typical ASTM distillation test for an automotive gasoline are given in Table 13-28, in which temperatures have already been corrected to a pressure of 101.3 kPa (760 torr). It is generally assumed that percent loss corresponds to volatile noncondensables that are distilled off at the beginning of the test. In that case, the percent recovered values in Table 13-28 do not correspond to percent evaporated values, which are of greater scientific value. Therefore, it is common to adjust the reported temperatures according to a linear interpolation procedure given in the ASTM test method to obtain corrected temperatures in terms of percent evaporated at the standard intervals as included in Table 13-28. In the example, the corrections are not large because the loss is only 1.5 vol %.

TABLE 13-28 Typical ASTM D 86 Test Results for Automobile Gasoline Pressure, 760 torr (101.3 kPa)

Percent recovered basis (as measured)			Percent evaporated basis (as corrected)		
Percent recovered	T, °F	Percent evaporated	Percent evaporated	T, °F	Percent recovered
0(IBP)	98	1.5	1.5	98	(IBP)
5	114	6.5	5	109	3.5
10	120	11.5	10	118	8.5
20	150	21.5	20	146	18.5
30	171	31.5	30	168	28.5
40	193	41.5	40	190	38.5
50	215	51.5	50	212	48.5
60	243	61.5	60	239	58.5
70	268	71.5	70	264	68.5
80	300	81.5	80	295	78.5
90	340	91.5	90	334	88.5
95	368	96.5	95	360	93.5
EP	408			408	(EP)

NOTE: Percent recovery = 97.5; percent residue = 1.0; percent loss = 1.5. To convert degrees Fahrenheit to degrees Celsius, °C = (°F − 32)/1.8.

Although most crude petroleum can be heated to 600°F (316°C) without noticeable cracking, when ASTM temperatures exceed 475 °F (246°C), fumes may be evolved, indicating decomposition, which may cause thermometer readings to be low. In that case, the following correction attributed to S. T. Hadden may be applied:

$$\Delta T_{\text{corr}} = 10^{-1.587 + 0.004735T} \tag{13-122}$$

where T = measured temperature, °F
ΔT_{corr} = correction to be added to T, °F

At 500 and 600°F (260 and 316°C), the corrections are 6 and 18°F (3.3 and 10°C), respectively.

As discussed by Nelson (op. cit.), virtually no fractionation occurs in an ASTM distillation. Thus, components in the mixture do distill one by one in the order of their boiling points but as mixtures of successively higher boiling points. The IBP, EP, and intermediate points have little theoretical significance, and, in fact, components boiling below the IBP and above the EP are present in the sample. Nevertheless, because ASTM distillations are quickly conducted, have been successfully automated, require only a small sample, and are quite reproducible, they are widely used for comparison and as a basis for specifications on a large number of petroleum intermediates and products, including many solvents and fuels. Typical ASTM curves for several such products are shown in Fig. 13-102.

Data from a *true boiling point* (TBP) distillation test provide a much better theoretical basis for characterization. If the sample contains compounds that have moderate differences in boiling points such as in

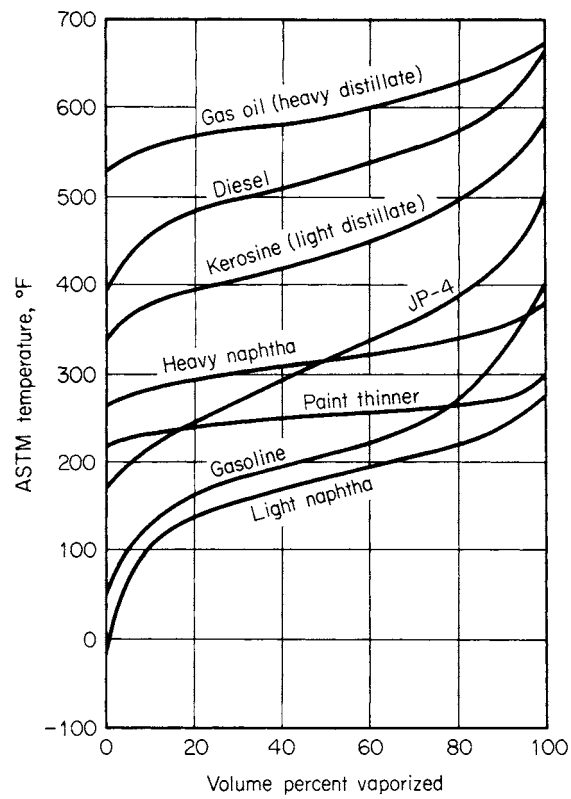

FIG. 13-102 Representative ASTM D 86 distillation curves.

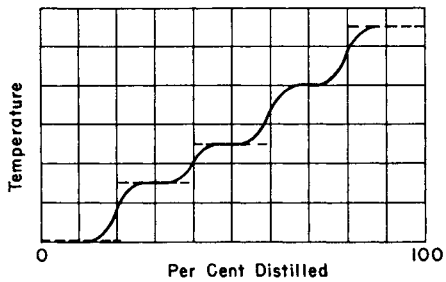

FIG. 13-103 Variation of boiling temperature with percent distilled in TBP distillation of light hydrocarbons.

a light gasoline containing light hydrocarbons (e.g., isobutane, *n*-butane, isopentane), a plot of overhead vapor distillate temperature versus percent distilled in a TBP test would appear in the form of steps as in Fig. 13-103. However, if the sample has a higher average boiling range when the number of close-boiling isomers increases, the steps become indistinct and a TBP curve such as that in Fig. 13-104 results. Because the degree of separation for a TBP distillation test is much higher than that for an ASTM distillation test, the IBP is lower and the EP is higher for the TBP method as compared with the ASTM method, as shown in Fig. 13-104.

A standard TBP laboratory distillation test method has not been well accepted. Instead, as discussed by Nelson (op. cit., pp. 95–99), batch distillation equipment that can achieve a good degree of fractionation is usually considered suitable. In general, TBP distillations are conducted in columns with 15 to 100 theoretical stages at reflux ratios of 5 or greater. Thus, the new ASTM D 2892 test method, which involves a column with 14 to 17 theoretical stages and a reflux ratio of 5, essentially meets the minimum requirements. Distillate may be collected at a constant or a variable rate. Operation may be at 101.3-kPa (760-torr) pressure or at a vacuum at the top of the column as low as 0.067 kPa (0.5 torr) for high-boiling fractions, with 1.3 kPa (10 torr) being common. Results from vacuum operation are extrapolated to 101.3 kPa (760 torr) by the vapor-pressure correlation of Maxwell and Bonner [*Ind. Eng. Chem.*, **49,** 1187 (1957)], which is given in great detail in the API *Technical Data Book—Petroleum Refining* (op. cit.) and in the ASTM D 2892 test method. It includes a correction for the nature of the sample (paraffin, olefin, naphthene, and aromatic content) in terms of the UOP characterization factor, UOP-K, as given by

$$\text{UOP-K} = \frac{(T_B)^{1/3}}{\text{SG}} \tag{13-123}$$

where T_B is the mean average boiling point in degrees Rankine, which is the arithmetic average of the molal average boiling point and the cubic volumetric average boiling point. Values of UOP-K for *n*-hexane, 1-hexene, cyclohexene, and benzene are 12.82, 12.49, 10.99, and 9.73, respectively. Thus, paraffins with their lower values of specific gravity tend to have high values, and aromatics tend to have low values of UOP-K. A movement toward an international TBP standard is discussed by Vercier and Mouton [*Oil Gas J.*, **77**(38), 121 (1979)].

A crude oil assay always includes a whole crude API gravity and a TBP curve. As discussed by Nelson (op. cit., pp. 89–90) and as shown in Fig. 13-105, a reasonably consistent correlation (based on more than 350 distillation curves) exists between whole crude API gravity and the TBP distillation curve at 101.3 kPa (760 torr). Exceptions not correlated by Fig. 13-105 are highly paraffinic or naphthenic crude oils.

An alternative to TBP distillation is simulated distillation by gas chromatography. As described by Green, Schmauch, and Worman [*Anal. Chem.*, **36,** 1512 (1965)] and Worman and Green [*Anal. Chem.*, **37,** 1620 (1965)], the method is equivalent to a 100-theoretical-plate TBP distillation; is very rapid, reproducible, and easily automated; requires only a small microliter sample; and can better define initial and final boiling points. The ASTM D 2887 standard test method is based on such a simulated distillation and is applicable to samples having a boiling range greater than 55°C (100°F) for temperature determinations as high as 538°C (1000°F). Typically, the test is conducted with a gas chromatograph having a thermal conductivity detector, a programmed temperature capability, helium or hydrogen carrier gas, and column packing of silicone gum rubber on a crushed firebrick or diatomaceous earth support.

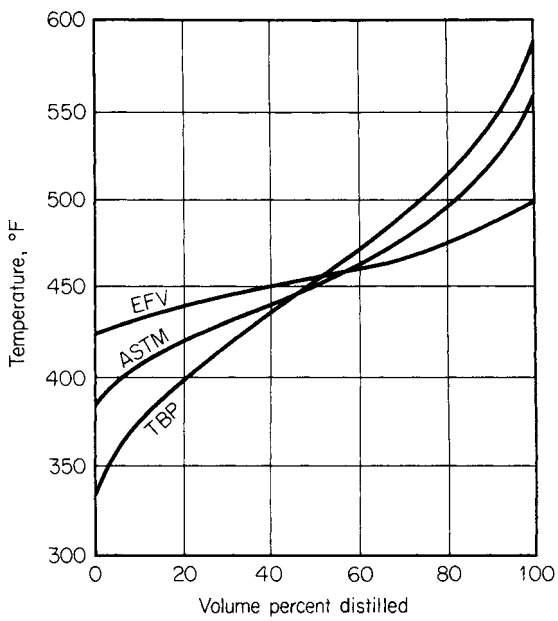

FIG. 13-104 Comparison of ASTM, TBP, and EFV distillation curves for kerosine.

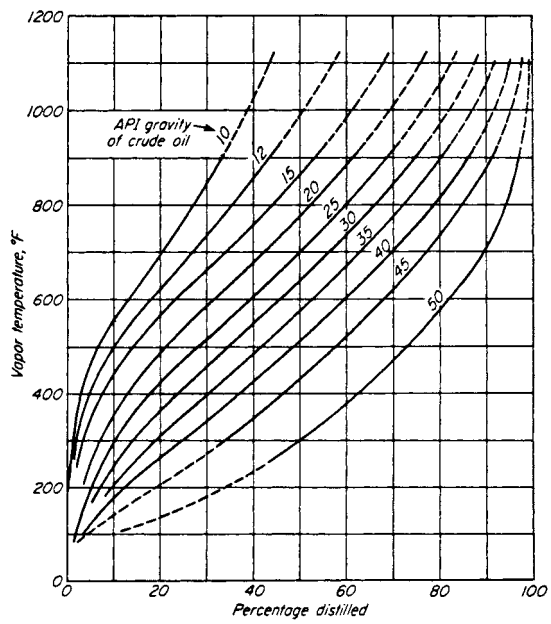

FIG. 13-105 Average true-boiling-point distillation curves of crude oils. *(From W. E. Edmister,* Applied Hydrocarbon Thermodynamics, *vol. 1, 1st ed., 1961 Gulf Publishing Company, Houston, Texas, Used with permission. All rights reserved.)*

It is important to note that simulated distillation does not always separate hydrocarbons in the order of their boiling points. For example, high-boiling multiple-ring-type compounds may be eluted earlier than normal paraffins (used as the calibration standard) of the same boiling point. Gas chromatography is also used in the ASTM D 2427 test method to determine quantitatively ethane through pentane hydrocarbons.

A third fundamental type of laboratory distillation, which is the most tedious to perform of the three types of laboratory distillations, is equilibrium flash vaporization (EFV), for which no standard test exists. The sample is heated in such a manner that the total vapor produced remains in contact with the total remaining liquid until the desired temperature is reached at a set pressure. The volume percent vaporized at these conditions is recorded. To determine the complete flash curve, a series of runs at a fixed pressure is conducted over a range of temperatures sufficient to cover the range of vaporization from 0 to 100 percent. As seen in Fig. 13-104, the component separation achieved by an EFV distillation is much less than that by the ASTM or TBP distillation tests. The initial and final EFV points are the bubble point and the dew point, respectively, of the sample. If desired, EFV curves can be established at a series of pressures.

Because of the time and expense involved in conducting laboratory distillation tests of all three basic types, it has become increasingly common to use empirical correlations to estimate the other two distillation curves when the ASTM, TBP, or EFV curve is available. Preferred correlations given in the API *Technical Data Book—Petroleum Refining* (op. cit.) are based on the work of Edmister and Pollock [*Chem. Eng. Prog.*, **44,** 905 (1948)], Edmister and Okamoto [*Pet. Refiner,* **38**(8), 117 (1959); **38**(9), 271 (1959)], Maxwell (*Data Book on Hydrocarbons,* Van Nostrand, Princeton, N.J., 1950), and Chu and Staffel [*J. Inst. Pet.*, **41,** 92 (1955)]. Because of the lack of sufficiently precise and consistent data on which to develop the correlations, they are, at best, first approximations and should be used with caution. Also, they do not apply to mixtures containing only a few components of widely different boiling points. Perhaps the most useful correlation of the group is Fig. 13-106 for converting between ASTM D 86 and TBP distillations of petroleum fractions at 101.3 kPa (760 torr). The ASTM D 2889 test method, which presents a standard method for calculating EFV curves from the results of an ASTM D 86 test for a petroleum fraction having a 10 to 90 vol % boiling range of less than 55°C (100°F), is also quite useful.

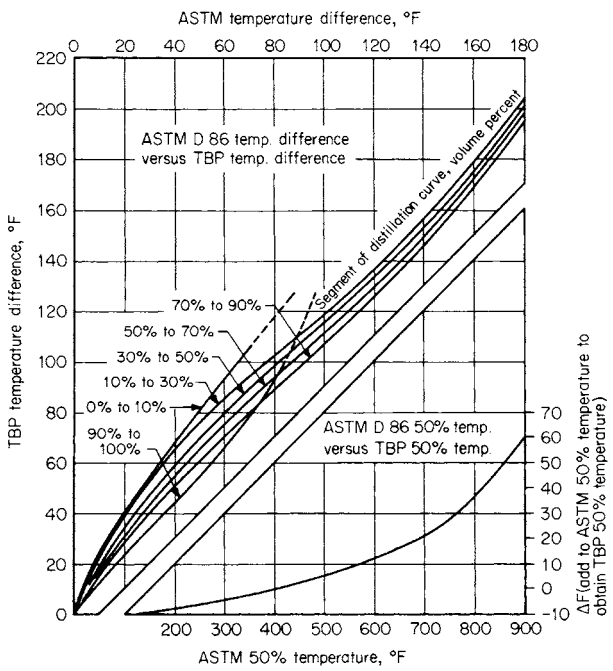

FIG. 13-106 Relationship between ASTM and TBP distillation curves. *(From W. C. Edmister,* Applied Hydrocarbon Thermodynamics, *vol. 1, 1st ed., 1961 Gulf Publishing Company, Houston, Tex. Used with permission. All rights reserved.)*

APPLICATIONS OF PETROLEUM DISTILLATION

Typical equipment configurations for the distillation of crude oil and other complex hydrocarbon mixtures in a crude unit, a catalytic cracking unit, and a delayed coking unit of a petroleum refinery are shown in Figs. 13-107, 13-108, and 13-109. The initial separation of crude oil into fractions is conducted in two main columns, shown in Fig. 13-107. In the first column, called the atmospheric tower or topping still, partially vaporized crude oil, from which water, sediment, and salt have been removed, is mainly rectified, at a feed tray pressure of no more than about 276 kPa (40 psia), to yield a noncondensable light-hydrocarbon gas, a light naphtha, a heavy naphtha, a light distillate (kerosine), a heavy distillate (diesel oil), and a bottoms residual of components whose TBP exceeds approximately 427°C (800°F). Alternatively, other fractions, shown in Fig. 13-102, may be withdrawn. To control the IBP of the ASTM D 86 curves, each of the sidestreams of the atmospheric tower and the vacuum and main fractionators of Figs. 13-107, 13-108, and 13-109 may be sent to side-cut strippers, which use a partial reboiler or steam stripping. Additional stripping by steam is commonly used in the bottom of the atmospheric tower as well as in the vacuum tower and other main fractionators.

Additional distillate in the TBP range of approximately 427 to 593°C (800 to 1100°F) is recovered from bottoms residuum of the atmospheric tower by rectification in a vacuum tower, also shown in Fig. 13-107, at the minimum practical overhead condenser pressure, which is typically 1.3 kPa (10 torr). Use of special low-pressure-drop trays or column packing permits the feed tray pressure to be approximately 5.3 to 6.7 kPa (40 to 50 torr) to obtain the maximum degree of vaporization. Vacuum towers may be designed or operated to produce several different products including heavy distillates, gas-oil feedstocks for catalytic cracking, lubricating oils, bunker fuel, and bottoms residua of asphalt (5 to 8 API gravity) or pitch (0 to 5 API gravity). The catalytic cracking process of Fig. 13-108 produces a superheated vapor at approximately 538°C (1000°F) and 172 to 207 kPa (25 to 30 psia) of a TBP range that covers hydrogen to compounds with normal boiling points above 482°C (900°F). This gas is sent directly to a main fractionator for rectification to obtain products that are typically gas and naphtha [204°C (400°F) ASTM EP approximately], which are often fractionated further to produce relatively pure light hydrocarbons and gasoline; a light cycle oil [typically 204 to 371°C (400 to 700°F) ASTM D 86 range], which may be used for heating oil, hydrocracked, or recycled to the catalytic cracker; an intermediate cycle oil [typically 371 to 482°C (700 to 900°F) ASTM D 86 range], which is generally recycled to the catalytic cracker to extinction; and a heavy gas oil or bottom slurry oil.

Vacuum-column bottoms, bottoms residuum from the main fractionation of a catalytic cracker, and other residua can be further processed at approximately 510°C (950°F) and 448 kPa (65 psia) in a delayed-coker unit, as shown in Fig. 13-109, to produce petroleum coke and gas of TBP range that covers methane (with perhaps a small amount of hydrogen) to compounds with normal boiling points that may exceed 649°C (1200°F). The gas is sent directly to a main fractionator that is similar to the type used in conjunction with a catalytic cracker, except that in the delayed-coking operation the liquid to be coked first enters into and passes down through the bottom trays of the main fractionator to be preheated by and to scrub coker vapor of entrained coke particles and condensables for recycling to the delayed coker. Products produced from the main fractionator are similar to those produced in a catalytic cracking unit, except for more unsaturated cyclic compounds, and include gas and coker naphtha, which are further processed to separate out light hydrocarbons and a coker naphtha that generally needs hydrotreating; and light and heavy coker gas oils, both of which may require hydrocracking to become suitable blending stocks.

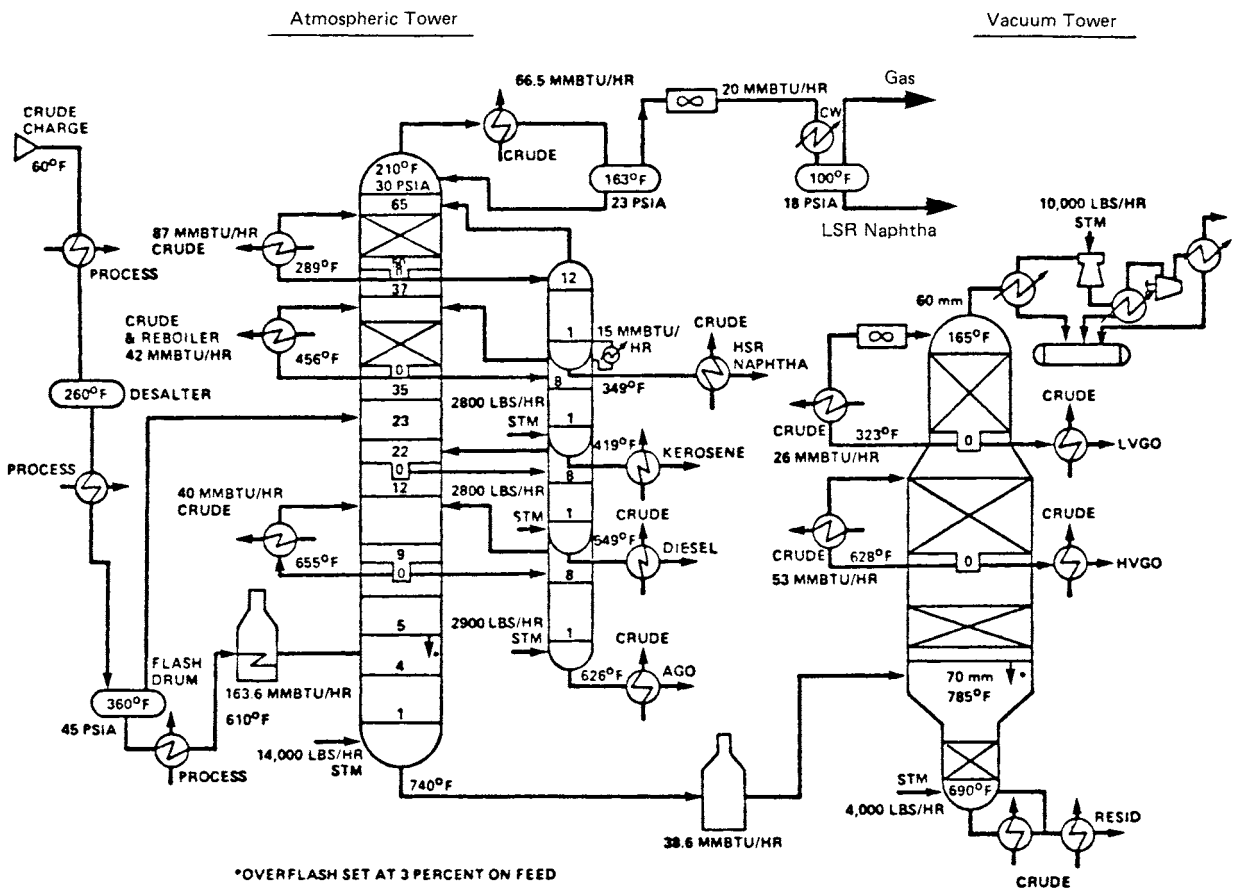

FIG. 13-107 Crude unit with atmospheric and vacuum towers. [*Kleinschrodt and Hammer,* Chem. Eng. Prog., ***79(7),*** *33 (1983).*]

DESIGN PROCEDURES

Two general procedures are available for designing fractionators that process petroleum, synthetic crude oils, and complex mixtures. The first, which was originally developed for crude units by Packie [*Trans. Am. Inst. Chem. Eng. J.*, **37,** 51 (1941)], extended to main fractionators by Houghland, Lemieux, and Schreiner [*Proc. API,* sec. III, *Refining,* 385 (1954)], and further elaborated and described in great detail by Watkins (op. cit.), uses material and energy balances, with empirical correlations to establish tray requirements, and is essentially a hand calculation procedure that is a valuable learning experience and is suitable for preliminary designs. Also, when backed by sufficient experience from previous designs, this procedure is adequate for final design.

In the second procedure, which is best applied with a digital computer, the complex mixture being distilled is represented by actual components at the light end and by perhaps 30 pseudocomponents (e.g., petroleum fractions) over the remaining portion of the TBP distillation curve for the column feed. Each of the pseudocomponents is characterized by a TBP range, an average normal boiling point, an average API gravity, and an average molecular weight. Rigorous material balance, energy balance, and phase equilibrium calculations are then made by an appropriate equation-tearing method, as shown by Cecchetti et al. [*Hydrocarbon Process.*, **42**(9), 159 (1963)] or a simultaneous-correction procedure as shown, e.g., by Goldstein and Stanfield [*Ind. Eng. Chem. Process Des. Dev.*, **9,** 78 (1970)] and Hess et al. [*Hydrocarbon Process.*, **56**(5), 241 (1977)]. Highly developed procedures of the latter type, suitable for preliminary or final design, are included in most computer-aided steady-state process design and simulation programs as a special case of interlinked distillation, wherein the crude tower or fractionator is converged simultaneously with the sidecut stripper columns.

Regardless of the procedure used, certain initial steps must be taken for the determination or specification of certain product properties and yields based on the TBP distillation curve of the column feed, method of providing column reflux, column-operating pressure, type of condenser, and type of sidecut strippers and stripping requirements. These steps are developed and illustrated with several detailed examples by Watkins (op. cit.). Only one example, modified from one given by Watkins, is considered briefly here to indicate the approach taken during the initial steps.

For the atmospheric tower shown in Fig. 13-110, suppose distillation specifications are as follows:

- Feed: 50,000 bbl (at 42 U.S. gal each) per stream day (BPSD) of 31.6 API crude oil.
- Measured light-ends analysis of feed:

Component	Volume percent of crude oil
Ethane	0.04
Propane	0.37
Isobutane	0.27
n-Butane	0.89
Isopentane	0.77
n-Pentane	1.13
	3.47

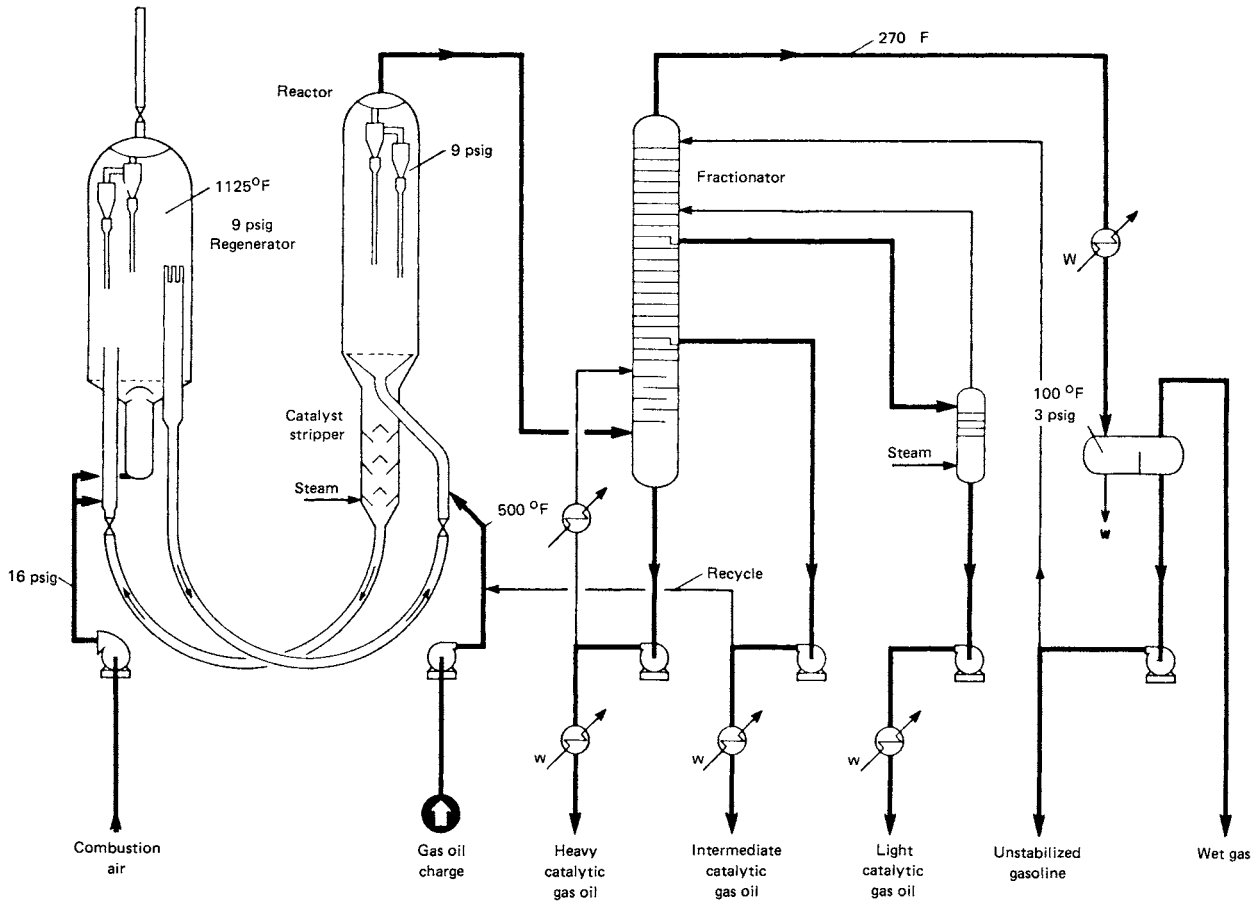

FIG. 13-108 Catalytic cracking unit. [*New Horizons*, Lummus Co., New York (1954)].

- Measured TBP and API gravity of feed, computed atmospheric pressure EFV (from API *Technical Data Book*), and molecular weight of feed:

Volume percent vaporized	TBP, °F	EFV, °F	°API	Molecular weight
0	–130	179		
5	148	275	75.0	91
10	213	317	61.3	106
20	327	394	50.0	137
30	430	468	41.8	177
40	534	544	36.9	223
50	639	619	30.7	273
60	747	696	26.3	327
70	867	777	22.7	392
80	1013	866	19.1	480

- Product specifications:

	ASTM D 86, °F		
Desired cut	5%	50%	95%
Overhead (OV)			253
Heavy naphtha (HN)	278	314	363
Light distillate (LD)	398	453	536
Heavy distillate (HD)	546	589	
Bottoms (B)			

NOTE: To convert degrees Fahrenheit to degrees Celsius, °C = (°F – 32)/1.8.

- TBP cut point between the heavy distillate and the bottoms = 650 °F.
- Percent overflash = 2 vol % of feed
- Furnace outlet temperature = 343°C (650 °F) maximum
- Overhead temperature in reflux drum = 49°C (120°F) minimum

From the product specifications, distillate yields are computed as follows: From Fig. 13-106 and the ASTM D 86 50 percent temperatures, TBP 50 percent temperatures of the three intermediate cuts are obtained as 155, 236, and 316°C (311, 456, and 600°F) for the HN, LD, and HD, respectively. The TBP cut points, corresponding volume fractions of crude oil, and flow rates of the four distillates are readily obtained by starting from the specified 343°C (650°F) cut point as follows, where CP is the cut point and T is the TBP temperature (°F):

$$\mathrm{CP}_{\mathrm{HD,B}} = 650°\mathrm{F}$$
$$\mathrm{CP}_{\mathrm{HD,B}} - T_{\mathrm{HD}_{50}} = 650 - 600 = 50°\mathrm{F}$$
$$\mathrm{CP}_{\mathrm{LD,HD}} = T_{\mathrm{HD}_{50}} - 50 = 600 - 50 = 550°\mathrm{F}$$
$$\mathrm{CP}_{\mathrm{LD,HD}} - T_{\mathrm{LD}_{50}} = 550 - 456 = 94°\mathrm{F}$$
$$\mathrm{CP}_{\mathrm{HN,LD}} = T_{\mathrm{LD}_{50}} - 94 = 456 - 94 = 362°\mathrm{F}$$
$$\mathrm{CP}_{\mathrm{HN,LD}} - T_{\mathrm{HN}_{50}} = 362 - 311 = 51°\mathrm{F}$$
$$\mathrm{CP}_{\mathrm{OV,HN}} = T_{\mathrm{HN}_{50}} - 51 = 311 - 51 = 260°\mathrm{F}$$

These cut points are shown as vertical lines on the crude oil TBP plot of Fig. 13-111, from which the following volume fractions and flow

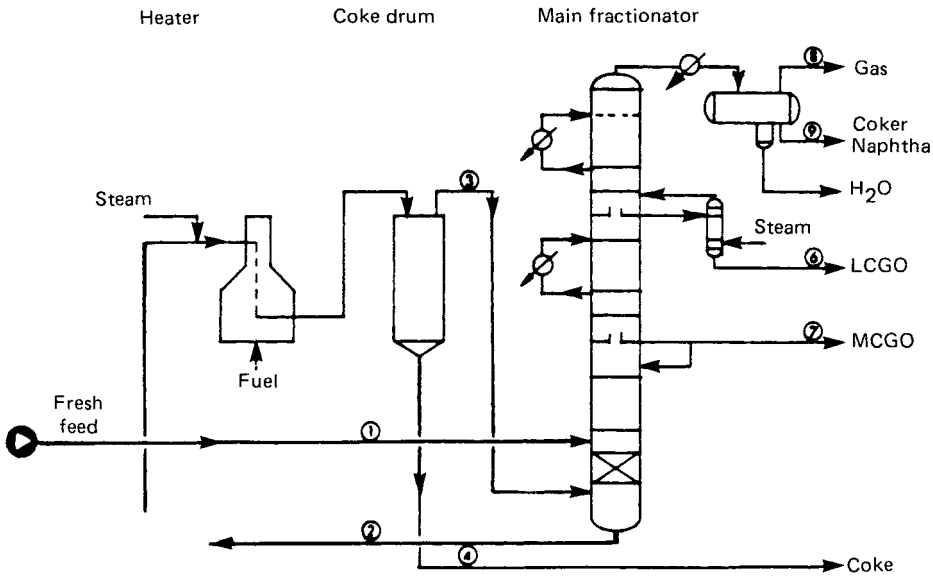

FIG. 13-109 Delayed-coking unit. (Watkins, *Petroleum Refinery Distillation*, 2d ed., Gulf, Houston, Tex., 1979).

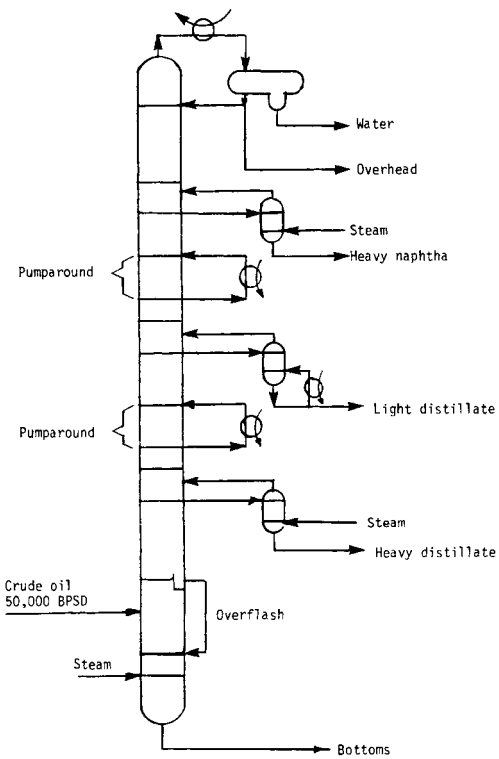

FIG. 13-110 Crude atmospheric tower.

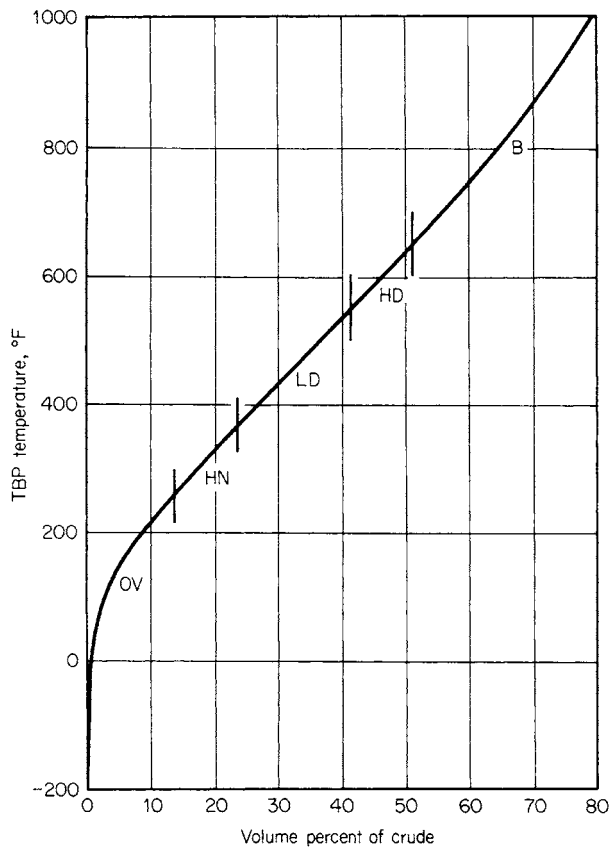

FIG. 13-111 Example of crude oil TBP cut points.

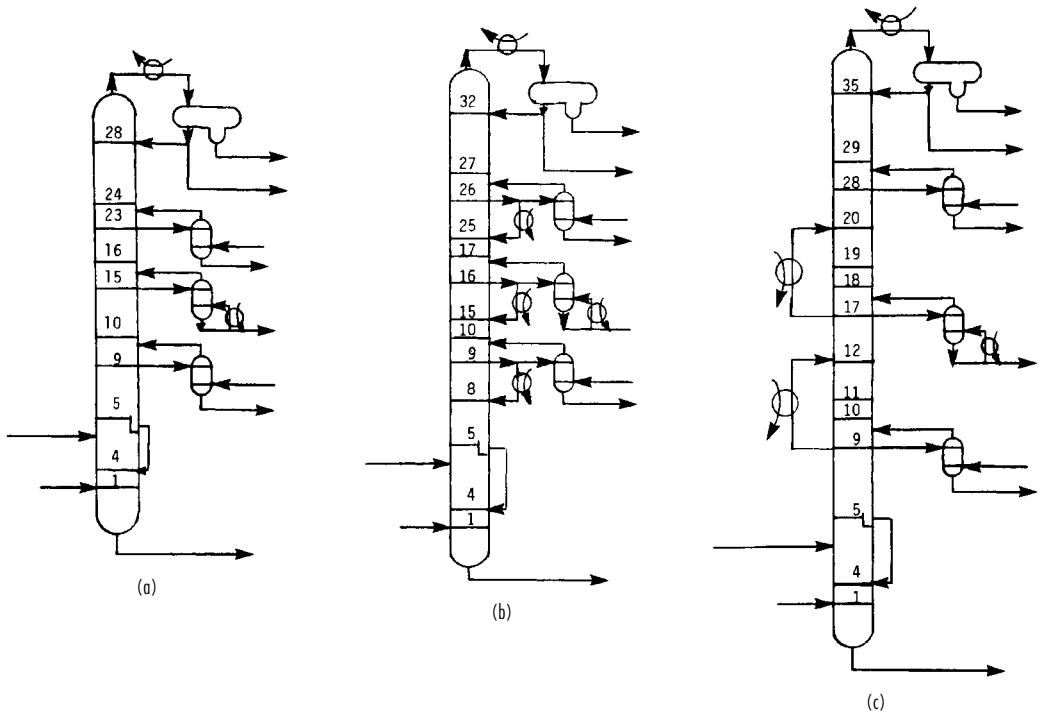

FIG. 13-112 Methods of providing reflux to crude units. (*a*) Top reflux. (*b*) Pump-back reflux. (*c*) Pump-around reflux.

rates of product cuts are readily obtained:

Desired cut	Volume percent of crude oil	BPSD
Overhead (OV)	13.4	6,700
Heavy naphtha (HN)	10.3	5,150
Light distillate (LD)	17.4	8,700
Heavy distillate (HD)	10.0	5,000
Bottoms (B)	48.9	24,450
	100.0	50,000

As shown in Fig. 13-112, methods of providing column reflux include *(a)* conventional top-tray reflux, *(b)* pump-back reflux from sidecut strippers, and *(c)* pump-around reflux. The latter two methods essentially function as intercondenser schemes that reduce the top-tray reflux requirement. As shown in Fig. 13-113 for the example being considered, the internal-reflux flow rate decreases rapidly from the top tray to the feed-flash zone for case *a*. The other two cases, particularly case *c*, result in better balancing of the column-reflux traffic. Because of this and the opportunity provided to recover energy at a moderate- to high-temperature level, pump-around reflux is the most commonly used technique. However, not indicated in Fig. 13-113 is the fact that in cases *b* and *c* the smaller quantity of reflux present in the upper portion of the column increases the tray requirements. Furthermore, the pump-around circuits, which extend over three trays each, are believed to be equivalent for mass-transfer purposes to only one tray each. Representative tray requirements for the three cases are included in Fig. 13-112. In case *c*, heat-transfer rates associated with the two pump-around circuits account for approximately 40 percent of the total heat removed in the overhead condenser and from the two pump-around circuits combined.

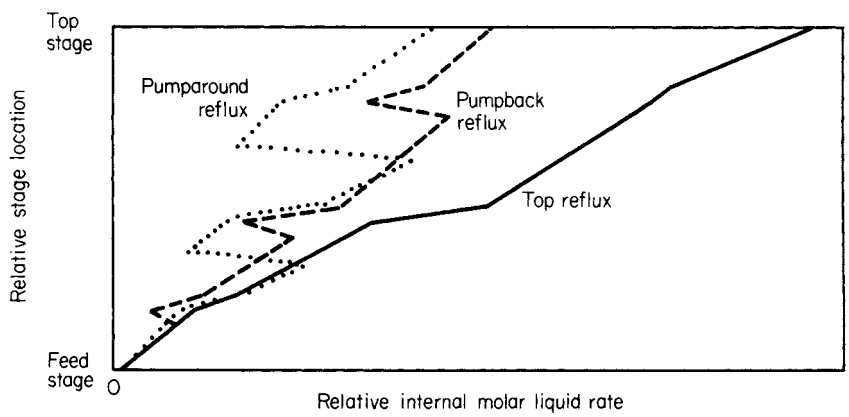

FIG. 13-113 Comparison of internal reflux rates for three methods of providing reflux.

Bottoms and three sidecut strippers remove light ends from products and may use steam or reboilers. In Fig. 13-112 a reboiled stripper is used on the light distillate, which is the largest sidecut withdrawn. Steam-stripping rates in sidecut strippers and at the bottom of the atmospheric column may vary from 0.45 to 4.5 kg (1 to 10 lb) of steam per barrel of stripped liquid, depending on the fraction of stripper feed liquid that is vaporized.

Column pressure at the reflux drum is established so as to condense totally the overhead vapor or some fraction thereof. Flash-zone pressure is approximately 69 kPa (10 psia) higher. Crude oil feed temperature at flash-zone pressure must be sufficient to vaporize the total distillates plus the overflash, which is necessary to provide reflux between the lowest sidestream-product drawoff tray and the flash zone. Calculations are made by using the crude oil EFV curve corrected for pressure. For the example being considered, percent vaporized at the flash zone must be 53.1 percent of the feed.

Tray requirements depend on internal reflux ratios and ASTM 5-95 gaps or overlaps and may be estimated by the correlation of Packie (op. cit.) for crude units and the correlation of Houghland, Lemieux, and Schreiner (op. cit.) for main fractionators.

Example 15: Simulation Calculation of an Atmospheric Tower The ability of a rigorous calculation procedure to simulate operation of an atmospheric tower with its accompanying sidecut strippers may be illustrated by comparing commercial-test data from an actual operation with results computed with the REFINE program of ChemShare Corporation, Houston, Texas. (See also DESIGN II program from WinSim, Inc., Sugar Land, Texas; http://www.winsim.com.) The tower configuration and plant operating conditions are shown in Fig. 13-114.

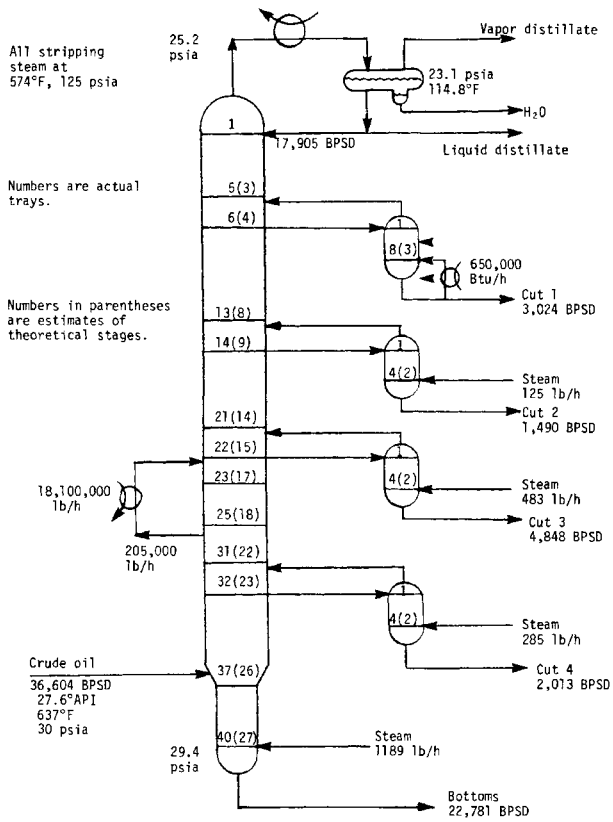

FIG. 13-114 Configuration and conditions for the simulation of the atmospheric tower of crude unit.

TABLE 13-29 Light-Component Analysis and TBP Distillation of Feed for the Atmospheric Crude Tower of Fig. 13-114

Light-component analysis	
Component	Volume percent
Methane	0.073
Ethane	0.388
Propane	0.618
n-Butane	0.817
n-Pentane	2.05

TBP distillation of feed		
API gravity	TBP, °F	Volume percent
80	−160.	0.1
70	155.	5.
57.5	242.	10.
45.	377.	20.
36.	499.	30.
29.	609.	40.
26.5	707.	50.
23.	805.	60.
20.5	907.	70.
17.	1054.	80.
10.	1210.	90.
−4.	1303.	95.
−22.	1467	100.

NOTE: To convert degrees Fahrenheit to degrees Celsius, °C = (°F − 32)/1.8.

TABLE 13-30 Pseudo-Component Representation of Feed for the Atmospheric Crude Tower of Fig. 13-114

No.	Component name	Molecular weight	Specific gravity	API gravity	(lb·mol)/h
1	Water	18.02	1.0000	10.0	.00
2	Methane	16.04	.3005	339.5	7.30
3	Ethane	30.07	.3561	265.8	24.54
4	Propane	44.09	.5072	147.5	37.97
5	*n*-Butane	58.12	.5840	110.8	43.84
6	*n*-Pentane	72.15	.6308	92.8	95.72
7	131 ABP	83.70	.6906	73.4	74.31
8	180 ABP	95.03	.7152	66.3	66.99
9	210 ABP	102.23	.7309	62.1	65.83
10	240 ABP	109.78	.7479	57.7	70.59
11	270 ABP	118.52	.7591	54.9	76.02
12	300 ABP	127.69	.7706	52.1	71.62
13	330 ABP	137.30	.7824	49.4	67.63
14	360 ABP	147.33	.7946	46.6	64.01
15	390 ABP	157.97	.8061	44.0	66.58
16	420 ABP	169.37	.8164	41.8	63.30
17	450 ABP	181.24	.8269	39.6	59.92
18	480 ABP	193.59	.8378	37.4	56.84
19	510 ABP	206.52	.8483	35.3	59.05
20	540 ABP	220.18	.8581	33.4	56.77
21	570 ABP	234.31	.8682	31.5	53.97
22	600 ABP	248.30	.8804	29.2	52.91
23	630 ABP	265.43	.8846	28.5	54.49
24	660 ABP	283.37	.8888	27.7	51.28
25	690 ABP	302.14	.8931	26.9	48.33
26	742 ABP	335.94	.9028	25.2	109.84
27	817 ABP	387.54	.9177	22.7	94.26
28	892 ABP	446.02	.9288	20.8	74.10
29	967 ABP	509.43	.9398	19.1	50.27
30	1055 ABP	588.46	.9531	17.0	57.12
31	1155 ABP	665.13	.9829	12.5	50.59
32	1255 ABP	668.15	1.0658	1.3	45.85
33	1355 ABP	643.79	1.1618	−9.7	29.39
34	1436 ABP	597.05	1.2533	−18.6	21.19
		246.90	.8887	27.7	1922.43

NOTE: To convert (lb·mol)/h to (kg·mol)/h, multiply by 0.454.

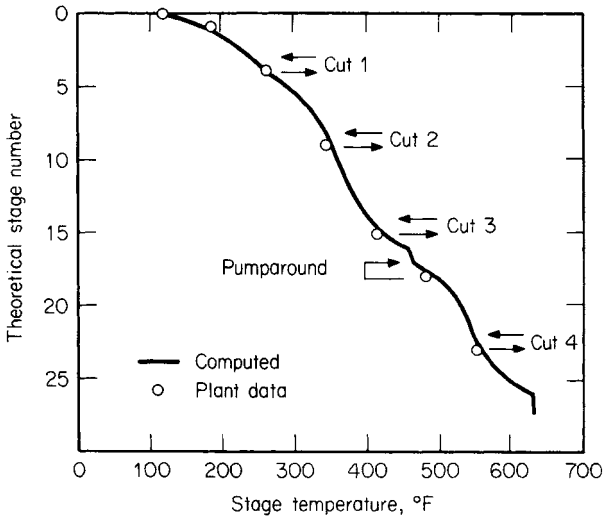

FIG. 13-115 Comparison of computed stage temperatures with plant data for the example of Fig. 13-114.

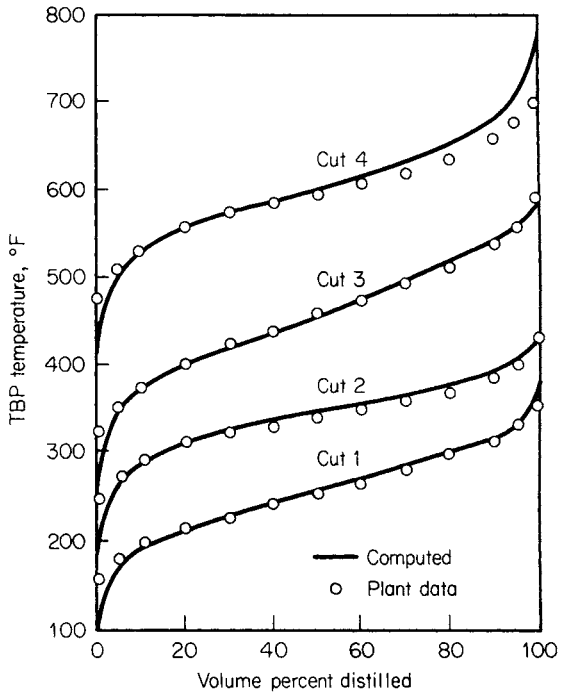

FIG. 13-116 Comparison of computed TBP curves with plant data for the example of Fig. 13-114.

Light-component analysis and the TBP and API gravity for the feed are given in Table 13-29. Representation of this feed by pseudocomponents is given in Table 13-30 based on 16.7°C (30°F) cuts from 82 to 366°C (180 to 690°F), followed by 41.7°C (75°F) and then 55.6°C (100°F) cuts. Actual tray numbers are shown in Fig. 13-114. Corresponding theoretical-stage numbers, which were determined by trial and error to obtain a reasonable match of computed- and measured-product TBP distillation curves, are shown in parentheses. Overall tray efficiency appears to be approximately 70 percent for the tower and 25 to 50 percent for the sidecut strippers.

Results of rigorous calculations and comparison to plant data, when possible, are shown in Figs. 13-115, 13-116, and 13-117. Plant temperatures are in good agreement with computed values in Fig. 13-115. Computed sidestream-product TBP distillation curves are in reasonably good agreement with values converted from plant ASTM distillations, as shown in Fig. 13-116. Exceptions are the initial points of all four cuts and the higher-boiling end of the heavy-distillate curve. This would seem to indicate that more theoretical stripping stages should be added and that either the percent vaporization of the tower feed in the simulation is too high or the internal reflux rate at the lower draw-off tray is too low. The liquid-rate profile in the tower is shown in Fig. 13-117. The use of two or three pump-around circuits instead of one would result in a better traffic pattern than that shown.

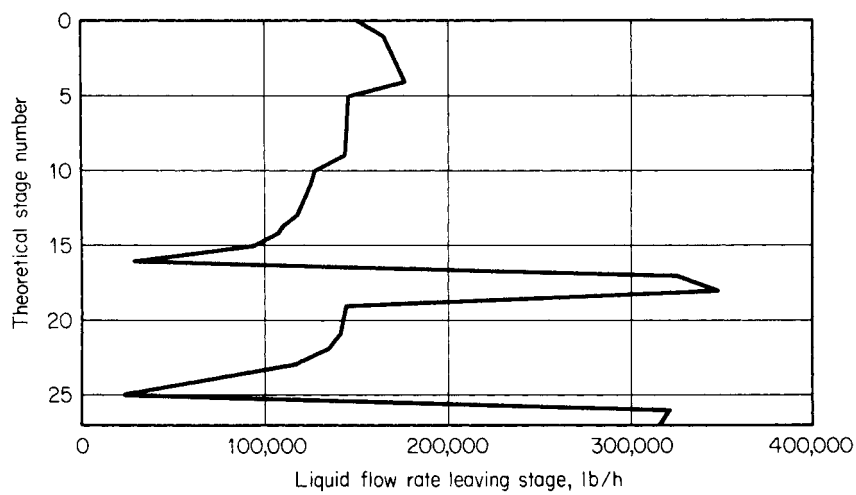

FIG. 13-117 Liquid rate profile for the example of Fig. 13-114.

BATCH DISTILLATION

Batch distillation, which is the process of separating a specific quantity (the charge) of a liquid mixture into products, is used extensively in the laboratory and in small production units that may have to serve for many mixtures. When there are C components in the feed, one batch column will often suffice where $C - 1$ simple continuous distillation columns would be required.

Many larger installations also feature a batch still. The material to be separated may be high in solids content, or it might contain tars or resins that would plug or foul a continuous unit. Use of a batch unit can keep solids separated and permit convenient removal at the termination of the process.

SIMPLE BATCH DISTILLATION

The simplest form of batch distillation consists of a heated vessel (pot or boiler), a condenser, and one or more receiving tanks. No trays or packing is provided. Feed is charged into the vessel and brought to boiling. Vapors are condensed and collected in a receiver. No reflux is returned. The rate of vaporization is sometimes limited to prevent "bumping" the charge and to avoid overloading the condenser, but other controls are minimal. This process is often referred to as a Rayleigh distillation.

If we represent the moles of vapor by V, the moles of liquid in the pot by H, the mole fraction of the more volatile component in this liquid by x, and the mole fraction of the same component in the vapor by y, a material balance yields

$$-y\,dV = d(Hx) \tag{13-124}$$

Since $dV = -dH$, substitution and expansion give

$$y\,dH = H\,dx + x\,dH \tag{13-125}$$

Rearranging and integrating give

$$\ln \frac{H_i}{H_f} = \int_{x_f}^{x_i} \frac{dx}{y - x} \tag{13-126}$$

where subscript i represents the initial condition and f the final condition of the liquid in the pot. The integration limits have been reversed to obtain a positive integral. Equation (13-126) is equivalent to an integrated form of the defining expression for residue curves in Eq. (13-116), with appropriate substitutions for the variable ξ (see below).

If phase equilibrium is assumed between liquid and vapor, the right-hand side of Eq. (13-126) may be evaluated from the area under a curve of $1/(y - x)$ versus x between the limits x_i and x_f. If the mixture is a binary system for which the relative volatility α can be approximated as a constant over the range considered, then the VLE relationship

$$y = \frac{\alpha x}{1 + (\alpha - 1)x} \tag{13-127}$$

can be substituted into Eq. (13-126) and a direct integration can be made:

$$\ln\left(\frac{H_f}{H_i}\right) = \frac{1}{\alpha - 1} \ln\left[\frac{x_f/(1 - x_f)}{x_i/(1 - x_i)}\right] + \ln\left(\frac{1 - x_i}{1 - x_f}\right) \tag{13-128}$$

For any two components A and B of a multicomponent mixture, if constant α values can be assumed for all pairs of components, then $dH_A/dH_B = y_A/y_B = \alpha_{A,B}(x_A/x_B)$. When this is integrated, we obtain

$$\ln\left(\frac{H_{Af}}{H_{A,i}}\right) = \alpha_{A,B} \ln\left(\frac{H_{Bf}}{H_{B,i}}\right) \tag{13-129}$$

where $H_{A,i}$ and $H_{A,f}$ are the moles of component A in the pot before and after distillation and $H_{B,i}$ and $H_{B,f}$ are the corresponding moles of component B. Mixtures that cannot be accurately described by using a constant relative volatility require some form of numerical or graphical integration for the solution of Eq. (13-126).

As an example, consider the distillation of an ethanol-water mixture at 101.3 kPa (1 atm). The initial charge is 100 mol of liquid containing 18 mol % ethanol, and the mixture must be reduced to a maximum ethanol concentration in the still of 6 mol %. By using equilibrium data interpolated from Gmehling and Onken [*Vapor-Liquid Equilibrium Data Collection*, DECHEMA Chemistry Data Ser., vol. 1, Part 1, Frankfurt (1977)], we get the following:

x	y	$y - x$	$1/(y - x)$
0.18	0.517	0.337	2.97
0.16	0.502	0.342	2.91
0.14	0.485	0.345	2.90
0.12	0.464	0.344	2.90
0.10	0.438	0.338	2.97
0.08	0.405	0.325	3.08
0.06	0.353	0.293	3.41

The area under a curve of $1/(y - x)$ versus x between $x = 0.06$ and 0.18 is $0.358 = \ln(H_i/H_f)$, so that $H_f = 100/1.43 = 70.0$ mol. The liquid remaining consists of $(70.0)(0.06) = 4.2$ mol of ethanol and 65.8 mol of water. By material balance, the total accumulated distillate must contain $18.0 - 4.2 = 13.8$ mol of alcohol and $82.0 - 65.8 = 16.2$ mol of water. The total distillate is 30 mol, and the average distillate composition is $13.8/30 = 0.46$ mole fraction ethanol. The time, rate of heating, and vapor rate required to carry out the process are related by the energy balance and operating policy, which can be considered separately.

Graphical solutions of models lend significant insight, but there are many cases where such solutions are not possible or where repeated solutions are desired for different conditions. Progress in computer-based models, ranging from specialized simulation software to more general-purpose tools, now permits rapid solutions of most models. One solution of the example above using a general-purpose modeling tool Mathematica® is shown in Fig. 13-118.

The simple batch still provides only one theoretical plate of separation. Its use is usually restricted to laboratory work or preliminary manufacturing in which the products will be held for additional separation at a later time, when most of the volatile component must be removed from the batch before it is processed further, for separation of the batch from heavy undesired components.

BATCH DISTILLATION WITH RECTIFICATION

To obtain products with a narrow composition range, a batch rectifying still is commonly used. The *batch rectifier* consists of a pot (or reboiler) as in simple distillation, plus a rectifying column, a condenser, some means of accumulating and splitting off a portion of the condensed vapor (distillate) for reflux, and one or more product receivers (Fig. 13-119).

The temperature of the distillate is controlled near the bubble point, and reflux is returned at or near the upper column temperature to permit a true indication of reflux quantity and to improve the column operation. A heat exchanger is used to subcool the remainder of the distillate, which is sent to a product receiver. The column may operate at an elevated pressure or at vacuum, in which case appropriate additional devices must be included to obtain the desired pressure. Equipment design methods for batch still components, except for the pot, typically follow the same principles as those presented for continuous distillation under the assumption of conditions close to a steady state (but see the comments below on the effects of holdup). The design should be checked for each mixture if several mixtures are to be processed. The design should be checked at more than one point for each mixture, since the compositions in the pot and in the column change as the distillation proceeds. The pot design is based on the batch size and the vaporization rate, which are related to the time and rate of heating and cooling available. For existing equipment, the pot size will determine the size of the batch or at least a range of feasible sizes H_i.

In operation, a batch of liquid is charged to the pot, and the system is first brought to steady state under total reflux. A portion of the overhead condensate is then continuously withdrawn in accordance with

```
In[1]:= ydata = {{0.18, 0.517}, {0.16, 0.502}, {0.14, 0.485},
         {0.12, 0.464}, {0.10, 0.438}, {0.08, 0.405},
         {0.06, 0.353}};

In[2]:= y = Fit[ydata, {1, x, x^2}, x]

Out[2]= 0.190167 + 3.27321 x - 8.18452 x^2


In[3]:= curve = Plot[y, {x, 0.06, 0.18},
         {DisplayFunction → Identity}];

In[4]:= points = ListPlot[ydata,
         {PlotStyle → PointSize[0.025],
          DisplayFunction → Identity}];

In[5]:= Show [curve, points,
        {DisplayFunction → $DisplayFunction,
         AxesOrigin → Last[ydata],
         AxesLabel → {"x", "y"}}];
```

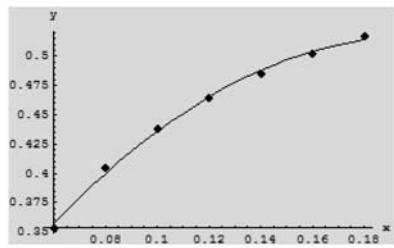


```
In[6]:= Integrate[{1 / {y - x}}, {x, 0.06, 0.18}]

Out[6]= {{0.35856}}
```

FIG. 13-118 Solution for a simple distillation example using Mathematica,® version 5.0.1.

the established reflux policy. "Cuts" are made by switching to alternate receivers, at which time the operating conditions, e.g., reflux rate, may also be altered. The entire column operates as an enriching or rectifying section. As time proceeds, the composition of the liquid in the pot becomes less rich in the more volatile components, and distillation of a cut is stopped when the accumulated distillate attains the desired average composition.

OPERATING METHODS

A batch distillation can be operated in several ways:

1. *Constant reflux, varying overhead composition.* The reflux is set at a predetermined value at which it is maintained for the entire run. Since the pot liquid composition is changing, the instantaneous composition of the distillate also changes. The progress of the distillate and pot compositions in a particular binary separation is illustrated in Fig. 13-120. The variation of the distillate composition for a multicomponent batch distillation is shown in Fig. 13-121 (these distillate product cuts have relatively low purity). The shapes of the curves are functions of volatility, reflux ratio, and number of theoretical plates. The distillation is continued until the average distillate composition is at the desired value. In the case of a binary mixture, the overhead is then typically diverted to another receiver, and an intermediate or "slop" cut is withdrawn until the remaining pot liquid meets the required specification. The intermediate cut is usually added to the next batch, which can therefore have a somewhat different composition from the previous batch. For a multicomponent mixture, two or more intermediate cuts may be taken between the product cuts. It is preferred to limit the size of the intermediate cuts as far as practical because they reduce the total amount of feed that can be processed.

2. *Constant overhead composition, varying reflux.* If it is desired to maintain a constant overhead composition in the case of a binary mixture, the amount of reflux returned to the column must be constantly increased throughout the run. As time proceeds, the pot is gradually depleted of the lighter component. The increase in reflux is typically gradual at first and more rapid near the end of a cut. Finally, a point is reached at which there is little of the lighter component remaining in the pot and the reflux ratio has attained a very high value. The receivers are then changed, the reflux is reduced, and an intermediate cut is taken as before. This technique can also be extended to a multicomponent mixture.

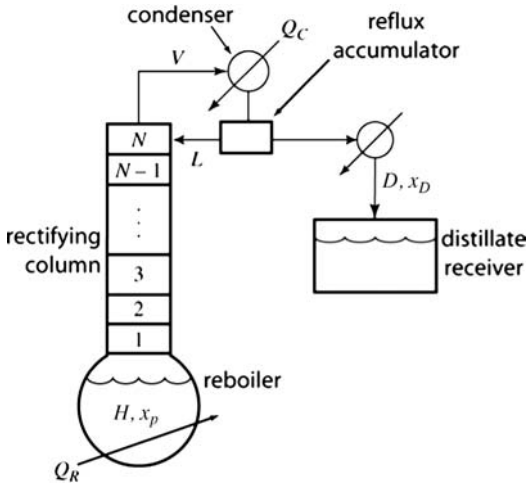

FIG. 13-119 Schematic of a batch rectifier.

3. *Other methods.* A cycling procedure can also be used for the column operation. The unit operates at total reflux until a steady state is established. The distillate is then taken as total drawoff for a short time, after which the column is returned to total reflux operation. This cycle is repeated throughout the course of distillation. Another possibility is to optimize the reflux ratio to achieve the desired separation in a minimum time. More complex operations may involve withdrawal of sidestreams, provision for intercondensers, addition of feeds to trays, and periodic feed additions to the pot.

APPROXIMATE CALCULATION PROCEDURES FOR BINARY MIXTURES

A useful analysis for a binary mixture employs the McCabe-Thiele graphical method. In addition to the usual assumptions of an adiabatic column and constant molar overflow on the trays, the following procedure assumes that the holdup of liquid on the trays, in the column,

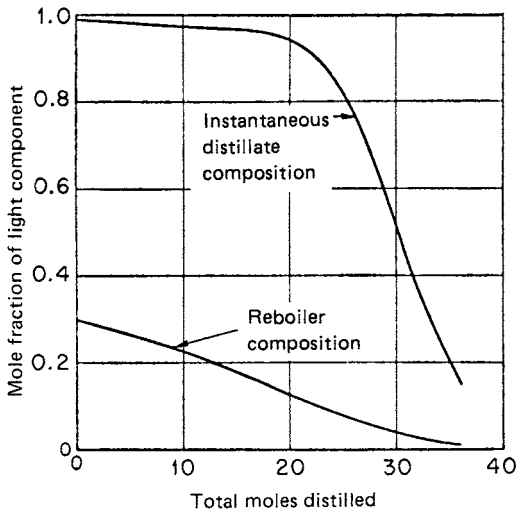

FIG. 13-120 Variation in distillate and reboiler compositions with the amount distilled in binary batch distillation at a constant reflux ratio.

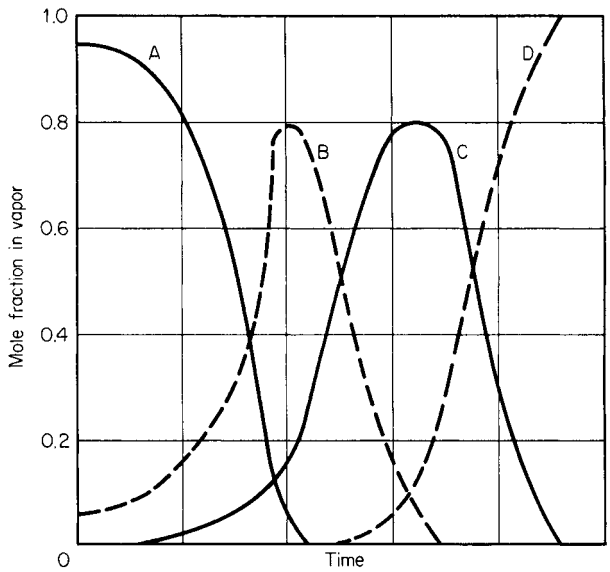

FIG. 13-121 Distillate composition for a batch distillation of a four-component mixture at a constant reflux ratio.

and in the condenser is negligible compared to the holdup in the pot. (The effects of holdup can be significant and are discussed in a later section.)

As a first step, the minimum reflux ratio should be determined. Point D in Fig. 13-122 represents the desired distillate composition and is located on the diagonal since a total condenser is assumed and $x_D = y_D$. Point F represents the initial composition in the pot x_{pi} and for the vapor entering the bottom of the rectifying column y_{pi}. The minimum internal reflux is found from the slope of the line DF

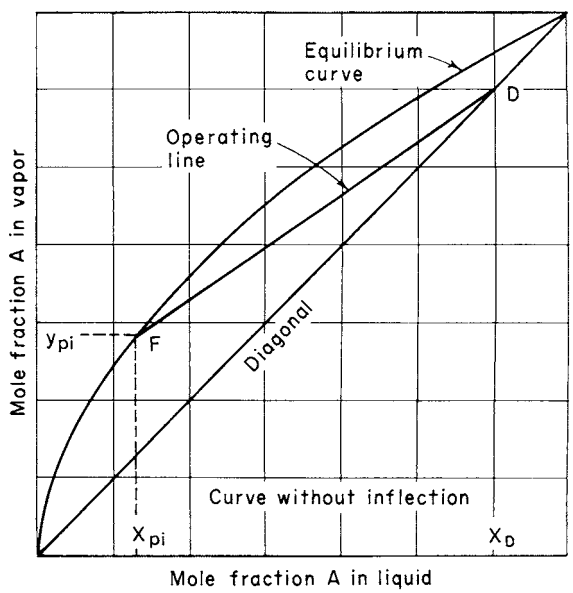

FIG. 13-122 Determination of the minimum reflux for a relatively ideal equilibrium curve.

$$\left(\frac{L}{V}\right)_{\min} = \frac{y_D - y_{pi}}{x_D - x_{pi}} \tag{13-130}$$

where L is the liquid flow rate and V is the vapor rate, both in moles per hour. Since $V = L + D$ (where D is distillate rate) and the external reflux ratio R is defined as $R = L/D$,

$$\frac{L}{V} = \frac{R}{R+1} \tag{13-131}$$

or

$$R_{\min} = \frac{(L/V)_{\min}}{1 - (L/V)_{\min}} \tag{13-132}$$

The condition of minimum reflux for an equilibrium curve with an inflection point P is shown in Fig. 13-123. In this case the minimum internal reflux is

$$\left(\frac{L}{V}\right)_{\min} = \frac{y_D - y_P}{x_D - x_P} \tag{13-133}$$

The operating reflux ratio is usually 1.5 to 10 times the minimum. By using the ethanol-water equilibrium curve for 101.3-kPa (1-atm) pressure shown in Fig. 13-123 but extending the line to a convenient point for readability, $(L/V)_{\min} = (0.800 - 0.695)/(0.800 - 0.600) = 0.52$ and $R_{\min} = 1.083$.

Batch Rectification at Constant Reflux Using an analysis similar to the simple batch still, Smoker and Rose [*Trans. Am. Inst. Chem. Eng.*, **36,** 285 (1940)] developed the following equation:

$$\ln \frac{H_i}{H_f} = \int_{x_{pf}}^{x_{pi}} \frac{dx_p}{x_D - x_p} \tag{13-134}$$

An overall material balance on the light component gives the average or accumulated distillate composition $x_{D,\text{avg}}$.

$$x_{D,\text{avg}} = \frac{H_i x_{pi} - H_f x_{pf}}{H_i - H_f} \tag{13-135}$$

If the integral on the right side of Eq. (13-134) is denoted by ξ, the time θ for distillation can be found by

$$\theta = (R+1)\frac{H_i(e^{\xi} - 1)}{Ve^{\xi}} \tag{13-136}$$

An alternative equation is

$$\theta = \frac{R+1}{V}(H_i - H_f) \tag{13-137}$$

Development of these equations is given by Block [*Chem. Eng.*, **68,** 88 (Feb. 6, 1961)]. The calculation process is illustrated schematically in Fig. 13-124. Operating lines are drawn with the same slope but intersecting the 45° line at different points. The number of theoretical plates under consideration is stepped off to find the corresponding bottoms composition (i.e., still pot composition) for each distillate composition. In Fig. 13-124, operating line $L - 1$ with slope L/V drawn from point D_1 where the distillate composition is x_{D1} and the pot composition is $x_{p1\text{-}3}$ for three theoretical plates, x_{D2} has a corresponding pot composition of $x_{p2\text{-}3}$, etc. By using these pairs of distillate and pot compositions, the right-hand side of Eq. (13-134) can be evaluated and $x_{D,\text{avg}}$ can be found from Eq. (13-135). An iterative calculation is required to find the value of H_f that corresponds to a specified $x_{D,\text{avg}}$.

To illustrate the use of these equations, consider a charge of 520 mol of an ethanol-water mixture containing 18 mol % ethanol to be distilled at 101.3 kPa (1 atm). Suppose that the vaporization rate is 75 mol/h, and the product specification is 80 mol % ethanol. Let $L/V = 0.75$, corresponding to a reflux ratio $R = 3.0$. If the column section has six theoretical plates and the pot provides an additional seventh, find how many moles of product will be obtained, what the composition of the pot residue will be, and the time that the distillation will take.

Using the vapor-liquid equilibrium data, plot a y-x diagram. Draw a number of operating lines at a slope of 0.75. Note the composition at the 45° intersection, and step off seven stages on each to find the equilibrium value of the bottoms pot composition. Some of the results are tabulated in the following table:

x_D	x_p	$x_D - x_p$	$1/(x_D - x_p)$
0.800	0.323	0.477	2.097
0.795	0.245	0.550	1.820
0.790	0.210	0.580	1.725
0.785	0.180	0.605	1.654
0.780	0.107	0.673	1.487
0.775	0.041	0.734	1.362

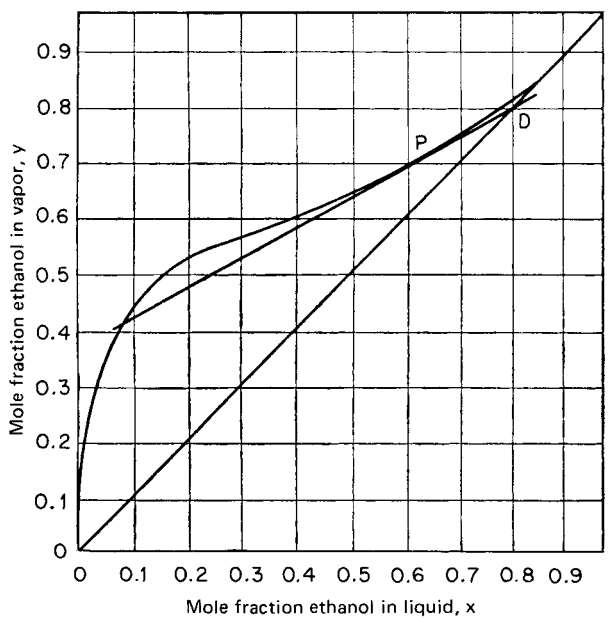

FIG. 13-123 Determination of minimum reflux for an equilibrium curve with an inflection point.

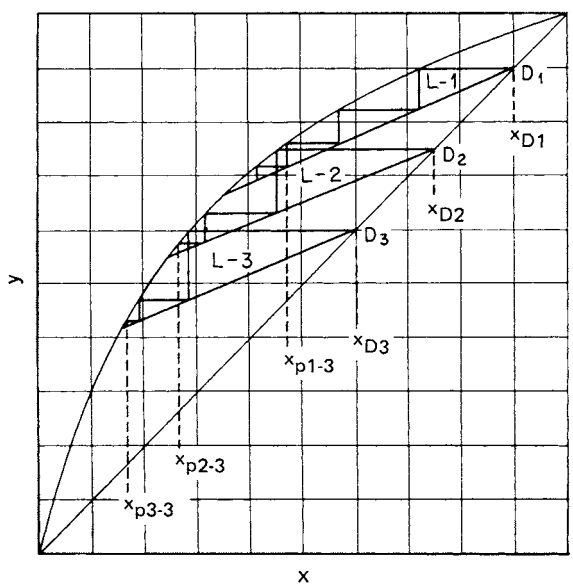

FIG. 13-124 Graphical method for constant-reflux operation.

By using an iterative procedure, integrating between x_{pi} of 0.18 and various lower limits, it is found that $x_{D,avg} = 0.80$ when $x_{pf} = 0.04$, at which time the value of the integral = 0.205 = ln (H_i/H_f), so that H_f = 424 mol. The product collected = $H_i - H_f$ = 520 − 424 = 96 mol. From Eq. (13-136),

$$\theta = \frac{(4)(520)(e^{0.205} - 1)}{75(e^{0.205})} = 5.2 \text{ h} \qquad (13\text{-}138)$$

Batch Rectification at Constant Distillate Composition Bogart [*Trans. Am. Inst. Chem. Eng.*, **33,** 139 (1937)] developed the following equation for constant distillate composition with the column holdup assumed to be negligible:

$$\theta = \frac{H_i(x_D - x_{pi})}{V} \int_{x_{pf}}^{x_{pi}} \frac{dx_p}{(1 - L/V)(x_D - x_p)^2} \qquad (13\text{-}139)$$

and where the terms are defined as before. The quantity distilled can then be found by material balance once the initial and final pot compositions are known.

$$H_i - H_f = \frac{H_i(x_{pi} - x_{pf})}{x_D - x_{pf}} \qquad (13\text{-}140)$$

A schematic example is shown in Fig. 13-125. The distillate composition is held constant by increasing the reflux as the pot composition becomes more dilute. Operating lines with varying slopes (= L/V) are drawn from the known distillate composition, and the given number of stages is stepped off to find the corresponding bottoms (still pot) compositions.

As an example, consider the same ethanol-water mixture used above to illustrate constant reflux but now with a constant distillate composition of $x_D = 0.90$. The following table is compiled:

L/V	R	x_p	$x_D - x_p$	$1/(1 - L/V)(x_D - x_p)^2$
0.600	1.50	0.654	0.147	115.7
0.700	2.33	0.453	0.348	27.5
0.750	3.00	0.318	0.483	17.2
0.800	4.00	0.143	0.658	11.5
0.850	5.67	0.054	0.747	11.9
0.900	9.00	0.021	0.780	16.4

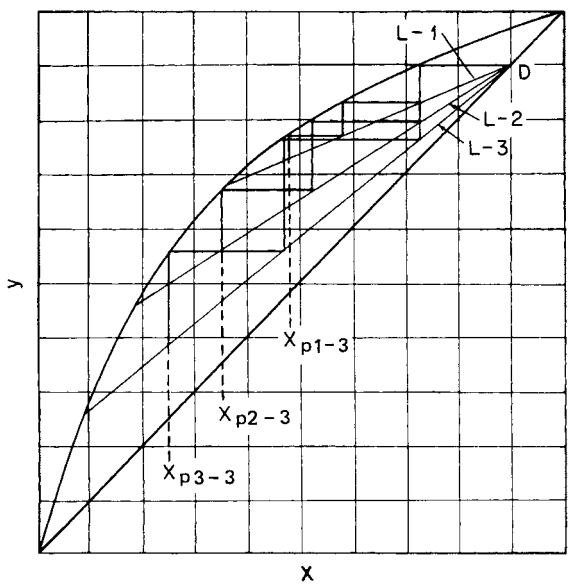

FIG. 13-125 Schematic of constant distillate composition operation.

If the right-hand side of Eq. (13-139) is integrated by using a limit for x_{pf} of 0.04, the value of the integral is 1.615 and the time is

$$\theta = \frac{(520)(0.800 - 0.180)(1.615)}{75} = 7.0 \text{ h} \qquad (13\text{-}141)$$

The quantity distilled can be found from Eq. (13-140):

$$H_i - H_f = \frac{(520)(0.180 - 0.040)}{0.800 - 0.040} = 96 \text{ mol} \qquad (13\text{-}142)$$

Other Operating Methods and Optimization A useful control method for difficult industrial or laboratory distillations is *cycling operation.* The most common form of cycling control is to operate the column at total reflux until steady state is established, take off the complete distillate for a short time, and then return to total reflux. An alternative scheme is to interrupt vapor flow to the column periodically by the use of a solenoid-operated butterfly valve in the vapor line from the pot. In both cases, the equations necessary to describe the system are complex, as shown by Schrodt et al. [*Chem. Eng. Sci.*, **22,** 759 (1967)]. The most reliable method for establishing the cycle relationships is by experimental trial on an operating column. Several investigators have also proposed that batch distillation be programmed to attain *time optimization* by proper variation of the reflux ratio. A comprehensive discussion was first presented by Coward [*Chem. Eng. Sci.*, **22,** 503 (1967)] and reviewed and updated by Kim and Diwekar [*Rev. Chem. Eng.*, **17,** 111 (2001)].

The *choice of operating mode* depends upon characteristics of the specific system, the product specifications, and the engineer's preference in setting up a control sequence. Probably the most direct and most common method is *constant reflux.* Operation can be regulated by a timed reflux splitter, a ratio controller, or simply a pair of flowmeters. Since composition is changing with time, some way must be found to estimate the average accumulated distillate composition in order to define the endpoint. This is no problem when the specification is not critical or the change in distillate composition is sharply defined. However, when the composition of the distillate changes slowly with time, the cut point is more difficult to determine. Operating with *constant composition* (varying reflux), the specification is automatically achieved if control can be linked to composition or some composition-sensitive physical variable. The relative advantage of the two modes depends upon the materials being separated and upon the number of theoretical plates in the column. A comparison of distillation rates using the same initial and final pot composition for the system benzene-toluene is given in Fig. 13-126. Typical control instrumentation is described by Block [*Chem. Eng.*, **74,** 147 (Jan. 16, 1967)]. Control procedures for *reflux and vapor cycling* operation and for the *time-optimal* process are largely a matter of empirical trial.

Effects of Column Holdup When the holdup of liquid on the trays and in the condenser and reflux accumulator is not negligible compared with the holdup in the pot, the distillate composition at constant reflux ratio changes with time at a different rate than when the column holdup is negligible because of two separate effects.

First, with an appreciable column holdup, the composition of the charge to the pot will be higher in the light component than the pot composition at the start of the distillation. The reason is that before product takeoff begins, the column holdup must be supplied, and due to the rectification, its average composition is higher in the lighter component than that of the liquid charged as feed to the pot. Thus, when overhead takeoff begins, the pot composition is lower than it would be if there were negligible column holdup and the separation is more difficult than expected based on the composition of the feed. The second effect of column holdup is to slow the rate of exchange of the components; the holdup exerts an inertial effect, which prevents compositions from changing as rapidly as they would otherwise, and the degree of separation is usually improved.

Both these effects occur at the same time and change in importance during the course of distillation. Although a number of studies were made and approximate methods developed for predicting the effect of liquid holdup during the 1950s and 1960s (summarized in the 6th edition of *Perry's Chemical Engineers' Handbook*), it is now best to use simulation methods to determine the effect of holdup on a case-by-case basis.

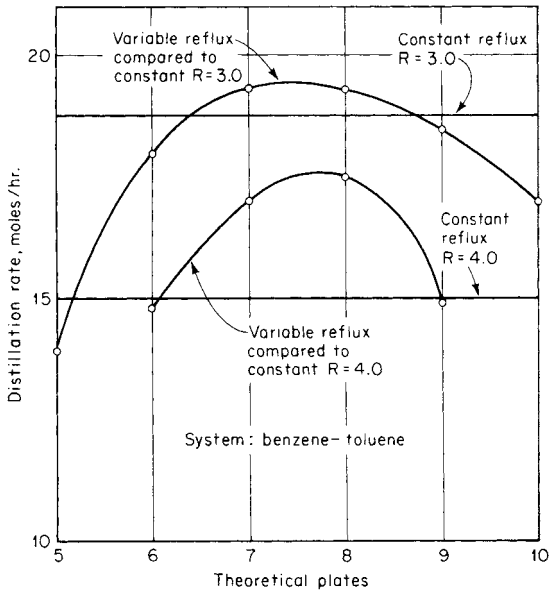

FIG. 13-126 Comparison of operating modes for a batch column.

As an example, consider a batch rectifier fed with a 1:1 mixture of ethanol and *n*-propanol. The rectifier has eight theoretical stages in the column and is operated at a reflux ratio of 19. The distillate and pot compositions are shown in Fig. 13-127 for various values of the holdups.

In Fig. 13-127*a*, the holdup on each stage is 0.01 percent of the initial pot holdup, and in the reflux accumulator it is 0.1 percent of the initial pot holdup (for a total of 0.108 percent). Because this model calculation does not begin with a total reflux period, there is a small initial distillate cut with relatively low ethanol purity. This is followed by a high-purity distillate cut. An intermediate cut of approximately 10 percent of the initial batch size can be collected, leaving the pot with a high purity of *n*-propanol. The column holdup for the case shown in Fig. 13-127*b* is 1 percent of the initial batch size on each stage while the reflux accumulator holdup remains small at 0.1 percent (for a total of 8.1 percent). In this case, both the first low-purity cut and the intermediate cut are somewhat larger for the same purity specifications. These effects are substantially larger when the reflux accumulator has a more significant holdup, as shown in Fig. 13-127*c*, corresponding to a holdup of 1 percent on each stage and 5 percent in the reflux accumulator (for a total of 13 percent). Similar effects are found for multicomponent mixtures. The impact of column and condenser holdup is most important when a high-purity cut is desired for a component that is present in relatively small amounts in the feed.

SHORTCUT METHODS FOR MULTICOMPONENT BATCH RECTIFICATION

For preliminary studies of batch rectification of multicomponent mixtures, shortcut methods that assume constant molar overflow and negligible vapor and liquid holdup are useful in some cases (see the discussion above concerning the effects of holdup). The method of Diwekar and Madhaven [*Ind. Eng. Chem. Res.*, **30,** 713 (1991)] can be used for constant reflux or constant overhead rate. The method of Sundaram and Evans [*Ind. Eng. Chem. Res.*, **32,** 511 (1993)] applies only to the case of constant reflux, but is easy to implement. Both methods employ the Fenske-Underwood-Gilliland (FUG) shortcut procedure at successive time steps. Thus, batch rectification is treated as a sequence of continuous, steady-state rectifications.

CALCULATION METHODS AND SIMULATION

Model predictions such as those shown in Fig. 13-126 or 13-127 are relatively straightforward to obtain by using modern simulation models and software tools. As discussed in earlier editions of this handbook, such models and algorithms for their solutions have been the subject of intensive study since the early 1960s when digital computing became practical. Detailed calculation procedures for binary and multicomponent batch distillation were initially focused on binary mixtures of constant relative volatility. For example, Huckaba and Danly [*AIChE J.*, **6,** 335 (1960)] developed a simulation model that incorporated more details than can be included in the simple analytical models described above. They assumed constant-mass tray holdups, adiabatic tray operation, and linear enthalpy relationships, but did include energy balances around each tray and permitted the use of nonequilibrium trays by means of specified tray efficiencies. Experimental data were provided to validate the simulation. Meadows [*Chem. Eng. Prog. Symp. Ser.* **46,** 59, 48 (1963)] presented a multicomponent batch distillation model that included equations for energy, material, and volume balances around theoretical trays. The only assumptions made were perfect mixing on each tray, negligible vapor holdup, adiabatic operation, and constant-volume tray holdup. Distefano [*AIChE. J.*, **14,** 190 (1968)] extended the model and developed a procedure that was used to simulate several commercial batch distillation columns successfully. Boston et al. (*Foundations of Computer-Aided Chemical Process Design,* vol. 2, Mah and Seider, eds., *American Institute of Chemical Engineers,* New York, 1981, p. 203) further extended the model, provided a variety of practical sets of specifications, and utilized modern numerical procedures and equation formulations to handle efficiently the nonlinear and often stiff nature of the multicomponent batch distillation problem.

It is important to note that in using computer-aided models for batch distillation, the various assumptions of the model can have a significant impact on the accuracy of the results; e.g., see the discussion of the effects of holdup above. Uncertainties in the physical and chemical parameters in the models can be addressed most effectively by a combination of sensitivity calculations using simulation tools, along with comparison to data. The mathematical treatment of stiffness in the model equations can also be very important, and there is often a substantial advantage in using simulation tools that take special account of this stiffness. (See the 7th edition of *Perry's Chemical Engineers' Handbook* for a more detailed discussion of this aspect).

The availability of detailed models and solution methods has enabled many new studies of complex, mixtures, configurations, and operating and control strategies for batch distillation.

CONSTANT-LEVEL DISTILLATION

Manipulation of the operating conditions such as reflux ratio or pressure during a batch distillation can be useful. In addition, the feed to the batch distillation may vary during the process. A common application is to replace one solvent with another in the presence of a heavy nonvolatile product, as may be encountered in pharmaceutical production. One option for switching solvents is to use simple distillation repeatedly. Initially, a portion of the first solvent is removed by boiling. Then the second solvent is added, and a simple distillation removes more of the first solvent along with some of the second. Repetition of the latter step can be used to reduce the concentration of the first solvent to very small levels.

Gentilcore [*Chem. Eng. Progr.*, **98**(1), 56 (Jan. 2002)] describes an alternative strategy of "constant-level" batch distillation where the replacement solvent is added at a rate to keep the volume of liquid in the pot constant. For simple distillation without rectification the analog of Eq. (13-126) is

$$\frac{S}{H} = \int_{x_f}^{x_i} \frac{dx}{y} \tag{13-143}$$

and the analog of Eq. (13-128) is

$$\frac{S}{H} = \frac{1}{\alpha} \ln \frac{x_i}{x_f} + \frac{\alpha - 1}{\alpha}(x_i - x_f) \tag{13-144}$$

where the mole fractions refer to the compositions of the original solvent and S is the amount of the second solvent added to the batch. The amount of solute, a nonvolatile heavy product, is small compared to the size of the batch (alternatively, the analysis can be done on a

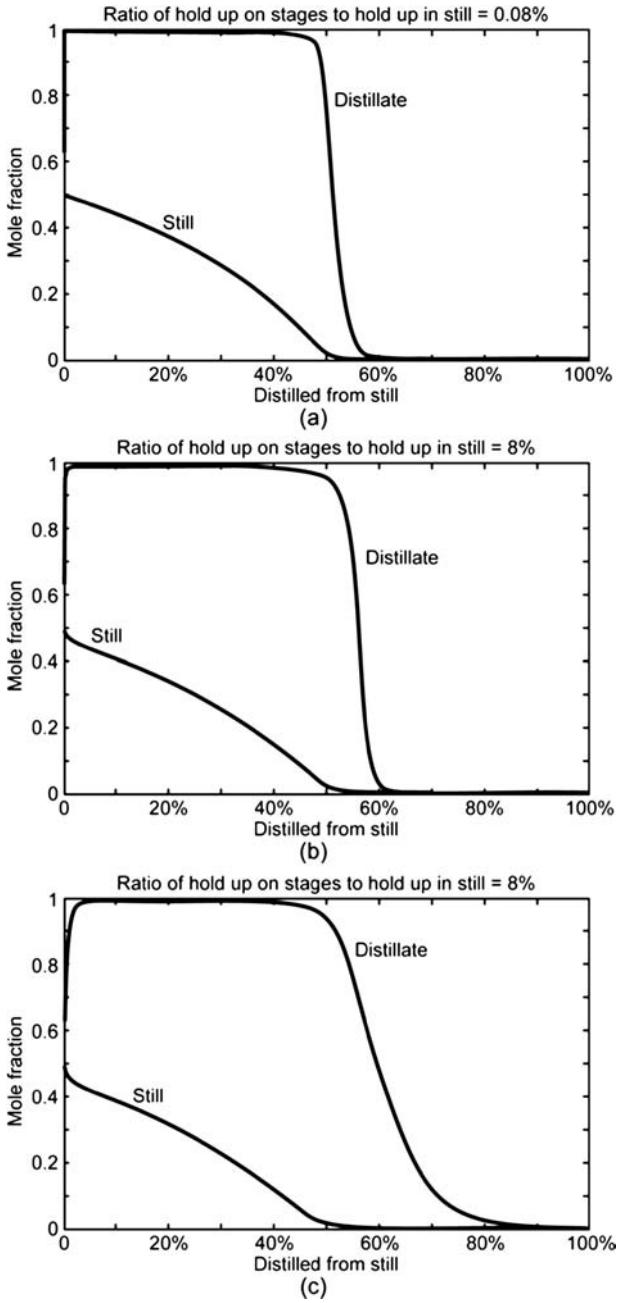

FIG. 13-127 Effects of holdup on batch rectifier.

solute-free basis). The second solvent is assumed to be pure, and the rate of addition is manipulated to keep a constant level in the pot. Compared to the repeated application of simple distillation, this semibatch operation can typically reduce solvent use by one-half or more depending on the volatility and the desired compositions. This is also a more efficient use of equipment at the expense of a somewhat more complex operation.

An example provided by Gentilcore considers a simple batch still that operates with an initial charge of 80 mol and a minimum of 20 mol. The original solvent use has a volatility $\alpha = 3$ relative to that of the replacement solvent. If simple distillation is used, 60 mol of the original solvent is initially boiled off and then 60 mol of the second solvent is added. A second distillation of this mixture begins with a composition $x_i = 0.25$ of the original solvent. The solution of Eq. (13-128) by trial and error or root finding gives $x_f = 0.03$ for $H_i = 80$ and $H_f = 20$. Of the 60 mol removed as distillate in this second distillation, 20 – 0.03 = 19.97 mol is the original solvent and 60 – 19.97 = 40.03 mol is the replacement. An alternative constant-level batch distillation in the same equipment according to Eq. (13-144) with $H = 20$, $x_i = 0.25$, and $x_f = 0.03$ requires the addition of $S = 35.6$ mol of replacement solvent. The still contains 20 mol of the solvent; 16.2 mol is distilled compared to 40.3 mol in the simple distillation. This 60 percent savings in the use of replacement solvent arises because the distillation takes place beginning with a higher concentration of the original solvent for the second step.

ALTERNATIVE EQUIPMENT CONFIGURATIONS

The batch rectifier shown schematically in Fig. 13-119 is by far the most common configuration of equipment. Several alternative special-purpose configurations have been studied and offer potential advantages in particular applications. Also see Doherty and Malone (*Conceptual Design of Distillation Systems,* McGraw-Hill, 2001, pp. 407–409, 417–419).

For instance, a simple batch distillation can be combined with a stripping column to give the batch stripper shown in Fig. 13-128. The pot holds the batch charge and provides liquid reflux into the stripping section. The reboiler provides vapor to the column and has relatively small holdup. The product stream B in the bottom is concentrated in the higher-boiling compound, and the pot gradually becomes more concentrated in the lighter component. Multiple "cuts" can be taken as products, and the reboil rate either can be constant or can be adjusted by analogy with the reflux ratio in the batch rectifier.

For mixtures containing large concentrations of a heavy component, the batch stripper can be advantageous.

The more complex "middle vessel" column combines aspects of both the batch rectifier and the batch stripper, as shown in Fig. 13-129. The middle vessel arrangement was described qualitatively by Robinson and Gilliland (*Elements of Fractional Distillation,* McGraw-Hill, 1950, p. 388) and analyzed by Bortolini and Guirase [*Quad. Ing. Chim. Ital.,* **6,** 150 (1970)]. This configuration requires more equipment and is more complex, but can produce both distillate and bottoms product cuts simultaneously. Barolo and Botteon [*AIChE J.,* **43,** 2601 (1997)] pointed out that the middle vessel configuration at total reflux and reboil and with the appropriate collection equipment for distillate and bottoms products (not shown in Fig. 13-129) can concentrate a ternary mixture into its three pure fractions. This and analogous configurations for mixtures with more components have been studied by Hasebe et al. [*J. Chem. Eng. Japan,* **29,** 1000 (1996); *Computers Chem. Engng.,* **23,**

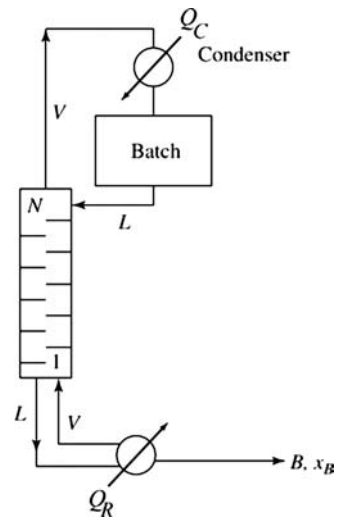

FIG. 13-128 Schematic of a batch stripper.

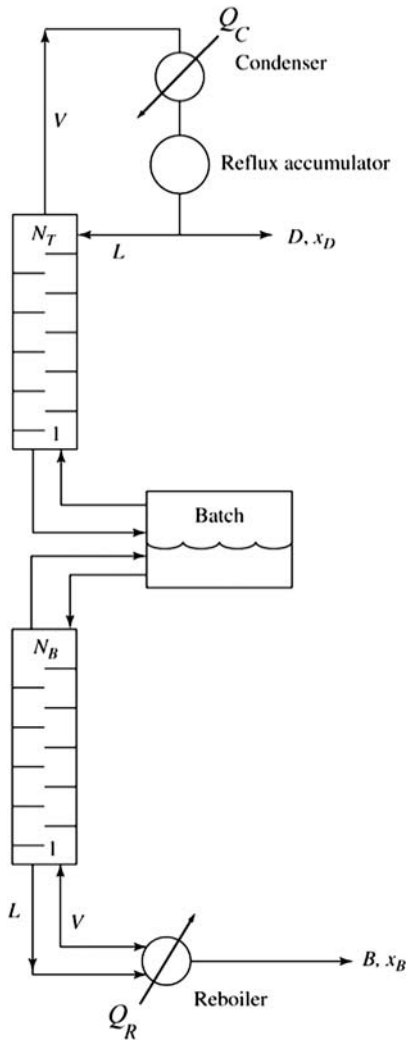

FIG. 13-129 Middle vessel batch distillation.

523 (1999)] and experimentally by Wittgens and Skogestad [*IChemE Symp Ser.*, **142,** 239 (1997).]

The batch stripper and the middle vessel configurations provide the capability to make separations for certain azeotropic mixtures that are not possible or that cannot be done efficiently in the batch rectifier.

BATCH DISTILLATION OF AZEOTROPIC MIXTURES

Although azeotropic distillation is covered in an earlier subsection, it is appropriate to consider the application of residue curve maps to batch distillation here. (See the subsection Enhanced Distillation for a discussion of residue curve maps.) An essential point is that the sequence, number, and limiting composition of each cut from a batch distillation depend on the form of the residue curve map and the composition of the initial charge to the still. As with continuous distillation operation, the set of reachable products (cuts) for a given charge to a batch distillation is constrained by the residue curve–map distillation boundaries. Furthermore, some pure components can be produced as products from the batch stripper, but not the batch rectifier and vice versa. Doherty and Malone (*Conceptual Design of Distillation Systems,* chap. 9, McGraw-Hill, 2001) give more details, but the main points are the following.

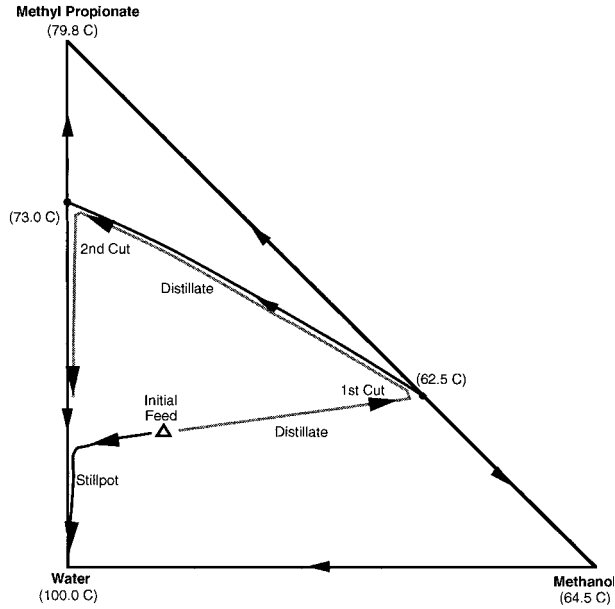

FIG. 13-130 Residue curve map and batch rectifier paths for methanol, methyl propionate, and water.

In the batch rectifier, the limiting cuts, obtainable with a sufficiently large number of stages and reflux, begin with the low-boiling node that defines the distillation region containing the feed composition. For the batch stripper, the first limiting cut is the high-boiling node. In either case, the subsequent cuts depend on the structure of the residue curve map.

For the batch rectifier, as the low-boiling component or azeotrope is removed, the still composition moves along a straight material balance line through the initial feed composition and the low-boiling node and away from the initial composition until it reaches the edge of the composition triangle or a distillation boundary. The path then follows the edge or distillation boundary to the high-boiling node of the region.

As an example, consider the residue curve map structure shown in Fig. 13-130 for a mixture of methanol, methyl propionate, and water at a pressure of 1 atm. There are two minimum-boiling binary azeotropes joined by a distillation boundary that separates the compositions into two distillation regions. Feeds in the upper and lower regions will have different distillate products. For the sample feed shown, and with a sufficient number of theoretical stages and reflux, the distillate will rapidly approach the low-boiling azeotrope of methanol and methyl propionate at 62.5°C. The still pot composition changes along the straight-line segment as shown until it is nearly free of methanol. At that point, the distillate composition changes rapidly along the distillation boundary to a composition for the second cut at or near the methyl propionate–water azeotrope. The still pot composition eventually approaches pure water. The rate of change and the precise approach to these compositions require more detailed study.

For the same feed, a batch stripper can be used to remove a bottoms product that approaches pure water. The pot composition (overhead) will contain all three components near the point of intersection of the distillation boundary with a straight line extended from the water vertex through the feed composition.

For this mixture it is not possible to isolate the pure components in a batch rectifier or batch stripper. The use of additional equipment such as a decanter to exploit liquid-liquid phase behavior or the addition of a fourth component or chemical reactions can sometimes be used to effect the separation.

The product cuts for azeotropic mixtures are also sensitive to the curvature of the distillation boundaries; see Doherty and Malone (*Conceptual Design of Distillation Systems,* McGraw-Hill, 2001; pp. 403–404) and additional references there.